Thèse de doctorat
de l'Université Sorbonne Paris Cité
Préparée à l'Université Paris Diderot
Ecole doctorale BIOSPC 562

Laboratoire d'Immunorégulation, Institut Pasteur, Paris

Exploring immunological mechanisms of human graft-versus-host disease after hematopoietic stem cell transplantation

Par Eleonora M. T. LATIS

Thèse de doctorat d'Immunologie

Dirigée par Dr Lars ROGGE

Présentée et soutenue publiquement à Paris, le 14 Décembre 2018

Jury :

Rapporteur	Dr Sophie BROUARD	Université de Nantes
Rapporteur	Dr Fréderic VELY	Aix Marseille Université
Examinateur	Dr Philippe BOUSSO	Institut Pasteur
Examinateur	Pr Antoine TOUBERT	Université Paris Diderot
Directeur de thèse	Dr Lars ROGGE	Institut Pasteur

Abstract

Allogeneic hematopoietic stem cell transplantation (HSCT) is a curative treatment for many hematologic malignancies. However, its success is hindered by graft-versus-host disease (GVHD), a potentially fatal complication deriving from alloreactive donor T cells attacking recipient tissues. Acute GVHD (aGVHD) prevalence lies between 40 and 80% depending on transplant characteristics. GVHD is the main cause of non-relapse morbidity and mortality after HSCT and despite the advances in the field, disease processes in humans remain poorly understood.

In this study we investigated the phenotypic and molecular characteristics of immune cells in patients after HSCT and in their HLA-identical sibling donors, with the goal of defining immune parameters associated with the recovery of donor-derived immunity and with the development of acute GVHD. We analysed 101 donor-recipient pairs in three independent cohorts for which blood was collected from the donors before transplantation and for the recipients either at aGVHD onset, before any treatment, or at day 30 or 90 post-HSCT for recipients that did not develop GVHD. On the donors' and recipients' samples we performed cellular profiling using spectral flow cytometry as well as gene expression analysis.

Immunophenotyping reveals an incomplete reconstitution of the T cell compartment in the recipients, with an inversion of the CD4/CD8 ratio, both at one and three months after HSCT. Moreover, the reconstituting T cell compartment is characterized by a shift in the effector/memory phenotype of these cells, with a parallel depletion of the naïve T cell pool. NK cell reconstitution is characterized by an expansion of the $CD56^{bright}$ subset, while monocytes undergo an expansion of $CD16^{+}$ cells. At aGVHD onset recipients have an increase of cells with a T stem cell memory-like ($T_{SCM\text{-}like}$) phenotype compared to recipients without aGVHD. These cells may represent a cellular reservoir for GVHD, maintaining the production of alloreactive T cells in the presence of host persistent antigens. Molecular profiling shows that donor T cells react to the environment of the host by acquiring an activated phenotype, with upregulation of genes associated with T cell activation, adhesion, migration and effector functions. T cell transcriptome profiling at aGVHD onset shows upregulation of inflammatory mediators as well as genes involved in cytokine signal transduction, cell migration and cell trafficking.

Our data demonstrate that comprehensive analysis of the distribution of different immune cell subsets with flow cytometry together with gene expression profiling can contribute to elucidate the processes involved in immune reconstitution and acute GVHD development in humans. In the future, studies with new technologies will hopefully bring insights into the mechanisms underlying GVHD development that will help design new preventive and therapeutic strategies to be applied in the clinics.

Keywords: Hematopoietic Stem Cell Transplantation; Immune Reconstitution; Acute GVHD; Immunophenotyping; Gene Expression; Human Immune System; Immune Signatures

Résumé

L'allogreffe de cellules souches hématopoïétiques est un traitement curatif pour de nombreuses maladies hématologiques. Cependant, le succès de cette procédure est entravé par la maladie du Greffon-contre-l'Hôte (GVH), une complication potentiellement fatale induite par l'attaque des tissues de l'hôte par les cellules T alloreactives du donneur. La GVH a une prévalence de 40 à 80%, selon les caractéristiques de la transplantation. La GVH est la cause principale de mortalité post-greffe en dehors des rechutes et, en dépit des nombreuses avancées dans le domaine de l'allogreffe, la physiopathologie de cette maladie est encore mal comprise à ce jour, en particulier chez l'homme.

Dans cette étude, nous nous sommes concentrés sur la caractérisation phénotypique et moléculaire du système immunitaire des patients greffés et de leurs donneurs. L'objectif de l'étude est de déterminer les facteurs liés à la reconstitution du système immunitaire et au développement de la GVH aigüe. Nous avons collecté le sang de 101 couples donneur /receveur apparentés HLA-identique provenant de trois cohortes indépendantes : avant transplantation pour les donneurs, à l'apparition des premiers symptômes chez les patients atteint de la GVH aigüe et 30 ou 90 jours post-greffe pour les patients non atteints. Nous avons caractérisé le profil cellulaire de ces échantillons par cytométrie spectrale et analysé leur profil transcriptomique.

L'immunophenotypage des patients nous a permis de montrer que la reconstitution du compartiment des cellules T est incomplète, avec une inversion du rapport CD4/CD8 après la greffe. De plus, le compartiment cellulaire T est enrichi en cellules possédant un phénotype effecteur/mémoire tandis que le réservoir des cellules T naïves est appauvri. La reconstitution des cellules NK est caractérisée par un enrichissement du sous-type $CD56^{bright}$ et celle des monocytes par l'enrichissement des cellules $CD16^{+}$. A l'apparition de la GVH, une augmentation de la fréquence des cellules possédant un phénotype semblable aux cellules souches mémoire est observée, par rapport aux patients non-atteints. Ces cellules pourraient représenter un réservoir cellulaire de la maladie, maintenant la production de cellules T alloréactives. Le profilage transcriptomique montre que les cellules T du donneur réagissent à l'environnement de l'hôte en acquérant un phénotype activé, avec une surexpression des gènes associés à l'activation, l'adhésion, la migration et les fonctions effectrices. Au commencement de la maladie, on observe que les cellules T surexpriment des gènes médiateurs de l'inflammation ainsi que des gènes impliqués dans la transduction du signal cytokinique et la migration cellulaire.

Nos données démontrent que l'analyse de la distribution des sous-types cellulaires par cytométrie associée au profilage transcriptomique peut contribuer à élucider les mécanismes impliqués dans la reconstitution immunitaire et dans le développement de la GVH humaine.

Mots-clés : Allogreffe de Cellules Souches Hématopoïétiques; Reconstitution Immunitaire, Maladie du Greffon-contre-l'Hôte; Immunophénotypage; Expression Génique; Système Immunitaire Humain; Signature Immunitaire

Table of contents

Introduction

Foreword

Blood is one of the most highly regenerative tissues. Every day billions of new cells are produced in the human body to replenish the blood system and replace blood cellular components that are lost in normal turnover processes or due to illness or trauma. A variety of mechanisms orchestrate hematopoiesis, the complex process through which blood cells are produced and homeostasis is maintained (Doulatov et al., 2012). Impairment or loss of these homeostatic mechanisms underlies a number of malignant hematologic disorders such as leukemias or lymphomas, but also non-malignant conditions such as immunodeficiencies.

Nowadays these disorders can be treated thanks to the possibility to replace the abnormal or defective lymphohematopoietic system with a normal one in a highly specialized and unique medical procedure called hematopoietic stem cell transplantation (HSCT).

The work presented in this thesis focuses on the study of the mechanisms involved in the reconstitution of the immune system after allogeneic HSCT and in acute graft-versus-host disease (aGVHD) in humans in the HLA-identical setting. In this introduction I will give an overview on HSCT, from its development in the early 1950s, to its wide application today in the clinics, exploring the different aspects of this procedure that has revolutionized the treatment of high-risk and otherwise fatal malignant and non-malignant hematologic diseases, becoming one of the most effective immunotherapies available to date. I will then describe two relevant and closely linked phenomena associated with the alloreactivity that accompanies allogeneic HSCT: the beneficial graft-versus-leukemia effect (GVL), in which alloreactive donor immune competent cells eradicate residual malignant cells in the host, and the adverse effect of graft-versus-host disease (GVHD), in which donor cells attack host tissues causing a life-threatening condition that remains a major source of morbidity and mortality after HSCT, limiting the broader applicability of this procedure.

1 Hematopoietic stem cell transplantation

Over the past 70 years, bone marrow transplantation (BMT), or hematopoietic stem cell transplantation (HSCT), has evolved from a highly experimental form of rescue from high-dose radiation exposure after the development of nuclear weapons during World War II, to an established curative treatment for a variety of life-threatening malignant and non-malignant diseases (Singh and McGuirk, 2016). Nowadays, HSCT represents one of the most unique and highly specialized medical procedures and it can be defined as the transfer of hematopoietic stem cells from a donor into a recipient in order to repopulate and replace the hematopoietic system in total or in part (Ljungman et al., 2010). It represents the standard of care for several diseases, including hematologic malignancies, immunodeficiency states, autoimmune diseases and enzymatic disorders (McDonald-Hyman et al., 2015), with more than 40,000 procedures performed in Europe annually, according to the European Bone Marrow Transplant (EBMT) 2016 activity survey (www.ebmt.org).

1.1 Brief historical overview of HSCT

1.1.1 Early work and first steps of HSCT into the clinic

The concept of hematopoietic stem cells capable of restoring hematopoiesis *in vivo* began to emerge following the recognition that the bone marrow was the most radiosensitive organ in the body and that marrow failure was the cause of death following radiation exposure (Thomas and Blume, 1999). In 1949, Jacobson and colleagues showed that mice could survive the otherwise lethal effects of ionizing radiation by shielding the spleen or the femur with a lead foil (Jacobson et al., 1949). A similar effect was described in 1951 by Lorenz et al. who reported that irradiated mice and guinea pigs could be protected by infusion of spleen or marrow cells (Lorenz et al., 1951). These observations led to the initial belief that the radiation protection phenomenon was mediated by some “humoral” factor in the spleen or in the bone marrow capable of stimulating the recovery of blood-forming tissue (“humoral hypothesis”) (Thomas and Blume, 1999). Subsequently, evidence for a “cellular hypothesis” was presented by Barnes and Loutit (Barnes and Loutit, 1954) and Main and Prehn (Main and Prehn, 1955) and by following studies in the mid-1950s showing that radiation protection was due to transplanted stem cells (Ford et al., 1956; Nowell et al., 1956). These findings, and the idea that the hematopoietic system could be destroyed

using ionizing radiation and subsequently reconstituted using hematopoietic stem cells from a healthy donor, pointed out the potential application of bone marrow grafting for the treatment of patients with life-threatening hematologic disorders. The initial rationale for HSCT came from the observation that most hematologic malignancies were chemo- and radio-sensitive in a dose-dependent manner. The ability to rescue hematopoiesis using stem cell grafts from a donor would allow clinicians to increase the intensity of the cytotoxic anticancer therapy beyond the irreversible bone marrow toxicity range, potentially increasing its efficacy (Little and Storb, 2002). Studies in animal models of bone marrow transplantation led to attempts to translate these discoveries into the clinic. The first allogeneic HSCT was pioneered by E. Donnall Thomas and colleagues in 1957. In this study, 6 patients with acute leukemia were treated with total body irradiation (TBI) and high-dose chemotherapy to eradicate the cancer, and then grafted with allogeneic fetal and adult bone marrow. Only two patients engrafted and all patients died within the first 100 days posttransplant (Thomas et al., 1957). Numerous reports followed these initial transplantation attempts, however all the early transplantation procedures performed in the late 1950s and early 1960s in human patients failed either for disease relapse, graft failure or immunological reactions in the host ("secondary disease" now known as graft-versus-host disease) (Juric et al., 2016; Thomas and Blume, 1999). In 1970, a review of about 200 human bone marrow transplants demonstrated unsuccessful outcomes with no long-term survivors (Bortin, 1970). In retrospect, it appears that these failures were due both to the lack of knowledge of human histocompatibility, probably because these procedures were based on work in inbred mice, which do not require histocompatibility matching, and to insufficient immunosuppression to prevent graft rejection (Thomas, 1999). However, despite disappointing results, these trials showed for the first time that high doses of donor bone marrow, properly prepared before infusion, could be safely administered to human patients, providing clinicians with a baseline for future studies (Little and Storb, 2002). Subsequent experiments, mainly in canine and non-human primate models, led to several important discoveries and renewed the interest to translate these findings into humans. Although murine studies had been critical in elucidating the fundamental principles of transplantation, canine models appeared to be particularly suitable owing to their outbred nature, wide genetic diversity, large litter size and short gestation period (Lupu and Storb, 2007). Based on the major histocompatibility complex (MHC) system in mice, an *in vitro* method to type MHC antigens in dogs, known as dog leukocyte antigen (DLA), was developed and allowed to investigate donor-

recipient combinations that were matched or mismatched for MHC antigens. These studies showed that recipients receiving bone marrow grafts from a DLA-matched donor survived significantly longer compared to their DLA-mismatched counterparts that died of graft rejection or graft-versus-host disease (GVHD). These observations highlighted the importance of MHC typing for successful transplantation and set the basis for HSCT between matched siblings in humans. Moreover, canine transplantation studies showed that mismatches across minor histocompatibility antigens (mHAs) could also induce GVHD and led to the development of posttransplant immunosuppressive protocols using the antimetabolite methotrexate (MTX) to control the graft-versus-host reaction. Taken together, the advances in understanding the MHC system, as well as the refinement of high-dose conditioning regimens and post-grafting immunosuppressive prophylaxis in preclinical models renewed the optimism for the use of HSCT in the clinic (Little and Storb, 2002; Thomas, 1999).

1.1.2 The second phase of clinical transplantation and the beginning of the modern era of human HSCT

Increased knowledge of the human MHC system led to the development of methods to identify and type human leukocyte antigens (HLA) allowing for donor-recipient HLA matching. By the 1970s, human clinical trials were carried out in patients with immunodeficiency diseases, such as severe combined immunodeficiency (SCID), aplastic anemia and advanced refractory hematologic malignancies using grafts from HLA-matched sibling donors. Advances were also made in the supportive care of transplanted patients, including transfusion of blood products, therapies to prevent opportunistic infections and improvements in GVHD prevention using methotrexate and T cell activation inhibitors such as cyclosporine (Little and Storb, 2002; Singh and McGuirk, 2016). In 1975 and 1977 E. Donnall Thomas and the Seattle Marrow Transplant team reviewed the outcome of 100 patients with end-stage leukemia/lymphoma and aplastic anemia treated with HSCT after conventional treatment had failed. These reports demonstrated that, despite high transplant-related mortality (TRM), long-term disease-free survival was achieved, showing for the first time that a small percentage of patients could be cured from otherwise lethal diseases. Moreover, these studies established that patients transplanted earlier in the course of the disease, when they were in good general condition, had better outcome than those with advanced disease, concluding that HSCT should be undertaken earlier in the management of patients with leukemia for which an HLA-identical sibling donor is available (Thomas et al., 1975, 1977).

In the 1980s and 1990s the field of transplantation witnessed important progress, and the use of HSCT to treat a variety of diseases increased as HLA typing technologies were refined, alternative graft donors and sources were found and conditioning regimens, GVHD prophylaxis protocols and measures to prevent death from opportunistic infections were implemented (**Figure 1**) (Appelbaum, 2007).

Figure 1 Timeline showing the number of bone marrow transplants performed and the milestones in the field of HSCT between 1957 and 2005
From 1980 the number of HSCT performed began to increase in parallel with advances in the field. BMT=bone marrow transplantation; HLA=human leukocyte antigen. Data are from the Centre for International Blood and Marrow Transplant Research. From Appelbaum, 2007.

Over the last two decades the field has continued to rapidly advance, broadening the range of indications for which HSCT is applied and improving the overall success of the procedure. The establishment of donor registries, with more than 30 million typed volunteers (as of September 2018, www.wmda.org) greatly enhanced a patient's chance of finding an haploidentical match outside their family. However, significant challenges remain as HSCT continues to be associated with significant mortality and morbidity in the clinic with relapse of primary disease, GVHD and infections representing the main hurdles to be addressed (D'Souza and Fretham, 2017).

1.2 Autologous and allogeneic HSCT

HSCT can be categorized into two types: (i) autologous, in which patients receive their own stem cell grafts following high-dose chemotherapy, and (ii) allogeneic, in which stem cell grafts from healthy donors are infused into the recipients following a conditioning regimen, in order to establish donor-derived hematopoiesis and immunity (Singh and McGuirk, 2016) (**Figure 2**, from Khwaja et al., 2016).

Figure 2 Autologous and allogeneic HSCT
In autologous HSCT stem cells from the patient are harvested and frozen and subsequently re-infused after high-dose cytotoxic therapy to enable hematopoietic recovery. In allogeneic HSCT, bone marrow or peripheral blood stem cells from a suitable donor are infused into a recipient, who received prior conditioning with cytotoxic and immunosuppressive therapy to allow engraftment and prevent graft rejection. From Khwaja et al, 2016.

1.2.1 Autologous HSCT

In autologous stem cell transplants, stem cells are harvested from the patient and cryopreserved. The patient then undergoes a myeloablative treatment to eradicate the underlying malignancy or to destroy the hematopoietic system in order to create a niche for the new hematopoietic stem cells (HSCs) to engraft. Collected stem cells are subsequently reinfused into the patient to recover hematopoiesis (Copelan, 2006), as shown in the lower part of **Figure 2**. As graft type for autologous HSCT, peripheral blood mobilized stem cells (PBSCs) are the preferred choice because of a faster hematopoietic reconstitution. Stem cell mobilization is achieved either with granulocyte colony-stimulating factor (G-CSF)-based regimens or with the use of inhibitors of the interaction between CX chemokine receptor 4 (CXCR4) and stromal derived factor-1 (SDF-1), such as plerixafor (Sureda et al., 2015). Autologous HSCT accounts for about 60% of all the transplants performed in the clinic today (EBMT 2016 transplant activity survey, www.ebmt.org) and is mainly used in case of direct correlation between chemotherapy dose and tumour response, with myelosuppression being the dose-limiting treatment toxicity (Hatzimichael and Tuthill, 2010). The most common indications for an autologous transplant are multiple myeloma, non-Hodgkin's lymphoma and Hodgkin's lymphoma. Less common indications include refractory/relapsing autoimmune diseases (multiple sclerosis, systemic sclerosis and Crohn's disease) and solid tumours (sarcoma, germinal tumours and neuroblastoma) (Henig and Zuckerman, 2014; McLornan, 2013). As the patient is at the same time the donor and the recipient of the stem cell graft, the main advantage of this form of transplant is the absence of any alloreactivity against the recipient. Therefore, it does not induce GVHD and posttransplant immunosuppression is not necessary. However, this lack of alloreactivity can also represent a disadvantage, as the beneficial graft-versus-tumour effect (GVT) is missing, reducing the effectiveness of the procedure. Moreover, contamination of the graft by neoplastic cells can occur and contribute to posttransplant relapse (Copelan, 2006).

1.2.2 Allogeneic HSCT

In allogeneic HSCT, patients are first treated with a conditioning regimen consisting of chemotherapy with or without radiotherapy. This allows the eradication of cancer cells, in case of hematologic malignancies, but also immunosuppression of the host to prevent graft rejection, and reduces the number of recipient hematopoietic stem cells creating "space" for the infused stem cells from the donor to engraft. Following the conditioning regimen, patients receive donor bone

marrow grafts, or now more commonly, peripheral blood mobilized stem cells (PBSCs) from donors that have been treated with G-CSF (**Figure 2,** upper panel). In the allogeneic setting, the anti-tumour efficacy is enhanced by alloreactive donor cells in the graft that elicit a potent GVT effect. Unfortunately, the same kind of alloreaction can also be induced against host normal tissues causing graft-versus-host disease. Therefore, administration of immunosuppressive therapy as GVHD prophylaxis is necessary following allogeneic HSCT (Shlomchik, 2007).

To date, allogeneic HSCT accounts for about 40% of the transplant procedures performed (EBMT 2016 transplant activity survey, www.ebmt.org), with the main indications being acute myeloid and lymphoid leukemia, myelodysplastic syndrome, myeloproliferative neoplasm and bone marrow failures. Other less common indications include lymphoma, myeloma, and hematologic disorders such as aplastic anemia and thalassemia (Henig and Zuckerman, 2014). The selection of the type of transplantation, autologous or allogeneic, depends on many factors such as the type of malignancy and its susceptibility to the graft-versus-tumour effect, the age of the patient, the availability of a suitable donor, the ability to collect a tumour-free autograft and the stage and status of the underlying disease (Champlin, 2003). The work presented in this thesis concerns allogeneic HSCT only.

1.3 Histocompatibility and allogeneic HSCT

Allogeneic HSCT became feasible in the early 1960s after the identification and typing of HLA, the human version of the major histocompatibility complex (MHC). In 1958, Van Rood and colleagues observed that during pregnancy about one-third of women made antibodies against HLA, paving the way for the unravelling of the genetics of the HLA system (Van Rood and Van Leeuwen, 1963; Van Rood et al., 1958). Subsequent studies elucidated the role of these antigens in HSCT, leading to a better understanding of the importance of HLA typing, and thus improving donor selection strategies. In particular, proof of the importance of leucocyte antigens in HSCT came from studies in canine models, demonstrating a clear link between DLA-matching and transplant outcome (Thomas, 1999). Since its discovery 60 years ago, several studies investigated the functional implications of HLA genetic diversity, and the development of molecular tools for typing allelic variants of HLA genes contributed to the extensive information on the role of HLA genes in transplantation available to date (Petersdorf, 2013).

1.3.1 The major histocompatibility complex

The major histocompatibility complex (MHC) is a group of cell surface proteins involved in binding and presentation of processed antigens to T lymphocytes, therefore playing an essential role in the initiation of adaptive immune responses. The human major histocompatibility complex comprises about 3 megabases (Mb) located on the short arm of chromosome 6 (6p21). The HLA region is characterized not only by a very high gene density (more than 200 genes), but also by extensive sequence variation (Erlich et al., 2001). The human MHC is divided in three regions: class I, class II and class III. Class I and II regions encode HLA molecules, whereas the class III region contains, among others, genes for complement components and tumour necrosis factors (TNFs). The classical HLA class I genes *HLA-A*, *-B* and *-C* encode the heavy chain of class I molecules. HLA class I molecules consist of an HLA-encoded glycoprotein chain associated with β2-microglobulin and are expressed by most nucleated cells. These molecules bind and present peptides derived primarily from endogenous proteins to $CD8^+$ T cells allowing cytotoxic $CD8^+$ T lymphocytes to identify and eliminate virally infected or cancer cells. The class II region comprehends the subregions HLA-DR, -DP and -DQ, each containing A and B genes coding for α and β chains of the class II molecules, respectively. HLA class II molecules consist of HLA-encoded α and β glycoprotein chains associated as heterodimers. Compared to HLA class I, HLA class II molecules have a more restricted distribution, and are normally expressed only on antigen presenting cells (APCs) such as dendritic cells, macrophages and B cells, activated T cells, and epithelial cells following inflammatory signals. MHC class II molecules bind processed peptides derived predominantly from extracellular proteins and from self-proteins degraded in the endosomal pathway and present them to $CD4^+$ T cells (Klein and Sato, 2000; Rock et al., 2016). The outstanding feature of MHC class I and class II molecules is their extreme polymorphism (more than 10,000 different alleles of MHC class I and more than 3,000 alleles of MHC class II molecules have been identified). The highly polymorphic nature of the MHC has functional consequences, enabling the presentation of many different peptides and thus conferring an advantage for the survival of the population. On the other hand, however, the disadvantage that accompanies MHC allelic diversity is transplant rejection (Rock et al., 2016). Early studies on T cell responses to allogeneic MHC molecules by the means of mixed lymphocyte reactions showed that about 1-10% of T cells in an individual will respond to stimulation by cells from an unrelated

donor. This type of immune response, called alloreactivity, represents the recognition of allelic variants in allogeneic MHC molecules (Janeway CA et al., 2001).

1.3.2 Minor histocompatibility antigens

The outcome of allogeneic HSCT is influenced by genetic disparity between the donor and the recipient at loci both inside and outside the MHC on chromosome 6. Peptides derived from proteins encoded by polymorphic genes outside the MHC that differ between the donor and the recipient and that are presented by MHC molecules are functionally defined as minor histocompatibility antigens (mHAs) (Warren et al., 2012). Negative selection of miHA-specific T cells in the donor thymus is absent due to lack of expression, thus T cell receptors with high affinity to recipient miHAs are present in low frequency within the donor T cell repertoire (Szyska and Na, 2016). Although the most potent transplantation antigens are HLAs encoded by genes located in the MHC, genetic disparity at loci outside the MHC that encode mHAs can elicit alloimmune responses in HSCT recipients receiving stem cell grafts from HLA-identical sibling donors. Genetic disparity of mHAs between donors and recipients can occur through a variety of mechanisms related to DNA sequence and structural variation. The most common mechanisms through which mHAs can be generated are represented by single nucleotide polymorphisms (SNPs) and deletions leading to differences in the amino acid sequence of homologous proteins between donor and recipient cells (Mullally and Ritz, 2007). Once these peptides derived from host polymorphic proteins are complexed to MHC class I and class II molecules, mHA-specific donor T cells may be able to recognize these differences, triggering an alloimmune response (Spierings, 2014). In human, mHAs are mostly restricted by HLA class I molecules (Gam et al., 2017). Unlike MHC antigens, that are encoded by a limited set of genes on chromosome 6, mHAs derive from genetic polymorphisms across the entire genome, thus matched unrelated donors are expected to harbour larger differences in minor histocompatibility antigens than HLA-matched siblings (Roy and Perreault, 2017).

In addition to autosomally encoded mHAs, several mHAs are encoded by genes on the Y chromosome, which display significant level of genetic variation with their X-chromosome homologues. The male-specific minor histocompatibility antigens encoded by these Y-chromosome genes are known as HY antigens and are the strongest mHAs. As a consequence, in the setting of sex-mismatched transplants in which male patients receive stem cell grafts from

female donors, male-specific (HY) antigens can be recognized as foreign and mediate alloreactivity (Roopenian et al., 2002).

Clinically, mHAs mismatches have been associated with an increased risk of developing GVHD and an improved GVL effect. The role of these mHAs in the alloresponse mediating GVHD and/or GVL is related to their differential cell and tissue expression and their immunogenicity. Most minor histocompatibility antigens identified to date are broadly expressed (e.g. HA-3, HA-8), likely contributing to both GVHD and GVL. However, mHAs selectively expressed by hematopoietic cells have been identified, such as HA-1, HA-2, LRH-1 and ACC-1, and might be able to enhance GVL responses without mediating GVHD. Such hematopoietic-restricted mHAs, as well as mHAs expressed by recipient tumour cells, represent an attractive target in immunotherapy trials to augment GVL and prevent relapse (Koyama and Hill, 2016; Roopenian et al., 2002; Spierings, 2014).

1.3.3 Mechanisms of alloreactivity

The immunological mechanisms involved in the recognition and rejection of foreign cells between genetically disparate individuals of the same species are collectively known as allorecognition (Zakrzewski et al., 2014). Following HSCT, recipient allogeneic cells can interact with and activate donor immune cells, including T lymphocytes, B lymphocytes and natural killer (NK) cells. T cells involved in allorecognition can be sensitized against alloantigens via three non-mutually exclusive mechanisms: the direct, indirect, and the semidirect pathways that differ in the origin of APCs, kinetics and contribution to the alloresponse (Afzali et al., 2008). In direct allorecognition, T cells are directly activated by allogeneic APCs or any cell expressing allogeneic MHC molecules (Zakrzewski et al., 2014). In the context of HSCT, direct allorecognition is initiated by residual host APCs which present allogeneic MHC-peptides complexes to donor T cells resulting in an alloresponse against the recipient. In transplant settings where MHC mismatches are present, donor T cells react to recipient APCs at a very high frequency (1% to 10%) (Koyama and Hill, 2016). Moreover, immunoglobulin (Ig) G HLA alloantibodies can directly recognize intact allogeneic HLA molecules that are present on the cell surface. Humoral responses directed against allogeneic HLA can occur upon exposure to HLA alloantigens during pregnancy, blood transfusions or previous transplantations (Geneugelijk et al., 2014).

In the indirect pathway, allogeneic proteins must be processed by autologous APCs and then the peptides derived from these allogeneic antigens are presented by autologous MHC II on

autologous APCs to T cells. Thus, indirect recognition results in alloresponses that are dominated by $CD4^+$ T cells. In HSCT, donor T cells recognize allogeneic recipient-derived peptides presented by MHC class II molecules expressed on donor APCs (Afzali et al., 2008; Koyama and Hill, 2016). Indirect T cell recognition is also involved in the formation of alloantibodies, since T cells can recognize HLA epitopes presented by B cells (Geneugelijk et al., 2014).

Finally, in semidirect allorecognition, allogeneic MHC class I and class II molecules are acquired and MHC-peptide complexes displayed by autologous APCs (Zakrzewski et al., 2014). This mechanism is based on the capacity of immune cells to exchange surface molecules. In particular, APCs are able to acquire intact MHC-peptide complexes from other APCs and endothelial cells and to present them to alloreactive T cells (Afzali et al., 2008). In HSCT, donor APCs can acquire recipient allogeneic MHC-peptide complexes through MHC transfer (and stimulate $CD8^+$ T cells via the direct pathway) as well present allogeneic histocompatibility antigens from phagocytosed material which is processed and presented by MHC class II to $CD4^+$ T cells via the indirect pathway (Afzali et al., 2008).

In contrast to alloreactivity mediated by T cells, the role of MHC molecules in NK cell allorecognition is different. These cells express a repertoire of activating and inhibitory receptors that regulate their function (Vivier et al., 2008). The principal inhibitory receptors regulating NK cell function recognize HLA class I molecules and include inhibitory killer-cell immunoglobulin-like receptors (KIRs), CD94/NKG2A, and LILRB1. Since HLA class I molecules are ubiquitously expressed on the majority of healthy cells, interactions between autologous HLA class I and inhibitory KIRs prevent NK cells from killing healthy autologous cells and therefore ensure self-tolerance (Locatelli et al., 2018). The absence of self MHC class I molecules triggers NK cell activation, whereas expression of self MHC I, engaging inhibitory receptors on NK cells, protects cells from NK cell-mediated killing. Thus, recipient allogeneic cells not expressing self MHC class I molecules are potential targets of donor NK cells (Zakrzewski et al., 2014).

Allorecognition through any of these pathways, especially in a proinflammatory environment such as the one following HSCT, leads to the activation of alloreactive T cells. Some of these cells will have effector functions and possibly mediate graft-versus-host reactions, while others with regulatory function will attempt to establish tolerance. The nature of activated cells, their interactions with other cells and the environment of the host after transplantation will determine the clinical outcome (Afzali et al., 2008).

The role of the different immune cell subsets in mediating the alloimmune responses leading to graft-versus-host disease and graft-versus-leukemia effect will be discussed in more detail in the following sections.

1.4 Donor types and donor selection

Because of its fundamental role in determining transplantation outcome, HLA compatibility has become the cornerstone of donor selection and most allogeneic transplants have been performed between HLA-matched individuals (Geneugelijk et al., 2014). HLA matching significantly reduces the risk of graft rejection and graft failure after solid organ transplantation, and the risk of not achieving a sustained engraftment and GVHD after HSCT. Improvements in HSCT would not have been possible without the significant advances in the understanding of the HLA system and the development of high-resolution (allele level) molecular HLA typing techniques. The HLA genes of greatest relevance to HSCT are the MHC class I genes *HLA-A, -B* and *-C* and the MHC class II genes *HLA-DRB1, -DQB1* and *-DPB1*.

The current state-of-the-art for donor selection is based on donor-recipient matching at HLA-A, -B, -C, -DRB1 and -DQB1 alleles if possible (Petersdorf, 2017a). The ideal donor for allogeneic HSCT is represented by an HLA-matched sibling of the patient who is identical in both alleles of each of the HLA-A, -B, -C, -DRB1 and -DQB1 loci. This donor is referred to as the "10/10 allele match" or "perfect match" (Nowak, 2008). Moreover, as mentioned above, genotypically identical related donors are also more likely to be compatible with regard to minor histocompatibility antigens. Given that all genes encoding HLA antigens located on chromosome 6 are tightly linked and tend to be inherited as haplotypes with low recombination frequencies, siblings have a 25% chance of being HLA-identical. An HLA-matched sibling donor is found in approximately 10-50% of patients requiring an allogeneic HSCT depending on patient age and race/ethnicity (Juric et al., 2016). In France, HSCTs from HLA-identical sibling donors represent about one third of the procedures performed (Lafarge, 2017). Other family members (parents and siblings) usually share one haplotype, and haploidentical donors are defined as family members in which only one haplotype is genetically identical with the patient (Sureda et al., 2015). Historically, due to the high degree of HLA disparity between the donor and the recipient, haploidentical HSCT has been associated with very poor survival. However, improvements in haploidentical HSCT outcome have

been possible thanks to the administration of posttransplant cyclophosphamide to eliminate donor alloreactive T cells (Norkin and Wingard, 2017).

Patients without a suitable family donor have 30-70% chance of finding an HLA-matched unrelated donor through international registries, depending on the frequency of the HLA genotype and the patient's ethnicity (Juric et al., 2016). The gold standard unrelated donor should be matched at HLA-A, -B, -C, -DRB1 (+/- DQB1), although single mismatches are often used in the clinic. A well-matched unrelated donor is defined as 10/10 or 8/8 identical donor based on high resolution typing for HLA-A, -B, -C, -DRB1 and -DQB1. A mismatched unrelated donor refers to a donor mismatched in at least one antigen or allele at HLA-A, -B, -C or -DR (Sureda et al., 2015). Evidence suggests that not all HLA mismatches are equal and that certain alleles may be more "permissive", potentially being less of a barrier to successful transplantation. For example, HLA-DQB1 mismatches seem to be the least risky, except when they occur in combination with other mismatches, while HLA-C antigen mismatches have been shown to be "non permissive" (Petersdorf, 2013). Moreover, polymorphisms outside of HLA may also play a role, further complicating the prediction of transplantation outcome (Passweg et al., 2012).

When patients lack an HLA-identical sibling or a matched unrelated donor, unrelated cord blood units can be used. The introduction of cord blood as a source of stem cells in HSCT has extended the access to this procedure especially to patients of racial and ethnic minorities (Ballen et al., 2013). The current standard for cord blood selection is donor-recipient matching at six loci: HLA-A and HLA-B antigen and HLA-DRB1 allele (Lafarge, 2017). In cord blood transplantation, donor cells are relatively immunologically naïve, which is associated with a higher tolerance for HLA mismatches compared to BM and PBSCs grafts. However, the major limitation of cord blood transplantation is represented by the low cell dose (total nucleated and $CD34^+$ cell dose), especially for adult recipients, and by a slower immune reconstitution that increases the risk of posttransplant complications (Norkin and Wingard, 2017; Petersdorf, 2008). To overcome the cell-dose limitation, double cord blood transplantation has been carried out. Compared to single unit transplantation, results concerning clinical outcome are controversial (Lafarge, 2017).

Nowadays, potential candidates for allogeneic HSCT that lack an HLA-matched donor (HLA-identical sibling or HLA-matched unrelated donor) have different options: mismatched unrelated donor, cord blood or haploidentical transplants. The choice of the donor may vary from centre to centre and if a donor is urgently required, cord blood and haploidentical donors are preferable to

mismatched unrelated donors (Sureda et al., 2015). Similar outcomes have been reported for transplants performed from allelic-matched unrelated donors and HLA-identical sibling donors (Ljungman et al., 2010).

1.5 Hematopoietic stem cell sources for allogeneic HSCT

Currently, three sources of hematopoietic stem cells (HSCs) are commonly used in the clinic for allogeneic HSCT, namely bone marrow (BM), peripheral blood-mobilized stem cells (PBSCs) and cord blood (CB). Historically, BM represented the first and only source of stem cells for HSCT, until the 1990s, when two new options, G-CSF mobilized PBSCs and cord blood became available for clinical use (Welniak et al., 2007).

Bone marrow grafts are harvested by aspiration from the posterior iliac crests under spinal or general anesthesia, filtered to remove particles and clots and subsequently infused into the recipient. HSCs can be mobilized from the BM into the peripheral blood by using G-CSF, which causes the proliferation of neutrophils and the release of proteases. Proteases degrade the proteins that maintain stem cells attached to the marrow stroma, and together with protease-independent mechanisms, lead to their release into the circulation. Mobilized stem cells are then collected by apheresis and transferred into the recipient. To avoid general anesthesia and other common complications of marrow harvesting, PBSCs have become the preferred source for HSCT today, accounting for about 75% of all procedures performed (Copelan, 2006; Juric et al., 2016; Passweg et al., 2012). The third source of HSCs, cord blood, can be safely and easily collected as a by-product of pregnancy. Blood from the umbilical cord and the placenta is rich in HSCs but limited in volume. It is collected immediately after birth and cord blood units are cryopreserved in biobanks and represent a valid option for patients lacking a suitable donor and urgently needing a transplant.

Each stem cell source is associated with specific advantages and disadvantages. All three sources have the ability to reconstitute hematopoiesis in the recipients, but the use of one source rather than another entails differences regarding the time of engraftment, the rate of graft failure, graft-versus-host disease, transplant-related mortality, and relapse risk. Evidence collected in the past years indicates that compared to BM grafts, PBSCs lead to faster hematopoietic engraftment and immune reconstitution, lower relapse rates, and increased risk of chronic but not acute GVHD, while the overall survival is similar. Unmodified PBSCs grafts contain up to one log more T cells

than BM grafts, explaining the increased incidence of chronic GVHD (cGVHD) as well as the lower relapse rate, likely due to an enhanced GVL effect. For patients with non-malignant diseases, such as aplastic anemia, who do not benefit from the GVL effect usually connected with cGVHD, BM is therefore considered as preferred choice (Markiewicz et al., 2013). Compared to BM and PBSCs, CB is associated with slower engraftment, leading to increased risk of posttransplant infectious complications and graft failure. The major limitation of CB is the small number of progenitors that make this option more difficult for adult recipients. However, advantages include rapid availability and, due to immunologic immaturity of transplanted T cells, higher tolerance of HLA-disparity and lower risk of GVHD.

The choice of the stem cell source to be used must therefore take into account several factors such as the underlying disease and the type of conditioning applied, clinical comorbidities, the age of the donor and the recipient, as well as the preferences of different centres and donors (Juric et al., 2016).

1.6 Conditioning regimens

An essential component of the HSCT procedure is the preparative or conditioning regimen that is administered to patients before the infusion of the stem cell graft.

1.6.1 Aims of the conditioning: “create space”, immunosuppression and disease eradication

Following HSCT, donor stem cells must be able to home to the bone marrow to re-establish hematopoiesis in the recipient. To allow adequate engraftment of the incoming donor stem cells, it is necessary to eradicate host stem cells from the bone marrow niches. Without conditioning, most BM niches are occupied and unavailable to accept donor stem cells. A second purpose of the conditioning is the immunosuppression of the host in order to prevent host-versus-graft reactions. The pretransplant preparative regimen, eradicating the host immune system, allows the establishment of donor-derived immunity without the risk of graft rejection. Finally, in case of patients with hematologic malignancies, the conditioning therapy has the aim to eradicate cancer cells reducing the tumour burden. The ability to rescue hematopoiesis thanks to the infusion of donor stem cells, allows the administration of high doses of cytotoxic anticancer drugs, beyond the limit of bone marrow toxicity (Gratwohl, 2008; Vriesendorp, 2003). Due to a deficiency in their own immune system, children with combined severe immune deficiency (SCID) and patients

with severe aplastic anemia with an identical sibling donor may be grafted without prior conditioning therapy (Bacigalupo et al., 2009).

1.6.2 Intensity of the conditioning

A broad spectrum of conditioning regimens exists. They induce different degrees of myeloablation and immunosuppression, depending on the dose and type of chemotherapy and radiotherapy administered. (Gill and Porter, 2013). An accepted classification based on the intensity defines two main types of conditioning: myeloablative (MAC) and non-myeloablative (NMA)/reduced-intensity (RIC) (Bacigalupo et al., 2009). Initial HSCTs were based on myeloablative conditioning regimens relying solely on TBI (1000-1600 rad) to eliminate malignant cells. However, while enabling engraftment, TBI alone proved to be insufficient for long-term control of the underlying disease. Cyclophosphamide (Cy) was introduced later in association with TBI to increase both anti-tumour activity and immune suppression. Radiation-free conditioning regimens were introduced by Santos and colleagues and combined the administration of Cy with busulfan (an alkylating anticancer agent) (Santos, 1989). Today, MAC include a combination of chemo- and radiotherapy at doses that lead to the destruction of hematopoietic stem cells in the host bone marrow causing irreversible pancytopenia and not allowing autologous hematologic recovery (Bacigalupo et al., 2009). These types of maximally intense regimens are associated with acute and long-term toxicities and with significant morbidity and mortality, limiting their applicability in older patients or patients with comorbidities (Gill and Porter, 2013).

A better understanding of the graft-versus-tumour biology led to the development of reduced intensity conditioning regimens with decreased organ toxicity, broadening the access to HSCT to older and less fit patients. In RIC the dose of alkylating agents or TBI is reduced by at least 30%. They provide sufficient immunosuppression to prevent graft rejection, and complete tumour eradication relies on immune-mediated effects of donor cells (Bacigalupo et al., 2009). In general, RIC and NMA conditionings result in varying degrees of mixed chimerism after transplant, with the presence of both donor and recipient cells, subsequently followed by conversion to full donor-derived hematopoiesis and immunity (Gyurkocza and Sandmaier, 2014).

No standard criteria are available for choosing the best conditioning to be administered prior to HSCT and several factors such as patient’s age, diagnosis and disease status, comorbidities, risk

of graft rejection and risk of relapse should be taken into consideration by clinicians as they might affect HSCT outcome (Gyurkocza and Sandmaier, 2014).

1.7 Immune reconstitution after HSCT

The goal of HSCT is to replace the abnormal or deficient lymphohematopoietic system of the recipient with a "normal" one from a healthy donor. The reconstitution of a fully functional, donor-derived immune system in the host is an important component of successful allogeneic HSCT and involves the coordinated regeneration of innate and adaptive immune cell subsets in the recipient (**Figure 3**).

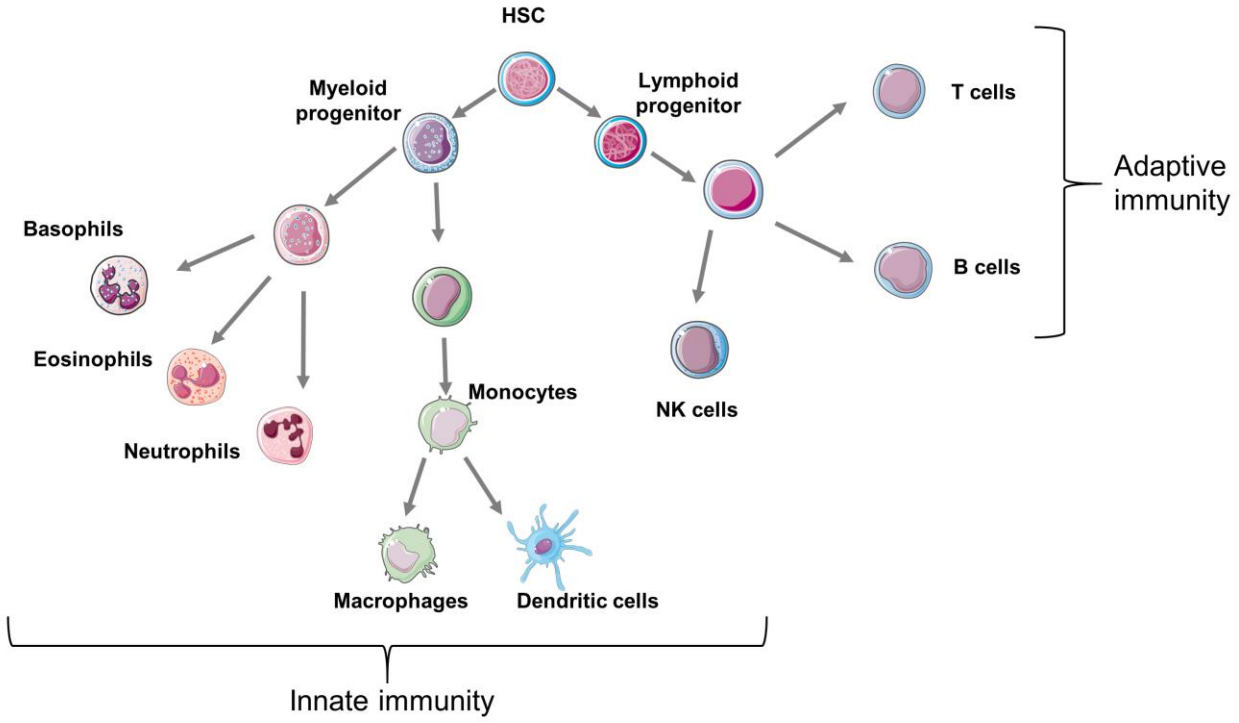

Figure 3 Overview of immune cell differentiation
Following HSCT, the reconstitution of innate immunity occurs rapidly (within 100 days), whereas reconstitution of adaptive immunity is delayed and can require up to 1-2 years after HSCT. Monocytes, granulocytes, dendritic cells and NK cells recover rapidly, while T and B cells, whose development requires specialized microenvironments, is typically delayed. HSC=Hematopoietic stem cell; NK= natural killer. Adapted from Fry and Mackall, 2005.

The reconstitution of the different immune cell subsets after transplantation is a highly dynamic process and it occurs with different kinetics. Innate immunity is rapidly restored, within the first months post-HSCT (<100 days), with recovery of monocytes, granulocytes and NK cells. In contrast, restoration of adaptive cellular and humoral immunity is much slower and recovery of a broad, functional T- and B-lymphocyte repertoire may take years, particularly in adults, in whom lymphocyte output and peripheral turnover are relatively low compared to children (**Figure 4**) (Fry and Mackall, 2005; Mackall et al., 2009; Stern et al., 2018).

Immune reconstitution is influenced by many factors such as the age of the donor and the recipient, the underlying disease, the type of conditioning regimen, the degree of genetic disparity between donor and recipient as well as the type of graft (PBSCs, BM or CB). Moreover, post-transplant events like GVHD, relapse and infection may negatively affect immune recovery (Toubert, 2008) (**Figure 4**).

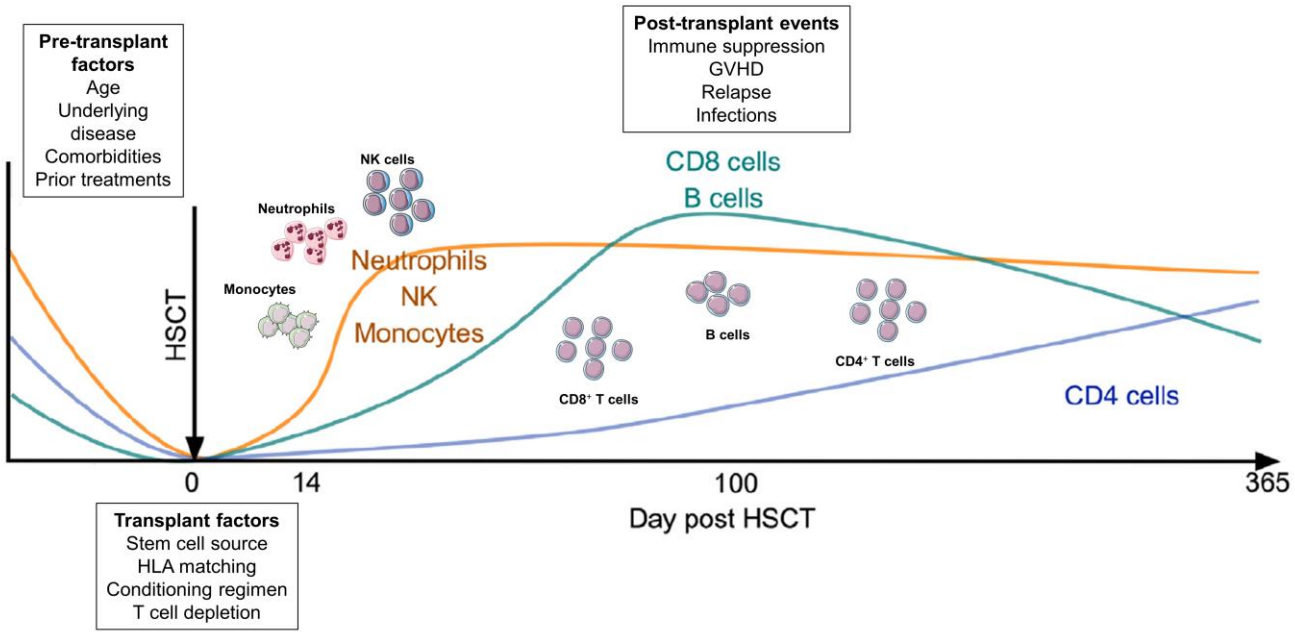

Figure 4 Immune reconstitution following HSCT
After allogeneic HSCT the different immune cell subsets recover with different kinetics under the influence of several factors including patient baseline characteristics, transplant factors and posttransplant events. Adapted from Stern et al, 2018.

Patients undergoing HSCT experience different degrees of immune deficiency according to the intensity of the conditioning regimen they receive. After myeloablative conditioning, immune recovery is determined by both the mature donor cells contained in the graft and the *de novo* production of myeloid and lymphoid cells that arise from engrafted committed progenitors and hematopoietic stem cells (Toubert, 2008). Recipients generally experience a period of profound pancytopenia, spanning days to weeks depending on the source of stem cells used. Immune incompetence together with epithelial and mucosal damage caused by the conditioning regimen make HSCT recipients particularly susceptible to infectious complications in the immediate posttransplant period. Following non-myeloablative transplants the degree and duration of pancytopenia is highly variable depending on the type of conditioning regimen. Although the myelosuppression is milder, recipients undergo an almost total lymphodepletion, thus lymphoid reconstitution occurs through mature lymphocytes and progenitors transplanted with the graft (Mackall et al., 2009).

1.7.1 Reconstitution of innate immunity

1.7.1.1 Phagocytes and antigen presenting cells

Following HSCT, the appearance of monocytes, granulocytes, NK cells and dendritic cells (DCs) in peripheral blood marks the start of cellular recovery. Monocytes are the first cells to recover, rapidly followed by granulocytes and NK cells, and monocytes counts normalize within the first month posttransplant. Host macrophages that resist the conditioning regimen are gradually replaced by donor cells over several months after the transplantation, whereas the first monocytes that appear in the circulation are produced from donor-derived HSCs. Although monocyte recovery is rapid, their function (e.g. cytokine production, antigen presentation) may remain suboptimal for up to one year following HSCT (Baron et al., 2006; Storek et al., 2008).

The kinetic of neutrophil engraftment depends on the type of graft, with a median time of 21 days for BM grafts, 14 days for PBSCs, and 30 days for CB. Early posttransplant neutrophil functions (e.g. chemotaxis, phagocytosis, superoxide production) might be impaired and neutrophils can remain dysfunctional for up to 2 months post-HSCT in the absence of GVHD or infectious complications (Mehta and Rezvani, 2016; Storek et al., 2008).

Dendritic cells (DCs) are APCs that process and present antigen peptides in the context of MHC class I and class II molecules to T cells. They produce different cytokines and express various costimulatory molecules and therefore play a key role in the regulation of the immune

response. Depending on the cytokine repertoire and expression of costimulatory molecules, DCs can polarize T helper cell responses and drive differentiation toward different types of T cell subsets. Circulating DCs are classified into two subtypes: $CD11c^+$ myeloid DCs (mDCs) and $CD123^+$ plasmacytoid DCs (pDCs) (Colonna et al., 2004). Following HSCT, DCs generated from grafted HSCs appear around 2-3 weeks posttransplant, but in the first three months cell counts remain low. Subsequently mDCs tend to normalize, while pDCs remain low for up to one year post-HSCT (Storek et al., 2008). In addition, while peripheral blood DCs are largely donor-derived, up to 70% of DCs in the tissues may remain of host origin up to one year post-HSCT (Williams and Gress, 2008).

1.7.1.2 NK cell reconstitution

Natural killer cells are innate lymphocytes which play an important role in the early immune response against infected and transformed cells both by cell-mediated cytotoxicity and by cytokine production. In humans, NK cells have been traditionally defined by the expression of the surface marker CD56, with or without CD16, and by the lack of the T cell marker CD3. The level of CD56 expression further subdivides human NK cells into two groups, the $CD56^{dim}$ and the $CD56^{bright}$ subsets, characterized by different functional and homing properties (Vivier et al., 2008). In peripheral blood the majority (around 90%) of NK cells are $CD56^{dim}$ $CD16^+$ and possess high cytotoxic potential. In contrast, $CD56^{bright}$ $CD16^-$ NK cells account for about 10% of circulating NK cells, exhibit little cytotoxicity and mainly produce immunoregulatory cytokines (Cooper et al., 2001a). After HSCT, NK cells are the first donor-derived lymphocytes to reconstitute, and full recovery of NK cell counts generally occurs within 1-2 months (Mackall et al., 2009). The rapid recovery of NK cells after HSCT is based on the expansion of the more immature, cytokine-producing $CD56^{bright}$ subset (Dulphy et al., 2008; Pical-Izard et al., 2015). This early expansion of the $CD56^{bright}$ subset gradually declines over time after HSCT, but it may persist for one year and the equilibrium between the two $CD56^{bright}$ and $CD56^{dim}$ NK subsets has been reported to be altered for one year after transplantation (Dulphy et al., 2008). Although NK cell reconstitute rapidly after HSCT, acquisition of immunophenotypic and functional characteristics found in healthy donors can take several months (Ullah et al., 2016). NK cells are believed to be important effectors against viral infections in the early-post transplant period, when adaptive immune responses are not fully recovered yet. Cytomegalovirus (CMV) reactivation is a common complication following HSCT

(Ljungman et al., 2011) and it can drive NK cell maturation (Chiesa et al., 2012) and promote the expansion of $NKG2C^{+}CD57^{+}$ NK cells in HSCT recipients (Foley et al., 2012).

1.7.2 Reconstitution of adaptive immunity

In contrast to innate immunity that recovers within the first months after HSCT, reestablishment of adaptive cellular and humoral immunity is a prolonged process that may take 1-2 years, with some patients showing immune deficits for several years after HSCT (Van Den Brink et al., 2015). Regeneration of the lymphocyte pool after HSCT occurs through two distinct pathways. In the first pathway, lymphocytes are *de novo* generated from donor-derived HSCs and progenitors that home to the recipient's hematopoietic microenvironment and engraft in the bone marrow niches. This pathway recapitulates ontogeny and gives rise to a naïve and clonally diverse lymphocyte pool, similarly to what is found in newborn children. B- and T-lymphopoiesis requires specialized microenvironments, namely the "bursal equivalent" in the bone marrow and the thymic epithelium/stroma, respectively. Moreover, adverse effects of the conditioning regimen, GVHD or its treatment on these specialized structures may negatively influence and further delay the reconstitution of a fully competent adaptive immune system after transplantation. In contrast, in the second pathway, immune reconstitution relies on the proliferation and peripheral expansion of mature cells contained within the allograft (Mackall et al., 2009).

1.7.2.1 Reconstitution of humoral immunity

B cells are primarily generated through the marrow-derived pathway from donor lymphoid progenitors and stem cells, while homeostatic expansion of mature B cells contained in the graft seems to contribute minimally to B cell reconstitution. B cells derived from infused donor B lymphocytes may thus predominate early after transplantation, whereas stem cell-derived B cells probably predominate at later timepoints (Mackall et al., 2009; Storek et al., 2008). Generally, B cell counts are low or undetectable during the first 2 months and recover within 12 months after HSCT (Storek et al., 2008). However, reestablishment of complete humoral competence requires the reconstitution of both naïve and memory B cells and may take up to 2 years (Mackall et al., 2009; Ogonek et al., 2016). The first B cells to emerge into the circulation are $CD19^{+}CD21^{low}CD38^{high}$ transitional B cells that subsequently decline, while mature $CD19^{+}CD21^{high}CD27^{-}$ naïve B cells progressively increase. Complete reconstitution of the B cell pool involves the recovery of both $CD19^{+}CD21^{high}CD27^{-}$ naïve and $CD19^{+}CD27^{+}$ memory B cells. Reconstitution of memory B cells takes place upon environmental or vaccine-based antigen

exposure and requires $CD4^+$ T cell help. Slow $CD4^+$ T cell recovery may therefore contribute to delayed B cell reconstitution and influence antibody production as T cell help is required for isotype switching. Immediately after HSCT, IgG production largely derives from recipient plasma cells that survived the preparative regimen. Naïve B cells predominate during the first 1-2 years after HSCT and produce IgM rather than IgG and IgA. Normal serum IgM levels are generally assessable 3-6 months posttransplant followed by normalization of IgG1/IgG3, IgG2/IgG4, and IgA similarly to what is observed in young children. Both acute and chronic GVHD negatively affect B cell reconstitution. Thus, regeneration of a complete repertoire of donor-derived IgG- and IgA-producing cells is generally delayed for several months posttransplant and is further hindered by GVHD (Fry and Mackall, 2005; Ogonek et al., 2016; Storek et al., 2008).

1.7.2.2 T cell immune reconstitution

T cell recovery after HSCT occurs through two pathways: a thymic-dependent pathway, that recapitulates ontogeny and that accounts for the long-term and clonally diverse reconstitution of the T cell compartment, and a thymic-independent pathway, known as "homeostatic peripheral expansion" (HPE), that involves the proliferation of adoptively transferred donor T cells within the allograft or recipient T cells that survive the conditioning regimen (Chaudhry et al., 2017; Mackall et al., 1997a; Toubert et al., 2012). In the early posttransplant period, initial recovery of the T cell compartment predominantly relies on the expansion of memory T cells, driven by T cell lymphopenia, cytokines and the presence of alloantigens. It is only at later time points that the production of naïve T cells in the thymus starts. The thymus-dependent pathway is a prolonged process involving the migration of early lymphoid progenitors derived from donor HSCs circulating in the periphery and seeding the recipient's thymus (Mackall et al., 2009; Seggewiss and Einsele, 2010). In younger patients, thymic regeneration usually occurs during the first year posttransplant and leads to the normalization of T cell counts. On the contrary, in older adults age-related thymic involution together with cytotoxic effects of the conditioning and GVHD result in prolonged thymic dysfunction. Recovery of total T cell counts is therefore delayed and might remain subnormal for years after HSCT (Fujimaki et al., 2001; Storek et al., 2008; Toubert et al., 2012). While the absolute numbers of $CD8^+$ T cells return to values within the normal range within months post-HSCT, $CD4^+$ T cells do not recover completely, even after as long as 5 years following transplantation (Baron et al., 2006; Fujimaki et al., 2001). Regardless of the stem cell source, $CD8^+$ T cell reconstitution is faster compared to $CD4^+$ T cells. This derives from the fact

that HPE is much more efficient for $CD8^+$ than for $CD4^+$ T cells and leads to an inversion of the CD4/CD8 ratio for several months following HSCT (Mackall et al., 1997b, 2009; Mehta and Rezvani, 2016). Memory T cells are the first to expand following HSCT as they respond faster and are easier to trigger than naïve T cells. Following HSCT, the lymphopenic environment of the host as well as the increased availability of homeostatic cytokines, such as interleukin (IL)7 and IL15, and the presence of alloantigens drive HPE of mature donor T cells transferred with the graft.

IL7 is a non-redundant homeostatic cytokine produced mainly by stromal cells from primary and secondary lymphoid organs (Thiant et al., 2016) and IL7 is required for sustaining naïve T cell expansion and survival. IL15 is produced mainly by monocyte/macrophages and DCs and is upregulated in inflammatory conditions. It enhances the proliferation of memory $CD8^+$ T cells, while both IL7 and IL15 are required for cell survival (Tchao and Turka, 2012). Homeostatic proliferation of memory $CD8^+$ T cells depends mainly on IL15, whereas memory $CD4^+$ T cells undergo homeostatic proliferation in response to both IL7 and IL15 signals (Boyman et al., 2009).

In contrast to thymopoiesis, HPE generates a qualitatively and quantitatively deficient T cell pool. In particular, cells undergo a high rate of apoptosis and the T cell repertoire that is produced during HPE is restricted by the T cell specificities contained in the graft and by the antigens that drive alloreactive T cell proliferation (Fry and Mackall, 2005). Regeneration of fully competent immune responses requires the reconstitution of a broad naïve T cell repertoire and necessitate a functional thymus to recapitulate ontogeny. In addition to generation of a broad T cell receptor (TCR) repertoire, the thymic-dependent pathway has the benefit of producing donor-derived T cells that are tolerant of both the graft and the recipient as these cells undergo positive and negative selection processes in the recipient's thymus (Welniak et al., 2007). Assessment of the reconstitution of naïve and memory cells after HSCT includes the analysis of surface markers such as CD45R0, CD45RA, CD27, CD28, CD62L, and CCR7 that are differentially expressed by naïve and memory T cell subsets. Moreover, T cell diversity and thymic function can be evaluated. T cell diversity is determined mainly by naïve T cells, thus after HSCT evaluation of the T cell repertoire diversity reflects the extent of the naïve T cell pool. Thymic output can be assessed measuring T cell receptor rearrangement excision DNA circles (TRECs) that are used as a marker for naïve T cell recovery occurring in the thymus (Seggewiss and Einsele, 2010; Toubert et al., 2012).

Establishment of a well-balanced immune system after HSCT is pivotal to maintain appropriate levels of peripheral tolerance and requires robust reconstitution of regulatory T cells (Tregs) as well as conventional T cells. Tregs are a subset of $CD4^+$ T cells characterized by the expression of the transcription factor Forkhead box P3 (Foxp3), whose function is to suppress immune responses and maintain tolerance (Josefowicz et al., 2012). In particular, in the context of HSCT, Tregs have been shown to play an important role in the establishment of tolerance between donor-derived immunity and host tissues (Matsuoka, 2018). During the first year after HSCT, Treg reconstitution has been reported to occur primarily through active proliferation rather than through thymic generation of naive Tregs. Moreover, this subset was shown to maintain a significantly higher level of proliferation compared with conventional $CD4^+$ T cells, but displayed increased susceptibility to apoptosis. In this study Treg proliferation was shown to be driven mainly by $CD4^+$ T lymphopenia, suggesting that Treg homeostasis might be modulated by the level of conventional T cell recovery. IL7 and IL15 levels were not found to be associated with Treg recovery following HSCT (Matsuoka et al., 2010). As for conventional $CD4^+$ T cells, Treg reconstitution after HSCT is delayed and Tregs counts remain below the normal range for up to 2 years after HSCT (Alho et al., 2016; Xhaard et al., 2014). The altered cytokine environment of the posttransplant period, rich in IL7 and IL15 and relatively deficient in IL2 could hinder Treg reconstitution, since IL2 is the essential cytokine regulating Treg homeostasis. Treatment with low doses of IL2 was shown to induce Treg expansion and has been investigated as potential therapy to restore immune balance after HSCT (Matsuoka, 2018).

Delayed immune reconstitution after allogeneic HSCT has been associated with significant morbidity and mortality including opportunistic infections and relapse of the underlying disease. Reconstitution of a fully functional lymphocyte pool is essential to control infections and to avoid the reappearance of leukemic cells after HSCT. In particular, T cell immunity is affected by many factors such as recipient's and donor's age, degree of HLA mismatch between donor and recipient, type of graft, intensity of the conditioning, type of GVHD prophylaxis as well as occurrence of GVHD (Van Den Brink et al., 2015; Toubert et al., 2012). Strategies to enhance immune reconstitution have been investigated in preclinical models as well as in clinical trials and include infusion of pathogen-specific T cells, transplantation of expanded lymphoid progenitors, transfer of suicide-gene-transduced donor T cells, sex steroid ablation, or the use of biological agents such

as IL7, IL2, keratinocyte growth factor (KGF) and growth hormone (GH) (Van Den Brink et al., 2004, 2015; Li and Sykes, 2012; Toubert et al., 2012).

1.8 Complications and risk factors for outcome following HSCT

1.8.1 Main complications following HSCT

Despite improvements in donor selection thanks to advances in HLA typing, prophylaxis against viral, fungal and bacterial infections, immunosuppressive drugs to prevent GVHD, development of reduced intensity conditioning regimens and a better supportive care, HSCT is associated with significant morbidity and mortality. Relapse of primary disease, GVHD, opportunistic infections, and conditioning-related toxicities remain the main complications limiting the efficacy of allogeneic HSCT (Henig and Zuckerman, 2014; Reis et al., 2016). Broadly, HSCT-related complications can be classified as infections, early non-infectious complications (within 3 months post-HSCT), late non-infectious complications (more than 3 months post-HSCT), and GVHD (Hatzimichael and Tuthill, 2010).

Chemo- and radiotherapy used in HSCT as conditioning regimen cause significant drug toxicities that vary according to the dose and agents administered. Conditioning-related toxicities usually include nausea, vomiting and mild skin erythema. Mucositis is the most common early complication of myeloablative preparative regimens and methotrexate (used as GVHD prophylaxis) and can involve the oral cavity and gastrointestinal tract. Another acute adverse effect of the conditioning is sinusoidal obstruction syndrome, in which damaged sinusoidal endothelium obstructs the hepatic circulation leading to hepatocyte injury (Appelbaum, 2003; Copelan, 2006).

Transplantation-related infections result from epithelial and mucosal damage caused by the conditioning regimen as well as from neutropenia and immunodeficiency that occur in the posttransplant period. Reduced-intensity preparative regimens are associated with lower rates of early infections compared to myeloablative regimens, however the long-term infectious risk seems to be comparable (Copelan, 2006). In the early posttransplant period (pre-engraftment phase), the most frequent causes of infection are bacteria deriving from the skin and gastrointestinal flora. Fungal infections with *Aspergillus* and *Candida* species are also common early after transplantation. During the post-engraftment phase, after the resolution of pancytopenia, CMV and other herpes virus infections represent a frequent problem. The risk of CMV infection/reactivation is higher for recipients that are CMV positive before the transplant and can be reduced by matching

donor and recipients according to the CMV serostatus (Hatzimichael and Tuthill, 2010; Kedia et al., 2013; Markiewicz et al., 2013).

Acute and chronic GVHD are major complications of allogeneic HSCT despite the use of prophylactic immunosuppressive regimens. The overall incidence of acute GVHD is around 40%, but varies from 10 to 80% according to transplant and patient's characteristics. Chronic GVHD occurs in around 50% of HLA-matched sibling HSCT and is the main cause of late morbidity and non-relapse mortality (Hill et al., 2018). The pathophysiology of acute GVHD will be described in more detail in the following section.

Relapse of the primary disease represents the main cause of treatment failure in the first 2-4 years after transplantation. The risk of relapse depends on the type of underlying disease and its stage at the time of transplantation as well as the GVHD prophylaxis administered, as profound immunosuppression, lowering the efficacy of the GVL effect, is associated with a higher risk of relapse. Moreover, patients with mild acute or limited chronic GVHD, report the longest survival time associated with lower relapse rates. Other long-term side effects after allogeneic HSCT include organ and tissue dysfunction, infections associated with impaired immune reconstitution and occurrence of secondary malignancies (Majhail, 2017).

1.8.2 Risk factors for outcome

The success of HSCT is influenced by many parameters related both to the patient and to the transplant procedure. Gratwohl and colleagues initially reported that the main factors affecting HSCT outcome were the stage of the underlying disease, the age of the patient, the delay between the diagnosis and the transplant and, for allogenic HSCT, the degree of genetic disparity between donor and recipient and the donor-recipient gender combination (EBMT risk score). Older patient age, advanced disease stage, increasing time between diagnosis and transplant, increase in HLA disparity and female donors for male recipients are associated with increased transplant-related mortality and decreased survival rates (Gratwohl et al., 1998). Among the several donor and recipient factors that predict outcome in HSCT the most important patient-associated parameters have been reported to be disease type and stage, age, comorbidities and CMV status, while donor-related factors mainly affecting HSCT success are the degree of HLA disparity, the gender, the age, and the KIR genotype (Anasetti, 2008). In order to integrate all parameters into the risk assessment for patients undergoing HSCT, HSCT-specific comorbidity indexes have been

developed and nowadays the evaluation of the transplantation-associated risk for every patient represent an important factor in the decision making for transplant (Sureda et al., 2015).

2 Alloresponses after HSCT: graft-versus-leukemia effect and graft-versus-host disease

Allogeneic HSCT is associated with reciprocal immune reactions between the donor and the recipient, related to histocompatibility, that have both deleterious and beneficial consequences. While alloimmune rejection is uniformly detrimental in solid organ transplantation, a delicate balance between immune complications and benefits deriving from alloreactivity exists following allogeneic HSCT. Allogeneic HSCT is a potent immunotherapy with curative potential for several hematologic disorders. In case of malignant diseases, the main therapeutic benefit derives both from the ability to treat the patients with intensive chemoradiotherapy to eradicate the cancer, but also from a strong antitumor effect mediated by engrafted donor cells that attack and eliminate residual malignant cells. This immune-mediated reaction, known as graft-versus-leukemia effect (GVL), represents an efficient form of cellular immune therapy for both hematologic malignancies and some solid tumours. Unfortunately, the same kind of alloreaction can also be induced against normal tissues of the host, giving rise to the severe complication graft-versus-host disease (GVHD) (**Figure 5**). Thus, allogeneic HSCT is associated with a reduction of malignant relapse owing to the beneficial GVL effect, but comes with the risk of GVHD. Maximising the GVL reaction while minimizing GVHD remains the main challenge in the field of HSCT (Jenq and van den Brink, 2010).

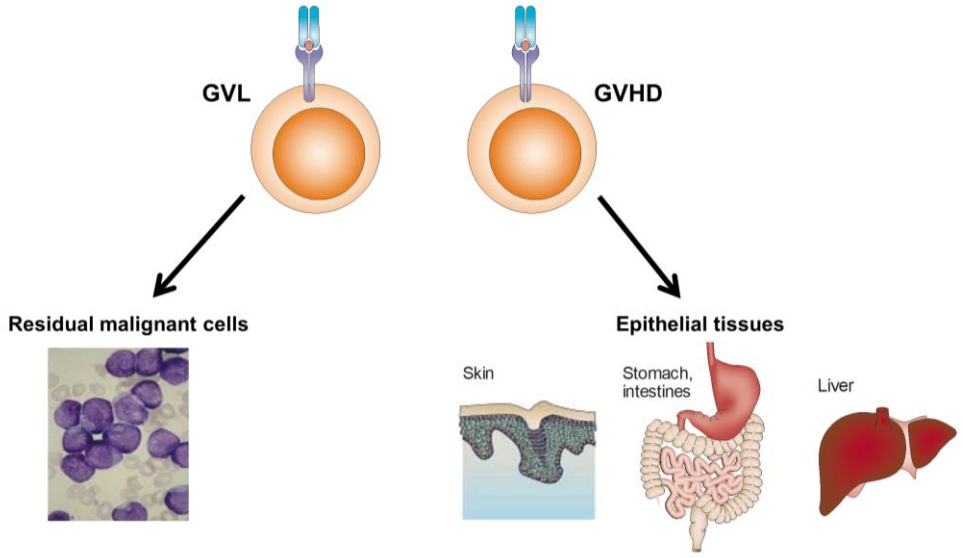

Figure 5 Graft-versus-leukemia effect and graft-versus-host disease following HSCT
Following allogeneic HSCT, alloreactive donor cells can attack and eradicate residual malignant cells mediating the beneficial graft-versus-leukemia effect (GVL). However, the same kind of alloreaction, if directed against host normal tissues, especially the skin the gut and the liver, gives rise to graft-versus-host disease (GVHD). Adapted from Bleakley and Riddell, 2004.

2.1 Graft-versus-leukemia effect

The graft-versus-leukemia (GVL) reaction refers to the ability of donor immune cells to eliminate residual host malignant cells after allogeneic HSCT (Vincent et al., 2011). A GVL effect was first reported by Barnes and colleagues in 1956, who observed that leukemic cells were eradicated in irradiated mice receiving allogeneic, but not syngeneic, bone marrow transplants. The authors suggested that a reaction of the donor bone marrow might kill cancer cells resulting in eradication of the leukemia. (Barnes and Loutit, 1957; Barnes et al., 1956). Following these observations, Mathé coined the term "adoptive immunotherapy" for the treatment of leukemia with allogeneic bone marrow transplantation in human patients. In this study, they also observed a "secondary syndrome", that will be later described as GVHD (Mathé et al., 1965). The relevance of the GVL reaction in humans was established in the late 1970s-early 1980s thanks to studies reporting reduced relapse rates in allogeneic HSCT recipients who developed acute (Weiden et al., 1979) and/or chronic GVHD (Sullivan et al., 1989; Weiden et al., 1981) compared to those without GVHD. Key insights into the mechanisms of the GVL effect were reported in a landmark study from the International Bone Marrow Transplant Registry in 1990 (Horowitz et al., 1990). This study involved 2254 patients receiving HLA-identical sibling bone marrow grafts for acute myeloid leukemia (AML), acute lymphoblastic leukemia (ALL) and chronic myeloid leukemia (CML) and clearly established the antileukemic effect of allogeneic grafts. In fact, recipients of genetically identical twin grafts showed the highest relapse rates. Relapse rates were lowest in patients developing both acute and chronic GVHD, higher in those that did not develop GVHD and highest in recipients of T cell-depleted or syngeneic grafts (**Figure 6**). This study also established a key role for T cells in mediating GVL responses, because recipients of T cell-depleted grafts had only slightly lower relapse rates than patients receiving allografts from identical twins. Moreover, reduction of the relapse risk in allogeneic recipients without GVHD compared to recipients receiving grafts from a twin donor also suggested the presence of a GVL effect that is independent of clinical GVHD (Horowitz et al., 1990).

Figure 6 Probability of relapse after allogenic and syngeneic bone marrow transplantation
Relapse rates following bone marrow transplantation are highest in patients receiving syngeneic or T-cell depleted grafts, lower in recipients of T-cell replete grafts without GVHD (No GVHD) and lowest in recipients of T-cell replete grafts developing both acute and chronic GVHD (AGVHD + CGVHD). Adapted from Horowitz et al, 1990.

The efficacy and potency of the GVL effect in mediating tumour eradication was further supported by the demonstration of complete remission in patients who relapsed post-HSCT through infusion of donor lymphocytes (Kolb et al., 1995; Slavin et al., 1995). Recognition of the power of the GVL effect in eradicating leukemic cells after HSCT, led to the introduction of non-myeloablative conditioning regimens and donor lymphocyte infusions (DLIs) (Bethge et al., 2004; Kolb et al., 1995). Nowadays, DLIs represent an effective post-transplant therapy to provide a GVL effect and DLIs can produce complete remissions in 20% to 80% of patients, but the success rate is highly dependent on the underlying malignancy. DLIs efficacy is limited in rapidly proliferating leukemias, while better outcomes are observed in patients with less rapidly proliferative diseases such as chronic myeloid leukemia (CML). A limitation of DLIs is the occurrence of GVHD, thus improvement of HSCT outcome will require the development of effective strategies for separating GVHD from GVL (Dickinson et al., 2017; Falkenburg and Warren, 2011; Singh and McGuirk, 2016).

2.1.1 Role of T cells and NK cells in the GVL effect

As mentioned above, demonstration of the central role of T cells as mediators of the GVL effect derived from the observation that T cell depletion was associated with an increase of relapse rates (Horowitz et al., 1990). Initially considered to be mainly T cell-mediated, the GVL effect is now recognized to be multifactorial. T and NK cells are the main cell subsets mediating cytotoxicity with adjuvant roles played by dendritic cells and B cells (Singh and McGuirk, 2016).

Induction of GVL reactions requires genetic disparity between donor and recipient and is mediated mainly by donor lymphocytes contained in the graft or derived from engrafted donor stem cells (Warren and Deeg, 2013). T cell alloreactivity involves the recognition of disparities of major and minor histocompatibility antigens by $CD4^+$ and $CD8^+$ T cells. Evidence from studies in several experimental models demonstrated that GVL reactions depend on the recognition of host histocompatibility antigens expressed on leukemic cells (Vincent et al., 2011). In transplants between non-HLA-matched individuals, MHC antigens are themselves target of donor T cells and are responsible for increased GVHD after transplant. If donor and recipient are HLA-identical, mHAs are the primary antigenic targets of donor T cells responsible for alloreactivity. Evidence indicates that T cell responses against both autosomal and Y chromosome-encoded mHAs can contribute to the GVL effect and the extent of the beneficial GVL versus detrimental GVHD responses is dependent on the mHAs expression profile and tissue distribution (Gam et al., 2017; Warren and Deeg, 2013). In addition to mHAs, proteins over- or aberrantly expressed by leukemic cells have emerged as potential targets for GVL reactions. T cell responses against tumour-specific antigens have been observed in HSCT recipients and might contribute to GVL activity (Bleakley and Riddell, 2004; Warren and Deeg, 2013).

In murine models, both $CD4^+$ and $CD8^+$ T cells have been reported to contribute to the GVL reaction and removal of either population diminished GVL efficacy, indicating that an optimal GVL response requires both $CD4^+$ and $CD8^+$ T cell subsets (Truitt and Atasoylu, 1991). After allogeneic HSCT in humans, both $CD4^+$ and $CD8^+$ T cells that recognize mHAs on recipient cells have been identified (Warren et al., 1998). Thus, in recipients receiving T cell replete grafts from HLA-matched donors, donor $CD4^+$ and $CD8^+$ T cells recognizing MHC-peptide complexes on the surface of recipient cells are the main mediators of the GVL reaction (Warren and Deeg, 2013).

Donor T cells recognizing recipient alloantigens are central, but not exclusive mediators of the GVL response, and donor NK cells have been reported to also play important roles in preventing

cancer relapse after HSCT. In particular, studies from the Velardi group showed that allogeneic, alloreactive NK cells promoted engraftment and GVL effect and reduced GVHD in patients with acute myeloid leukemia (AML) treated with T cell–depleted haploidentical HSCT. They showed that HSCT outcomes were significantly better in patients exhibiting KIR ligands mismatched with those from their donors (Ruggeri et al., 2002, 2007). Functional heterogeneity of NK cell populations derives from the differential expression of various activating and inhibitory receptors, which recognize stress-induced antigens and absence of self-MHC class I antigens (Vivier et al., 2008). The genes encoding KIRs and HLA are located on different chromosomes and segregate independently, thus two HLA-matched individuals, even related, may still be KIR-mismatched (Gill et al., 2009). In HLA-mismatched HSCT, the patients lack KIR ligands that are present in the donors and donor NK cells can recognize and attack host cells in virtue of the absence of self MHC class I ("missing self") (Petersdorf, 2017b; Wu and Ritz, 2006). In HLA-matched transplants, patients lacking KIR ligands ("missing ligand") have been shown to have a lower risk of relapse and improved overall survival. Moreover, several clinical studies suggest that expression of specific activating NK cell receptors on donor cells is associated with a decreased risk of AML relapse (Vincent et al., 2011). Several line of evidence demonstrated that KIR ligand mismatches in the graft-versus-host direction are important for the success of haploidentical HSCT (Juric et al., 2016).

Similarly to NK cells, KIR expression on TCR $\gamma\delta^+$ lymphocytes has been reported to regulate their antitumor activity (Dolstra et al., 2001). At the interface between innate and adaptive immunity, γδ T cells are a subset of "non-conventional" T cells displaying several innate-like features that allow their rapid activation during the early phase of an immune response (Bonneville et al., 2010). In humans, γδ T cells represent 1-20% of total circulating $CD3^+$ lymphocytes but are enriched in skin and mucosal tissues (Handgretinger and Schilbach, 2018). Detection of stress-induced molecules is achieved through both TCR and non-TCR molecules, such as Toll-like receptors and natural killer receptors, leading to activation of effector functions related to cytotoxicity and cytokine production (Bonneville et al., 2010). γδ T cells have been described to exert tumoricidal activity against various solid tumours and hematologic malignancies. Given their antitumor abilities and the fact that they are not HLA-restricted for antigen recognition, γδ T cells have been investigated as mediators of GVL reactions in the absence of GVHD (Handgretinger and Schilbach, 2018). In particular, increased frequencies of γδ T cells have been associated with

a better disease-free survival in patients with leukemia undergoing T cell depleted bone marrow transplantation from partially HLA-mismatched donors. However, γδ T cell alloreactivity is not as well characterized as the one of NK cells. It is not clear whether KIR expression defines alloreactive and non-alloreactive γδ T cells and whether the donor KIR genotype plays a role in allogeneic HSCT (Handgretinger and Schilbach, 2018).

2.2 Graft-versus-host disease

An important limitation of allogeneic HSCT for the treatment of hematologic malignancies is that alloreactive T lymphocytes not only contribute to eradicate residual neoplastic cells, but also frequently cause a life-threatening immune complication referred to as graft-versus-host disease (GVHD). GVHD is defined as a complex disease resulting from donor T cell recognition of a genetically disparate recipient that is unable to reject donor cells following allogeneic HSCT (Welniak et al., 2007). The overall incidence of GVHD is around 40%, but varies from 10 to over 80% depending on patient- and transplant-related characteristics. Despite the advances in the field of HSCT and GVHD prophylaxis, acute GVHD remains a major factor contributing to non-relapse morbidity and mortality and it is the second cause of death, after disease relapse, accounting for about 15% of deaths after allogenic HSCT (Nassereddine et al., 2017; Sung and Chao, 2013).

2.2.1 Historical descriptions and definition

The first descriptions of what would be later named GVHD date back to the late 1950s, when Barnes et al., Van Bekkum et al., and Billingham et al. observed that irradiated animals infused with allogenic bone marrow and spleen cells died from a “wasting” or “secondary” syndrome characterized by weight loss, diarrhea, skin changes and liver disturbance (Barnes and Loutit, 1957; Van Bekkum et al., 1959; Billingham and Brent, 1959). Similar observations were reported also in humans (Mathé et al., 1965). In 1966, Billingham formulated the three requirements for the development of GVHD that still hold true today: (i) the graft must contain sufficient numbers of immunologically competent cells, (ii) the recipient must express tissue antigens that are not present in the transplant donor and, (iii) the recipient must be incapable of mounting an effective immune response against the graft (Billingham, 1966). More than 50 years later, it is now known that the immunologically competent cells within the graft mediating GVHD are alloreactive donor T cells

and that the tissue antigens responsible for the graft-versus-host reaction are major and minor histocompatibility antigens mismatched between donor and recipient.

2.2.2 Classification and clinical manifestations

Clinical GVHD has an acute and a chronic form, involving distinct pathological processes and manifestations. Acute GVHD (aGVHD) has strong inflammatory components and is characterized by damage mainly to the skin (81% of patients), the gastrointestinal (GI) tract (54%) and the liver (50%), although other sites such as the lung, the thymus and secondary lymphoid organs may be affected. Skin lesions are usually the first manifestation arising around the time of engraftment and affected patients typically present a maculopapular erythematous rash. Gastrointestinal manifestations include abdominal pain and diarrhea, as well as anorexia, nausea, and vomiting. Hepatic aGVHD can be more difficult to diagnose and distinguish from other forms of liver disfunction after HSCT (such as veno-occlusive disease, toxic drug effects or viral infection). Liver disease is caused by damage to the small bile ducts, leading to cholestasis with hyperbilirubinemia. The hematopoietic system is also commonly affected leading to thymic atrophy and cytopenias. Chronic GVHD (cGVHD) displays more autoimmune and fibrotic features and is characterized by a wider range of manifestations. It can target the skin and mucosa, but it also involves serous membranes and exocrine glands. Clinical features range from edema, erythematous rash, mucositis and diarrhea, to more fibrotic and chronic manifestations such as scleroderma-like skin and fasciitis (Blazar et al., 2012; Ferrara et al., 2009; Shlomchik, 2007; Sung and Chao, 2013).

Historically, acute and chronic GVHD have been classified depending on the time of onset after HSCT using a cut-off of 100 days. Acute GVHD was defined as arising within the first 100 days following allogeneic HSCT, while cGVHD included any clinical manifestation of GVHD that occurred beyond 100 days after HSCT. However, this classification has been challenged by recognition of signs of acute and chronic GVHD outside of these delineated periods and the current consensus is that the clinical symptoms rather than the time of onset should be used to define whether GVHD is considered acute or chronic. A more recent classification recognizes two main categories of GVHD, each with two subcategories. The broad category of acute GVHD includes classic aGVHD and also persistent, recurrent and late-onset aGVHD occurring more than 100 day after HSCT. The broad category of chronic GVHD includes classic cGVHD and an overlap syndrome characterized by clinical manifestations of cGVHD together with features of aGVHD (**Figure 7**) (Pavletic and Fowler, 2012). Late-onset aGVHD and the overlap syndrome have been

reported to occur more frequently in HSCT recipients after reduced intensity conditioning regimen (Ferrara et al., 2009).

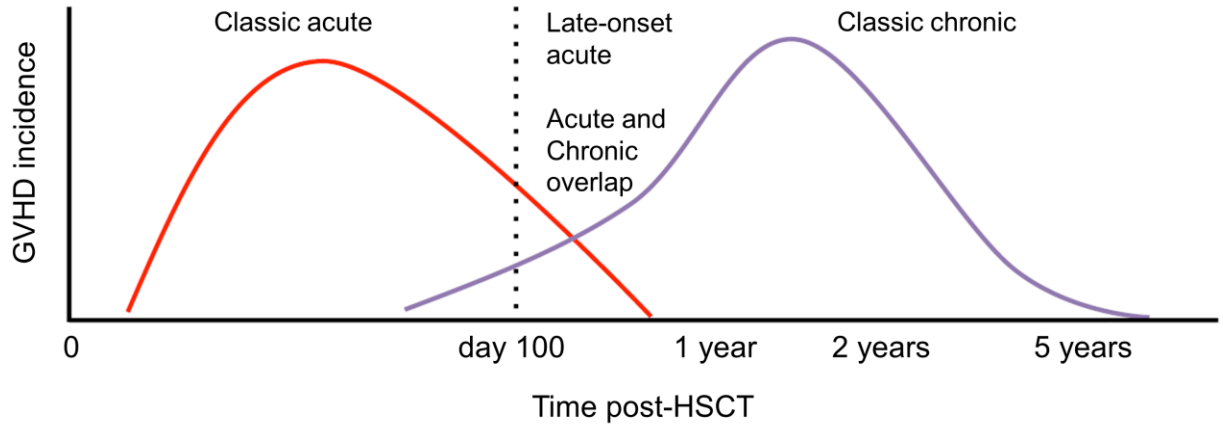

Figure 7 GVHD classification
Schematic representation of GVHD onset after HSCT. The current consensus is that clinical manifestations and not the time after transplantation should determine whether the clinical syndrome is considered acute or chronic GVHD. A National Institutes of Health classification includes also late-onset acute GVHD (after day 100) and an overlap syndrome with features of both acute and chronic disorders. Adapted from Pavletic and Fowler, 2012.

Clinically significant aGVHD occurs in approximately 40% of patients undergoing HLA-matched HSCT and in 50-70% of patients receiving grafts from unrelated donors (Jagasia et al., 2012), while cGVHD affects 40-70% of long-term survivors of allogeneic HSCT (Arai et al., 2015). As our study involved only patients with acute GVHD, in the following sections I will describe more in detail the pathophysiology of this clinical form only.

2.2.3 Pathophysiology of acute GVHD

Much of our understanding of the pathophysiology and immunological mechanisms of GVHD derives from studies in mouse models. However, differences between human and murine physiology and immunological functions as well as transplantation procedures and microbiome should be considered when drawing conclusions from studies in animal models and translating these findings to human patients. In particular, the main aspects that differentiate the studies performed in mouse models from the clinical setting in humans are the following:

(i) Conditioning regimen: in mouse models of GVHD irradiation alone is typically used, and only few studies have used chemotherapy for myeloablative conditioning. On the contrary, in human patients chemotherapy is more frequently applied with or without TBI.

(ii) Source of donor cells: following the conditioning regimen, bone marrow grafts are used in murine models to re-establish hematopoiesis and T cells from the spleen or lymph nodes are added to provide a sufficient dose of T cells to induce GVHD. In contrast, in the clinic, PBSCs or BM grafts are typically used as graft and are sufficient to trigger GVHD.

(iii) Immunologic disparity between donor and recipient: murine studies utilize several inbred strain combinations, resulting in a variety of MHC- and miHAs-mismatched models in which $CD4^+$ and $CD8^+$ T effector cells are differently involved in mediating the disease. The situation in humans is much more complex, in particular regarding the genetic differences that lie outside the MHC loci and environmental factors.

(iv) Microbiome: while humans are exposed to a wide range of pathogens throughout life, mice are usually housed under specific pathogen-free conditions since birth leading to differences in innate and adaptive immune responses influenced by the environment.

(v) Age of donors and recipients: murine studies primarily employ young adult mice while in human studies both young and older patients are included. Clinically, the age of the donor and the recipient can influence the development and severity of GVHD (Hülsdünker and Zeiser, 2015; Welniak et al., 2007).

Thus, compared to murine models, patients undergoing HSCT tend to be older, sicker and exposed to a wide range of pathogens. Moreover, they undergo a procedure that is very different from the one applied in animals. These differences need to be critically taken into account when findings in on system are extrapolated into the other (Hülsdünker and Zeiser, 2015; Socie and Blazar, 2009; Welniak et al., 2007). Nonetheless, studies in murine models provided invaluable information regarding the pathophysiologic mechanisms involved in GVHD and are extremely useful for developing and testing new treatment approaches. In addition to studies in mice, canine models have been critical for the development of clinically useful strategies for GVHD prophylaxis and treatment and for the development of donor leukocyte infusions. Canine and non-human primate models represent now robust preclinical models to analyse the efficacy of pharmacological agents before translation to clinical trials (Ferrara et al., 2009; Markey et al., 2014).

The clinical symptoms of acute GVHD reflect an exaggerated inflammatory response leading to damage of target organs. Underlying this clinical presentation is a complex immune-mediated process involving an intricate cascade of humoral and cellular interactions between donor and host cells (Blazar et al., 2012; Magenau et al., 2016). Integrating insights from animal models with

clinical data Ferrara et al. proposed a model summarizing the mechanisms underlying aGVHD pathogenesis as a three-phase process: (i) priming of the immune response leading to antigen presenting cells (APCs) activation, (ii) donor T cell activation, expansion, differentiation and migration, and (iii) cellular and inflammatory effector phase (Ferrara and Reddy, 2006; Reddy and Ferrara, 2003). The three phases involved in the pathophysiology of GVHD and the closely linked GVL effect are depicted in **Figure 8**.

2.2.3.1 Phase 1: priming of the immune response

The initiation phase of aGVHD begins before the infusion of the stem cell graft, with host tissue damage caused by the underlying disease and exacerbated by the conditioning regimen. The cytoreductive conditioning induces tissue damage and the release of proinflammatory cytokines, such as tumour necrosis factor-alpha (TNFα), IL1 and IL6, that promote the activation and maturation of APCs. Epithelial damage to the gastrointestinal tract allows the systemic translocation of lipopolysaccharide (LPS) and other microbial products that further enhance APCs activation. These "danger signals", damage- and pathogen-associated molecular patterns (DAMPs and PAMPs, respectively), activate host tissues, including APCs, contributing to the "cytokine storm", and mediate profound changes to the tissue microenvironment with increased expression of adhesion molecules, costimulatory molecules, MHC antigens and chemokine gradients that promote the infiltration of immune effectors. Overall, these early events set the stage for subsequent T cell priming and expansion. Evidence from both animal and human studies indicates that the intensity of the conditioning and the degree of tissue damage is correlated with the risk of aGVHD. RIC regimens are associated with less morbidity and with a delayed GVHD onset (Choi et al., 2010; Magenau et al., 2016; Socie and Blazar, 2009; Welniak et al., 2007).

2.2.3.2 Phase 2: donor T cell activation, expansion, differentiation and migration

The second phase of aGVHD induction involves the activation and subsequent proliferation and differentiation of donor alloreactive cells in response to activated APCs. Donor T cells can recognize alloantigens on both host and donor APCs that are present in secondary lymphoid organs. APCs are the primary "sensors" of the initial inflammatory signals and are required to present alloantigens to donor T cells via MHC molecules and provide critical co-stimulatory and cytokine signals that influence the type and the quality of the effector response. Several types of APCs are capable of contributing to graft-versus-host reactions. These include residual host hematopoietic APCs that survive the conditioning regimen, host non-hematopoietic APCs as well

as donor APCs transferred within the allograft (Blazar et al., 2012; Holtan et al., 2014). In mouse models in which genetic differences between the donor and the recipient can be tightly controlled, $CD4^+$ T cells induce GVHD to MHC class II differences, while $CD8^+$ T cells induce GVHD to MHC class I differences (Ferrara et al., 2009). In the clinic, the majority of transplants are performed between MHC-matched individuals, related or unrelated. In this setting, mHAs are presented within MHC class I and class II molecules, and both $CD4^+$ and $CD8^+$ T cells are involved in GVHD (Koyama and Hill, 2016). Murine studies in mHAs-mismatched models indicated that host antigens presented in the context of MHC I on host APCs are crucial for CD8-dependent GVHD induction and donor APCs can augment this response by acquiring and presenting host antigens. Both donor and host APCs can present alloantigens in the context of MHC II to donor $CD4^+$ T cells. In a murine MHC-mismatched model, Koyama and colleagues showed that donor $CD4^+$ T cells can also be activated within the target organs by recipient non-hematopoietic APCs that express MHC class II molecules such as myofibroblasts (Koyama et al., 2012). Parenchymal tissue cells can acquire APC function and promote alloreactive donor T cell activation in the GI tract. Thus, in the absence of functional host professional APCs, mHAs can be presented by donor APCs or host non-hematopoietic APCs and lead to T cell activation and GVHD induction. However, in humans it is difficult to evaluate the relative contribution of different APC subsets and assess the impact of these alternative pathways (Blazar et al., 2012; Nassereddine et al., 2017).

Following TCR engagement, T cells must receive a "second signal" mediated by costimulatory molecules on APCs in order to proliferate and acquire effector functions. Several costimulatory pathways have been studied in the context of GVHD induction. These pathways include the positive regulatory pathways such as CD28 and Inducible Co-stimulator (ICOS, CD278), the TNFR superfamily receptors CD40L (CD154), OX40 (CD134), and 4-1BB (CD137), and the negative regulatory pathways anti-cytotoxic T-lymphocyte-associated antigen 4 (CTLA4), programmed death 1 (PD1)-PDL1, and B7-H3 among others (Magenau et al., 2016; Welniak et al., 2007). Blockade of these costimulatory or inhibitory interactions has been shown to reduce or exacerbate GVHD, suggesting possible therapeutic targets (McDonald-Hyman et al., 2015; Zeiser et al., 2016). The "third signal" required for sustained T cell activation and survival is provided by cytokines. Several cytokines have been implicated in GVHD pathogenesis, including IL1, TNFα, IL6, IFNγ and IL2. During the second phase of GVHD induction, the cytokines present in the microenvironment play a key role in driving T cell differentiation and expansion. Type 1 or

Th1/Tc1 differentiation is believed to be central to GVHD induction, however, Th2/Tc2 and Th17/Tc17 subsets are also involved in aGVHD pathology and the balance between the different cell subsets determines GVHD severity and organ specificity (Henden and Hill, 2015). Cytokines are also important for T cell survival, especially the IL2 receptor common γ chain (IL2Rγ, CD132) cytokines IL2, IL7 and IL15. Therapeutic approaches under investigation to prevent or treat GVHD include strategies targeting signals mediated by inflammatory cytokines such as inhibition of IL6 or IL12 and IL23, IL2Rγ blockade, or inhibition of downstream signals via Janus kinase (JAK)1/2 or JAK3 inhibitors (McDonald-Hyman et al., 2015; Zeiser et al., 2016). However, blockade of cytokines or costimulatory signals for GVHD prevention has to be considered with caution, as these approaches could be associated with a loss of the beneficial GVL effect (Zeiser et al., 2016).

Once activated, donor T cells undergo proliferation and differentiation into effector subsets and initiate transcriptional programs that result in the release of proinflammatory mediators that contribute to the "cytokine storm" and amplify the immune response. Following activation within secondary lymphoid organs, alloreactive donor T cells migrate toward GVHD target tissues by means of chemotaxis involving chemokine-receptor, selectin- and integrin-mediated interactions (Wysocki et al., 2005). Activated T cells downregulate L-selectin (SELL, CD62L) and C-C chemokine receptor type 7 (CCR7) to leave lymph nodes and enter into the circulation, and upregulate selectin ligands such as P-selectin ligand 1 (PSGL1) and CD44, enabling them to efficiently roll on inflamed endothelium expressing the counter receptors P- and E-selectin. Although transplantation antigens (mHAs) are broadly expressed in host tissues, GVHD preferentially affects organs such as the skin, the gut and the liver (Ferrara et al., 2009). T cell recruitment into specific organs has been proposed to be regulated by unique combinations of signals present in the tissue microenvironment and corresponding receptors on T cells. Chemokine gradients, together with upregulation of adhesion molecules within GVHD target tissues drive T cell recruitment. Upregulation of chemokines such as C-C motif ligand (CCL)2, CCL3, CCL4, CCL5, CXC ligand (CXCL)9, CXCL10 and CXCL11 in GVHD target organs plays a key role in this homing process. Activated T effector cells upregulate different receptors for inflammatory chemokines that modulate their trafficking and homing to different tissues. Expression of the chemokine receptor CCR9 by alloreactive T cells facilitates recruitment into the gut and skin; CCR4 and CCR10 are important for skin homing and CXCR3 has been shown to recruit Th1 cells

to inflamed tissues (Blazar et al., 2012; Wysocki et al., 2005). CCR5 is upregulated in alloreactive T lymphocytes and directs recruitment to target tissues such as the GI tract. Strategies targeting chemokine receptors and homing molecules are under investigation for GVHD prevention. For example, maraviroc, a CCR5 inhibitor, was shown to reduce the incidence of gut GVHD in patients following HSCT (Moy et al., 2017). In contrast to the hypothesis that T cell homing properties are the main determinants of GVHD target organs involvement, Michonneau et al. showed that cytotoxic T lymphocytes (CTLs) activity within different organs is determined, at least in part, by the distinct expression of PD1 ligands encountered in different tissue microenvironments that regulate T cell sensitivity to antigen. The authors propose that the PD1 pathway contributes to spatially compartmentalize CTL activity during allogeneic HSCT and that organs with high and low CTL activity might be sites for GVHD or tumour escape, respectively (Michonneau et al., 2016).

2.2.3.3 Cellular and inflammatory effector phase

The effector phase of aGVHD involves a complex cascade of cellular and inflammatory mediators that synergize to amplify local tissue injury and further promote inflammation and end-organ damage. Alloreactive donor T cells that infiltrate GVHD target organs can mediate tissue destruction through both direct cytotoxic activity and the recruitment of other leukocytes (Welniak et al., 2007). Both innate and adaptive immune cells contribute to exacerbate T cell-induced inflammation. Although cytotoxic T cells are the major cellular effectors of aGVHD, other cellular mediators such as NK cells, neutrophils and macrophages contribute to tissue damage during this phase, further augmenting tissue injury and resulting in a self-perpetuating inflammation that once initiated is difficult to control (Blazar et al., 2012). Cytotoxic lymphocytes mediate target cell lysis mainly through Fas-Fas ligand (FasL) and perforin/granzyme pathways (Van Den Brink and Burakoff, 2002). The expression of Fas and FasL has been reported to be increased on donor $CD4^+$ and $CD8^+$ T cells during aGVHD both in murine models and in patients, and serum levels of soluble FasL and Fas were found to correlate with GVHD severity or the response to therapy. The Fas-FasL pathway seems to predominate in hepatic GVHD, while the perforin/granzyme pathway appear to be more important in the skin and GI tract (Ferrara et al., 2009). Moreover, TNF-related apoptosis-inducing ligand (TRAIL) and TNF-like weak inducer of apoptosis (TWEAK) have been proposed as alternative cytotoxic pathways for CTLs and NK cells (Van Den Brink and Burakoff, 2002). The role of NK cells in GVHD is not completely understood and evidence from both

preclinical models and studies in humans suggests that NK cell could either promote or prevent GVHD. Alloreactive, donor-derived NK cells have been shown to kill recipient APCs and activated T cells, thus preventing GVHD. On the other hand, NK cells can contribute to GVHD development by producing proinflammatory cytokines that may act directly to induce cell damage or indirectly by increasing T cell mediated tissue damage (Simonetta et al., 2017).

In addition to direct cytolytic pathways, production of proinflammatory mediators such as TNFα and IL1 also contributes to tissue injury. In particular, TNFα plays a central role in GVHD pathogenesis and acts at different stages, enhancing APCs maturation, promoting cellular trafficking and T cell responses and directly inducing tissue injury. Tissue damage can be further enhanced by nitride oxide (NO) and other inflammatory mediators produced by macrophages (Morris and Hill, 2007).

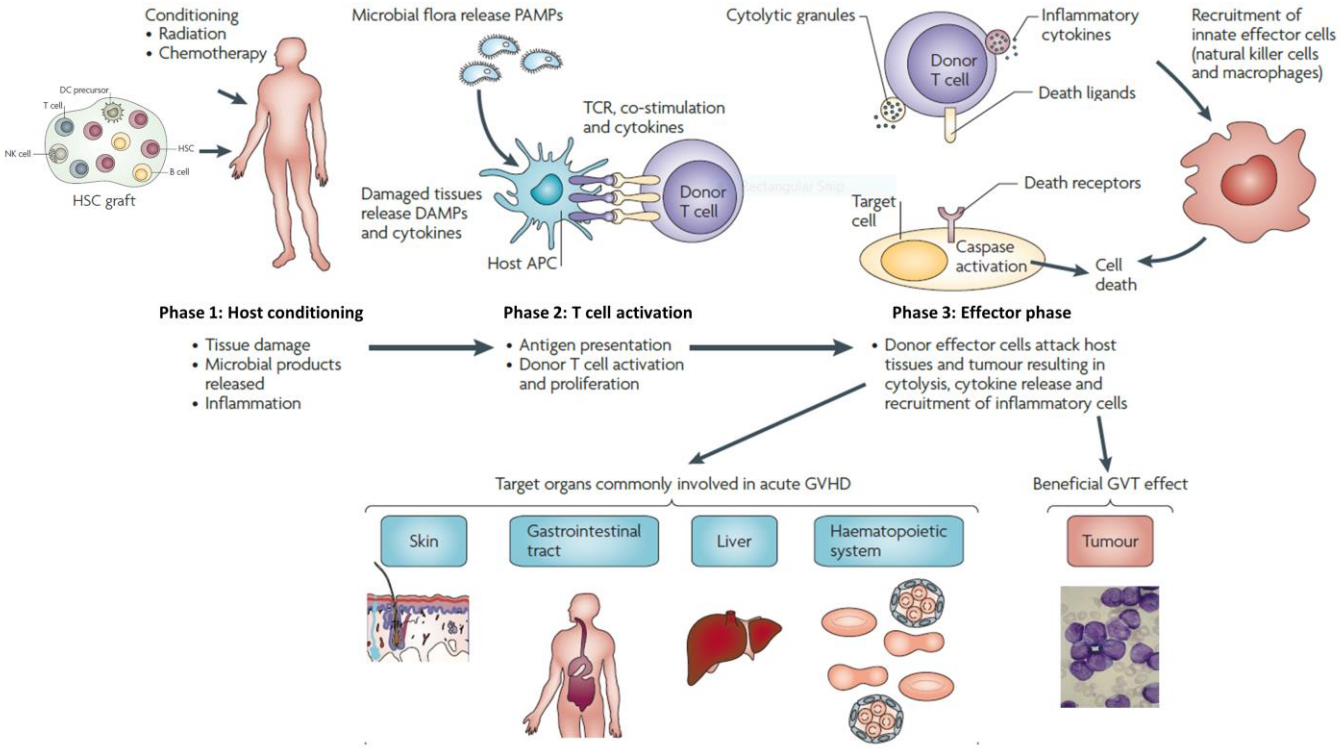

Figure 8 Alloresponses following HSCT: GVHD and GVL effect

Three phases of graft-versus-host disease (GVHD) and graft-versus-leukemia effect (GVL) following allogeneic HSCT. Phase 1: the host conditioning damages host tissues determining the release of inflammatory mediators and microbial products and leading to activation of APCs. Phase 2: Antigen presentation leads to donor T cell activation and proliferation. Phase 3: Activated alloreactive donor T cells attack both host tissues, leading to GVHD, and residual malignant cells, mediating the beneficial GVL effect. APC=antigen-presenting cell; DAMP=damage-associated molecular pattern; HSC=hematopoietic stem cell; LPS=lipopolysaccharides; MHC=major histocompatibility complex; PAMP=pathogen-associated molecular pattern; TCR=T cell receptor. Adapted from Jenq and Van Den Brink, 2010.

2.2.3.4 T cell subsets in GVHD pathogenesis

T cell replete grafts contain large numbers of mature T cells. The central role of T lymphocytes in mediating GVHD has been demonstrated by the complete abrogation of GVHD following T cell depletion from the graft (Blazar et al., 2012). During the last decade T cell subsets have been investigated to better understand and to predict the onset of aGVHD. Differential expression of surface molecules including, among others, CD62L, CD45RA/R0, CCR7 and CD27 allows to phenotypically define naïve and memory T cells subsets. Naïve T cell (T_N) express the lymph node homing molecules CD62L and CCR7 and are characterized by CD45RA and CD27 expression. As T_N, central memory T cells (T_{CM}) express CD62L, CCR7 and CD27, but express CD45R0 instead of CD45RA. Effector memory T cells (T_{EM}) do not express the lymph node homing molecules CD62L and CCR7 and therefore preferentially traffic to peripheral tissues, and express the marker CD45R0 (Gattinoni et al., 2017; Mahnke et al., 2013). Moreover, a T cell subset characterized by the expression of both naïve and memory markers and endowed with self-renewal potential has been identified in both mice (Zhang et al., 2005) and humans (Gattinoni et al., 2011). These cells, named T memory stem cells (T_{SCM}), were reported to sustain GVHD upon serial transplantation into allogeneic hosts and to reconstitute all memory and effector subsets while maintaining their own pool size through self-renewal (Zhang et al., 2005). Human T_{SCM} have been identified by Gattinoni and colleagues and similar to their murine counterpart have been shown to express a naïve-like phenotype, being $CD45RA^+CD45R0^-CCR7^+CD62L^+CD27^+CD28^+$, while overexpressing Fas (CD95) and other markers of memory cells such as IL2 receptor beta (IL2Rβ) and CXCR3 (Gattinoni et al., 2011, 2017). Phenotypic, functional, and gene expression properties of these T cell subsets (Gattinoni et al., 2011; Lugli et al., 2013) suggest that human memory T cell differentiation follows a linear progression where less differentiated cells give rise to more differentiated progeny in response to antigenic stimulation or, potentially, homeostatic signaling. According to this hierarchical model T_N progressively differentiate into T_{SCM}, T_{CM}, T_{EM} and ultimately into terminally differentiated effectors (T_{EFF}) (Gattinoni et al., 2017).

In preclinical models, donor naïve T cells have been shown to play a key role in mediating aGVHD, while memory T cell subsets are less alloresponsive and do not seem to initiate GVHD to the same degree (Chen et al., 2007; Dutt et al., 2007; Zhang et al., 2012). In mice, naïve $CD44^{lo}CD62^{hi}CD8^+$ T cells have been shown to generate and sustain allogeneic $CD8^+$ T cell subsets in graft-versus-host reaction (Zhang et al., 2005) while memory T cells do not cause

GVHD but sustain the GVL effect (Huang and Chao, 2017). Collectively, data in the literature indicate that memory T cells mediate a different type of alloreactivity compared to naïve T cells in GVHD, but the biological mechanisms underlying this difference are not clear (Huang and Chao, 2017). In humans, it has been shown that alloreactive T cells preferentially derive from $CD45RA^+$ naïve T cells (Chérel et al., 2014; Distler et al., 2011). However, the precise role of $CD4^+$ and $CD8^+$ naïve and memory subsets in GVHD pathogenesis is still incompletely understood, with some conflicting studies associating either the proportion of naïve (Chang et al., 2009; Yakoub-Agha et al., 2006) or memory (Loschi et al., 2015) T cells present in the graft with the risk of developing aGVHD after HSCT. In a recent pilot study, depletion of naïve $CD45RA^+$ T cells from the donor graft did not reduce the incidence of aGVHD, but possibly improved the response to corticosteroid treatment, as GVHD was steroid sensitive in all patients. Moreover, selective transfer of effector memory T cells was associated with a reduced risk of cGVHD and with sustained antiviral and antitumor immunity (Bleakley et al., 2015). Clinical trials in which viral antigen-specific T cells were transferred after HSCT, showed increased antiviral immunity without increased risk of aGVHD and therefore suggest that adoptive transfer of enriched memory T cells can preserve antiviral and GVL effects without causing GVHD, making it an ideal strategy for GVHD prevention in HSCT (Huang and Chao, 2017).

Following recognition of alloantigens and subsequent activation, donor T cells proliferate and differentiate into various effector subsets. Naïve T cells can differentiate into distinct subsets such as Th1/Tc1, Th2/Tc2, Th17/Tc17 and T regulatory (Treg) cells secreting specific cytokine repertoires and expressing different chemokine receptors. In contrast to the classical view according to which these subsets behave like lineages and have an inflexible phenotype, it is currently recognized that T helper cells have a plastic phenotype and can change their profile of cytokine production and express more than one master regulator according to the cytokine milieu and the stimulus they receive (O'Shea and Paul, 2010). Traditionally, acute GVHD has been considered as a Th1/Tc1-type (IL12, IL2 and IFNγ) disease based on the features of cytotoxic T cell-mediated pathology and increased production of type 1 cytokines, including IFNγ (Nikolic et al., 2000). However, other subsets such as Th2/Tc2 and Th17/Tc17 have been implicated in aGVHD pathogenesis, and GVHD manifestations, organ specificity and severity have been proposed to be influenced by the proportion of naïve cells maturing along Th1/Tc1, Th2/Tc2, Th17/Tc17 or Treg phenotypes and by the dynamic balance between the different subsets and the

cytokines they produce (Henden and Hill, 2015; Yi et al., 2009; Zhang et al., 2016). $CD4^+CD25^+Foxp3^+$ Tregs are a functionally distinct subset of mature T cells endowed with suppressive activity that play a pivotal role in the maintenance of peripheral tolerance and control of immune responses (Fontenot et al., 2003; Sakaguchi et al., 1995). In recent years, several preclinical and clinical studies have demonstrated the importance of Tregs in improving transplantation outcome for both HSCT and solid organ transplantation (Di Ianni et al., 2011; Juvet et al., 2014; Romano et al., 2017). Following HSCT, the reconstituting immune system must include critical regulatory cell populations as well as effector cells that provide immune surveillance. Previous studies have suggested that a deficiency of $CD4^+$ Tregs after transplantation is associated with increased alloreactivity and increased risk of developing GVHD (Edinger et al., 2003; Josefowicz et al., 2012; Miura et al., 2004; Yuan et al., 2014).

Cytokines such as TNFα, IFNγ, IL2, IL10 and others appear to be essential in regulating leukocyte recruitment and tissue destruction. Cytokine-mediated effects can vary during the different phases of GVHD and dose and timing of cytokine production is critical in determining their role in GVHD pathogenesis and make the effects of individual cytokines difficult to predict (Welniak et al., 2007).

2.2.4 Acute GVHD diagnosis and grading system

The diagnosis of aGVHD is based on the evaluation of clinical symptoms and the involvement of the target organs is assessed by means of clinical and laboratory analyses and biopsy (Zeiser and Blazar, 2017). The severity of aGVHD is staged and graded according to a number of scoring systems considering the extent of involvement of the three main target organs (skin, liver and GI tract). The modified Glucksberg criteria are commonly used for this purpose (**Table 1**, adapted from Choi et al, 2010) (Przepiorka et al., 1995). Each organ is independently assessed and assigned a clinical stage. Skin involvement is defined by assessing the percentage of body surface affected by the rash, liver involvement is assessed by measuring serum levels of bilirubin and GI tract involvement by measuring the stool output per day. These organ stages are then combined to determine an overall clinical grade (I-IV) that defines the overall severity of aGVHD. The overall grades are classified as I (mild), II (moderate), III (severe), and IV (very severe). Disease severity has been shown to correlate with mortality and a poor prognosis is associated with severe grades III and IV (Choi et al., 2010).

Clinical stage	SKIN (extent of rash)	LIVER (serum bilirubin)	GI TRACT (diarrhea volume/day)
0	0	<2 mg/dl	<500 ml
1	< 25% body surface	2-3 mg/dl	500-1000 ml *
2	25-50% body surface	3.1-6 mg/dl	1000-1500 ml
3	Generalized erythroderma	6.1-15 mg/dl	>1500 ml
4	Bullae/Desquamation	>15 mg/dl	>2000 ml**

* or persistent anorexia, nausea and vomiting
** or severe abdominal pain with or without ileus

Overall Clinical grade	
0	Stage 0 in every organ
I	Skin stage 1-2 Liver and GI tract stage 0
II	Skin stage 3 and/or Liver and/or GI tract stage 1
III	Skin stage 0-3 with Liver stage 2-3 and/or GI tract stage 2-3
IV	Skin stage 4 Liver and/or GI tract involvement

Table 1 Acute GVHD staging and grading criteria

Diagnosis of aGVHD based on clinical symptoms is frequently not straightforward due to the difficulties in differentiating immune-mediated GVHD damage from tissue injury induced by other processes. Diagnosis can be confirmed by biopsies of affected organs, however, the histologic severity on the biopsy does not consistently correlate with the clinical outcome. A panel of plasma biomarkers including IL2 receptor α chain (IL2Rα/sCD25), tumour necrosis factor receptor 1 (TNFR1), IL8 and hepatocyte growth factor (HGF) has been suggested as a confirmatory tool for the diagnosis of aGVHD at the onset of clinical symptoms (Morris and Hill, 2007; Nassereddine et al., 2017; Paczesny et al., 2009). Moreover, target-specific biomarkers that allow the discrimination of skin and GI GVHD from other forms of rashes or other forms of enteritis have been described and could replace the use of invasive biopsies. These include elafin for skin aGVHD and regeneration islet-derived 3α (REGα) and T cell immunoglobulin mucin 3 (Tim-3) for GI aGVHD (Paczesny, 2018). A limitation in aGVHD research and treatment is that diagnosis and prognosis rely almost entirely on the presence of clinical symptoms and currently, no validated laboratory tests exist to predict aGVHD development prior to its onset, responsiveness to treatment, or patient survival (Paczesny, 2018; Paczesny et al., 2013).

2.2.5 Acute GVHD prophylaxis and treatment

Prophylactic immunosuppression is central to the management of GVHD in clinical practice. Based on preclinical trials, posttransplant methotrexate (MTX) has been the first widely used GVHD prophylaxis, followed by cyclosporine A (CSA). MTX, a folate antagonist, and CSA, a calcineurin inhibitor, exert their immunosuppressive effects interfering with purine synthesis and calcium-dependent signal transduction downstream the TCR, respectively, resulting in inhibition of T cell activation. Tacrolimus has a mechanism of action similar to CSA and is also widely used in clinical practice. Today the backbone of conventional acute GVHD prophylaxis regimens used in most T cell replete transplant includes two drugs: a calcineurin inhibitor such as CSA, plus MTX or mycophenolate mofetil (MMF), an inhibitor of purine synthesis. Combination of CSA and a short course of MTX is usually administered in matched sibling transplants after myeloablative conditioning. CSA in association with MMF is more frequently used in reduced intensity and cord blood transplants. Administration of high-dose cyclophosphamide (Cy) shortly after HSCT is used to deplete highly proliferating alloreactive T cells while preserving Tregs. This approach is mainly used in transplants from haploidentical donors. Additional approaches to prevent GVHD include T cell depletion of the graft. However, although effective in reducing GVHD, T cell depletion is associated with an increased incidence of graft rejection, relapse and infectious complications. It can be achieved *ex vivo,* for example through $CD34^+$ selection or through T cell subset depletion methods targeting CD3 or αβ T cell, or *in vivo* via administration of drugs such as anti-thymocyte globulin (ATG) and anti-CD52 antibody (alemtuzumab) (Holtan et al., 2014; Ruutu et al., 2014). Other preventive strategies under investigation in clinical trials include for example targeting leukocyte migration (e.g. CCR5 inhibition that blocks lymphocyte chemotaxis), reduction of inflammatory cytokines such as IL6, inhibition of Nuclear factor kappa-light-chain-enhancer of activated B cells (NF-κB) with the proteasome inhibitor bortezomib or cell-based therapies such as Treg infusions and adoptive transfer of mesenchymal stem cells, multipotent adult stem cells with immunoregulatory properties (Holtan et al., 2014; McDonald-Hyman et al., 2015).

Despite prophylaxis, clinically significant aGVHD still occurs and needs treatment. The first-line therapy is represented by corticosteroids, with potent anti-lymphocyte and anti-inflammatory activity. Treatment should be tailored according to the severity of the disease: initial therapy for aGVHD ranges from topical corticosteroids for skin GVHD of stage I or II to high-dose systemic treatment for patients with more severe disease (Nassereddine et al., 2017). However, about half

of the patients do not respond to the therapy and the likelihood of response in aGVHD is inversely correlated with the severity of the disease. Patients with higher risk of treatment failure are those with hyperacute GVHD, sex-mismatched HSCT or with certain patterns of organ involvement. ST2, the receptor for IL33, has been reported to be a biomarker correlated with the resistance to initial GVHD therapy and mortality (Vander Lugt et al., 2013). Patients with steroid-refractory (SR) aGVHD have a poor prognosis and the mortality rate is about 70-80%, as response to second-line treatments is poor (Hill et al., 2018; Magenau et al., 2016). Alternative therapies for SR-aGVHD include immune suppressants such as ATG, CSA, MMF, sirolimus or TNF blockers such as etanercept or infliximab, and novel procedures such as extracorporeal photochemotherapy. However, to date no proven second-line therapy for SR-aGVHD has been uniformly adopted and there are no sufficient data to compare the different regimens (Hill et al., 2018; Nassereddine et al., 2017; Zeiser and Blazar, 2017). Emerging therapies currently under investigation include kinase inhibitors (such as JAK1/2 inhibitors), proteasome inhibitors, cytokine modulators such as α-1 antitrypsin, monoclonal antibodies such as natalizumab that interferes with leukocyte migration, adoptive cell therapy with mesenchymal stem cells and microbiome restoration with fecal microbiota transplantation (Hill et al., 2018; Zeiser and Blazar, 2017).

2.2.6 Acute GVHD and the gut microbiota

Healthy individuals have a diverse intestinal bacterial flora that plays important roles in modulating the immune system during homeostasis and intestinal disease (Staffas et al., 2017). During HSCT procedures the diversity of the gut microbiota significantly decreases in transplant recipients. Antibiotic treatment, intestinal inflammation and changes in the diet are believed to be the main factors determining this loss of bacterial diversity (Shono and Van Den Brink, 2018; Staffas et al., 2017). The importance of the GI tract and its microbiota in GVHD pathogenesis was recognized in early studies showing a significant decrease in mortality and acute GVHD in germ-free mice and mice decontaminated with high-dose antibiotics before the transplant (Van Bekkum et al., 1974; Jones et al., 1971). Similar benefits were observed in a human study involving patients with aplastic anemia undergoing HSCT, in which gut decontamination and infection prophylaxis in isolated environment were shown to reduce the incidence of GVHD (Storb et al., 1983). However, more recently, broad spectrum antibiotics were shown to increase GVHD-related mortality in both patients and mice (Shono et al., 2016). The GI tract is a primary GVHD target organ and plays a major role in GVHD pathogenesis (Hill and Ferrara, 2000). Damage to the

intestinal barrier caused by the conditioning regimen for HSCT results in increased permeability that allows the translocation of bacterial products that participate to the activation of innate and adaptive immune responses. In line with this, Toll-like receptors (TLR) that recognize these products have been linked to GVHD development. In particular, mutations in the gene encoding TLR4 (receptor for LPS) and TLR4 inactivation have been associated with lower risk of acute GVHD (Lorenz et al., 2001; Zhao et al., 2013). On the contrary, mutations in the intracellular peptidoglycan receptor nucleotide-binding oligomerization domain-containing 2 (NOD2/CARD15) have been associated with acute GVHD and worse survival after HCT (Holler et al., 2006).

Collectively, data in the literature support the idea that loss of bacterial diversity affects HSCT outcome. In particular, microbiota injury and imbalances in the intestinal flora ("dysbiosis") with loss of some species (e.g. reduction in commensals from the genus *Blautia*) and expansion of others (e.g. *Enterococcus* spp., *Bacteroides* spp. or *Prevotella* spp.) have been correlated with GVHD incidence and transplant outcome. Studies have shown that the intestinal microbiota is significantly altered in patients developing GVHD and that these alterations correlate with GVHD pathogenesis and severity. Microbial metabolites can affect host immune responses and it has been reported that microbiome-derived metabolites modulate intestinal cell damage and mitigate GVHD (Mathewson et al., 2016). For example, the short chain fatty acid (SCFA) butyrate was shown to increase the recovery of intestinal epithelial cell damage and induce Treg cells in the intestine, linking the intestinal metabolism to GVHD, as Tregs can suppress GVHD. Local changes of microbial metabolites can reduce epithelial tissue damage and mitigate GVHD severity. Thus, it is currently recognized that the microbial metabolome has an impact on intestinal immune homeostasis and consequently also on GVHD. Increasing evidence indicates that the gut microbiota significantly affects the immune response in allogeneic HSCT and strategies to manipulate the intestinal microbiome in a favourable manner to improve HSCT outcome remain an area of active research. These include, for example, selecting antibiotics with a more narrow spectrum to spare beneficial anaerobic bacteria (such as *Blautia* spp.), administration of prebiotics to favour production of bacterial metabolites such as SCFAs, introduction of selected strains of bacteria through fecal microbiota transplantation or provide bacterial metabolic products (for example butyrate) directly (Magenau et al., 2016; Shallis et al., 2017; Shono and Van Den Brink, 2018; Zeiser et al., 2016).

2.2.7 Risk factors for GVHD development and biomarkers for outcome

The main risk factor for GVHD development is represented by the degree of HLA disparity between the donor and the recipient and single mismatches at HLA-A, -B, -C or -DRB1 are associated with significantly increased risk of acute GVHD (Petersdorf, 2008, 2013). Transplants from unrelated donors are associated with higher risk for aGVHD than matched sibling donors (Lee et al., 2013b).

In the HLA-matched setting, mHAs mismatches between donor and recipient provide the necessary tissue disparity to produce GVHD and have been clinically associated with an increased risk of GVHD (Spierings, 2014). For example, mismatches for HA-1, HA-2, HA-4 and HA-5 between donor and recipient have been described to be associated with an increased risk of GVHD (Dickinson and Charron, 2005; Goulmy, 1996). A recent genome wide association study (GWAS) showed that the number of mHAs mismatches is 2 fold higher in unrelated versus sibling HLA-matched transplants, but this had less impact on GVHD than mismatching at the HLA-DP locus (Martin et al., 2017).

Moreover, male-specific mHAs (encoded by the Y chromosome) are involved in HLA-matched sex-mismatched HSCT, and female-to-male transplants are more susceptible to GVHD. Thus, gender mismatch, in particular female donor for male recipient, increases the risk of developing GVHD (Dickinson and Charron, 2005). In addition, polymorphisms in genes involved in immune responses have been associated with the risk of developing GVHD. In particular, polymorphisms in genes coding for cytokines such as IL10, TNFα, IFNγ and IL6 have been linked to an increased risk of GVHD (Gam et al., 2017). As mentioned above, polymorphisms in NOD2/CARD15 gene, involved in innate immune response to bacterial cell wall products, have been implicated in both the incidence and the severity of aGVHD (Holler et al., 2006). Donor SNPs in the gene *IL1RL1* (coding for ST2 or IL33 receptor) showed an association with the risk of developing aGVHD with potential implication for donor selection (Paczesny, 2018).

Other risk factors for occurrence of aGVHD include older age of both donor and recipient, ineffective GVHD prophylaxis, intensity of the conditioning (some studies reported increased GVHD risk and severity associated with higher conditioning intensity and with TBI), graft source (PBSCs graft have been associated with increased risk of cGVHD) and pre-transplant comorbidities (Nassereddine et al., 2017).

In addition to strategies aimed at reducing the pre-transplantation risk to improve transplant outcome, such as optimal HLA matching, extensive effort has been made to define biomarkers able to anticipate GVHD onset, facilitate diagnosis or predict prognosis of posttransplant complications. Paczesny and colleagues reported the first biomarker panel for aGVHD diagnosis including IL2Rα, TNFR1, IL8 and HGF (Paczesny et al., 2009). Other target-specific biomarkers, released from injured tissues, such as elafin and REG3α, have been proposed as confirmatory tools for GVHD diagnosis (Paczesny, 2018). The serum level of ST2 has been reported to be an important biomarker for steroid resistance and mortality (Vander Lugt et al., 2013).

Other studies investigated gene expression signatures, either in bulk peripheral blood mononuclear cells (PBMCs) or in sorted cell populations, to identify pathways and drivers of GVHD in animal models and human patients (Buzzeo et al., 2008; Furlan et al., 2015, 2016; Takahashi et al., 2008; Verner et al., 2012), or used flow and mass cytometry to discover new cell populations associated with GVHD (Li et al., 2016). MicroRNAs (miRs) have also been studied as potential biomarkers for HSCT outcome (Gam et al., 2017). A miRNA-based model including miR-423, miR199a-3p, miR93 and miR377, has been investigated in a clinical study to predict the risk of aGVHD. Elevated levels of these miRNAs were detected in plasma before the onset of GVHD and their expression was associated with GVHD severity and poor overall survival (Xiao et al., 2013). Another study profiling 48 miRNAs in plasma of aGVHD patients, identified miR-586 as being decreased at aGVHD onset. In this study, the patients who developed aGVHD had a higher expression level of miR-586 at day 7 post-HSCT and the authors propose that the plasma level this miRNA early after transplant (at day 7 post-HSCT) might be a biomarker for predicting the occurrence of aGVHD (Wang et al., 2015). However, to date, no validated laboratory tests exist that are routinely applied in the clinic to predict aGVHD development prior to its onset, responsiveness to treatment, or patient survival (Paczesny, 2018; Paczesny et al., 2013).

Goals of the study

Allogeneic HSCT has become a standard therapy for many patients with life-threatening hematologic disorders. Advances in the necessary technology and the increased donor availability have allowed a rapid expansion of HSCT over the last two decades. New conditioning regimens with lower intensity have broadened the use of HSCT to patients that are ineligible for conventional allografting because of age or comorbidities. Moreover, the source of stem cells, initially limited to bone marrow cells, has been extended to peripheral blood stem cells and umbilical cord blood. However, despite the progress in the field, HSCT outcome is still heavily conditioned by GVHD, which is the main factor contributing to non-relapse morbidity and mortality. After six decades of HSCT, some progress has been made for GVHD prophylaxis, but very little in the treatment of the disease. Much of our knowledge on the pathophysiology and the immunological mechanisms involved in acute GVHD derives from studies performed in animal models, in particular the mouse system. However, direct translation of these experimental results to the clinical setting in human has proven to be difficult and progress in the clinical diagnosis, prognosis, prophylaxis and treatment of GVHD requires a better understanding of the disease processes in humans. Moreover, the lack of biomarkers for the early diagnosis and prognosis, in particular to predict GVHD resistance to steroid treatment, contributes to the high mortality of the disease.

To address these issues, the main goals of my thesis project were (i) to investigate the cellular and molecular mechanisms involved in the reconstitution of a functional immune system in recipients after HSCT and (ii) to explore the mechanisms of acute GVHD to improve our understanding of the immunological processes of this disease in humans.

In particular, the specific questions that we addressed in this study are:

1) How does the donor immune system react to the environment of the host after HSCT?
   To this end, we assessed the cellular and molecular characteristics of immune reconstitution in patients without acute GVHD after HSCT and compared them with their respective HLA-identical sibling donors before transplant to identify changes associated with the transplantation procedure and with immune reconstitution in the absence of the graft-versus-host reaction.
2) What are the cellular and molecular correlates associated with acute GVHD onset?
   To address this question, we compared on one hand, the cellular profile in patients at GVHD onset and in patient without GVHD, to identify potential “pathogenic” cell

populations associated with GVHD development and, on the other hand, the molecular characteristics of sorted immune cell populations to identify a gene expression signature associated with GVHD onset.

3) Can we identify “dangerous donors”, stronger alloresponders that are more likely to elicit acute GVHD in their recipients?

For this aim, we compared the cellular and gene expression profiles in donors whose recipients developed acute GVHD to donors whose recipients did not develop aGVHD, to identify donors whose grafts are associated with a higher risk of developing aGVHD for the recipients.

Materials and Methods

1 Study design and description of the cohorts

This study was performed in close collaboration with the team of Pr. Gérard Socié, director of the Service Hematologie-Greffe at St. Louis Hospital in Paris, and with CRYOSTEM, a national, multicentric biobank. Three independent cohorts of patients undergoing allogeneic HSCT and their respective HLA-matched sibling donors were recruited and included in this study. All participants had given written informed consent to participate in research studies in accordance with the Declaration of Helsinki. The first cohort includes donor-recipient couples for which peripheral blood mononuclear cells (PBMCs) and serum samples have been prospectively collected at St. Louis hospital in Paris and cryopreserved (cohort 1). The second cohort includes PBMCs and serum samples from donors and recipients couples provided by CRYOSTEM biobank (cohort 2) and the third cohort includes freshly collected blood samples from donor-recipient pairs recruited at St. Louis hospital in Paris (cohort 3). For all the three cohorts blood samples from the donors were collected before the transplantation procedure, and for the recipients samples were collected either at the onset of acute GVHD, before any treatment, or at day 90, for cohort 1 and 2, or day 30 post-HSCT for cohort 3 for the patients that did not develop acute GVHD.

2 Allogeneic HSCT and GVHD diagnosis

Patients received a myeloablative or reduced intensity conditioning regimen, depending on disease type, age and comorbidities, followed by infusion of the donor graft. The source of stem cells was either peripheral blood G-CSF-mobilized stem cells (PBSCs) or bone marrow (BM). Alleles at the HLA-A, -B, -C, -DRB1, and -DQB1 loci were identified for all patients and donors by DNA typing method. All donor-recipient pairs in our study are HLA-identical siblings.

The day of the donor graft infusion was day 0. After HSCT patients were administered a GVHD prophylaxis with cyclosporin A (CSA) alone or in association with methotrexate (MTX) or mycophenolate mofetil (MMF) and broad-spectrum antibiotics. Clinical characteristics of donors and recipients are summarized in **Table 3** in the Results section. Acute GVHD diagnosis was performed at onset of clinical symptoms and confirmed by skin, gut or liver biopsy if necessary. Overall GVHD grade was determined according to the Glucksberg criteria (Glucksberg et al., 1974). Donor chimerism was assessed at day 90 (cohorts 1 and 2) or at day 30 (cohort 3) post-HSCT by microsatellites amplification (polymerase chain reaction, PCR) in whole blood samples (total chimerism).

3 Collection and processing of blood samples

Cryopreserved cohorts (cohorts 1 and 2): recipients' blood samples were collected either at day 90 after HSCT, for recipients that did not develop aGVHD, or at aGVHD onset, before the start of systemic therapy. Donors' samples were collected before HSCT. Isolated PBMCs in fetal calf serum (FCS) + dimethyl sulfoxide (DMSO) and serum samples were cryopreserved at the biobank. Samples were stored in liquid nitrogen, shipped in dry ice and re-stored in liquid nitrogen until thawing at the Pasteur Institute in Paris. On the day of fluorescence-activated cell sorting (FACS) sorting and flow cytometric analysis, cells were removed from liquid nitrogen and transferred to a 37°C water bath until thawing. Samples were always thawed in less than 5 minutes. The thawed cell suspension was quickly transferred into a 15 or 50ml falcon tube, according to the number of vials per patient/donor, and 1ml of pre-warmed medium Roswell Park Memorial Institute (RPMI) 1640 (Gibco Life Technologies, Oslo, Norway) + 20% FCS (HyClone, Fisher Scientific) + Penicillin + Streptomycin per cryovial was added drop by drop. After incubation at 37°C for 10 minutes, 5ml of thawing medium per cryovial were added and cells were centrifuged at 1400 revolutions per minute (rpm) for 10 minutes at room temperature. Viable cells were counted after Trypan blue staining both manually in a Neubauer chamber and automatically with a Countess Automated Cell Counter (Thermo Fisher Scientific). Thawed PBMCs were then stained for FACS sorting and for immunophenotyping. In case of low cell numbers after thawing, either FACS sorting or flow cytometric analysis was performed.

Cohort of freshly collected samples (cohort 3): recipients' blood samples were collected either at day 30 after HSCT, for recipients that did not develop aGVHD, or at aGVHD onset, before the start of systemic therapy. Donors' samples were collected before the transplantation procedure. Venous blood samples were collected into sterile Lithium-Heparin tubes for PBMCs isolation or in gel tubes for serum separation (BD Vacutainer, Becton-Dickenson; Franklin Lakes, NJ, USA). PBMCs were isolated by density gradient centrifugation (Lymphocyte separation medium, Eurobio, France) of whole blood diluted 1:3 with room temperature Phosphate Buffer Saline (PBS, Fisher Scientific), counted and immediately processed for FACS sorting and flow cytometric analysis. Cells to be counted were re-suspended in a known volume of medium or PBS. Ten microlitres of cell suspension and 10µl 0.4% Trypan Blue were mixed in a 1.5ml eppendorf tube and 10µl was transferred to a Neubauer chamber. Mean numbers of live cells were counted from 3 squares. The total number of cells was calculated with the formula:

Total cells= Mean cell count*dilution factor*volume (ml) x 10^4. Viable cells were also counted automatically with a Countess Automated Cell Counter (Thermo Fisher Scientific).

Serum was obtained immediately by centrifugation of the gel tubes at 2400 rpm for 20 minutes and stored at -80°C until further processing.

4 Flow cytometry

4.1 TBNK TruCount assay

In order to assess the distribution of the main immune cell populations and evaluate immune reconstitution in HSCT recipients, absolute counts of mature T, B, and NK lymphocyte populations were determined in 50µl of whole blood from donors and recipients of cohort 3 using the TBNK reagent (Multitest 6-color TBNK reagent, BD) following the manufacturer's instructions. This assay is based on the use of fluorochrome-labelled antibodies that bind specific leukocyte surface antigens, and subsequent acquisition on a flow cytometer that allows identification and enumeration of cells belonging to the different cell subsets analysed. BD Multitest 6-color TBNK reagent is provided in 1ml of buffered saline with 0.1% sodium azide. It contains FITC-labelled CD3 (clone SK7), PE-labelled CD16 (clone B73.1), PE-labelled CD56 (clone NCAM16.2), PerCP-Cy5.5–labelled CD45 (clone 2D1 (HLe-1)), PE-Cy7–labelled CD4 (clone SK3), APC-labelled CD19 (clone SJ25C1), and APC-Cy7–labelled CD8 (clone SK1). The BD TruCount tubes used contain a lyophilized pellet that dissolves when the blood and the reagents are added, releasing a known number of fluorescent beads. During analysis, the absolute number (cells/µl) of positive cells in the sample can be determined by comparing cellular events to bead events. Samples were acquired on a FACS Canto (BD) at St. Louis Hospital or on a LSR II (BD) at Pasteur Institute in Paris. Absolute numbers (cells/µl) of the different leukocyte populations were determined using the formula:

$$\frac{\#\text{events in cell population}}{\#\text{events in absolute count bead region}} \times \frac{\#\text{beads/test}^*}{\text{test volume}} = \text{cell population absolute count}$$

* This value is found on the BD Trucount tube foil pouch label and can vary from lot to lot.

4.2 Fluorescence-activated cell sorting (FACS)

Cells to be sorted were stained in the dark, at 4°C for 20 minutes in FACS buffer (PBS 1X + 1% FCS) with anti-human CD3-APC (Clone BW264/56, Miltenyi Biotech), anti-human CD4-APC-Vio770 (Clone M-T466, Miltenyi Biotech) and anti-human CD8-PerCP-Vio700 (Clone BW135/80, Miltenyi Biotech). For a part of the samples of the second cohort, $CD56^+$ NK cells and $CD14^+$ monocytes were also sorted in addition to $CD4^+$ and $CD8^+$ T cells using the following antibodies: anti-human CD3-APC (Clone BW264/56, Miltenyi Biotech), anti-human CD19-APC (Clone SJ25C1, BD), anti-human TCRαβ-APC (Clone BW242/412, Miltenyi Biotech), anti-human TCRγδ-APC (Clone 11F2, Miltenyi Biotech), anti-human CD14-FITC (Clone TUK4, Miltenyi Biotech), anti-human CD16-PE-Vio770 (Clone eBioCB16, eBioscience), anti-human CD4-APC-Vio770 (Clone M-T466, Miltenyi Biotech) and anti-human CD8-PerCP-Vio700 (BW135/80, Miltenyi Biotech), anti-human CD56-PE (Clone NCAM16.2, BD). After incubation, cells were washed with 4°C FACS buffer, passed through a 35µm nylon mesh filter (Corning Falcon Test Tube with Cell Strainer Snap Cap, Thermo Fisher Scientific) and 1µl/ml of 4′,6-diamidino-2-phenylindole (DAPI) was added for dead cell discrimination. Cells were sort-purified on a FACS Aria II (BD Biosciences, San Jose, CA) at the Centre d'Immunologie Humaine (CIH) at the Pasteur Institute in Paris. Prior to sort, stream alignment into the collection tubes was verified and drop delay of the stream was set using Accudrop beads (BD Biosciences, San Jose, CA). A purity mask was selected. The purity of each population was confirmed with post-sort analysis. Cells were collected into medium-coated 1.5ml eppendorf tubes, pelleted at 3500 rpm for 5 minutes and lysed immediately in 350µl of Buffer RLT plus (Qiagen RNeasy Micro Kit, Valencia, CA). Cell lysates were stored at -80°C until RNA extraction.

4.3 Immunophenotyping using Spectral Flow Cytometry

Multicolour flow cytometric analysis was performed on donors and recipients' samples using a SP6800 Spectral Cell Analyzer (SONY Biotechnology Inc.) at the Centre d'Immunologie Humaine (CIH) at the Pasteur Institute in Paris.

Cryopreserved cohorts (cohorts 1 and 2): thawed cells were incubated for 1 hour in thawing medium at room temperature prior to staining to allow DMSO release. Cells for analysis were transferred into 5ml FACS tubes and washed with 2ml 4°C PBS 1X, re-suspended in 1ml PBS 1X

and stained with Viability Dye eF520 (eBioscience) for 30 minutes in the dark at 4°C. After incubation cells were washed with 2ml FACS buffer.

For cohort 1, cells were stained for 20 minutes at 4°C in the dark with the following anti-human monoclonal antibodies: anti-CD95-BV421 (Clone DX2, SONY), anti-CD3-V450 (Clone UCHT1, BD), anti-CD4-V500 (Clone RPA-T4, BD), anti-CD8-BV570 (Clone RPA-T8, SONY), anti-CD27-BV650 (Clone L128, BD), anti-CD196 (CCR6)-BV711 (Clone, 11A9, BD), anti-CD45RA-BV786 (Clone HI100, SONY), anti-CD45R0-BB515 (Clone UCHL1, BD), anti-CXCR5-PerCP-Cy5.5 (Clone RF8B2, BD), anti-CRTH2-PE-CF594 (Clone BM16, BD) and anti-CXCR3-PE-Vio770 (Clone REA232, Miltenyi Biotech), anti-TCRγδ-PE (Clone 11F2, Miltenyi Biotech), anti-TCRVδ2-PE (Clone 123R2, Miltenyi Biotech). Dump channel included anti-CD11c-FITC (Clone MJ4-27G12, Miltenyi Biotech), anti-CD14-FITC (Clone TUK4, Miltenyi Biotech), anti-CD19-FITC (Clone LT19, Miltenyi Biotech) and anti-CD34-FITC (AC136, Miltenyi Biotech). The complete antibody panel used is summarized in **Annex Table 4**. Cells were washed with 2ml FACS buffer and fixed in 250µl FACS buffer + 1% paraformaldehyde (PFA). Fixed samples were stored at 4°C in the dark until acquisition on the SP6800 Spectral Cell Analyzer (SONY Biotechnology Inc.)

A second antibody panel including intracellular markers was used to analyse T regulatory cells (Treg) (**Annex Table 5**). After incubation with the Viability Dye, cells were stained for 20 minutes at 4°C in the dark with the following anti-human monoclonal antibodies: anti-CD95-BV421 (Clone DX2, SONY), anti-CD3-V450 (Clone UCHT1, BD), anti-CD4-V500 (Clone RPA-T4, BD), anti-CD8-BV570 (Clone RPA-T8, SONY), anti-CD27-BV650 (Clone L128, BD), anti-CD279 (PD1)-BV711 (Clone, EH12.2H7, SONY), anti-CD45RA-BV786 (Clone HI100, SONY), anti-CD278 (ICOS)-PerCP-Cy5.5 (Clone REA192, Miltenyi Biotech), anti-HLA-DR-PE-Vio770 (Clone AC122, Miltenyi Biotech). Cells were washed with 2ml FACS buffer and incubated at 4°C in the dark for 30-60 minutes with 1ml Foxp3 Fixation/Permeabilization buffer (kit eBioscience) to permeabilize the cells prior to intracellular staining. Cells were washed with 2 ml Perm/Wash buffer 1X and stained with anti-Foxp3-PE (Clone PCH101, eBioscience), anti-Ki67-BV605 (Clone Ki-67, SONY) and anti-CD152 (CTLA4)-PE-CF594 (Clone BNI3, BD) for 30 minutes in the dark at room temperature. Cells were washed twice with 2ml Perm/Wash buffer 1X, resuspended in 250µl Fixation buffer (kit eBioscience) and stored at 4°C in the dark until acquisition on the SP6800 Spectral Cell Analyzer (SONY Biotechnology Inc.).

For cohort 2, cells were first stained for 20 minutes at 37°C in the dark with the following anti-human monoclonal antibodies: anti-CXCR5-PerCP-Cy5.5 (Clone RF8B2, BD), anti-CRTH2-PE-CF594 (Clone BM16, BD) and anti-CXCR3-PE-Vio770 (Clone REA232, Miltenyi Biotech) and then washed with 2ml FACS buffer. Cells were then stained for 20 minutes at 4°C in the dark with the following anti-human monoclonal antibodies: anti-CD95-BV421 (Clone DX2, SONY), anti-CD3-V450 (Clone UCHT1, BD), anti-CD45RO-VioGreen (Clone REA611, Miltenyi Biotech), anti-CD8-BV570 (Clone RPA-T8, SONY), anti-CD279 (PD1)-BV605 (Clone, EH12.2H7, SONY), anti-CD27-BV650 (Clone L128, BD), anti-CD196 (CCR6)-BV711 (Clone, 11A9, BD), anti-CD4-BV750 (Clone SK3, BD), anti-CD45RA-BV786 (Clone HI100, SONY), anti-CD122 (IL2RB)-PE (Clone Mik-b3, BD). Dump channel included anti-CD11c-FITC (Clone MJ4-27G12, Miltenyi Biotech), anti-CD14-FITC (Clone TUK4, Miltenyi Biotech), anti-CD19-FITC (Clone LT19, Miltenyi Biotech) and anti-CD34-FITC (AC136, Miltenyi Biotech) (**Annex Table 4**). Cells were washed with 2ml FACS buffer and fixed in 250µl FACS buffer + 1% paraformaldehyde (PFA). Fixed samples were stored at 4°C in the dark until acquisition on the SP6800 Spectral Cell Analyzer (SONY Biotechnology Inc.)

A second antibody panel including intracellular markers was used to analyse T regulatory cells (Treg) (**Annex Table 5**). After incubation with the Viability Dye, cells were stained for 20 minutes at 4°C in the dark with the following anti-human monoclonal antibodies: anti-CD25-BV421 (Clone M-A251, BioLegend), anti-CD3-V450 (Clone UCHT1, BD), anti-CD4-V500 (Clone RPA-T4, BD), anti-CD8-BV570 (Clone RPA-T8, SONY), anti-CD27-BV650 (Clone L128, BD), anti-CD279 (PD1)-BV711 (Clone, EH12.2H7, SONY), anti-CD45RA-BV786 (Clone HI100, SONY), anti-CD278 (ICOS)-PerCP-Cy5.5 (Clone REA192, Miltenyi Biotech), anti-CD127-PE-Vio770 (Clone REA614, Miltenyi Biotech). Cells were washed with 2ml FACS buffer and incubated at 4°C in the dark for 30-60 minutes with 1ml Foxp3 Fixation/Permeabilization buffer (kit eBioscience) to permeabilize the cells prior to intracellular staining. Cells were washed with 2ml Perm/Wash buffer 1X and stained with anti-Foxp3-PE (Clone PCH101, eBioscience), anti-Ki67-BV605 (Clone Ki-67, SONY) and anti-CD152 (CTLA4)-PE-CF594 (Clone BNI3, BD) for 30 minutes in the dark at room temperature. Cells were washed twice with 2ml Perm/Wash buffer 1X, resuspended in 250µl Fixation buffer (Kit eBioscience) and stored at 4°C until acquisition on the SP6800 Spectral Cell Analyzer (SONY Biotechnology Inc.). For this cohort, a reference sample of frozen PBMCs from the same healthy donor was processed together with the patient and

donor samples at every experiment to assess and guarantee the reproducibility of our staining procedure.

Samples in cohort 3 were analysed using different versions of the antibody panels described above, as some changes were introduced in the experimental protocol during the phase of design and validation of the antibody panels. The staining procedure used was the same as the one described for cohorts 1 and 2, but not all samples were analysed with the same antibody panel. The different versions of the panels with the list of antibodies used are summarized in **Annex Table 4** and **Table 5**.

Fluorescence minus one (FMO) controls were performed for the markers CD95, CXCR3 (panel 1) and PD1 (panel 2).

Data were analysed using Sony Software (SONY Biotechnology Inc.) and FlowJo analysis software version 10 (Tree Star, Ashland, OR).

5 Gene Expression Analysis

5.1 RNA extraction, Quantification and Quality control

Total RNA from sorted $CD4^+$ T cells, $CD8^+$ T cells, NK cells and monocytes was isolated using an RNeasy Micro Kit (Qiagen RNeasy Micro Kit, Valencia, CA) following the protocol provided by the manufacturer. RNA concentration was estimated using Qubit RNA HS Assay Kit (Life Technologies, Grand Island, New York, USA) according to the manufacturer's instructions.

RNA quality was assessed on a selection of random samples across the cohorts using the RNA 6000 Nano Kit on an Agilent BioAnalyzer 2100 system (Agilent Technologies, Palo Alto, CA). The RNA integrity number (RIN) was determined using the LabChip System software. RNA aliquots were stored at -80°C until use.

5.2 Gene Expression Analysis with NanoString nCounter Technology

Gene expression in purified $CD4^+$ T cells, $CD8^+$ T cells, NK cells and monocytes was assessed using NanoString nCounter Gene Expression Assay (NanoString Technologies, Inc. Seattle, Washington 98109 USA). The gene expression profile of $CD4^+$ and $CD8^+$ T cells was assessed for donors and recipients of the three cohorts, whereas NK cells and monocytes were analysed only for ten couples of the second cohort. T cells were analysed using the NanoString Human

Immunology V2 codeset, including 594 immune-related genes. For NK cells and monocytes, we used the NanoString Human PanCancer Immune profile codeset, including 770 genes covering both the adaptive and innate immune response. All nCounter assays were performed at the Centre for Translational Research (CRT) of the Pasteur Institute in Paris. Total RNAs were diluted with RNase-free water at 5 ng/µl (Cohort1), 10 ng/µl (Cohort2) or 20 ng/µl (Cohort3) into 0.2ml tubes of the 12-strip provided by NanoString. 25, 50 or 100ng (5µl total volume) of total RNA from each sample were analysed according to manufacturer's instructions.

NanoString nCounter technology detects messenger ribonucleic acids (mRNAs) within a sample and is based on the direct molecular barcoding of target molecules using colour-coded probe pairs followed by digital detection. The analysis is multiplexed, allowing simultaneous detection of up to 800 mRNAs and does not necessitate any amplification. The probe pair consists of a Capture probe, which carries a biotin on the 3' end, and a Reporter probe, which carries the barcode on its 5' end. The Capture probe contains a 35-50-base sequence complementary to a particular target mRNA plus a short common sequence coupled to a biotin. The Reporter probe contains a second 35-50-base sequence complementary to the target mRNA, coupled to a colour-coded tag that provides the detection signal. The colour codes carry six positions and each position can be one of four colours, thus thousands of barcodes combinations are possible. Unique pairs of Capture and Reporter probes are constructed to detect transcripts for each gene of interest (Geiss et al., 2008).

Hybridization reactions were performed in 12-tube PCR strips. First 5µl of each sample were added. Next, a mix containing hybridization buffer and Reporter probes was added. Finally, the Capture probes were added and PCR strips were quickly transferred to a thermocycler set at 65°C. Samples were hybridized at 65°C for 22 hours. Hybridization results in the formation of tripartite structures composed of a target mRNA bound to its specific Reporter and Capture probes. After hybridization, 12 samples at a time were processed using the handling robot Prep Station (process time 3h25min). Unbound excess Reporter and Capture probes are removed by affinity purification, and the remaining complexes are immobilized on a cartridge coated with streptavidin and aligned in an elongated state. Each mRNA of interest is identified by the colour code generated by the ordered fluorescent segments present on the Reporter probe (barcode). The level of expression is measured by counting the number of barcodes for each mRNA (Geiss et al., 2008). Cartridges

were read on a nCounter Digital Analyzer at the highest resolution (555 fields-of-view (FOV) collected per flow cell) to yield a Reporter Code Count (RCC) data set.

5.3 Analysis of gene expression data generated with the nCounter system

Each sample was analysed in a separate multiplexed reaction including in each, eight negative probes and six serial concentrations of positive control probes. Negative control analysis was performed to determine the background level for each sample.

Raw data (RCC files) were imported into nSolver Analysis software (version 3.0) for quality control and normalization. Data normalization included positive control normalization, negative control normalization and reference (housekeeping) gene normalization. For the positive control normalization, that allows to correct for technical variation, we calculated for each sample the geometric mean of the positive probes counts, then we calculated the average of the geometric means across all samples. To calculate a scaling factor, this average was divided by the geometric mean of the sample. For each sample, we multiplied all the counts (positive and negative controls and all gene counts) by the corresponding scaling factor. For negative controls normalization, we subtracted the mean of the negative controls + 2 standard deviations (SD) from the gene counts. Finally, to normalize for differences in mRNA input we used the same method as in the positive control normalization, except that geometric means were calculated over selected housekeeping genes. Samples from cohorts 1 and 2 were normalized together, while samples from cohort 3 were normalized separately. Using the geNorm method (Vandesompele et al., 2002) we selected the following housekeeping genes: *CD44*, *CD48*, *PPIA* and *RPL19* for $CD4^+$ and $CD8^+$ T cells in the three cohorts; *CD164*, *LAMP2*, *TXNIP* and *PPIA* for NK cells; and *CD44*, *CSF3R*, *HMGB1* and *TBP* for monocytes.

$CD4^+$ and $CD8^+$ T cells were analysed using the Human Immunology V2 codeset that contains probes for a total of 594 immune-related genes. Of these, 314 genes (cohorts 1 and 2) and 369 genes (cohort 3) were included in downstream analysis after removing probes with low counts (272 for cohorts 1 and 2 and 214 for cohort 3), probes mapping to multiple genes or probes aligning to polymorphic regions with greater than two SNPs (8 probes) (Urrutia et al., 2016) and probes used for housekeeping gene normalization.

NK cells and monocytes were analysed using the NanoString Human PanCancer Immune profile codeset, including 770 genes. Of these, 456 genes (NK cells) and 457 genes (monocytes)

were included in downstream analysis after removing probes with low counts (303 for NK cells and 306 for monocytes), probes mapping to multiple genes or probes aligning to polymorphic regions with greater than two SNPs (Urrutia et al., 2016) and probes used for housekeeping gene normalization. We defined probes with low counts if they were below the background level (defined as mean of the negative controls+2SD) in more than 80% of donors' samples and in more than 80% of recipients' samples.

6 Statistical Analysis and Data Visualization

A Wilcoxon's 2-tailed matched pairs test was performed to compare flow cytometry data between donors and recipients without GVHD (donors vs recipients in the absence of GVHD). A Mann-Whitney 2-tailed U test was used for comparison of flow cytometry data between recipients in the presence or absence of GVHD (GVHD onset vs No GVHD). Paired and unpaired Student t tests adjusted for multiple comparisons using the Benjamini-Hochberg method (Benjamini and Hochberg, 1995) were used for comparison of gene expression data between donors and recipients and between recipients in the presence or absence of GVHD, respectively. Comparison of clinical parameters between the different cohorts was performed using a Mann-Whitney 2-tailed U test for continuous variables and a Chi-square test for discrete variables. Statistical analyses were performed using GraphPad Prism version 7 (GraphPad Software, San Diego, CA) and R Studio. Unless otherwise indicated, horizontal bars represent the median.

Principal Component Analysis (PCA), hierarchical clustering, paired and unpaired t-tests were performed with Qlucore Omics Explorer version 3.0 (Qlucore, Lund, Sweden) and R Studio. Before applying PCA and hierarchical clustering, mRNA expression levels were log-transformed, mean-centred and scaled to unit variance. Q-values, defined as false discovery fate (FDR)-adjusted P-values (Benjamini and Hochberg, 1995), were used to define statistical significance in the t-tests.

Quantitative Set Analysis of Gene Expression (QuSAGE) was performed to identify differences in gene sets by quantifying gene-set activity using a probability density function. The analysis was performed in collaboration with the Bioinformatics and Biostatistics Hub at the Pasteur Institute, using the QuSAGE package (Yaari et al., 2013) in R Studio (version 3.5.1).

Results

1 Description of the cohorts

This study was performed in collaboration with the team of Pr. Gérard Socié, director of the Service Hematologie-Greffe at St. Louis Hospital in Paris, and with CRYOSTEM, a national, multicentric biobank in which almost 200.000 biological samples from patients before and after transplant and from donors have been collected since its establishment in 2011 (data December 2017).

To investigate the cellular and molecular mechanisms involved in the immune reconstitution after transplantation and to explore the mechanisms of acute GVHD (aGVHD) in humans, we analysed three independent cohorts of patients undergoing hematopoietic stem cell transplantation to treat hematologic diseases and their respective HLA-identical sibling donors. The first cohort includes 37 donor-recipient couples for which PBMCs and serum samples have been prospectively collected at St. Louis Hospital and cryopreserved (cohort 1). To assess the reproducibility of our findings and to increase the strength of our analysis, we analysed a second cohort of 38 donor-recipient pairs that was provided by CRYOSTEM biobank (cohort 2). Samples from this second cohort were selected in order to match the inclusion criteria used for cohort 1 and samples were obtained with the same kinetics. In order to assess immune reconstitution also at an early time point after transplantation, we analysed a third cohort that includes freshly collected samples from 26 donor-recipient pairs recruited at St. Louis Hospital (cohort 3). For all the three cohorts blood samples from the donors were collected before the transplantation procedure, and for the recipients samples were collected either at the onset of aGVHD or at day 90, for cohort 1 and 2, or day 30 for cohort 3 for the patients that did not develop aGVHD. The samples included in the study are summarized in **Table 2**.

Cohort 1 (Monocentric- St Louis)		
N° couples Donor – Recipient 37		
	D	**R**
NO GVHD (day 90)	21	18
GVHD (onset)	21	19
	42	**37**

Cohort 2 (Multicentric-Cryostem)		
N° couples Donor - Recipient 38		
	D	**R**
NO GVHD (day 90)	22	22
GVHD (onset)	17	16
	39	**38**

Cohort 3 (Monocentric- St Louis)		
N° couples Donor - Recipient 26		
	D	**R**
NO GVHD (day 30)	16	15
GVHD (onset)	15	11
	31	**26**

Table 2 Summary of the samples included for flow cytometry and gene expression analysis

2 Design of the study

To investigate the cellular and molecular mechanisms involved in the immune reconstitution after transplantation and to explore the mechanisms of acute GVHD in humans we collected donors' blood samples prior to hematopoietic stem cell transplantation and recipients' samples either at the onset of aGVHD, before the start of the steroid therapy, or at day 30 or 90 for the recipients that did not develop aGVHD. On the donors' and recipients' samples we performed (i) immunophenotyping using spectral flow cytometry to define the frequencies of different T-cell subpopulations, (ii) molecular profiling of cell populations involved in aGVHD pathogenesis using nCounter technology as well as (iii) metabolomic profiling of plasma samples (**Figure 9**). Cellular and molecular profiling were performed on all the three cohorts and results for these two approaches will be presented in this thesis. The metabolomic profiling of serum samples was assessed in cohorts 1 and 2 by Metabolon Inc. and analysis was performed by our collaborators at St. Louis Hospital and will not be presented in this thesis manuscript.

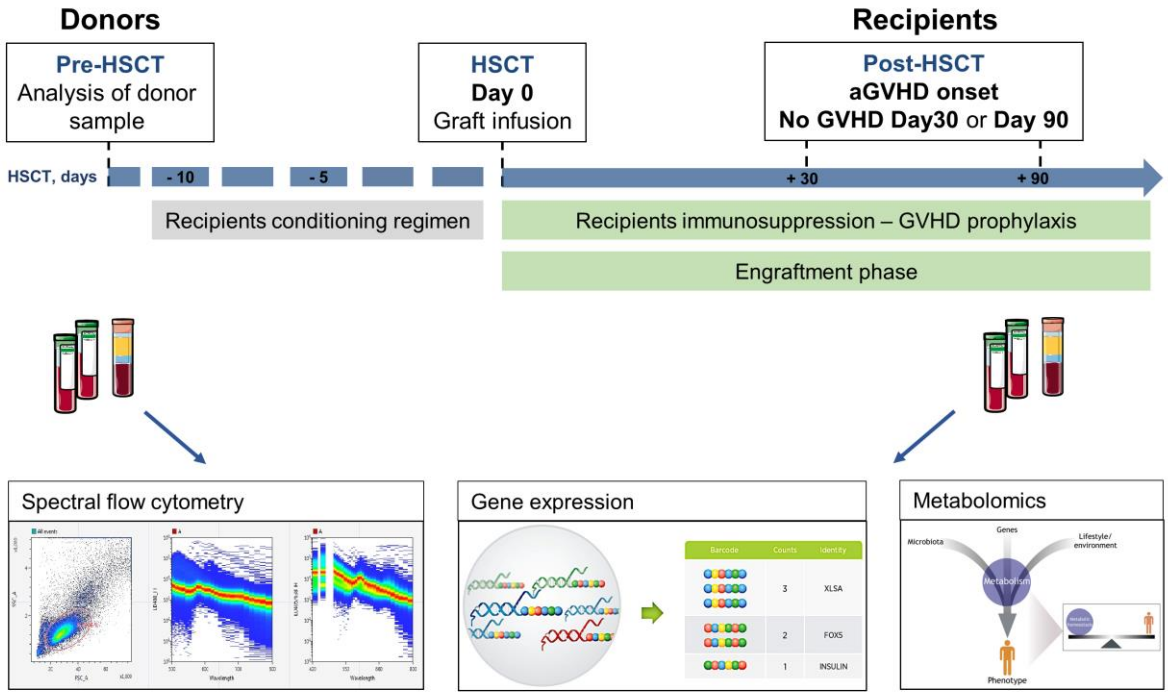

Figure 9 Design of the study
Blood samples from the donors were collected before stem cell mobilization prior to HSCT. The bone marrow or PBSC graft was infused in the recipients on D0, after administration of a preparative regimen. Blood samples were collected from HSCT recipients either at the onset of aGVHD or during the engraftment phase, at day 90 (cohorts 1 and 2) or day 30 (cohort3), for the recipients do not developing aGVHD.

3 Patients and donors' characteristics

Demographics and clinical characteristics of the patients and donors included for immunophenotyping and gene expression profiling are summarized in **Table 3** and **Figure 10**. All patients in this study received peripheral blood stem cells (PBSCs) or bone marrow (BM) grafts from an HLA-identical sibling donor after receiving a myeloablative (MAC) or reduced intensity (RIC) conditioning regimen to treat hematologic disorders. After HSCT patients were administered a GVHD prophylaxis with cyclosporine A (CSA) alone or in association with methotrexate (MTX) or mycophenolate mofetil (MMF). Only one patient in cohort 1 did not receive any GVHD prophylaxis because transplanted from an HLA-identical twin donor. A total of 19, 16 and 11 recipients who developed aGVHD were included in cohort 1, cohort 2 and cohort 3, respectively. GVHD diagnosis was performed at onset of clinical symptoms and confirmed by skin, gut or liver biopsy if necessary. GVHD grading was determined according to the Glucksberg criteria (Glucksberg et al., 1974).

As shown in **Figure 10**, no significant differences were seen in the age and gender distribution in the donors' and recipients' groups between the three cohorts. We observed a lower percentage of donor chimerism in recipients from cohort 3 compared to cohorts 1 and 2. This is consistent with the fact that for this cohort blood was collected at day 30 posttransplant, whereas for recipients in cohorts 1 and 2 blood was collected at day 90 post-HSCT for the recipients that did not develop GVHD. In the three cohorts, blood was collected from recipients that developed GVHD at the time of diagnosis, before the start of the steroid therapy. The median delay of GVHD onset after HSCT was comparable in the three cohorts (median day of GVHD onset: 36, 29 and 39 in cohort 1, 2 and 3 respectively).

A higher proportion of patients received a myeloablative conditioning regimen in cohort 2 (52.6%) compared to cohort 1 (13.5%). The majority of the recipients in cohorts 1 and 3 received as GVHD prophylaxis CSA+MMF (70.3 and 69.2% respectively), while in cohort 2 the higher proportion of recipients received CSA+MTX (57.9%).

Overall demographics and clinical characteristics of donors and recipients in the three cohorts were comparable.

Variable	Cohort 1		Cohort 2		Cohort 3	
	Donors (n=42)	Recipients (n=37)	Donors (n=39)	Recipients (n=38)	Donors (n=31)	Recipients (n=26)
Age						
Median age, y (range)	52.5 (15-67)	53 (22-67)	49.5 (14-65)	46 (17-68)	45 (19-68)	51 (20-68)
Gender, n (%)						
Female	24 (57.1%)	19 (51.4%)	18 (46.2%)	19 (50%)	12 (38.7%)	10 (38.5%)
Male	18 (42.9%)	18 (48.6%)	20 (51.3%)	19 (50%)	19 (61.3%)	16 (61.5%)
Unknown	-	-	1 (2.6%)	-	-	-
Donor type, n (%)						
HLA-identical sibling	100%		100%		100%	
Graft type, n (%)						
Bone marrow	3 (8.1%)		11 (28.9%)		5 (19.2%)	
Peripheral blood	34 (91.9%)		26 (68.4%)		21 (80.8%)	
Unknown	-		1 (2.6%)		-	
Sex match, n (%)						
Male to male	7 (18.9%)		10 (26.3%)		11 (42.3%)	
Female to female	11 (29.7%)		9 (23.7%)		4 (15.4%)	
Male to female	8 (21.6%)		10 (26.3%)		6 (23.1%)	
Female to male	11 (29.7%)		8 (21.1%)		5 (19.2%)	
Unknown	-		1 (2.6%)		-	
Conditioning regimen, n (%)						
Reduced intensity		32 (86.5%)		17 (44.7%)		20 (76.9%)
Myeloablative		5 (13.5%)		20 (52.6%)		6 (23.1%)
Unknown		-		1 (2.6%)		-
Total body irradiation, n (%)						
Yes		4 (10.8%)		12 (31.6%)		4 (15.4%)
No		33 (89.2%)		25 (65.8%)		22 (84.6%)
Unknown		-		1 (2.6%)		-
Chimerism, median % (range)						
No GVHD		100% (60-100)		100% (86-100)		98% (86-100)
GVHD		100% (97-100)		100% (81-100)		99% (95-100)
Unknown		-		4 (10.5%)		-
GVHD status, n (%)						
GVHD		19 (51.4%)		16 (42.1%)		11 (42.3%)
No GVHD		18 (48.6%)		22 (57.9%)		15 (57.7%)
GVHD grade, n (%)						
Grade 1		1 (5.3%)		8 (50%)		2 (18.2%)
Grade 2		16 (84.2%)		5 (31.3%)		5 (45.5%)
Grade 3		1 (5.3%)		1 (6.3%)		4 (36.4%)
Grade 4		1 (5.3%)		1 (6.3%)		-
Unknown		-		1 (6.3%)		-
Delay between sample and graft						
Donors, median days (range)	-27 (-119/-1)		-27 (-136/0)		-23 (-110/10)	
GVHD onset, median days (range)		36 (9/94)		29 (12/91)		39 (15/63)
No GVHD, median days (range)		90 (77/95)		91 (27/108)		31 (28/36)
GVHD prophylaxis, n (%)						
CSA		2 (5.4%)		7 (18.4%)		1 (3.8%)
CSA+MMF		26 (70.3%)		8 (21.1%)		18 (69.2%)
CSA+MTX		8 (21.6%)		22 (57.9%)		7 (26.9%)
None		1 (2.7%)		0		0
Unknown		-		1 (2.6%)		-
Diagnosis, n (%)						
Acute leukemia		13 (35.1%)		17 (45.9%)		11 (29.7%)
Myeloproliferative neoplasm		8 (21.6%)		3 (8.1%)		3 (8.1%)
Lymphoma		5 (13.5%)		8 (21.6%)		1 (2.7%)
Myeloma		3 (8.1%)		2 (5.4%)		2 (5.4%)
Myelodysplasic syndrome		2 (5.4%)		4 (10.8%)		5 (13.5%)
Aplastic anemia		3 (8.1%)		1 (2.7%)		2 (5.4%)
Chronic lymphoid leukemia		2 (5.4%)		1 (2.7%)		1 (2.7%)
Other diagnosis		1 (2.7%)		2 (5.4%)		1 (2.7%)
CMV serostatus						
Positive	23 (54.8%)	29 (78.4%)	22 (56.4%)	20 (52.6%)	16 (51.6%)	14 (53.8%)
Negative	19 (45.2%)	8 (21.6%)	16 (41%)	16 (42.1%)	15 (48.4%)	12 (46.2%)
Unknown	-	-	1 (2.6%)	2 (5.3%)	-	-
D+ / R+		21 (56.8%)		13 (34.2%)		10 (38.5%)
D- / R-		7 (18.9%)		8 (21.1%)		9 (34.6%)
D+ / R-		1 (2.7%)		8 (21.1%)		3 (11.5%)
D- / R+		8 (21.6%)		7 (18.4%)		4 (15.4%)

Table 3 Demographics and clinical characteristics of donors and patients in the three cohorts

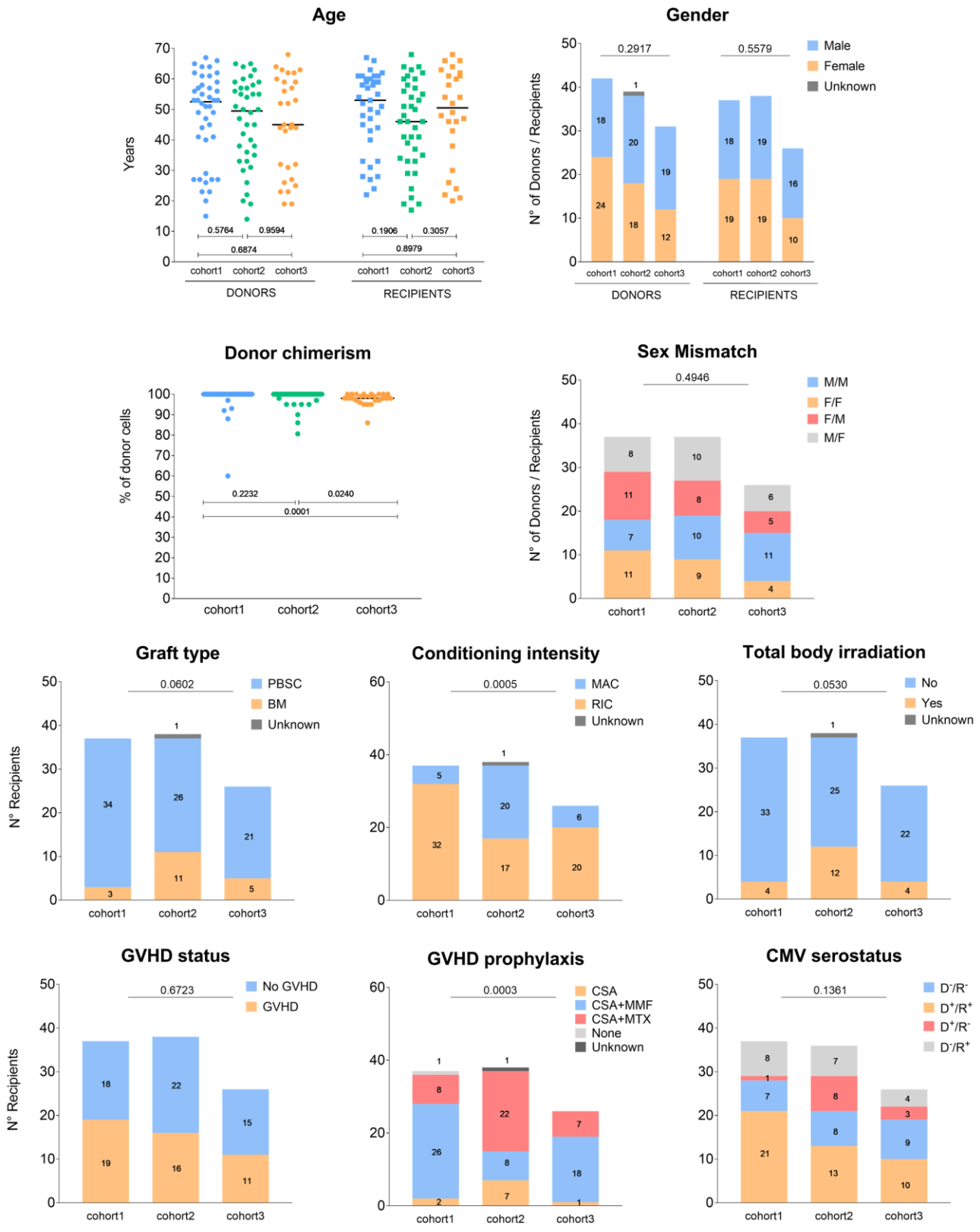

Figure 10 Demographic and clinical characteristics of donors and recipients in the three cohorts

Each dot point represents a donor or recipient in the three cohorts. Bar chart graphs indicate the proportion of donors/recipients in each group for the clinical parameter depicted in the three cohorts. P-values were calculated using a Mann-Whitney test for continuous variables and a Chi-square test for discrete variables (comparison between cohorts) and are indicated above the graph.

4 Cellular profiling using spectral flow cytometry

Polychromatic flow cytometry is a powerful analytical tool that enables high-resolution identification and quantification of large numbers of cells and the assessment of their subset distribution, activation status and other cellular functions. This technology has become, in the last decades, an invaluable tool in the study of complex cellular networks such as the immune system. Multiparameter flow cytometric analyses have been applied for immunophenotyping in clinical and research settings (Henel and Schmitz, 2007) and are currently used in the diagnosis, classification, staging and monitoring of disease states (e.g. hematologic malignancies) as well as in biomarker discovery (Craig and Foon, 2008; Stikvoort et al., 2017).

The goal of this part of the project was to characterize the composition of the immune cell compartment in donors' and recipients' samples using spectral flow cytometry, to define cellular correlates of immune reconstitution following allogeneic HSCT, and to identify potential "pathogenic" cell subsets associated with aGVHD onset. Since T cells play a key role in GVHD pathogenesis (Ferrara et al., 2009), we have focused our analysis on this lymphocyte population.

In conventional flow cytometry, mirrors and filters are used to select specific wavelength ranges of emitted fluorescence light for signal detection. In contrast, the recently developed hyperspectral cytometry takes advantage of dispersive optics, such as prisms or gratings, to disperse the collected light across a detector array, allowing to measure the full spectra from each particle. The different shapes of the fluorochromes emission spectra are distinguished along a large range of continuous wavelengths and the resulting data consist of a series of "spectral fingerprints" characterizing every analysed cell. In conventional systems, overlapping fluorescence is subtracted using colour compensation leading to photon loss. Instead, spectral flow cytometers sum the fluorescence together and then use unmixing deconvolution algorithms to mathematically separate the colours (**Figure 11**). This results in increased sensitivity and enhanced detection of weak signals. Moreover, having the ability to determine the spectral profile of autofluorescence from a cell, spectral cytometry allows to remove it from the stained samples, improving signal-to-noise and data accuracy (Grégori et al., 2014).

A

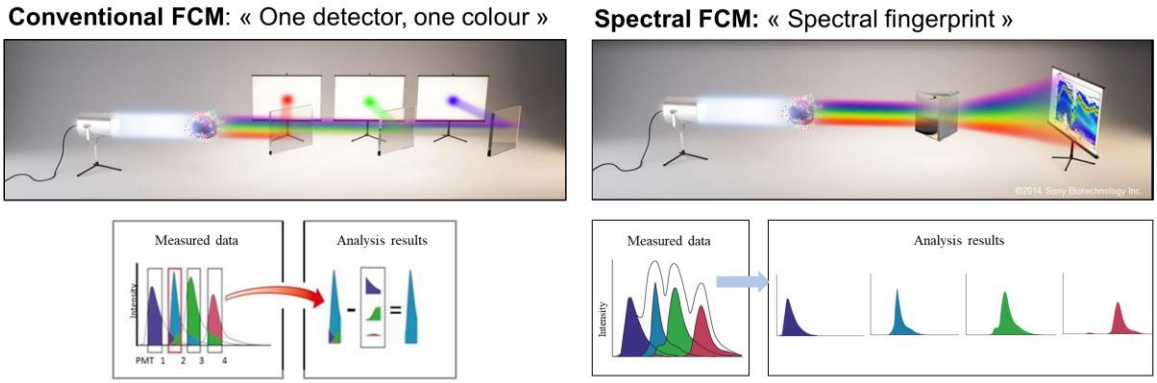

B

	Conventional FCM	Spectral FCM
Signal detection	Discrete ranges of wavelengths	Full spectra of emission
Autofluorescence correction	No	Yes
Overlapping emissions correction	Complex compensation matrices	Unmixing deconvolution algorithms
Use of close fluorescence wavelength peaks	Optimize fluorochromes combinations to minimize spill over	Discrimination of reagents with very similar waveforms

Figure 11 Conventional *versus* Spectral flow cytometry
(A) Schematic representation of the different method of signal detection in conventional (left panel) and spectral (right panel) flow cytometry. (B) Table summarizing the main differences between the two technologies. FCM= flow cytometry. Adapted from www.sony.net

4.1 Design and validation of the flow cytometry panels

To study the dynamics of reconstitution of different T cell subsets after transplantation and to investigate whether aGVHD development is associated with imbalances in specific immune cell populations, two flow cytometry panels were designed to enable detection of all major T cell subsets and their proliferative status in donors' and recipients' PBMCs.

Panel 1 (surface staining) is a 14-colour panel including surface markers that allow discrimination of different $CD4^+$ and $CD8^+$ T cell subpopulations. aGVHD has been initially described as a Th1-mediated disease (Antin and Ferrara, 1992), however, it was reported that also donor T cells deficient in IFNγ induced exacerbated acute GVHD (Murphy et al., 1998). Several studies implicated other T helper subsets, such as Th2 and Th17 in the pathophysiology of aGVHD and the exact role of each subset is still not completely understood (Kappel et al., 2009; Murphy et al., 1998; Nikolic et al., 2000; Yi et al., 2009). We therefore assessed whether the frequency of peripheral Th1 cells as well as other T helper subsets such as Th2, Th17 and T follicular helper (Tfh), was affected in recipients after HSCT or correlated with aGVHD development. Definition

of the different T helper subsets has been traditionally based on the expression of master transcription factors that guide cell differentiation (e.g. T-bet, GATA3, RORγt and Foxp3 for Th1, Th2, Th17 and Treg, respectively), and on the production of specific cytokines. In addition to differences in the cytokine repertoire, effector T cells exhibit distinct homing and migration properties thanks to the differential expression of chemokine receptors, selectins and integrins. Expression of chemokine receptors can be exploited to identify different T helper subsets based on their migratory capacity (Mahnke et al., 2013; Sallusto and Lanzavecchia, 2009). We therefore included in our surface panel the chemokine receptors CXCR3, CCR6, CXCR5 and CRTH2 to define Th1-, Th17-, Tfh- and Th2-like $CD4^+$ T cell subsets, respectively. For identification of Tfh cells we also included the inhibitory receptor programmed cell death 1 (PD1) that has been reported to be expressed on these cells (Crotty, 2011). We decided to apply this strategy for the identification of the different T helper subsets because the standard procedure for the identification of cytokine-producing cells via intracellular cytokine detection requires relatively high numbers of cells, a limiting factor at early time points after HSCT when the T cell compartment is not fully reconstituted. To allow discrimination of naïve and memory T cell subsets panel 1 includes the markers CD27, CD45RA, CD45R0 and CD95. We decided to use CD27 instead of CD62L for the identification of naïve cells because CD62L is lost with freezing and thawing procedures, leading to an unreliable quantification on cryopreserved cells (Mahnke et al., 2013). We identified the following subsets: T naïve ($CD45RA^+CD27^+CD45R0^-CD95^-$), T stem cell memory ($CD45RA^+CD27^+CD45R0^-CD95^+$), T central memory ($CD45RA^-CD27^+$), T effector memory ($CD45RA^-CD27^-$) and T effector memory re-expressing the naïve marker CD45RA ($CD45RA^+CD27^-$). This panel includes one fluorescence channel devoted to exclude cell types not of interest, termed "dump" channel. Markers in this channel include the viability dye to exclude dead cells, CD19 to exclude B cells, CD14 to exclude monocytes, CD11c to exclude myeloid dendritic cells and CD34 to exclude hematopoietic progenitors. Before identifying $CD4^+$ T cells as $CD3^+CD4^+CD8^-$ and $CD8^+$ T cells as being $CD3^+CD4^-CD8^+$, we gated for the lack of expression of the "dump" markers. For cohort 2 we modified this panel by removing TCRγδ and Vδ2 markers in order to add IL2Rβ, in an attempt to better characterize the T stem cell memory (T_{SCM}) subset. The complete list of markers included in panel 1 is summarized in **Annex Table 4**.

Given the importance of regulatory T cells in GVHD prevention and HSCT outcome (Edinger et al., 2003; Matsuoka et al., 2010), we designed a second 13-colour panel (panel 2, intracellular

staining) including amongst others the markers Foxp3, CTLA4, PD1 and ICOS to investigate Treg cell homeostasis. This panel also includes Ki-67, a nuclear antigen expressed by proliferating cells, irrespective of the cell cycle phase, but absent in resting cells (Scholzen and Gerdes, 2000), thus allowing us to assess the proliferative state of $CD4^+$ and $CD8^+$ T cell populations. For cohort 2 some modifications were applied to this panel compared to cohort 1. We encountered some technical difficulties to obtain a good and reproducible Foxp3 staining in cohort 1, and we therefore decided to substitute the markers CD95 with CD25, and HLA-DR with CD127 in order to identify the Treg subset also using cell surface markers. The complete list of markers included in panel 2 is summarized in **Annex Table 5**.

4.2 T cell dynamics following allogeneic HSCT

Reconstitution of a functional, donor-derived immune system is of utmost importance for the long-term recovery and survival of patients after allogeneic HSCT. A potent immune reconstitution is essential to limit the risk of infection and is associated with a favourable outcome after HSCT (Seggewiss and Einsele, 2010). Recovery of the T cell compartment relies initially on the peripheral expansion of memory T cells and it is only at a later time point that the production of naïve T cells in the thymus occurs. $CD4^+$ and $CD8^+$ T cells reconstitute within the first year after HSCT and are important for the defence against viral and fungal infections as well as for the eradication of residual malignant cells (GVL effect).

4.2.1 Incomplete reconstitution of the T cell compartment after HSCT

We first evaluated the reconstitution patterns of major T cell subsets at day 90 after transplantation, in recipients that did not develop aGVHD, compared to their respective sibling donors before transplant. We decided to include in this analysis only donor-recipient pairs not developing aGVHD to avoid potential confounding effects of aGVHD.

Cellular profiling of recipients three months after HSCT showed an incomplete reconstitution of the T cell compartment with a decrease of $CD3^+$ T lymphocytes compared to their respective sibling donors. This decrease reached statistical significance in cohort 2, whereas a trend towards a decrease approaching statistical significance was observed in cohort 1. Within the $CD3^+$ T cell population, we observed a significant decreased frequency of $CD4^+$ T cells accompanied by an increase of $CD8^+$ T cells in both cohorts **(Figure 12A**). Reconstitution of $CD8^+$ T cells is faster than that of $CD4^+$ T cells, which usually occurs around day 100 post-transplant or later, leading to

an inversion of the normal CD4/CD8 ratio (**Figure 12B**) that has been described to be characteristic of the post-transplant period (Seggewiss and Einsele, 2010). No significant differences were detected in the frequency of TCR $\gamma\delta^+$ T cells between donors and recipients. This cell subset was assessed only in cohort 1 and not in cohort 2 (data not shown).

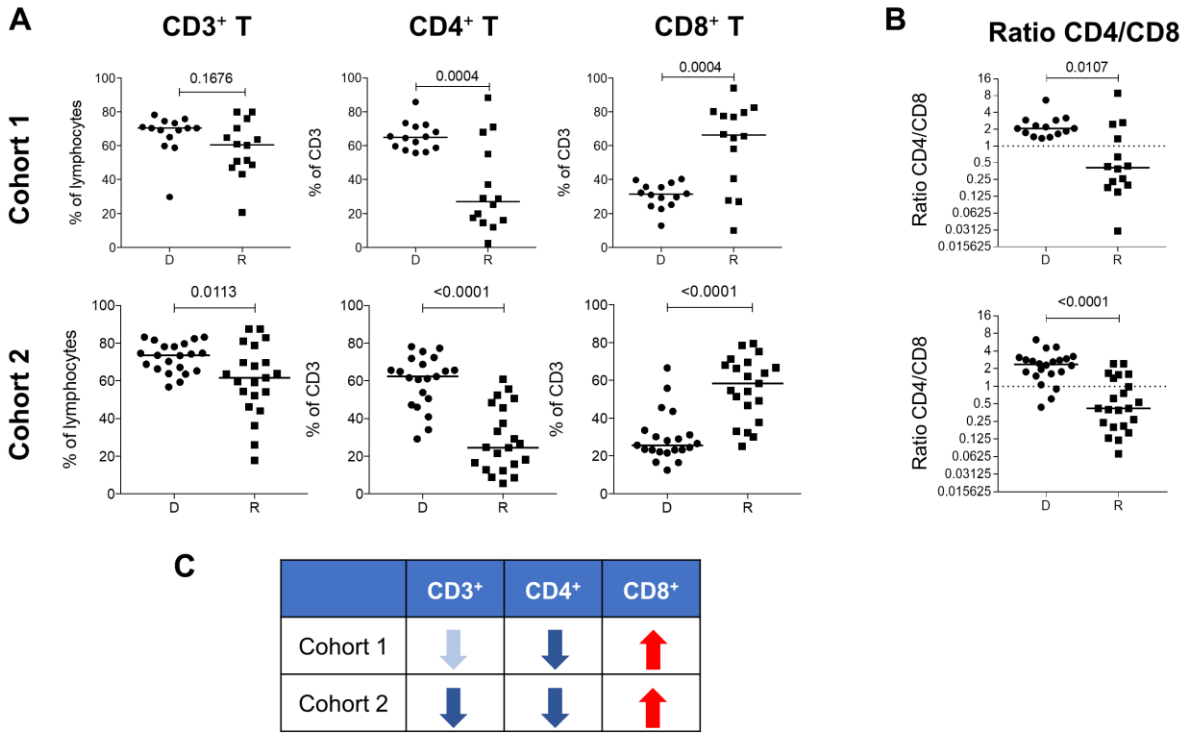

Figure 12 Incomplete reconstitution of the T cell compartment in recipients after HSCT
Shown are the (A) frequency of $CD3^+$ T cells within the lymphocyte population and the frequencies of $CD4^+$ and $CD8^+$ T cells within $CD3^+$ T cells and (B) the ratio of $CD4^+$ and $CD8^+$ T cells in recipients (R) at day 90 post-HSCT compared to their respective sibling donors (D) in cohort 1 (top graph) and cohort 2 (bottom graph). Horizontal bars indicate the median. P-values were calculated using a Wilcoxon matched-pairs t test (donor *versus* respective recipient) and are indicated above the graph. Differences are considered significant for P-values < 0.05. (C) Summary table of the differences observed in recipients compared to their donors. Red and blue arrows indicate a statistically significant increase or decrease of the cell population, whereas pink and light blue arrows indicate a trend towards an increase or decrease approaching statistical significance.

4.2.2 T cells migratory properties and T helper subsets

As shown in **Figure 13**, $CD4^+$ and $CD8^+$ T lymphocytes were identified on live $dump^-CD3^+$ T cells and within the $CD4^+$ T cell population we defined the following Th-like subsets: Th17-like as $CCR6^+CXCR3^-$, Th1-like as $CXCR3^+CCR6^-$, Th2-like as $CXCR3^-CCR6^-CRTH2^+$ and Tfh-like as $CXCR3^-CCR6^-CRTH2^-CXCR5^+$. PD1, initially included in the panel to better characterize Tfh cells, was not used for final quantification of Tfh cells due to insufficient events within the $CXCR5^+$ gate.

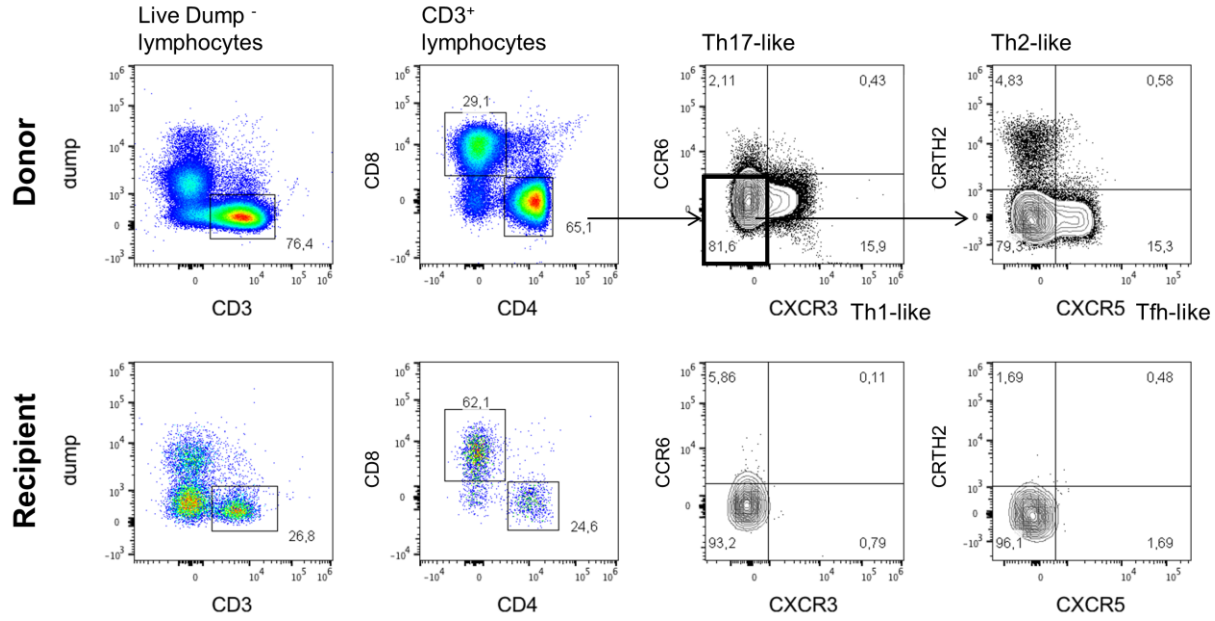

Figure 13 Identification of T cell subsets in donors and recipients
Gating strategy used to identify the different T cell subsets by polychromatic spectral flow cytometry. Representative example of staining on a donor sample (top panel) with the corresponding recipient (bottom panel).

Analysis of the expression of different chemokine receptors within the $CD4^+$ T cell compartment revealed no statistically significant differences between donors and recipients in cohort 1, whereas in cohort 2 we observed a decrease of the frequency of $CXCR3^+$ and $CXCR5^+$ cells and an increase of $CCR6^+$ cells in the recipients compared to their donors. No significant differences were observed concerning the expression of the Th2 marker CRTH2 (**Figure 14**). The discrepancy of results between the two cohorts could be explained by the fact that the staining procedure has been modified from cohort 1 to cohort 2 for the chemokine receptors CXCR3, CXCR5 and CRTH2. While the staining for the samples of cohort 1 has been carried out at 4°C,

in the second cohort we performed the staining for these markers at 37°C, leading to a more sensitive identification of expressing cells (Berhanu et al., 2003). We thus consider more reliable the results obtained in this second cohort.

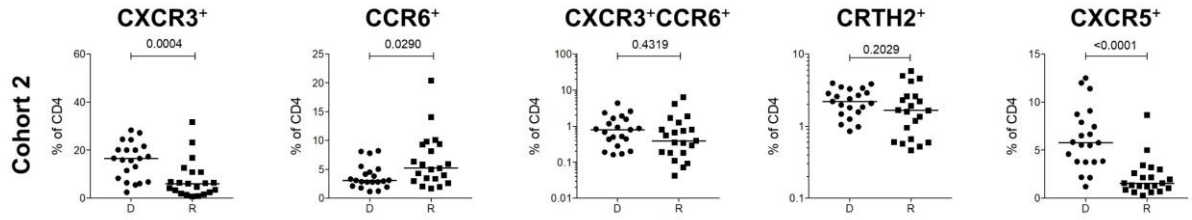

Figure 14 Chemokine receptors expression on CD4$^+$ T cells from donors and recipients
Frequencies of CXCR3$^+$, CCR6$^+$, CXCR3$^+$CCR6$^+$, CRTH2$^+$ and CXCR5$^+$ cells within the CD4$^+$ T cell compartment in recipients (R) at day 90 post-HSCT compared to their respective sibling donors (D) in cohort 2. Horizontal bars indicate the median. P-values were calculated using a Wilcoxon matched-pairs t test (donor *versus* respective recipient) and are indicated above the graph. Differences are considered significant for P-values < 0.05.

To gain insight into the migratory properties of CD8$^+$ T cells after transplantation, we also analysed the expression of CXCR3, CCR6, CRTH2 and CXCR5 within this cell subset (**Figure 15)**. This analysis was performed only in cohort 2, for which the chemokine receptors staining gave more reliable results (performed at 37°C). Compared to their respective donors, recipients had a significant lower frequency of CXCR3$^+$ CD8$^+$ T cells, similarly to what we observed within CD4$^+$ T cells. On the contrary, we found a significant increase of CXCR5$^+$ CD8$^+$ T cells in the recipients. However, the percentage of CD8$^+$ CXCR5$^+$ cells is low, being less than 2% of total CD8$^+$ T cells. No significant differences were observed in the frequency of CCR6$^+$, CXCR3$^+$CCR6$^+$ and CRTH2$^+$ cells.

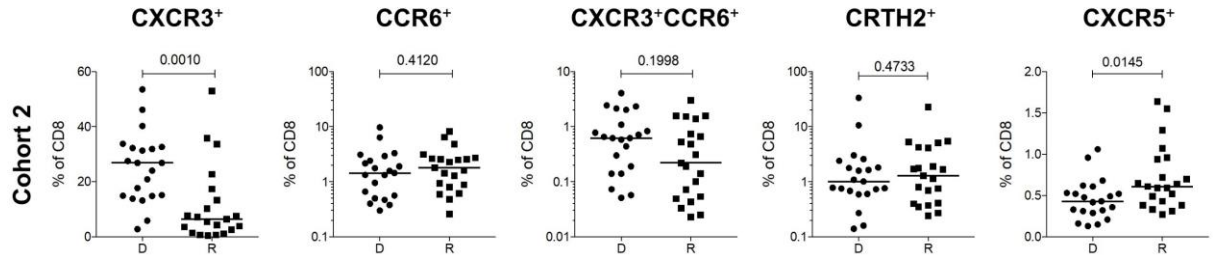

Figure 15 Chemokine receptors expression on CD8$^+$ T cells from donors and recipients
Frequencies of CXCR3$^+$, CCR6$^+$, CXCR3$^+$CCR6$^+$, CRTH2$^+$ and CXCR5$^+$ cells within the CD8$^+$ T cell compartment in recipients (R) at day 90 post-HSCT compared to their respective sibling donors (D) cohort 2. Horizontal bars indicate the median. P-values were calculated using a Wilcoxon matched-pairs t test (donor *versus* respective recipient) and are indicated above the graph. Differences are considered significant for P-values < 0.05.

CXCR3 and CCR6, while absent on naïve T cells, are upregulated upon T cell activation and are highly expressed on effector and memory T cells. CXCR3 is preferentially expressed on Th1 lymphocytes and effector $CD8^+$ T and regulates the migration of these cells towards sites of inflammation (Groom and Luster, 2011; Sallusto et al., 1998). CCR6 is expressed on several immune cells including IL17-producing Th17 cells, T regulatory cells and a subset of $CD8^+$ T cells with effector memory phenotype (Kondo et al., 2007; Singh et al., 2008; Yamazaki et al., 2008). Since its ligand CCL20 is expressed in tissues such as intestine and colon, it is thought that T cells expressing CCR6 are involved in mucosal immunity (Lee et al., 2013a).

CXCR5 has been identified as one of the defining hallmarks of Tfh cells and is important for entering the B cell zones in secondary lymphoid organs (Crotty, 2011; Moser, 2015). In the blood, $CD4^+CXCR5^+$ T cells are believed to represent a circulating memory compartment of Tfh lineage cells (Schmitt et al., 2014). CXCR5 is also expressed on a subset of memory $CD4^+$ T cells which have been proposed to be in a resting state and not involved in ongoing immune responses (Schaerli et al., 2000) as well as on a subset of effector memory $CD8^+$ T cells (Quigley et al., 2007).

Our results indicate that, in the absence of aGVHD, the transplantation procedure is associated with alterations of the migratory properties of both $CD4^+$ and $CD8^+$ T cells in the recipients compared to their respective donors. In particular we noted in the $CD4^+$ compartment an increase of cells able to migrate to mucosal sites ($CCR6^+$), whereas cells with a Th1-like ($CXCR3^+$) and Tfh-like ($CXCR5^+$) profile are decreased. The decrease of $CXCR3^+$ cells was also observed in the $CD8^+$ T cell population. On the other hand, within the $CD8^+$ compartment the percentage of $CXCR5^+$ cells is increased in the recipients, contrarily to what was observed within $CD4^+$ T cells.

The enrichment of $CCR6^+$ cells within the $CD4^+$ compartment could be linked to the inflammatory environment present in the recipients as a result of the tissue injury caused by the conditioning regimen administered prior to the infusion of the graft. Mucosal damage induced by the preparative regimen triggers the release of proinflammatory mediators, including TNFα, IL1 and IL6 leading to the establishment of an inflammatory milieu (Ramadan and Paczesny, 2015). The expression of both CCR6 and its ligand CCL20 has been reported to be upregulated by inflammatory stimuli (Lee et al., 2013a), suggesting that the increased frequency of CCR6-expressing cells after transplantation could be induced by inflammatory signals released as a consequence of the transplantation procedure.

In peripheral blood, $CXCR5^+CD8^+$ T cells were shown to be negative for CD69 and express CD127 (IL7Rα), suggesting to be in an inactive state and equipped to receive IL7 survival signals (Quigley et al., 2007). The increased percentage of $CXCR5^+CD8^+$ T cells in the recipients after transplantation could thus be due to an IL7-driven expansion of this cell subset. $CD4^+$ and $CD8^+$ $CXCR5^+$ T cells display different migratory properties (Quigley et al., 2007). The change in opposite direction observed in the recipients in these two cell types, decrease in $CD4^+$ and increase in $CD8^+$ T cells, regarding the percentage of CXCR5-expressing cells, could therefore reflect a different response of these two cell populations to the host environment post-HSCT.

4.2.3 Identification of naïve and memory T cell populations

We next assessed whether T cell reconstitution was associated with imbalances in naïve and memory T cell subsets distribution in the recipients after transplantation. In **Figure 16** is represented the gating strategy used to identify naïve and memory T cell populations in donors' and recipients' samples.

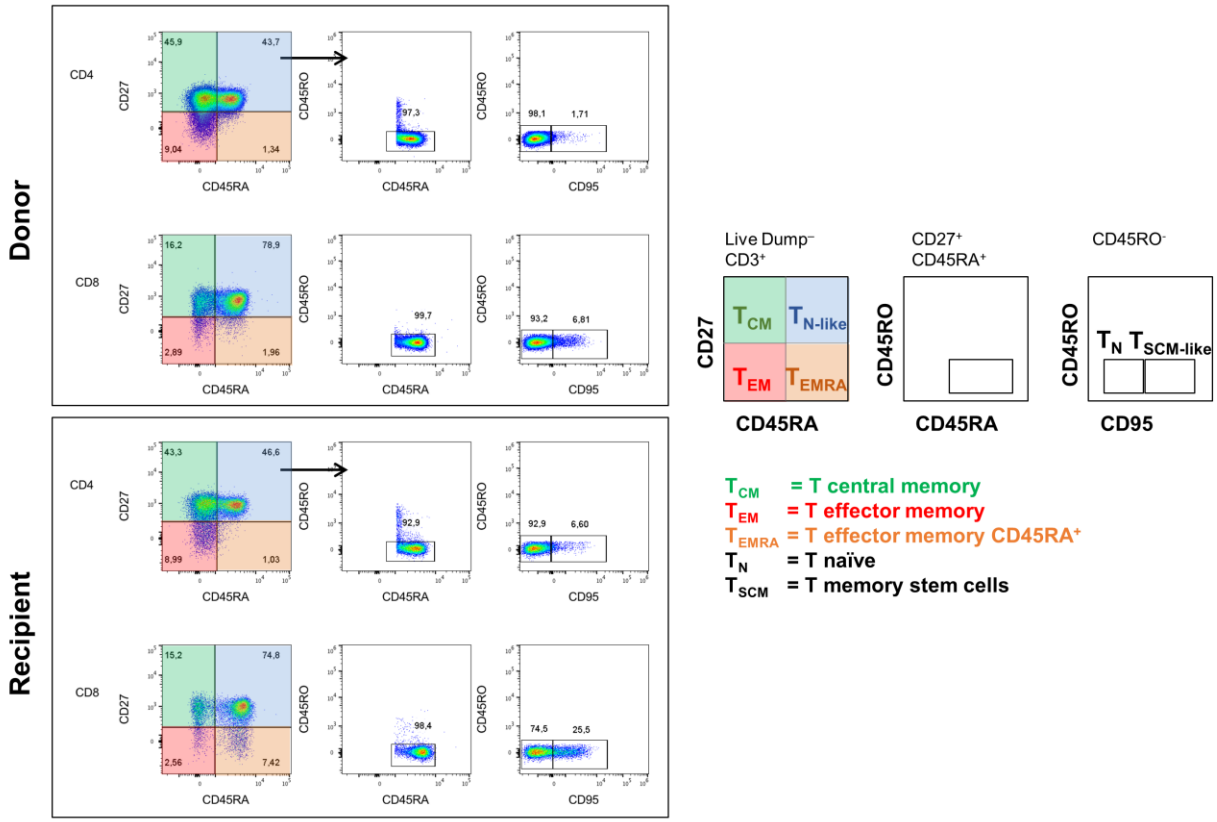

Figure 16 Identification of naïve and memory T cell subsets
Gating strategy used to identify naïve and memory subsets within the $CD4^+$ and $CD8^+$ T cell compartments in donors and recipients after transplantation by polychromatic flow cytometry. Representative example of staining on a donor (top panel) sample with the corresponding recipient (bottom panel).

We determined the frequency of naïve and memory subsets based on the expression of CD45RA and CD27 within $CD4^+$ and $CD8^+$ T lymphocytes: $CD45RA^+CD27^+$ naïve-like ($T_{N\text{-}like}$), $CD45RA^-CD27^+$ central memory (T_{CM}), $CD45RA^-CD27^-$ effector memory (T_{EM}), and $CD45RA^+CD27^-$ effector memory re-expressing the naïve marker CD45RA (T_{EMRA}). Within the $T_{N\text{-}like}$ subset we confirmed the negativity for the memory marker CD45R0 and we discriminated the real naïve cells from T stem cell memory ($T_{SCM\text{-}like}$) with the expression of CD95.

T_{SCM} represent a long-lived memory T cell subset with stem cell-like properties, characterized by the expression of markers reminiscent of naïve T cells (CD45RA and CD62L), but differently from naïve T cells and similarly to other memory subsets they express CD95 (Gattinoni et al., 2017). These cells have been shown to possess superior immune reconstitution ability, giving rise to all memory and effector T cell subsets, while maintaining their own pool size through self-renewal. They also display high anti-tumour activity in mice (Gattinoni et al., 2011; Zhang et al., 2005). Human T_{SCM} can be identified as $CD45RA^+$ $CD45R0^-$ $CCR7^+$ $CD62L^+$ $CD28^+$ $CD27^+$ $IL7R\alpha^+$ $CXCR3^+$ $CD95^+$ $CD11a^+$ $IL2R\beta^+$ $CD58^+$ $CD57^-$ cells (Gattinoni et al., 2017). Given the limited number of markers used in our study to define this cell subset compared to the extensive phenotypic characterization described in the literature, we will refer to these cells as $T_{SCM\text{-}like}$, indicating the expression of CD95 on an otherwise phenotypically naïve T cell subset.

Compared to their donors, recipients post-HSCT had a significant reduction of $CD4^+$ naïve T cells paralleled by an increase of effector memory T cells in both cohorts. We also observed an increase of the terminally differentiated T_{EMRA} subset in the recipients, but this increase reached statistical significance only in cohort 1, while just a trend towards an increase is present in cohort 2. No significant differences were observed in the frequency of $T_{SCM\text{-}like}$ and T_{CM} cells between donors and recipients (**Figure 17**).

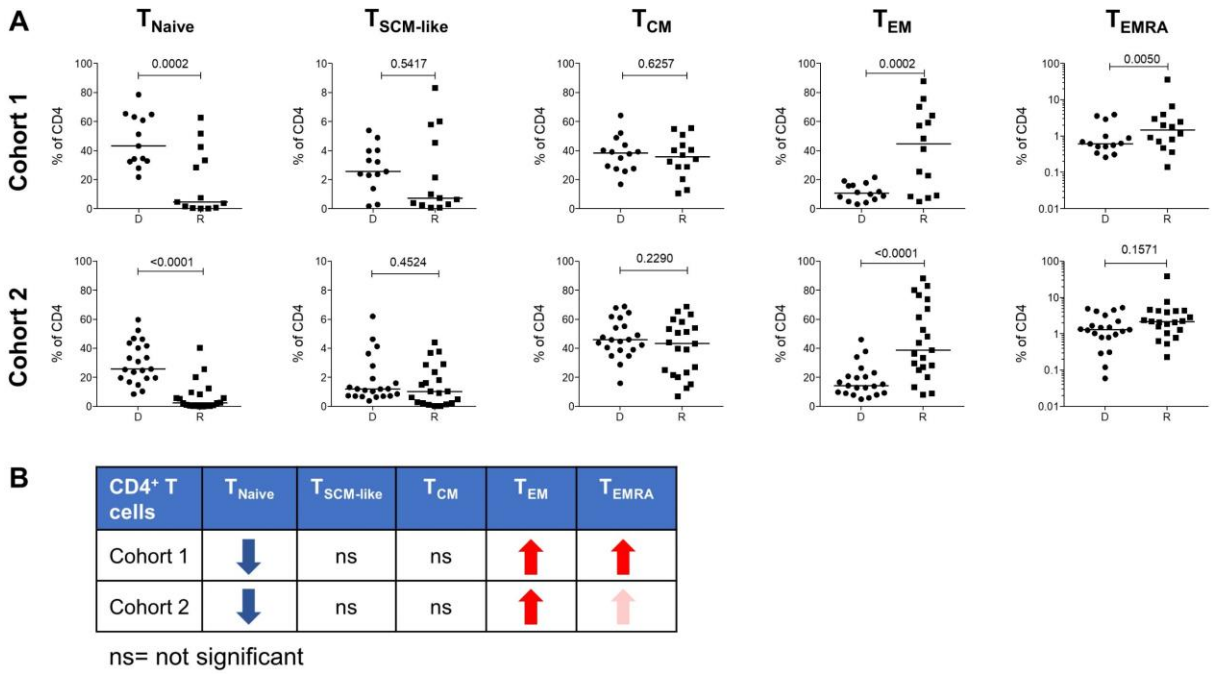

Figure 17 Depletion of CD4$^+$ naïve T cells and increase of cells with an effector memory phenotype in recipients after transplantation

(A) Frequencies of T_{Naive}, $T_{SCM\text{-}like}$, T_{CM}, T_{EM} and T_{EMRA} cells within the CD4$^+$ T cell compartment in recipients (R) at day 90 post-HSCT compared to their respective sibling donors (D) in cohort 1 (top graph) and cohort 2 (bottom graph). Horizontal bars indicate the median. P-values were calculated using a Wilcoxon matched-pairs t test (donor *versus* respective recipient) and are indicated above the graph. Differences are considered significant for P-values < 0.05. (B) Summary table of the differences observed in recipients compared to their donors. Red and blue arrows indicate a statistically significant increase or decrease of the cell population whereas pink and light blue arrows indicate a trend towards an increase or decrease approaching statistical significance.

Within CD8$^+$ T cells (**Figure 18**), we observed a very similar picture than in the CD4$^+$ T cell compartment, with an important decrease of naïve T cells in the recipients and an increase of cells with an effector memory phenotype. Moreover, we noted a decrease of $T_{SCM\text{-}like}$ (significant in cohort 1, trend in cohort 2) and a decrease of T_{CM} cells (cohort 1) in the recipients. More striking than in the CD4$^+$ compartment is the increase of T_{EMRA} cells in the recipients, consistent with their initial identification within CD8$^+$ T cells (Hamann et al., 1997) and with the more extensive body of literature characterizing these cells within the CD8$^+$ compartment (Sallusto et al., 1999; Tilly et al., 2017; Verma et al., 2017; Willinger et al., 2005; Yap et al., 2014). T_{EMRA} cells have been characterized as a terminally differentiated subset (Sallusto et al., 1999), a proportion of which expresses the senescence marker CD57 (Hamann et al., 1997; Verma et al., 2017). These cells respond vigorously to IL15 stimulation (Tilly et al., 2017), thus the enrichment we observe in the

recipients after transplantation could be driven by the increased availability of this cytokine in the post-HSCT environment (Dulphy et al., 2008; Matsuoka et al., 2010) as well as the chronic stimulation induced by host alloantigens.

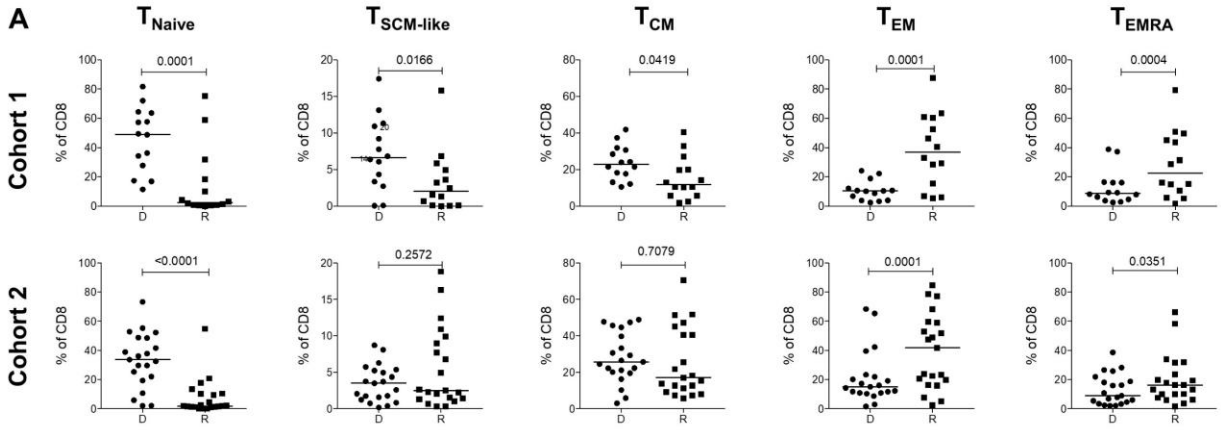

B

CD8⁺ T cells	T_{Naive}	$T_{SCM\text{-}like}$	T_{CM}	T_{EM}	T_{EMRA}
Cohort 1	↓	↓	↓	↑	↑
Cohort 2	↓	↓	ns	↑	↑

ns= not significant

Figure 18 Depletion of CD8⁺ naïve T cells and increase of cells with an effector memory phenotype in recipients after transplantation

(A) Frequencies of T_{Naive}, $T_{SCM\text{-}like}$, T_{CM}, T_{EM} and T_{EMRA} cells within the $CD8^+$ T cell compartment in recipients (R) at day 90 post-HSCT compared to their respective sibling donors (D) in cohort 1 (top graph) and cohort 2 (bottom graph). Horizontal bars indicate the median. P-values were calculated using a Wilcoxon matched-pairs t test (donor *versus* respective recipient) and are indicated above the graph. Differences are considered significant for P-values < 0.05. (B) Summary table of the differences observed in recipients compared to their donors. Red and blue arrows indicate a statistically significant increase or decrease of the cell population whereas pink and light blue arrows indicate a trend towards an increase or decrease approaching statistical significance.

Our data revealed that recovering T cells at day 90 post-HSCT display a phenotype of effector memory T cells with a depletion of the naïve T cells pool in both $CD4^+$ and $CD8^+$ compartments. Results observed in cohort 1 were replicated in the second cohort. Our observations are in line with data in the literature showing that recovery of the T cell compartment early after transplantation relies mainly on the thymic-independent peripheral expansion of memory T cells present in the graft inoculum, driven by cytokines as well as allogeneic antigens encountered in the host (Fry and Mackall, 2005; Toubert et al., 2012).

4.2.4 Proliferation of T cells in recipients after HSCT

Throughout adult life, the size and the composition of the peripheral T cell pool is tightly regulated and, in the absence of disease states, the number of circulating lymphocytes is maintained at a relatively constant level through mechanisms of cell survival, division and death (Freitas and Rocha, 2000; Goldrath and Bevan, 1999a).

In the HSCT clinical setting, the preparative regimen administered to the patients before the infusion of the stem cell graft has the dual purpose of eradicating cancer cells, when the disease is neoplastic, and suppress the recipient's immune system to allow the engraftment of the transplanted donor's stem cells (Vriesendorp, 2003). Following HSCT, the recovery of the peripheral T cell pool is a dynamic process that also relies on homeostatic signals to restore normal levels of each T cell population. Once transplanted in the host, donor cells encounter a lymphopenic environment with high bioavailability of the homeostatic cytokines IL7 and IL15 and undergo proliferation to replenish the lymphocyte pool (Tchao and Turka, 2012).

To assess the proliferative response of donor T cells in recipients after HSCT, we quantified the expression of Ki-67 within the different naïve and memory T cell subsets described in the previous section. Ki-67 is a critical protein for cell division and is expressed exclusively by proliferating cells (Scholzen and Gerdes, 2000). Compared to the donors, we observed in the recipients a statistically significant increase of proliferation of all the T cell subsets investigated in both the $CD4^+$ and $CD8^+$ compartments as depicted in **Figure 19**. For $CD8^+$ T_{EMRA} in cohort 1, the increase of proliferating cells in the recipients did not reach statistical significance, but a trend towards an increase is present. Proliferation of the $T_{SCM\text{-}like}$ subset could be assessed only for cohort 1, as for cohort 2 the intracellular staining panel was modified and the marker CD95 was removed to include CD25 and CD127 to better identify T regulatory cells. Naïve T cells are thus defined in the second cohort as $CD45RA^+CD27^+$ without further discrimination of T_{SCM} cells with CD95 expression.

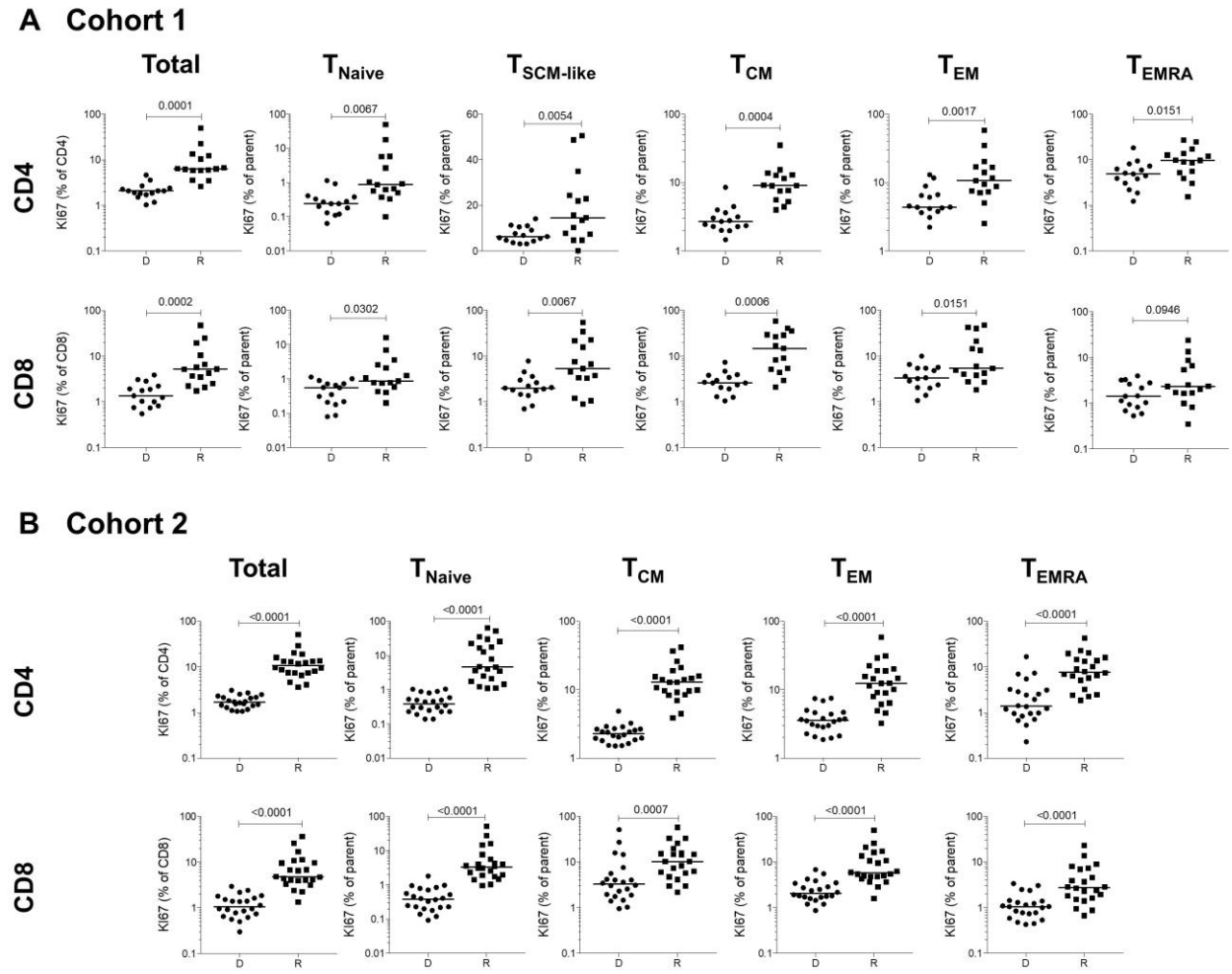

Figure 19 Proliferation of T cell subsets in recipients after transplantation
Frequency of proliferating Ki-67$^+$ cells in total CD4$^+$ and CD8$^+$ T cells and in the different naïve and memory subsets in both the CD4$^+$ and CD8$^+$ compartements in donors (D) and recipients (R) from cohort 1 (A, top panel) and cohort 2 (B, bottom panel). The frequency of Ki-67$^+$ cells is represented as percentage of Ki-67-expressing cells within total CD4$^+$ or CD8$^+$ T cells and as percentage Ki-67-expressing cells within the parent gate for T_{Naive}, $T_{SCM-like}$, T_{CM}, T_{EM} and T_{EMRA} subsets. Horizontal bars indicate the median. P-values were calculated using a Wilcoxon matched-pairs t test (donor *versus* respective recipient) and are indicated above the graph. Differences are considered significant for P-values < 0.05

Taken together, the results described in this section, showed that in recipients not developing aGVHD, three months after transplantation there is an incomplete reconstitution of the T cell compartment, especially for CD4$^+$ T cells that recover later than CD8$^+$ T cells. This observation is in line with a more efficient homeostatic expansion within the CD8$^+$ compartment, that leads to the characteristic inversion of the CD4/CD8 ratio post-HSCT (Seggewiss and Einsele, 2010).

We also observed in the recipients a depletion of the naïve T cell pool with an increase of cells with an effector memory phenotype. This might be explained by the fact that initial recovery of

the T cell compartment relies on the expansion of memory cells and by the fact that naïve T cells undergoing lymphopenia-induced proliferation acquire phenotypical and functional features of memory cells, thus leading to a skewing of the lymphocyte pool toward a memory phenotype (Sprent and Surh, 2011; Tchao and Turka, 2012).

We noted that the frequency of the different T cell subpopulations, in particular $CD4^+$, $CD8^+$ T cells and naïve and memory subsets, is highly heterogeneous in the recipients group compared to the donors, indicating a high degree of inter-individual variation amongst the recipients with respect to the recovery of the different T cell populations.

Assessment of Ki-67 expression revealed an increased proliferation of $CD4^+$ and $CD8^+$ naïve and memory T cell subsets in the recipients compared to their donors despite the administration of immunosuppressive GVHD prophylactic regimen (CSA, CSA+MTX or CSA+MMF). This important proliferation may be driven by the homeostatic cytokines IL7 and IL15, whose availability is increased in the lymphopenic environment of the host (Matsuoka et al., 2010; Thiant et al., 2016), and by the presence of alloantigens. It has been reported that homeostatic peripheral expansion results in an augmented propensity of cells to proliferate in response to weak antigens in lymphopenic environments (Fry and Mackall, 2005), suggesting that the extensive proliferation of all cell subsets analysed in the recipients in the absence of aGVHD may represent an homeostatic mechanism to replenish the T cell pool in the “empty” host following transplantation.

4.2.5 Regulatory T cell homeostasis after HSCT

We next investigated the dynamics of reconstitution of $CD4^+$ Treg cells in patients not developing aGVHD after transplantation compared to their donors. As depicted in **Figure 20**, we defined Treg cells within the $CD4^+$ population based on the expression of Foxp3. Within the $CD4^+Foxp3^+$ Treg population we assessed the expression of the functional markers CTLA4, ICOS and PD1 as well as the proliferation marker Ki-67. Statistical analysis of the frequency of Treg cells as well as of the percentages of CTLA4-, ICOS- and PD1-expressing cells within the $Foxp3^+$ population was performed only for cohort 2, due to technical difficulties in obtaining a reproducible Foxp3 staining in cohort 1.

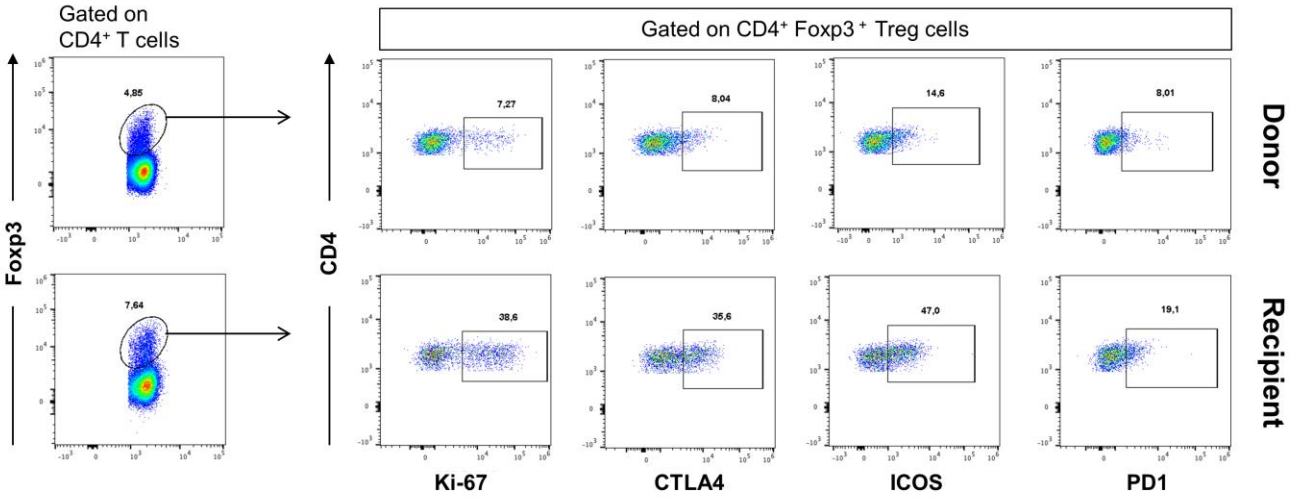

Figure 20 Treg homeostasis in recipients after HSCT
Gating strategy used to identify $Foxp3^+$ Treg cells within the $CD4^+$ T cell compartment (left part of the panel) and analysis of the expression of Ki-67, CTLA4, ICOS and PD1 within the Treg subset (right part of the panel) in donors and recipients after transplantation by polychromatic flow cytometry. Representative example of staining on a donor sample (top) with the corresponding recipient (bottom).

Interestingly, in the absence of aGVHD, three months after transplantation we observed in the recipients a significant increase of $CD4^+Foxp3^+$ Treg cells compared to the donors (**Figure 21**). In addition, we noted an increased frequency of Ki-67^+ Treg cells in the recipients. Consistent with the study from Matsuoka and colleagues describing increased proliferation within Treg cells compared to conventional T cells after HSCT, also our data revealed an increased frequency of Ki-67^+ cells in the Treg population as compared to conventional $CD4^+$ T cells in recipients following transplantation (median Ki-67^+ cells within Treg=22.35%, $CD4^+$ T cells=10.37%, P-value < 0.0001). These data indicate that in the lymphopenic environment of the host both

conventional CD4$^+$ T cells and Treg cells undergo strong proliferation compared to healthy donors and cell proliferation is most evident for Treg cells after HSCT (Matsuoka et al., 2010).

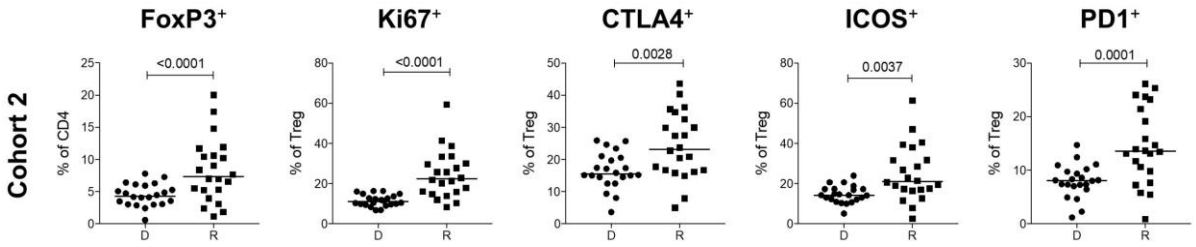

Figure 21 Treg homeostasis in recipients after HSCT
Frequency of Foxp3$^+$ cells within the CD4$^+$ population and frequencies of Ki-67$^+$, CTLA4$^+$, ICOS$^+$ and PD1$^+$ cells within the Foxp3$^+$ Treg population in donors (D) and recipients (R) at day 90 post-HSCT in cohort 2. Horizontal bars indicate the median. P-values were calculated using a Wilcoxon matched-pairs t test (donor *versus* respective recipient) and are indicated above the graph. Differences are considered significant for P-values < 0.05.

In the recipients after HSCT, we also observed an enrichment of CTLA4$^+$, ICOS$^+$ and PD1$^+$ Treg cells. CTLA4 is a crucial molecule for the immunosuppressive function of Tregs. It has been shown to interact with CD86 and CD80 on dendritic cells limiting their ability to stimulate naïve T cells through CD28 and thus resulting in immune suppression (Wing et al., 2008). ICOS is a costimulatory receptor expressed on activated T cells. Based on the expression of ICOS, Ito and colleagues identified two subsets of Treg cells with different properties. In particular, they found that ICOS$^+$ Foxp3$^+$ Treg cells used IL10 to suppress dendritic cell function and transforming growth factor β (TGFβ) to suppress T cell function, whereas ICOS$^-$Foxp3$^+$ Treg cells used TGFβ only (Ito et al., 2008). PD1, a coinhibitory receptor, has been reported to be upregulated on Treg cells during IL2 therapy to treat cGVHD. The authors propose that PD1 might be implicated in the homeostatic regulation of Tregs by inhibiting excessive proliferation and stabilizing Treg homeostasis during IL2 therapy (Asano et al., 2017). Upregulation of these markers within the Treg population in recipients without aGVHD after transplantation might suggest a mechanism aimed at counterbalancing the proinflammatory environment of the host in order to suppress alloreactivity and maintain tolerance.

4.3 Analysis of immune reconstitution early after HSCT

In order to assess immune reconstitution and T cell dynamics also at an early time point after transplantation, we analysed a third cohort that includes freshly collected samples from 26 donor-recipient pairs recruited at St. Louis Hospital (cohort 3). In this cohort donors' samples were collected before the transplantation procedure as for the two cohorts described in the previous sections, and recipients' samples were collected either at aGVHD onset or at day 30 (instead of day 90) for recipients that did not develop aGVHD. In this part of the project we thus aimed at characterizing the T cell compartment at the time of engraftment, 30 days after transplantation.

4.3.1 Absolute numbers of T, B and NK cells in recipients early after HSCT

Because immune reconstitution is highly variable after HSCT, it is of critical importance to have precise cell counts of the major lymphocyte populations in the recipients, in particular at an early time point after transplantation. We therefore performed TBNK TruCount assays (BD Biosciences) that allow to determine the absolute counts of T cells ($CD3^+$, $CD4^+$, $CD8^+$ T cell subsets), B cells ($CD19^+$) and Natural Killer cells ($CD56^+CD16^{+/-}$) in only 50µl of whole blood. The detailed procedure and the formula used to determine the absolute cell counts are described in the Materials and Methods section. The gating strategy used to define the lymphocyte subsets is depicted in **Figure 22.**

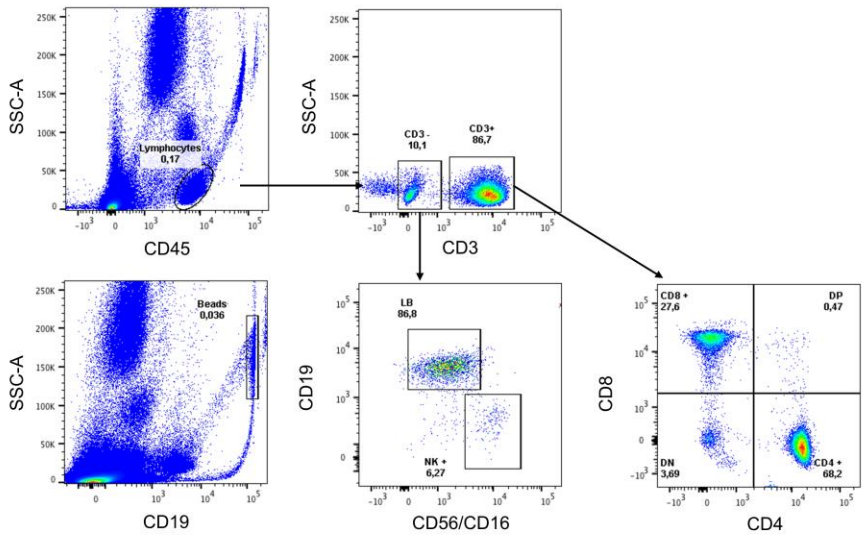

Figure 22 TBNK TruCount assay gating strategy
Representative flow cytometric profile of a donor's sample depicting the gating strategy used to define T, B and NK cell absolute counts in donors and recipients' samples. DP= $CD4^+CD8^+$ double positive T cells; DN= $CD4^-CD8^-$ double negative T cells; LB= $CD19^+$ B cells; NK= $CD56^+CD16^{+/-}$ Natural Killer cells.

Absolute counts showed a decrease of all the major lymphocyte subsets in recipients at day 30 post-HSCT compared to their donors, except for the Natural Killer (NK) cell population that remained stable **(Figure 23A**). Even if the median level of NK cells in the recipients is comparable to the one present in the donors, the distribution is highly heterogenous within the recipients' group, ranging from zero to more than 600 cells/µl, indicating a high degree of variability in the reconstitution of this cell subset at this early time point. Consistent with data in the literature reporting a delayed recovery of B lymphocytes after HSCT (Ogonek et al., 2016), the absolute counts of these cells were very low in the recipients (median=3 cells/µl) at day 30 post-HSCT.

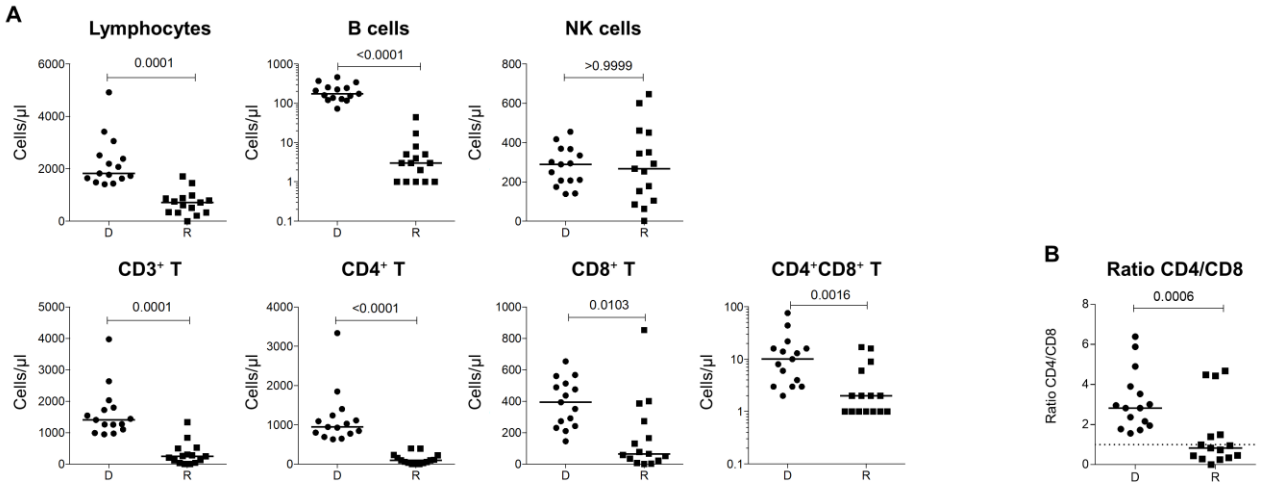

Figure 23 Decrease of all major lymphocyte populations in recipients early after HSCT
Absolute counts of total lymphocytes, CD19$^+$ B cells, CD56$^+$CD16$^{+/-}$Natural Killer (NK) cells; CD3$^+$ T cells, CD4$^+$ T cells, CD8$^+$ T cells and CD4$^+$CD8$^+$ double positive T cells (A) and the ratio of CD4$^+$ and CD8$^+$ T cells (B) in donors (D) and recipients (R) 30 days after HSCT in cohort 3. Cell counts are expressed as number of cells/µl of whole blood. Horizontal bars indicate the median. P-values were calculated using a Wilcoxon matched-pairs t test (donor *versus* respective recipient) and are indicated above the graph. Differences are considered significant for P-values < 0.05.

4.3.2 T cell dynamics early after HSCT

Similarly to what we observed three months after transplantation, at day 30 post-HSCT we found, in the absence of aGVHD, a decreased frequency of CD3$^+$ T cells in the recipients compared to their donors and within the CD3$^+$ population we noted a decrease of CD4$^+$ and an increase of CD8$^+$ T cells. Absolute counts showed a decrease of both CD4$^+$ and CD8$^+$ T cells in the recipients, however, within the CD3$^+$ population the frequency of CD4$^+$ is decreased and the one of CD8$^+$ cells is increased, showing that the inversion of the CD4/CD8 ratio observed at day 90 post-HSCT is already detectable at this early time point. The ratio between CD4$^+$ and CD8$^+$ T cells in donors

and recipients calculated on the absolute cell counts and on the cell frequencies is shown in **Figure 23B** and **Figure 24B**, respectively. The frequency of TCRγδ$^+$ T cells was not significantly different, even though a trend towards an increase is present in the recipients **(Figure 24A**).

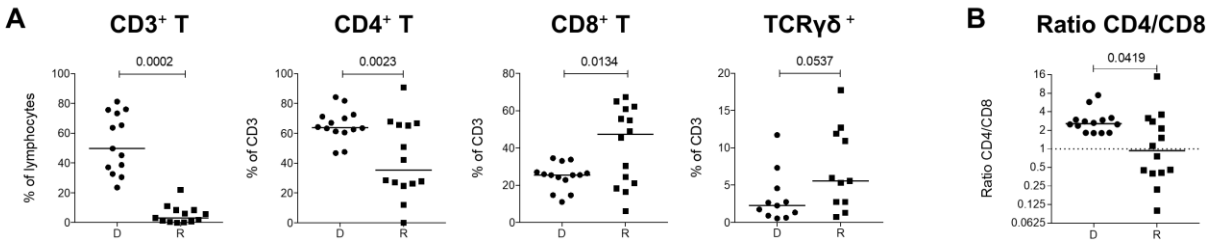

Figure 24 Decrease of CD4$^+$ and increase of CD8$^+$ T cells in recipients early after HSCT
Frequency of CD3$^+$ T cells within the lymphocyte population and the frequencies of CD4$^+$, CD8$^+$ and TCRγδ$^+$ T cells within CD3$^+$ T cells (A) and the ratio of CD4$^+$ and CD8$^+$ T cells (B) in recipients (R) at day 30 post-HSCT compared to their respective sibling donors (D) in cohort 3. Horizontal bars indicate the median. P-values were calculated using a Wilcoxon matched-pairs t test (donor *versus* respective recipient) and are indicated above the graph. Differences are considered significant for P-values < 0.05.

Analysis of the different naïve and memory subsets early after HSCT showed a decrease of the naïve T cell pool in both CD4$^+$ and CD8$^+$ compartments in the recipients. This decrease was statistically significant within CD4$^+$ T cells and approaching significance in the CD8$^+$ compartment. Contrarily to what we observed at day 90 post-HSCT, at this early time point we could not detect the increase of effector memory cells in the recipients. However, a trend towards an increase of T_{EM} is present within the CD4$^+$ population. No significant differences were found in the frequency of $T_{SCM\text{-}like}$, T_{CM} and T_{EMRA} subsets between donors and recipients (**Figure 25**).

Due to technical difficulties in obtaining a reproducible Foxp3 staining and changes in the flow cytometry panel within this cohort of samples, statistical analysis of the cell proliferation of the different naïve and memory subsets and assessment of the Treg population is not reported.

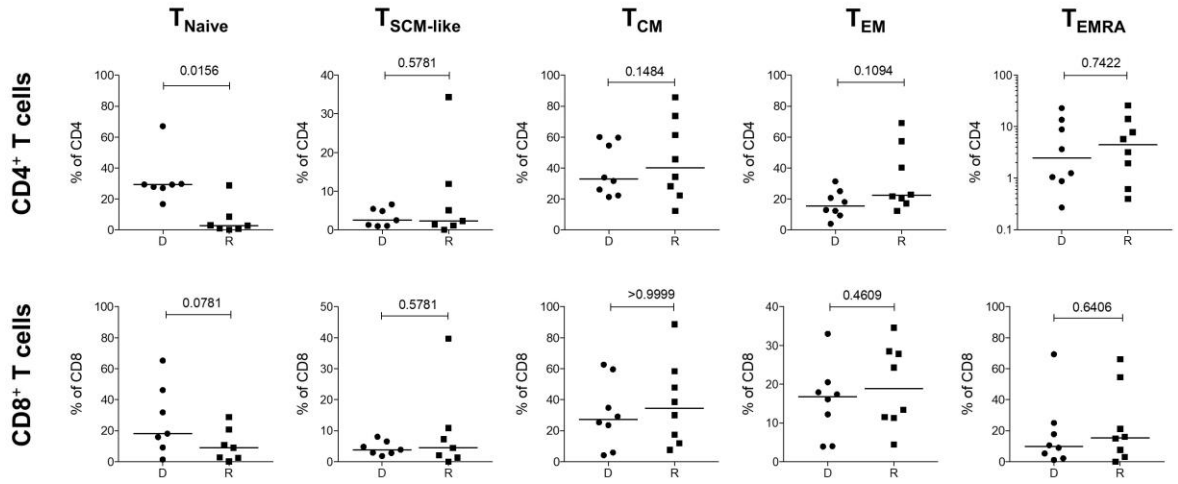

Figure 25 Decrease of naïve T cells in recipients early after HSCT
Frequencies of T_{Naive}, $T_{SCM\text{-}like}$, T_{CM}, T_{EM} and T_{EMRA} cells within the $CD4^+$ (top graph) and $CD8^+$ (bottom graph) T cell compartment in recipients (R) at day 30 post-HSCT compared to their respective sibling donors (D) in cohort 3. Horizontal bars indicate the median. P-values were calculated using a Wilcoxon matched-pairs t test (donor *versus* respective recipient) and are indicated above the graph. Differences are considered significant for P-values < 0.05.

In summary, immunophenotyping to assess T cell reconstitution in recipients after HSCT revealed several homeostatic imbalances compared to the donor's immune system before transplant. In particular, we observed an incomplete reconstitution of the T cell compartment, especially for $CD4^+$ T cells, with an inversion of the CD4/CD8 ratio both at one and three months after transplantation. Moreover, the reconstitution of the T cell compartment is characterized by a marked shift in the effector memory phenotype of these cells, with a depletion of the naïve T cell pool. While the decrease of naïve T cells was already detectable at day 30 post-HSCT, skewing of the T cell compartment toward a memory phenotype was observed only three months after transplantation. In the recipients all naïve and memory T cell subsets displayed increased proliferation compared to the donors, suggesting that in the "empty" environment of the host following the preparative regimen, donor cells undergo extensive proliferation to replenish the lymphocyte pool. Interestingly, we also observed an increased percentage of $CD4^+$ $Foxp3^+$ Treg cells in the recipients after transplantation. Within the Treg subset in the recipients we found increased percentages of proliferating cells as wells as an enrichment of CTLA4-, PD1- and ICOS-expressing cells, suggesting that also Treg homeostasis might be altered by the lymphopenic and proinflammatory environment of the host after HSCT.

4.4 Cellular correlates of GVHD onset

Immune competent donor cells transplanted with the graft are essential for providing immune surveillance and mediating the beneficial GVL effect. However, donor T cells can also mediate the detrimental graft-versus-host reaction, in which host normal tissues are recognized as foreign and attacked (Korngold and Sprent, 1978; Porter et al., 1994).

Amongst the patients included in our analysis, 19 in cohort 1, 16 in cohort 2 and 11 in cohort 3 developed aGVHD within day 100 post-HSCT (median day of GVHD onset: cohort 1=36; cohort 2=29; cohort 3=39). Given the key role of T cells in mediating GVHD, we thus assessed whether the frequency of different T cell subsets and their proliferative status was altered in recipients developing aGVHD compared to patients without aGVHD in order to identify potential "pathogenic" cell subsets associated with aGVHD onset.

4.4.1 Increased frequency of $CD4^+$ T cells and decrease of $CD8^+$ T cells at GVHD onset

We first evaluated the frequency of $CD3^+$, $CD4^+$ and $CD8^+$ T cells in recipients at aGVHD onset, before administration of the steroid therapy, compared to the recipients without aGVHD. $CD4^+$ and $CD8^+$ T cell subsets have been defined with the same gating strategy described previously in **Figure 13**. As shown in **Figure 26**, at GVHD onset we observed a significant decrease of the percentage of $CD3^+$ T cells within the lymphocyte population, but this decrease reached statistical significance only in cohort 1. The $CD3^+$ T cell compartment of recipients at GVHD onset was characterized by an increased frequency of $CD4^+$ T cells and a decrease of $CD8^+$ T cells. However, the increase in $CD4^+$ T cells was statistically significant only in cohort 1, while a trend towards an increase approaching significance is present in cohort 2. Recipients at GVHD onset are thus characterized by a CD4/CD8 ratio that is generally, but not in all patients, greater than one, indicating increased percentages of $CD4^+$ T cells and decreased $CD8^+$ T cells (**Figure 26B**). No significant differences were observed in the frequency of TCR $\gamma\delta^+$ T cells at GVHD onset in cohort 1 (data not shown).

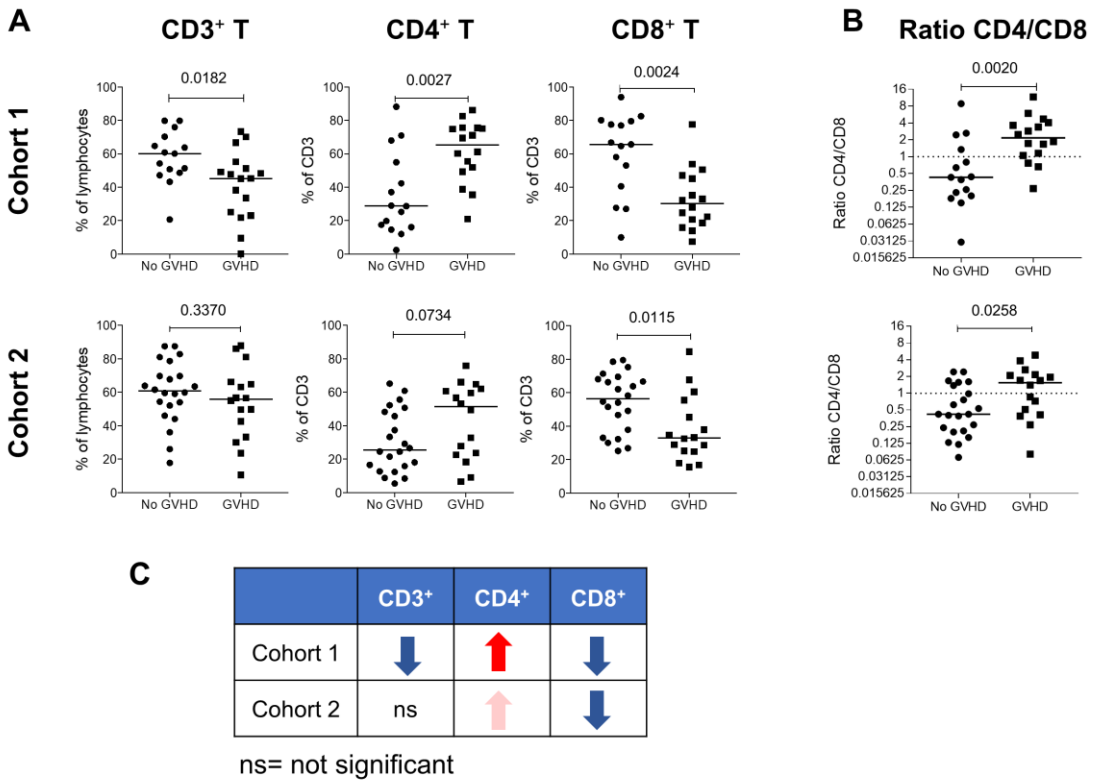

Figure 26 Increase of CD4$^+$ and decrease of CD8$^+$ T cells at GVHD onset compared to recipients without GVHD

Frequency of CD3$^+$ T cells within the lymphocyte population and frequencies of CD4$^+$, CD8$^+$ and TCR$\gamma\delta^+$ T cells within CD3$^+$ T cells (A) and the ratio of CD4$^+$ and CD8$^+$ T cells (B) in recipients at GVHD onset compared to recipients without GVHD in cohort 1 (top graph) and cohort 2 (bottom graph). Horizontal bars indicate the median. P-values were calculated using a Mann-Whitney test (GVHD *versus* No GVHD) and are indicated above the graph. Differences are considered significant for P-values < 0.05. (C) Summary table of the differences observed in recipients at GVHD onset compared to recipients without GVHD. Red and blue arrows indicate a statistically significant increase or decrease of the cell population whereas pink and light blue arrows indicate a trend towards an increase or decrease approaching statistical significance.

We next wanted to characterize the frequency of the different T cell subsets based on their migratory properties at GVHD onset. However, when comparing recipients with and without GVHD for the relative frequency of CXCR3$^+$, CCR6$^+$, CXCR3$^+$CCR6$^+$, CRTH2$^+$ and CXCR5$^+$ cells within the CD4$^+$ T cell compartment we could not detect any significant differences. **(Figure 27A)**. Within CD8$^+$ T cells, we observed at GVHD onset an increase of CXCR3$^+$CCR6$^+$, of CRTH2$^+$ and of CXCR5$^+$ cells (**Figure 27B)**. Shown are the data for cohort 2, for which the staining was performed at 37°C.

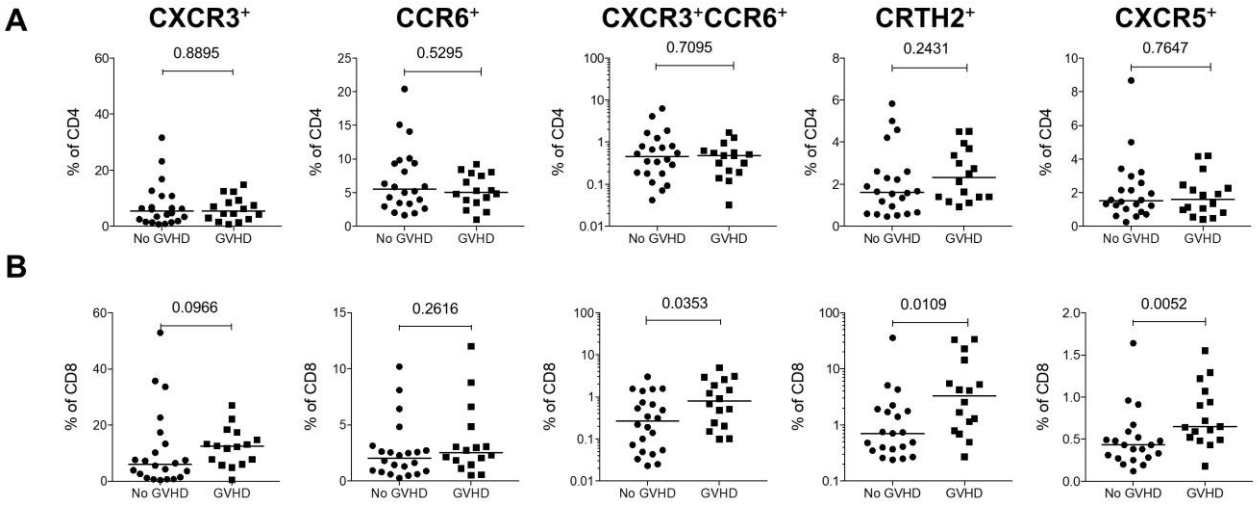

Figure 27 No significant differences in Th-like subsets at GVHD onset
Frequencies of CXCR3$^+$, CCR6$^+$, CXCR3$^+$CCR6$^+$, CRTH2$^+$ and CXCR5$^+$ cells within the CD4$^+$ (A) and CD8$^+$ (B) T cell compartments in recipients at GVHD onset compared to recipients without GVHD in cohort 2. Horizontal bars indicate the median. P-values were calculated using a Mann-Whitney test (GVHD *versus* No GVHD) and are indicated above the graph. Differences are considered significant for P-values < 0.05.

Taken together, these data indicate that within circulating T cells at GVHD onset there is a decreased frequency of CD8$^+$ T cells and an increase of CD4$^+$ T cells with no significant differences in the migratory properties of the latter. However, within CD8$^+$ T cells we could detect an increased percentage of cells able to migrate to inflamed and mucosal tissues (CXCR3$^+$CCR6$^+$) suggesting that these cells could be more prone to leave the periphery to migrate to GVHD target organs.

CRTH2 expression has been described on both CD4$^+$ and CD8$^+$ T cells and is associated with a Th2/Tc2 phenotype (Cosmi et al., 2000). Tc2 cells mediate cytotoxic effects mainly through perforin-mediated cytolysis (Fowler and Gress, 2000) and they appear to offer a favourable profile with regard to their ability to mediate GVL rather than GVHD (Fowler et al., 1996). However, in these studies Tc2 cells were defined based on their cytokine secretion profile without assessment of CRTH2 expression. The role of CRTH2-expressing CD8$^+$ T cells in the context of human acute GVHD remains unclear.

Within the CD8$^+$ T cell compartment CXCR5 has been reported to be expressed on a subset of effector memory cells (Quigley et al., 2007). Although being mainly localized within lymphoid organs, a minor fraction of human CXCR5$^+$ CD8$^+$ T cells also circulate in peripheral blood. However, the phenotype of these circulating cells is different compared to the one of cells confined

in the lymphoid follicles. In particular, it was described that these cells express higher CD62L and CD127, lower CCR5 and CD69 and lack CCR7. This suggests that these cells could egress from lymphoid organs, enter the circulation, and possibly migrate to inflamed tissues (Perdomo-Celis et al., 2017).

4.4.2 Increase of $T_{SCM\text{-}like}$ cells at GVHD onset

Evidence from studies conducted in the past decade has shown that different T cell subsets play different roles in GVHD and GVL in both murine models and human patients. Naïve T cells are believed to be the main cell subset involved in mediating GVHD, whereas memory T cells do not seem to cause GVHD, while preserving T cell immunity for GVL and protection against infections. Collectively, evidence suggests that memory T cells mediate a different type of alloreactivity compared to naïve T cells (Huang and Chao, 2017). However, the precise role of $CD4^+$ and $CD8^+$ naïve and memory subsets in GVHD pathogenesis is still incompletely understood, with studies associating the proportion of either naïve (Yakoub-Agha et al., 2006) or memory (Loschi et al., 2015) subsets present in the graft with the risk of developing aGVHD after HSCT.

We thus assessed whether the frequency of the different $CD4^+$ and $CD8^+$ naïve and memory T cell subsets was altered in recipients at the time of GVHD onset compared to patients without GVHD. Interestingly, as shown in **Figure 28**, we observed that recipients at GVHD onset had a significant increase of cells with a $T_{SCM\text{-}like}$ phenotype compared to recipients without GVHD, in both cohorts. We also noted an increase of T_{CM} cells, but only reaching significance in cohort 1. A trend towards a decreased frequency of T_{EM} cells is present in cohort 2, while no significant differences were observed regarding T_{Naive} and T_{EMRA} cells within the $CD4^+$ compartment.

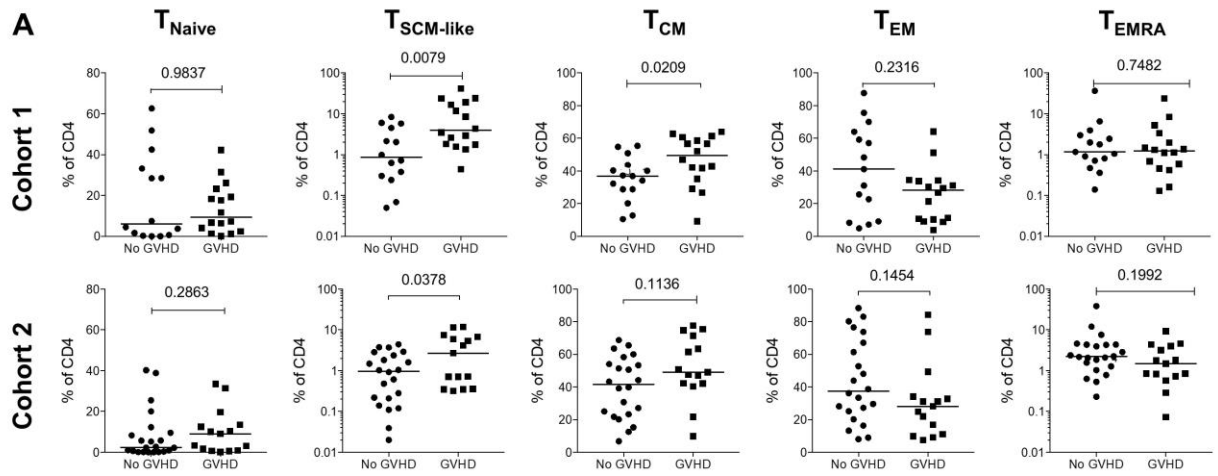

B

CD4⁺ T cells	T_{Naive}	$T_{SCM\text{-}like}$	T_{CM}	T_{EM}	T_{EMRA}
Cohort 1	ns	↑	↑	ns	ns
Cohort 2	ns	↑	↑	↓	ns

ns= not significant

Figure 28 Increase of CD4⁺ $T_{SCM\text{-}like}$ cells at GVHD onset
(A) Shown are the frequencies of T_{Naive}, $T_{SCM\text{-}like}$, T_{CM}, T_{EM} and T_{EMRA} cells within the CD4⁺ T cell compartment in recipients at GVHD onset compared to recipients without GVHD in cohort 1 (top graph) and cohort 2 (bottom graph). Horizontal bars indicate the median. P-values were calculated using a Mann-Whitney test (GVHD *versus* No GVHD) and are indicated above the graph. Differences are considered significant for P-values < 0.05. (B) Summary table of the differences observed in recipients at GVHD onset compared to recipients without GVHD. Red and blue arrows indicate a statistically significant increase or decrease of the cell population whereas pink and light blue arrows indicate a trend towards an increase or decrease approaching statistical significance.

This increase of $T_{SCM\text{-}like}$ cells at the onset of GVHD was also observed within the CD8⁺ T cell compartment in both cohorts, but only reached statistical significance in cohort 1, as shown in **Figure 29**. For CD8⁺ T cells we observed an increase of T_{CM} and a decrease of T_{EM} cells at GVHD onset, similar to what was observed for CD4⁺ T cells. Again, these results are significant in cohort 1, but a trend is present in cohort 2. We did not find any differences in the frequency of CD8⁺ $T_{Naïve}$ and T_{EMRA} subsets at GVHD onset.

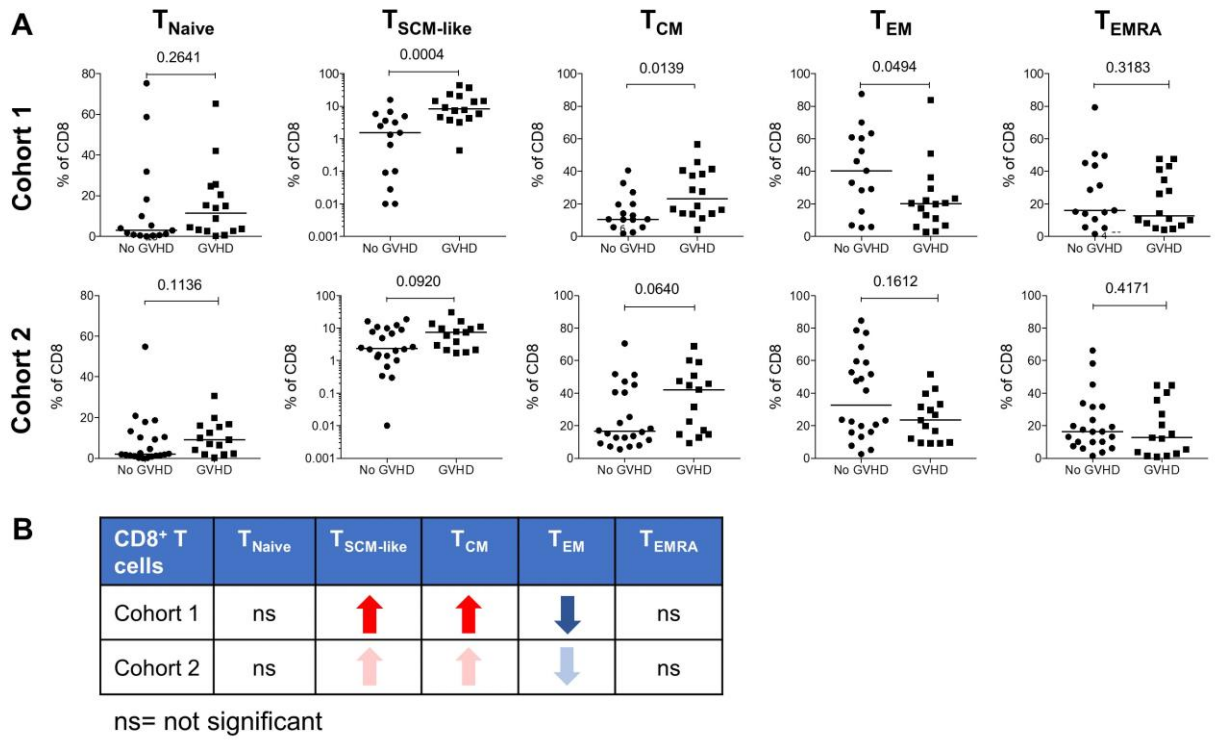

Figure 29 Increase of CD8$^+$ $T_{SCM\text{-}like}$ cells at GVHD onset

(A) Frequencies of T_{Naive}, $T_{SCM\text{-}like}$, T_{CM}, T_{EM} and T_{EMRA} cells within the CD8$^+$ T cell compartment in recipients at GVHD onset compared to recipients without GVHD in cohort 1 (top graph) and cohort 2 (bottom graph). Horizontal bars indicate the median. P-values were calculated using a Mann-Whitney test (GVHD *versus* No GVHD) and are indicated above the graph. Differences are considered significant for P-values < 0.05. (B) Summary table of the differences observed in recipients at GVHD onset compared to recipients without GVHD. Red and blue arrows indicate a statistically significant increase or decrease of the cell population whereas pink and light blue arrows indicate a trend towards an increase or decrease approaching statistical significance.

Despite the increased frequency of CD4$^+$ and CD8$^+$ $T_{SCM\text{-}like}$ and T_{CM} cells observed at GVHD onset, we didn't find any clear difference in the proliferative status of the different cell subsets between recipients with and without GVHD. We noted an increase of Ki-67$^+$ cells in total CD4$^+$ and CD8$^+$ T cells, CD4$^+$ T_{CM} and CD4$^+$ T_{EM} cells in cohort 1, while in cohort 2 we did not observe any significant difference in proliferating cells within the different subsets (**Figure 30**).

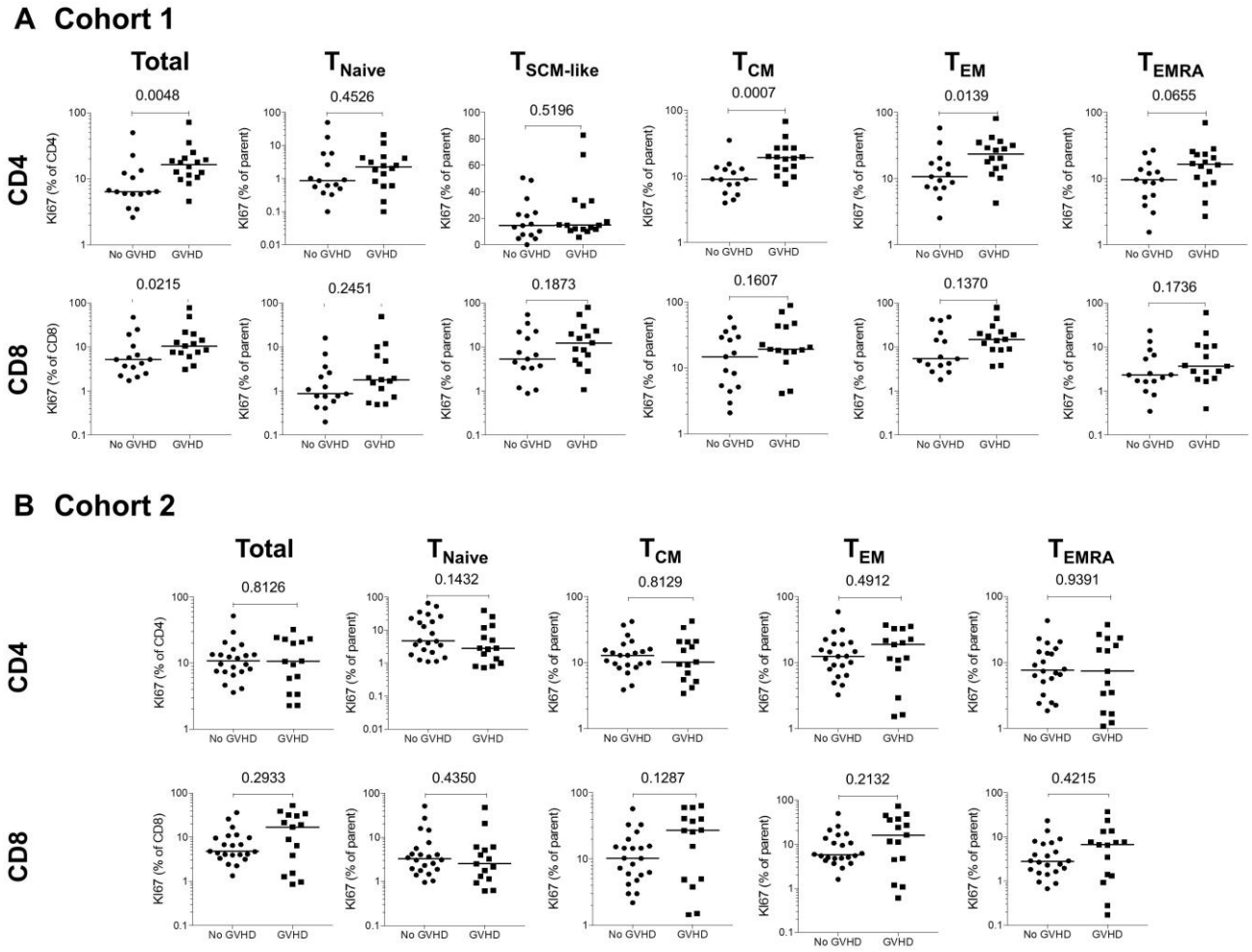

Figure 30 T cell subsets proliferation at GVHD onset

Frequency of proliferating Ki-67$^+$ cells in total CD4$^+$ and CD8$^+$ T cells and in the different naïve and memory subsets in both the CD4$^+$ and CD8$^+$ compartements recipients with (GVHD) or without (No GVHD) GVHD from cohort 1 (A, top panel) and cohort 2 (B, bottom panel). The frequency of Ki-67$^+$ cells is represented as percentage of Ki-67-expressing cells within total CD4$^+$ or CD8$^+$ T cells and as percentage Ki-67-expressing cells within the parent gate for T_{Naive}, $T_{SCM\text{-}like}$, T_{CM}, T_{EM} and T_{EMRA} subsets. Horizontal bars indicate the median. P-values were calculated using a Mann-Whitney test (GVHD *versus* No GVHD) and are indicated above the graph. Differences are considered significant for P-values < 0.05

4.4.3 Treg homeostasis at GVHD onset

Previous work from our laboratory investigating Treg homeostasis at the time of engraftment (15-30 days after transplantation), revealed that the overall frequency of $CD4^+Foxp3^+$ T cells and their suppressive activity were preserved. However, this study showed a marked depletion of Tregs with a naïve phenotype and increased Treg proliferation in patients developing aGVHD compared to patients without aGVHD (Dong et al., 2013). To investigate regulatory T cells dynamics in the context of aGVHD development, we analysed the frequency of $CD4^+Foxp3^+$ T cells and the expression of the functional markers CTLA4, ICOS and PD1 as well as Ki-67 within the Treg population in recipient at GVHD onset and in recipients without GVHD. Statistical analysis of the frequency of Treg cells and as well as the percentages of CTLA4-, ICOS- and PD1-expressing cells within the $Foxp3^+$ population was performed only for cohort 2, due to technical difficulties in obtaining a reproducible Foxp3 staining in cohort 1.

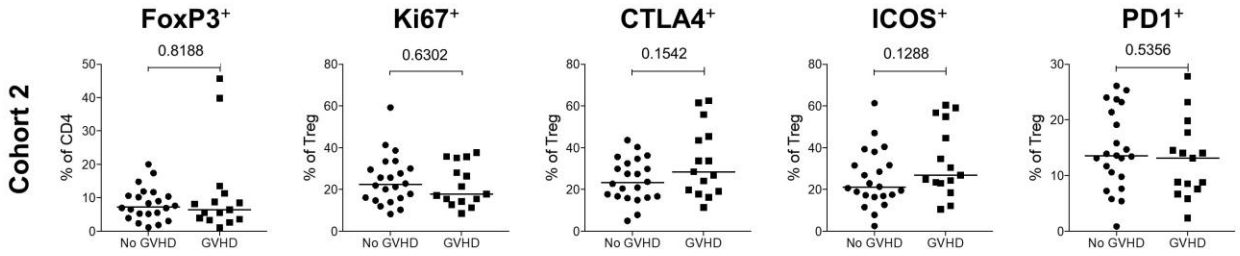

Figure 31 Treg homeostasis at GVHD onset
Frequency of $Foxp3^+$ cells within the $CD4^+$ population and frequencies of Ki-67^+, $CTLA4^+$, $ICOS^+$ and $PD1^+$ cells within the $Foxp3^+$ Treg population in recipients at GVHD onset (GVHD) compared to recipients without GVHD (No GVHD) in cohort 2. Horizontal bars indicate the median. P-values were calculated using a Mann-Whitney test (GVHD *versus* No GVHD) and are indicated above the graph. Differences are considered significant for P-values < 0.05.

We did not find any significant difference neither in the frequency of $CD4^+$ $Foxp3^+$ Treg cells nor in the expression of the functional (CTLA4, ICOS, PD1) and proliferation (Ki-67) markers in recipients at GVHD onset compared to recipients without GVHD **(Figure 31).** Conversely to solid organ transplantation, in which a positive correlation between graft survival and the number of circulating Tregs has been shown, studies investigating the correlation between the presence of Tregs and the incidence of GVHD have yielded conflicting results (Beres and Drobyski, 2013; Roncarolo and Battaglia, 2007). Dong and colleagues observed at GVHD onset a decrease of $CD4^+Foxp3^+$ T cells with a $CD45RA^+$ phenotype, but no significant differences in the overall

frequency of $CD4^+Foxp3^+$ T cells within the $CD4^+$ T cell compartment were found. This could suggest that the frequency of specific Treg subpopulations rather than that of the total pool of Tregs may be altered in patients developing aGVHD (Dong et al., 2013).

Taken together, the data presented in this section indicate that in peripheral blood of recipients at aGVHD onset there is an increase of cells belonging to less differentiated subsets, in particular $T_{SCM\text{-}like}$ and T_{CM} cells, while cells with an effector memory phenotype showed a trend towards a decrease especially in the $CD8^+$ compartment. This observation is consistent with the notion that T memory cells do not seem to trigger GVHD (Huang and Chao, 2017). Particularly interesting is the increase of $T_{SCM\text{-}like}$ cells observed at GVHD onset. In a mouse model of human GVHD against minor histocompatibility antigens, T_{SCM} have been shown to be capable of sustaining alloreactive T cells mediating GVHD upon serial transplantation into allogeneic hosts (Zhang et al., 2005). Since effector memory T cells represent pre-terminally differentiated cells, persistent antigen stimulation after HSCT could result in exhaustion and/or deletion of antigen-specific T cells, as proposed in chronic viral infection (Wherry, 2011). T cell-mediated immune reactions to persistent antigens require the continuous generation of antigen-specific effectors. The subset of $T_{SCM\text{-}like}$ cells that we observed to be increased at GVHD onset, could represent a cellular reservoir for alloreactive T cells in recipients developing GVHD, sustaining the production of alloreactive donor T cells in the presence of host persistent antigens.

4.5 Cellular profiling at GVHD onset in cohort 3

In order to reproduce the results observed in the first two cohorts and further investigate the cellular correlates associated with GVHD onset thanks to the assessment of absolute cell counts (TBNK TruCount assay), we compared the cellular profile of recipients at GVHD onset and recipients without GVHD in cohort 3. It has to be noted, however, that for this cohort, samples from recipients that did not develop GVHD were collected at day 30 post-HSCT and not at day 90 as for cohorts 1 and 2.

4.5.1 Absolute numbers of T, B and NK cells in recipients at GVHD onset

As depicted in **Figure 32**, absolute counts at GVHD onset showed an increase of $CD3^+$ and $CD4^+$ T cells compared to patients in the absence of GVHD. No significant differences were observed for B cells, NK cells and $CD8^+$ T cells. However, even if not statistically significant, a

trend towards increased counts of $CD8^+$ T cells seems to be present at GVHD onset. It is also worth noting that, compared to recipients without GVHD, absolute counts of total lymphocytes, B cells and $CD3^+$ T cells display a higher degree of heterogeneity at GVHD onset, suggesting that disease onset might affect immune cell composition in different ways in the patients.

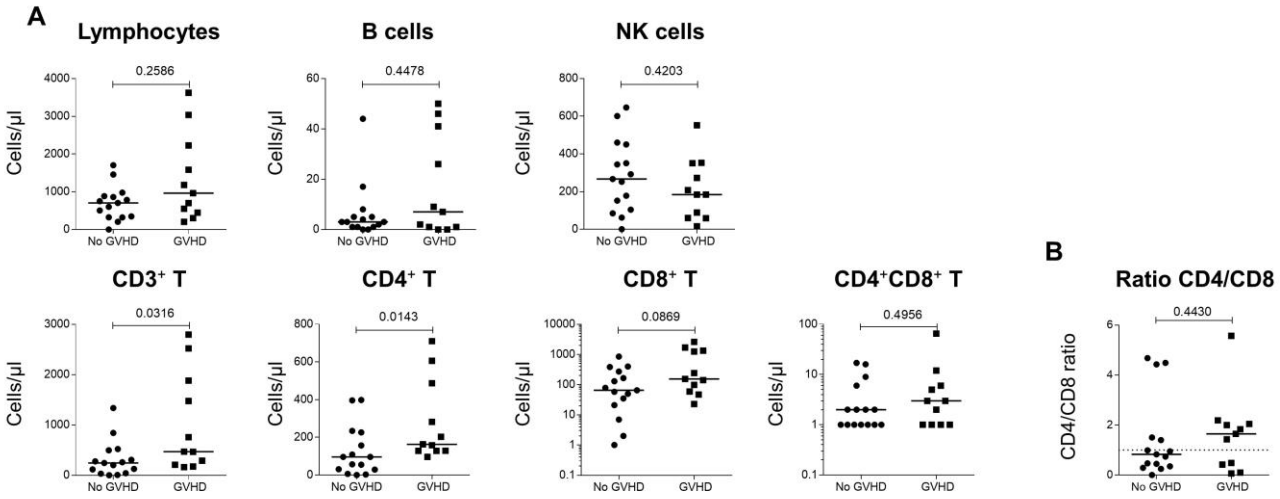

Figure 32 Absolute counts of T, B and NK cells at GVHD onset
Absolute counts of total lymphocytes, $CD19^+$ B cells, $CD56^+CD16^{+/-}$ Natural Killer (NK) cells; $CD3^+$ T cells, $CD4^+$ T cells, $CD8^+$ T cells and $CD4^+CD8^+$ double positive T cells (A) and the ratio of $CD4^+$ and $CD8^+$ T cells (B) in recipients at GVHD onset (GVHD) compared to recipients without GVHD (No GVHD) in cohort 3. Cell counts are expressed as number of cells/µl of whole blood. Horizontal bars indicate the median. P-values were calculated using a Mann-Whitney test (GVHD *versus* No GVHD) and are indicated above the graph. Differences are considered significant for P-values < 0.05.

4.5.2 Increased frequency of $CD3^+$ T cells at GVHD onset

Consistent with the increased absolute counts of $CD3^+$ T cells at GVHD onset, we also observed an increased frequency of $CD3^+$ T cells within the lymphocyte population in recipients developing GVHD compared to No GVHD patients, as shown in **Figure 33**. Compared to the results observed in cohort 1 and 2, however, we did not find significant differences in the frequency of $CD4^+$ and $CD8^+$ T cells at GVHD onset. In addition, we observed in cohort 1 a decreased frequency of $CD3^+$ T cells in GVHD recipients compared to patients without GVHD, while in cohort 3, both absolute counts and percentage of $CD3^+$ T cells indicate an increase of this cell subset at GVHD onset. This discrepancy could be explained by the fact that for cohorts 1 and 2 the samples for the recipients not developing GVHD were collected at day 90, whereas for cohort 3 No GVHD patients were sampled at day 30 posttransplant. In the three cohort the median day of

GVHD onset is around day 30, therefore the decreased frequency of $CD3^+$ T cells observed in the first cohort might represent an imbalance in immune reconstitution due to the different time point rather than an effect associated with GVHD onset. In cohort 3, in which the samples for the GVHD and No GVHD groups are more "time-matched" we observe an increase of T cells associated with GVHD onset, consistent with the key role of these cells in mediating the disease.

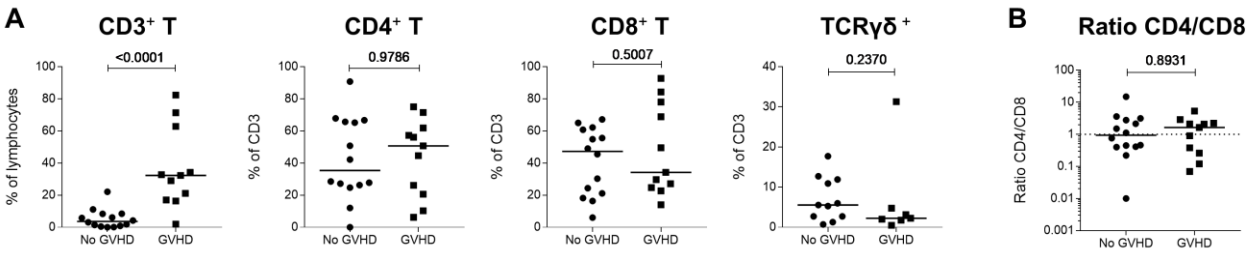

Figure 33 Increased frequency of $CD3^+$ T cells at GVHD onset
Frequency of $CD3^+$ T cells within the lymphocyte population and frequencies of $CD4^+$, $CD8^+$ and $TCR\gamma\delta^+$ T cells within $CD3^+$ T cells (A) and the ratio of $CD4^+$ and $CD8^+$ T cells (B) in recipients at GVHD onset compared to recipients without GVHD at day 30 in cohort 3. Horizontal bars indicate the median. P-values were calculated using a Mann-Whitney test (GVHD *versus* No GVHD) and are indicated above the graph. Differences are considered significant for P-values < 0.05.

For this cohort, due to changes in the flow cytometry panel and staining procedure, analysis of the different T helper subsets based on chemokine receptors expression, Treg homeostasis and T cell proliferation could not be performed. No significant differences were observed in the distribution of T naïve and memory subsets in this cohort (data not shown).

4.6 Immune profile of donors' samples before HSCT

In this study we also addressed whether in donors before transplantation differences in the frequency and numbers of the different T cell subsets could indicate an increased risk of developing GVHD for the recipients. We thus compared the absolute counts (only for cohort 3) as well as the distribution and the proliferative status of the different T cell subsets in donors whose recipients developed GVHD compared to donors whose recipients did not develop GVHD in the three cohorts we collected.

No significant differences were observed in the absolute numbers of the major lymphocyte populations (T, B, NK cells analysed with TBNK assays) in the two donors' groups in cohort 3 except for an increase of $CD8^+$ T cell counts in the donors whose recipients developed GVHD compared to the ones whose recipients did not develop GVHD (P=0.0366, data not shown). Moreover, we did not find any significant differences in the frequency of $CD3^+$, $CD4^+$, $CD8^+$ and $TCR\gamma\delta^+$ T cells, chemokine receptors expression as well as naïve and memory T cell subsets distribution and proliferation status in the two donors' groups in the three cohorts (data not shown). As a representative example, **Figure 34** shows the frequencies of the different naïve and memory subsets within the $CD4^+$ T cell compartment in donors whose recipients developed GVHD compared to donors whose recipients did not develop GVHD in the three cohorts.

In summary, in our cohorts, with our experimental setting, we could not detect in the peripheral blood of the donors before transplantation major differences in immune cell composition that could indicate a higher risk for the recipients to develop GVHD and thus identify a cellular signature of "dangerous donors" whose grafts are more likely to cause GVHD in the recipients.

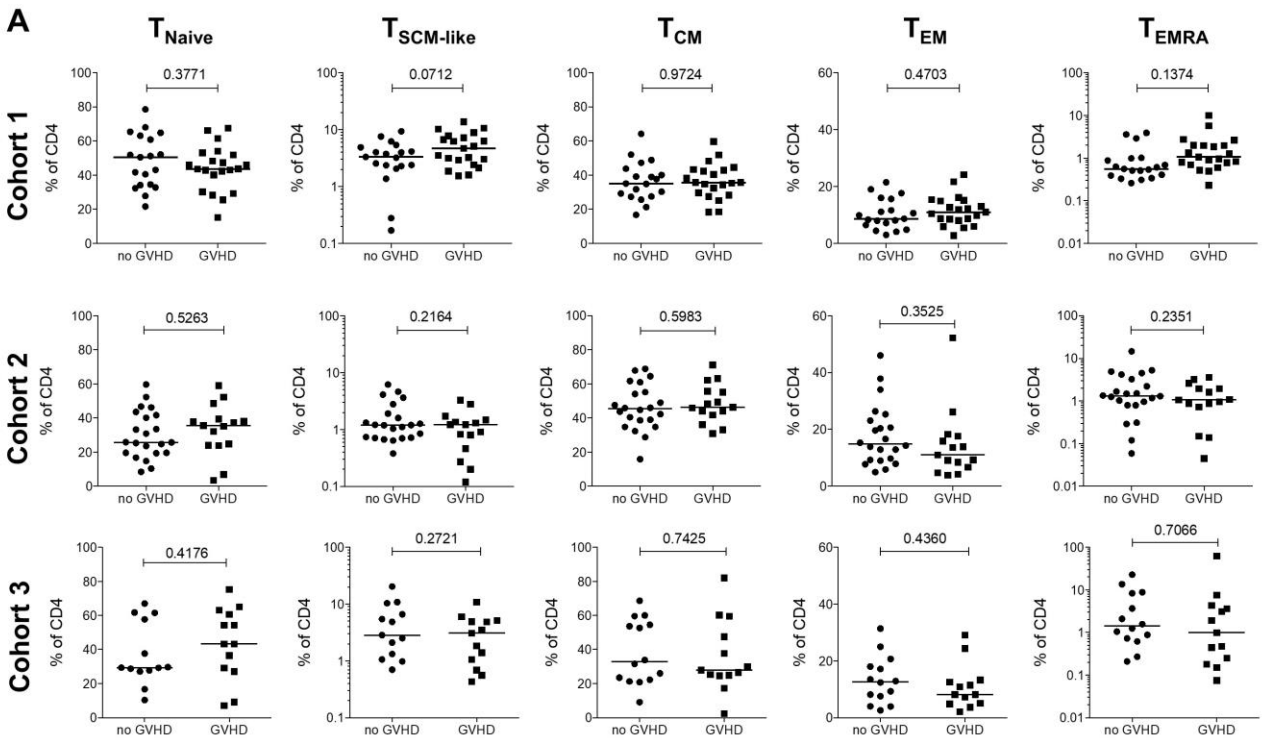

B

CD4⁺ T cells	T_{Naive}	$T_{SCM\text{-}like}$	T_{CM}	T_{EM}	T_{EMRA}
Cohort 1	ns	ns	ns	ns	ns
Cohort 2	ns	ns	ns	ns	ns
Cohort 3	ns	ns	ns	ns	ns

ns= not significant

Figure 34 Naïve and memory subsets within CD4⁺ T cells in donors before HSCT

(A) Frequency of T_{Naive}, $T_{SCM\text{-}like}$, T_{CM}, T_{EM} and T_{EMRA} cells within the $CD4^+$ T cell compartment in donors whose recipients did not develop GVHD (no GVHD) and in donors whose recipients developed GVHD (GVHD) in cohort 1 (top graph), cohort 2 (middle graph) and cohort 3(bottom graph). Horizontal bars indicate the median. P-values were calculated using a Mann-Whitney test (GVHD *versus* no GVHD) and are indicated above the graph. Differences are considered significant for P-values < 0.05. (B) Summary table of the differences observed between the two donors' groups.

5 Molecular profiling of immune cell populations involved in acute GVHD pathogenesis

The control of alloreactivity after allogeneic HSCT reflects a complex network of interactions between the innate and the adaptive immune systems. Diverse cell populations, such as T cells, antigen presenting cells (APCs), Natural Killer (NK) cells and regulatory T cells have been reported to play immune-modulatory roles in HSCT and in acute GVHD (Morris and Hill, 2007). Several studies have investigated the gene expression profile of GVHD target organs, such as the liver and the skin in murine models. These studies showed upregulation of genes coding for chemokines and their receptors, adhesion molecules, molecules involved in antigen processing and presentation, regulators of apoptosis, and genes associated with the attraction and activation of donor T cells (Ichiba et al., 2003; Sadeghi et al., 2013; Sugerman et al., 2004). However, despite providing valuable information on the molecular mechanisms involved in aGVHD, these studies assessed the gene expression profile of the target tissue as a whole, making it difficult to infer information on the individual cell populations involved. In HSCT recipients, Takahashi and colleagues identified 55 differentially expressed genes in peripheral blood mononuclear cell (PBMC) subpopulations during aGVHD in comparison with the recovery phase following cord blood transplantation. This study showed the important role of proinflammatory and immunoregulatory genes in the pathophysiology of aGVHD (Takahashi et al., 2008). Verner et al. performed microarray analysis on PBMCs from patients developing GVHD and described genes having a differential expression between the groups with favourable *versus* unfavourable outcomes after aGVHD (Verner et al., 2012). Studies related to acute GVHD have used sorted T cells, given their key role in disease pathogenesis. Using sorted $CD3^+$ T cells from non-human primate (NHP) models of GVHD and human patients, Furlan and colleagues reported gene expression signatures associated with aGVHD and identified pathways induced in both NHP and human alloreactive T cells (Furlan et al., 2015, 2016). On the contrary, few studies investigated gene expression signatures associated with immune reconstitution in the absence of GVHD (Pidala et al., 2015; Trop-Steinberg et al., 2015), and to our knowledge a comparison of the transcriptomic profile of different immune cell subsets in transplant recipients without GVHD and in the corresponding donors before transplant has not been performed. Therefore, the molecular mechanisms underlying

the behaviour of different immune cell populations during immune reconstitution following HSCT and in acute GVHD in humans are still incompletely understood.

To address this question, we defined the molecular characteristics of cell populations involved in the alloresponse after HSCT. To investigate the molecular changes associated with HSCT and with aGVHD, we performed transcriptomic profiling of cell populations important for GVHD development, in particular $CD4^+$ and $CD8^+$ T cells from donors and recipients with or without GVHD. Our work focused mainly on the study of T cell responses, given their key role in mediating GVHD (Ferrara et al., 2009), however, for a subgroup of donor-recipient couples we also investigated the frequency and the transcriptomic profile of NK cells and monocytes. Data for these two cell populations will be presented separately.

A major limitation of gene expression assays in patients undergoing HSCT is the number of circulating lymphocytes available, especially at early time points. Low numbers of cells can lead to high variability in the results, due to the multiple steps of RNA extraction, reverse transcription, and amplification. The NanoString nCounter technology is based on RNA hybridization with barcoded probes and allows quantification of gene expression without any amplification step and enzymatic reaction. This technology allows to detect the abundance of up to 800 transcripts in parallel in a biological sample using as little as 20ng of total RNA with high sensitivity and linearity across a broad range of expression levels. Thanks to the use of barcoded probes recognizing specific mRNA targets, the abundance of every gene is quantified resulting in a "digital count" of the individual mRNA transcripts (Geiss et al., 2008). The detailed experimental protocol is described in the Materials and Methods section. Briefly, total RNA was extracted from unstimulated $CD4^+$ T cells, $CD8^+$ T cells, $CD56^+$ NK cells and $CD14^+$ monocytes sorted from donors and recipients. RNA quality was assessed using the Agilent BioAnalyzer, confirming good RNA quality. The gene expression profile of $CD4^+$ and $CD8^+$ T cells was assessed for donors and recipients of the three cohorts, whereas NK cells and monocytes were analysed only for ten couples of the second cohort. T cells were analysed using the NanoString Human Immunology V2 codeset, including 594 immune-related genes. For NK cells and monocytes, we used the NanoString Human PanCancer Immune profile codeset, including 770 genes covering both the adaptive and innate immune response, as genes expressed in these two cell types were more represented in this panel. Expression data were normalized using nSolver Analysis Software (NanoString technologies) and the housekeeping genes were selected using the geNORM method, an

established algorithm for identifying the best housekeeping genes within a dataset (Vandesompele et al., 2002). Probes with low counts, at or below the level of background, and some probes mapping to multiple genes or aligning to polymorphic regions with more than two SNPs (see Materials and Methods for details) were removed and not considered for further analysis.

5.1 Transcriptomic profile of CD4$^+$ and CD8$^+$ T cells from donors and recipients without GVHD three months after HSCT

To investigate the molecular changes associated with T cell expansion after allogeneic HSCT, we profiled mRNA expression in sorted CD4$^+$ and CD8$^+$ T cells isolated from donors before transplant and on day 90 post-HSCT from recipients in the absence of GVHD (cohorts 1 and 2). First, to assess the structure of the data, we performed principal component analysis (PCA), a dimensionality reducing method used to identify the determinants of variation in complex data (Ringnér, 2008) (**Figure 35**).

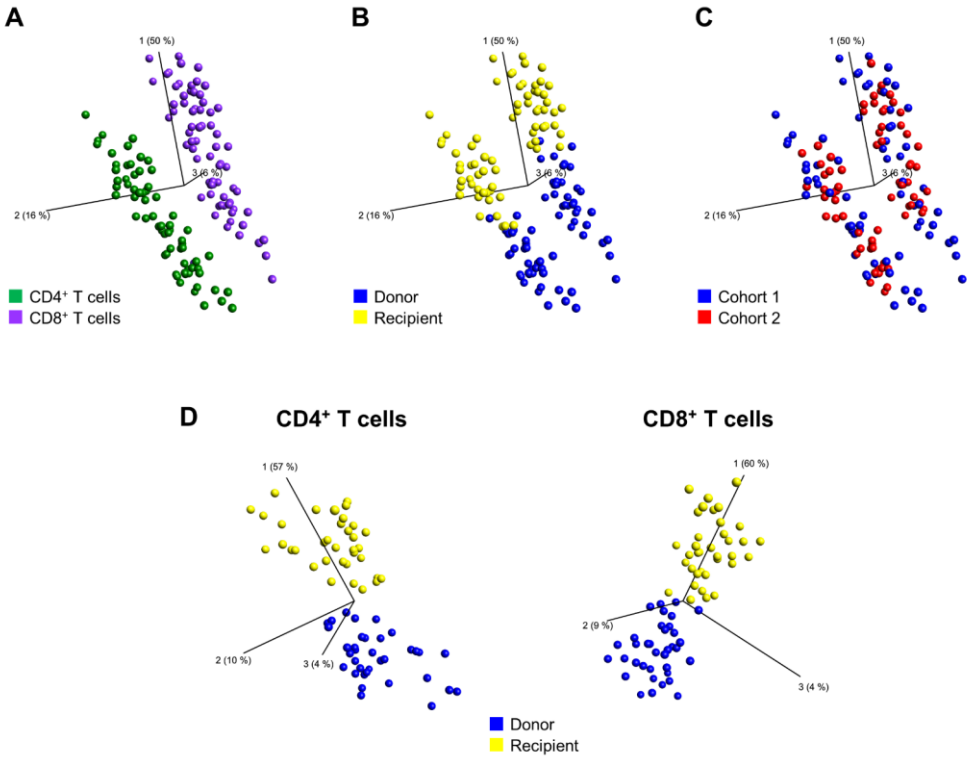

Figure 35 Gene expression analysis of CD4$^+$ and CD8$^+$ T cells in donors and recipients after HSCT

Principal component analysis (PCA) was performed on the gene expression data of CD4$^+$ and CD8$^+$ T cells from 71 donors and their corresponding recipients in the absence of GVHD after HSCT in cohorts 1 and 2. Each dot represents a sample, coloured according to (A) cell type, (B) donor/recipient group and (C) cohort. In (D) are represented samples from donors and recipients within CD4$^+$ (left) and CD8$^+$ (right) T cells. Prior to performing the PCA, values for each gene were log2 transformed, centred to a mean value of zero and scaled to unit variance.

This allowed us to determine the degree to which the T cell transcriptome of the HSCT recipients differed from the one of the donors, and the degree to which transcriptional variation was shared between the two cohorts. As shown in **Figure 35**, the PCA analysis revealed a clear separation of the $CD4^+$ (green) and $CD8^+$ (violet) T cell subsets from donors and recipients in the two cohorts, supporting the importance of analysing individual cell populations separately. In the PCA, the main factor driving the cluster separation (Principal Component (PC)1, explaining 50% of the variance) is the cell type (**Figure 35A**). The samples from the donors (yellow) and the recipients (blue) are also well separated (**Figure 35B**), while samples from the two cohorts are homogeneously mixed together (**Figure 35C**), refuting a possible "batch" or "cohort" effect. When analysing the two cell populations separately (**Figure 35D**), the majority of the variance is explained by PC1 (explaining 57% of the variance for $CD4^+$ T cells and 60% for $CD8^+$ T cells), driving the separation between the donors' and the recipients' groups, indicating that HSCT is associated with major transcriptomic changes in $CD4^+$ and $CD8^+$ T cell populations.

5.1.1 HSCT is associated with major transcriptomic changes in $CD4^+$ and $CD8^+$ T cells

To identify biological changes associated with immune reconstitution and gain insight into the molecular mechanisms underlying T cell expansion after allogeneic HSCT, we compared the gene expression profiles of $CD4^+$ and $CD8^+$ T cells from recipients that did not develop GVHD with the ones of their donors before transplantation. As for the cellular profiling, also for this analysis we included only donor-recipient pairs in the absence of aGVHD, to avoid confounding effects due to the graft-versus-host reaction. As shown in **Figure 36A**, in $CD4^+$ T cells, we identified 214 genes differentially expressed between donors and recipients in cohort 1 (FDR correction Q=1%). Of these, 207 are upregulated and only 7 are downregulated in the recipients after transplantation. In cohort 2, we identified 206 genes differentially expressed between donors and recipients (FDR correction Q=1%), of which 199 are upregulated and 7 are downregulated in the recipients compared to their donors. In $CD8^+$ T cells (**Figure 36B**), we identified 234 genes differentially expressed in cohort 1 and 221 in cohort 2 (FDR correction Q=1%). As for $CD4^+$ T cells, the majority of the genes are upregulated and only a few genes are downregulated in the recipients compared to their donors (cohort 1: 217 genes upregulated and 17 genes downregulated; cohort 2: 205 genes upregulated and 16 genes downregulated). Comparative analysis of the differentially expressed transcripts between donors and recipients demonstrated that there is an important overlap of the differentially expressed genes between the two cohorts. In particular, we found that

75% (180 genes) and 79% (201 genes) of the differentially expressed genes were shared between the two cohorts in $CD4^+$ and $CD8^+$ T cells respectively and changed in the same direction.

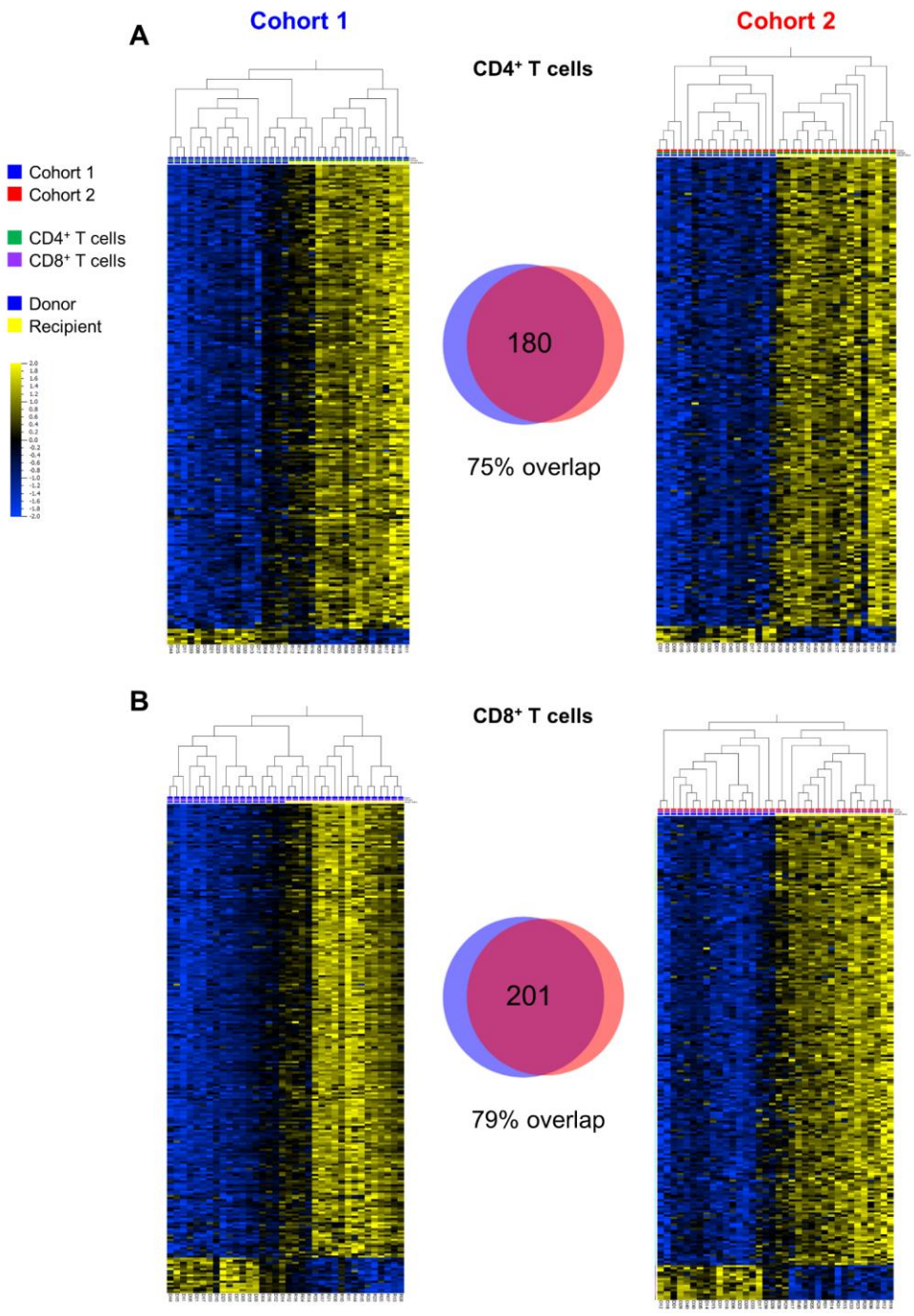

Figure 36 T cell transcriptomic profiles in donors and recipients after HSCT

Heatmaps showing the gene expression profiles of $CD4^+$ (A, top) and $CD8^+$ (B, bottom) T cells in donors and recipients at day 90 post-HSCT in cohort 1 (left) and cohort 2 (right). In the heatmap columns represent samples and are ordered by hierarchical clustering, while rows represent genes and are ranked by fold change. Yellow indicates high levels of expression and blue indicates low levels of expression. Paired t-test (donors *versus* recipients) with false discovery rate correction Q=1%. Values for each gene were log2 transformed, centred to a mean value of zero and scaled to unit variance. The weighted Venn diagrams depict the number of transcripts differentially expressed that are shared between cohorts 1 and 2 when comparing donors and recipients (paired t-test with FDR correction at Q=1%). Cohort 1 includes 18 donor-recipients couples for both cell populations. Cohort 2 includes 18 couples for $CD4^+$ T cells and 17 couples for $CD8^+$ T cells.

5.1.2 Modular transcriptional framework to investigate the biological pathways and the molecular processes altered in T cells following HSCT

To specifically characterize the signaling pathways and the molecular functions altered in T cells following allogeneic HSCT, we performed pathway analysis on the transcriptomic profiles of $CD4^+$ and $CD8^+$ T cells from donors and recipients after transplantation. During the past few years, a plethora of pathway analysis methods has been developed to facilitate the interpretation of high-throughput data and guide the identification of relevant biological pathways associated with specific clinical or experimental conditions (Dutta et al., 2012; Huang et al., 2009; Khatri et al., 2012). One of the most widely used tests for this purpose, Gene Set Enrichment Analysis (GSEA), allows to determine whether *a priori* defined sets of genes show statistically significant differential expression between two biological groups starting from genome-wide transcriptomic profiles (Subramanian et al., 2005). Since the nCounter technology does not allow a genome-wide gene expression analysis, we could not apply the classical GSEA approach. We therefore used the Quantitative Set Analysis for Gene Expression (QuSAGE) (Yaari et al., 2013) method, an approach that is compatible with the limited number of genes assessed with the NanoString panels used in our experimental setting. The same method has been successfully applied in another study performed in our laboratory in which whole-blood gene expression signatures associated with anti-TNF treatment responses have been assessed using nCounter technology (Menegatti et al., submitted) and in the literature (Banchereau et al., 2016). To perform this analysis, we designed gene modules by grouping sets of genes belonging to specific signaling pathways (e.g. TCR signaling), associated with a particular cellular phenotype (e.g. activation or differentiation state), or associated with a specific cellular function (e.g. cytotoxicity). These gene modules were constructed based on curated gene sets available in molecular Signatures Database (mSigDB), a high-quality collection of annotated gene sets (Liberzon et al., 2011), on gene and pathway annotation databases such as Gene Ontology (GO), Kyoto Encyclopedia of Genes and Genomes (KEGG) and Reactome, and based on current knowledge in the literature. The same gene could be included in several modules, since its redundancy does not have any impact on the final analysis. Concerning the size of the modules, we set as a cut-off a minimum of 3 genes for the module to be included in the analysis, while we did not impose any size limitation for the largest gene set, which is represented by the module *Memory* including 64 genes. We next applied the QuSAGE algorithm to identify biological pathways and molecular functions most affected in recipients

following HSCT compared to their donors before transplant. With this approach, given two biological groups to compare, the gene set activity (pathway activity) is quantified as a shift in the mean differential expression of the individual genes that compose the set (Yaari et al., 2013). The advantage of this system is that instead of treating hundreds of individual transcripts separately, the number of variables is reduced by grouping the genes into a new entity, the module, thus facilitating the functional interpretation of the results and improving the power of the analysis Moreover, compared to other gene set analysis approaches, the QuSAGE method (i) accounts for inter-gene correlations, (ii) does not require large numbers of samples in each group because it does not compute permutations, (iii) does not assume that the standard deviation for individual genes is the same across groups and (iv) does not assume that all genes have the same variance. The complete list of the 54 modules we designed, with the genes included in each module, is summarized in **Annex Table 6**. Due to the removal from the datasets of the genes with low counts, three modules containing less than 3 genes (*IL6 signaling*, *NOD signaling* and *FcRs* modules) for cohorts 1 and 2, and one module (*IL6 signaling*) for cohort 3, were excluded from the analysis.

5.1.3 Pathway enrichment in recipients 90 days after HSCT compared to their donors

To understand the molecular mechanisms underlying T cell immune reconstitution and functionally interpret the differentially expressed genes in $CD4^+$ and $CD8^+$ T cells from recipients at day 90 post-HSCT compared to their donors, we applied the QuSAGE algorithm using 51 gene modules we designed. In $CD4^+$ T cells the analysis revealed that 47 modules in cohort 1 and 46 modules in cohort 2 had a statistically significant increased pathway activity in the recipients compared to the donors. On the contrary, only few gene sets showed a decreased pathway activity and none of these reached statistical significance (**Figure 37**). The QuSAGE plots in **Figure 37** represent the mean expression levels of the different gene modules (pathway activity) in $CD4^+$ T cells from recipients after transplantation compared to their respective sibling donors in cohort 1 (A) and in cohort 2 (B). In the two cohorts the ranking of the modules based on the pathway activity is almost overlapping, further indicating the reproducibility of our observations in these two independent cohorts. Amongst the modules with the highest pathway activity increase in the recipients and the lowest FDR, we noted the *NLR-inflammasome* module; the *Memory* module, that includes genes known to be enriched in memory T cells; the *Th1 profile* and *CTL-Cytotoxicity* modules; followed by gene sets related to T cell activation, IFN-induced genes, proapoptotic genes and genes associated with exhausted cells. In contrast, the modules showing a reduction in pathway

activity in the recipients, although not statistically significant, are the *Naïve* module, regrouping genes described to be upregulated in naïve T cells; the *NF-κB negative regulators* and the *WNT signaling* modules in cohort 1, and the *Naïve* and *WNT signaling* modules in cohort 2.

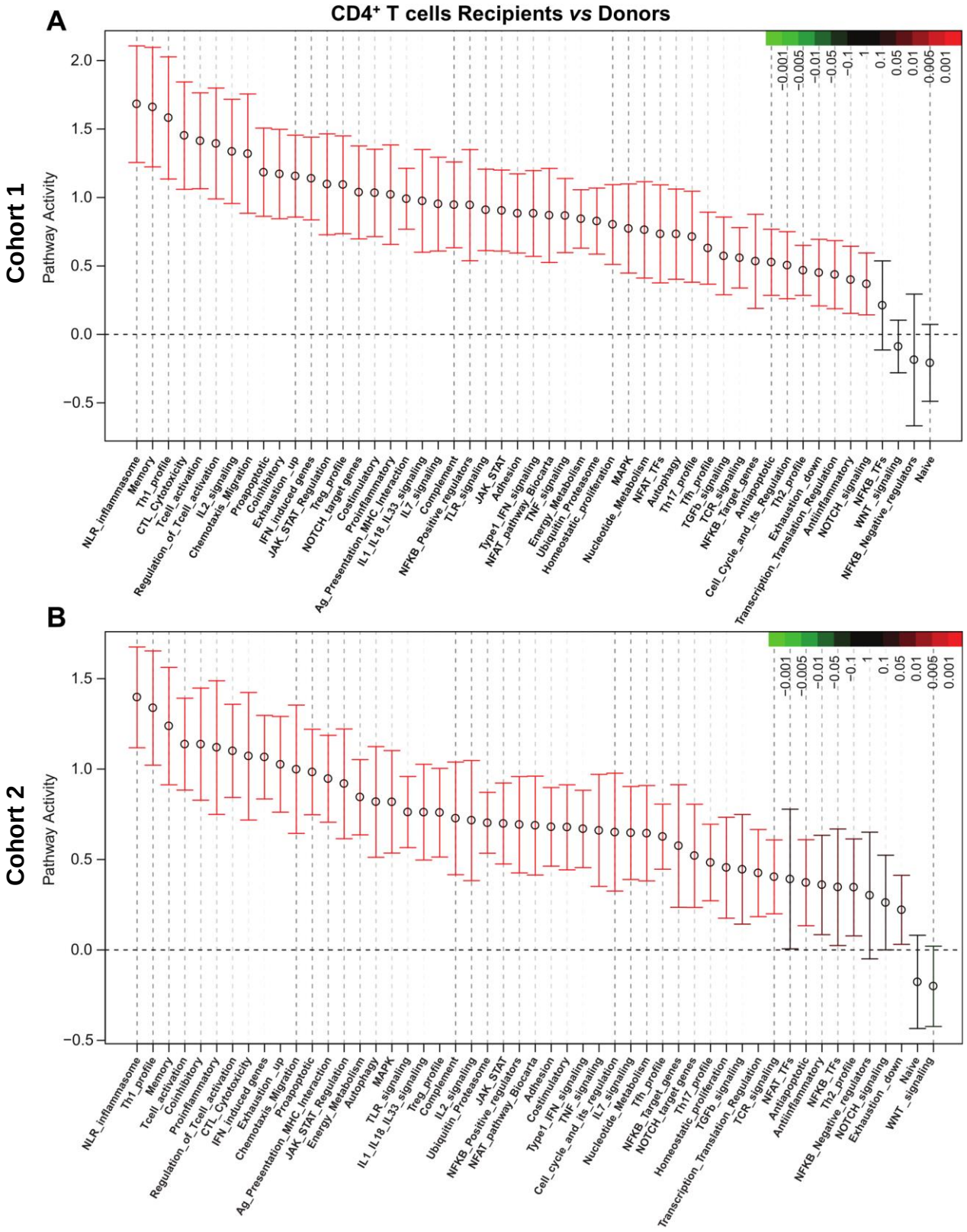

Figure 37 Molecular signatures in CD4⁺ T cells after HSCT

QuSAGE analysis on CD4⁺ T cell transcriptome in recipients at day 90 post-HSCT compared to their respective donors before transplant, in cohort 1 (A) and in cohort 2 (B). For each pathway, the mean fold change and the 95% confidence interval are plotted and colour-coded according to their False Discovery Rate (FDR)-corrected P-values when compared to zero. Red and green bars indicate a statistically significant increased or decreased pathway activity respectively, in the recipients compared to the donors.

QuSAGE analysis on the transcriptomic profile of $CD8^+$ T cells (**Figure 38**) showed 46 genes modules significantly different between donors and recipients in cohort 1. Of these, 44 had a significant increase in pathway activity, whereas two displayed a significant decrease in pathway activity in the recipients. In cohort 2, we observed 43 gene modules that reached statistical significance, of which three were downregulated in the recipients. Amongst the gene sets displaying the strongest increase in pathway activity with the lowest FDR, we found co-inhibitory molecules (*Coinhibitory*), genes shown to be upregulated in memory T cells (*Memory*), MHC molecules and genes involved in antigen presentation (*Ag Presentation and MHC Interaction*), proapoptotic genes (*Proapoptotic*), genes reported to be upregulated in exhausted cells (*Exhaustion-up*) as well as interferon-induced genes (*IFN-induced*) and genes related to T cell activation and autophagy. Interestingly, in $CD8^+$ T cells we also observed modules displaying a significant reduction in pathway activity in the recipients compared to the donors. In particular, the *WNT signaling* and the *Naïve* gene modules had decreased pathway activity in recipients in both cohorts, while the *Exhaustion-down* module, including genes reported to be downregulated in exhausted T cells had decreased pathway activity only in cohort 2.

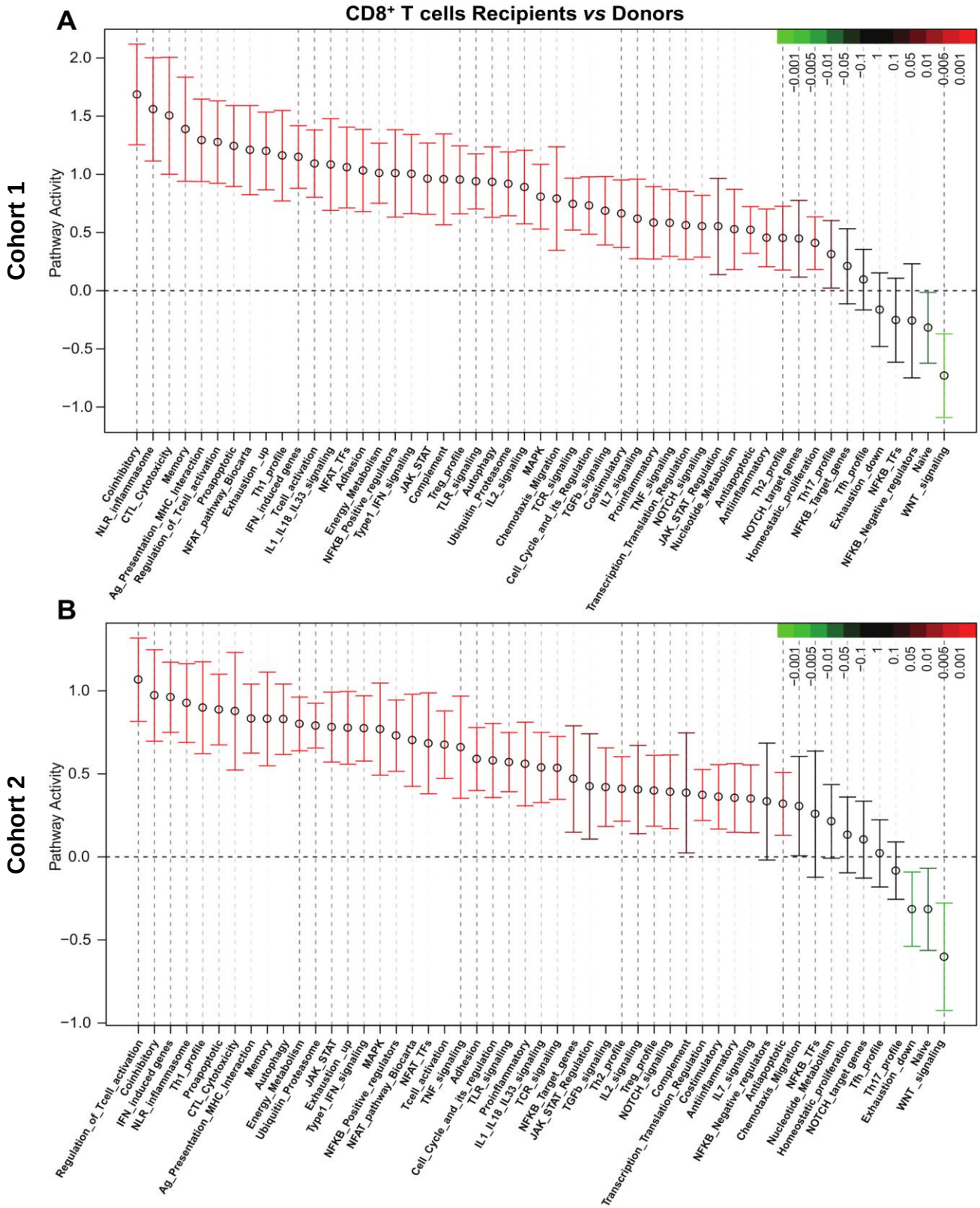

Figure 38 Molecular signatures in CD8⁺ T cells after HSCT

QuSAGE analysis on CD8⁺ T cell transcriptome in recipients at day 90 post-HSCT compared to their respective donors before transplant, in cohort 1 (A) and in cohort 2 (B). For each pathway, the mean fold change and the 95% confidence interval are plotted and colour-coded according to their False Discovery Rate (FDR)-corrected P-values when compared to zero. Red and green bars indicate a statistically significant increased or decreased pathway activity respectively, in the recipients compared to the donors.

5.1.4 Differential gene expression in T cells from HSCT recipients and their donors

Analysis of the transcriptomic profile of $CD4^+$ T cells (**Figure 39**) revealed that allogeneic HSCT is associated with major changes in gene expression in the recipients, with upregulation of genes involved in T cell activation and its regulation (*ZAP70, LCK, MAPKs, JAK-STATs, PTPN2, PTPN22, PTPN6, PTPRC*), adhesion (*ITGB1, ITGB2, ITGA4, ITGAL, ITGAM, ICAM3*), chemotaxis (*CX3CR1, CCR5, CXCR3, CXCR6, CCR2*) and effector functions, especially linked to Th1 profile and cytotoxicity (*TBX21, IFNG, GZMA, GZMK, PRF1, GNLY*). We also observed that the inflammasome pathway seems to be activated after HSCT, as suggested by the upregulation of genes involved in inflammasome biology such as *IL18R1, IL18RAP, CASP1, GBP5* and *PYCARD*. Although the inflammasome is most commonly attributed to the innate immune system (Martinon et al., 2007), it has been suggested that it is also active in adaptive immune cells (Arbore et al., 2016; Furlan et al., 2015). Moreover, we noted an upregulation of many genes associated with exhausted T cells (*CTLA4, PDCD1, LAG3, TIGIT, BTLA, KLRG1* and *SH2D1A*) (Crawford et al., 2014; Man et al., 2017; Thorp et al., 2015; Wherry et al., 2007) and proapoptotic genes (*BAX, TP53, BCL2L11, CASP1, CASP2, CASP3, CASP8, CRADD, PML*). Following chemotherapy $CD4^+$ T cells have been reported to be more susceptible to apoptosis when stimulated with mitogens compared to cells from healthy donors (Hakim et al., 1997). Upregulation of proapoptotic genes post-HSCT could therefore be related to an activation-induced apoptotic process. Consistent with the cellular profiling presented in the previous section, showing in the recipients a depletion of the naïve T cell pool and an increase of cells with an effector memory phenotype, also at the transcriptomic level we observed that many genes reported to be expressed in memory T cells are enriched in the recipients (*CD45R0, IFNG, CCL5, CD74, CXCR3, KLRG1, CX3CR1*), while naïve T cell-associated genes are underrepresented (*PTK2, IL6ST* in both cohorts; *CD45RA* only in cohort 1; *CCR7* and *TCF7* only in cohort 2) (Weng et al., 2012; Willinger et al., 2005).

Figure 39 HSCT is associated with major transcriptomic changes in CD4$^+$ T cells
(A) Heatmap showing the gene expression profile of CD4$^+$ T cells in donors and recipients at day 90 post-HSCT in cohort 2. In the heatmap columns represent samples and are ordered by hierarchical clustering, while rows represent genes and are ranked by fold change. Yellow indicates high levels of expression and blue indicates low levels of expression. Paired t-test (donors *versus* recipients) with false discovery rate correction Q=1%. 206 genes are differentially expressed between donors and recipients (17 donor-recipient pairs). Comparable results are observed in cohort 1 (heatmap not shown). (B) Histograms representing selected genes upregulated in the recipients compared to the donors in cohort 1 (blue bars) and in cohort 2 (red bars). The log2 of the fold change between recipients and donors is shown for each gene in the two cohorts. The presented genes were grouped according to their presumed function based on information available in public databases or in the literature.

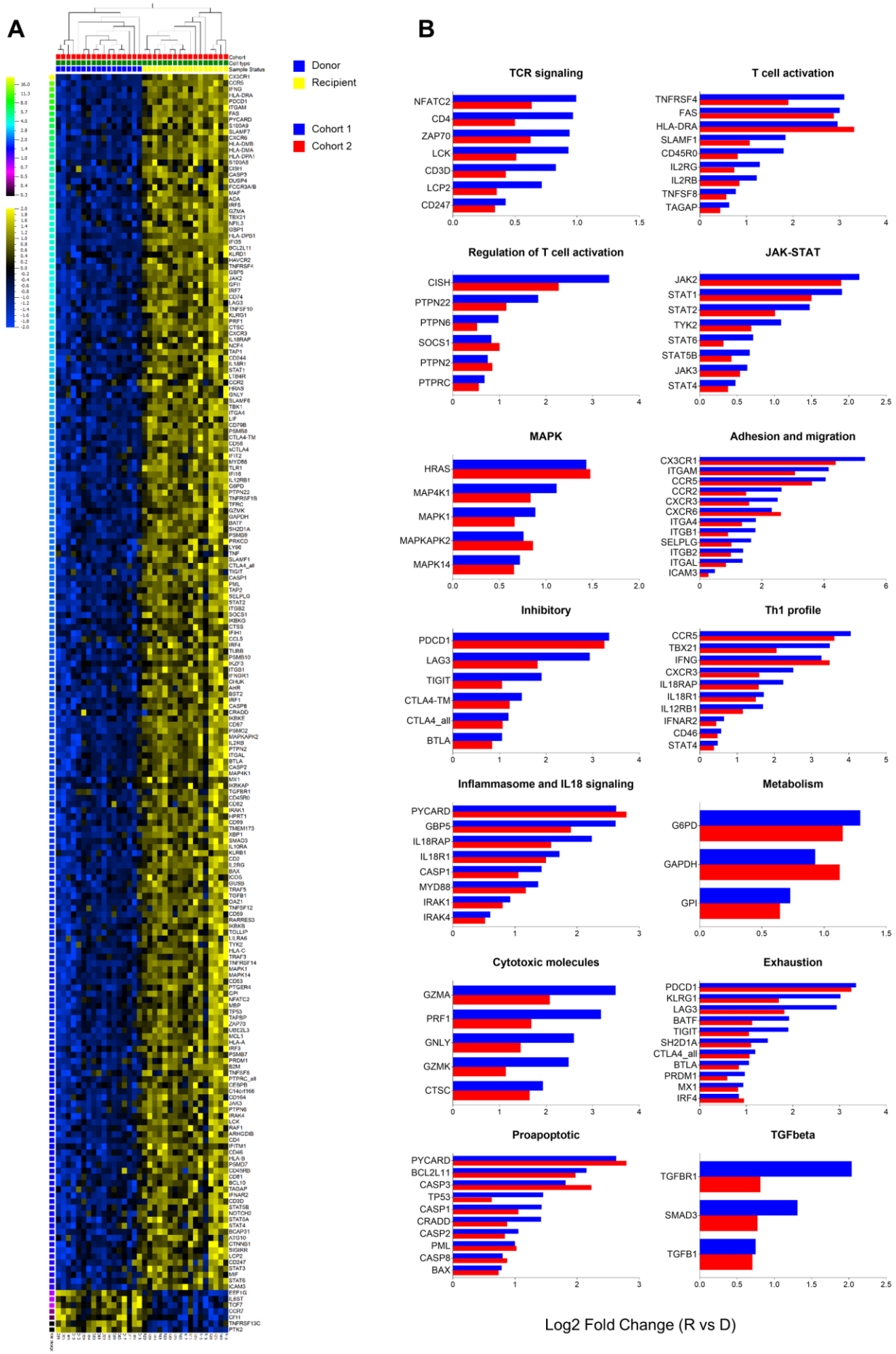
A
Donor
Recipient
Cohort 1
Cohort 2
B
TCR signaling
NFATC2
CD4
ZAP70
LCK
CD3D
LCP2
CD247
T cell activation
TNFRSF4
FAS
HLA-DRA
SLAMF1
CD45RO
IL2RG
IL2RB
TNFSF8
TAGAP
Regulation of T cell activation
CISH
PTPN22
PTPN6
SOCS1
PTPN2
PTPRC
JAK-STAT
JAK2
STAT1
STAT2
TYK2
STAT6
STAT5B
JAK3
STAT4
MAPK
HRAS
MAP4K1
MAPK1
MAPKAPK2
MAPK14
Adhesion and migration
CX3CR1
ITGAM
CCR5
CCR2
CXCR3
CXCR6
ITGA4
ITGB1
SELPLG
ITGB2
ITGAL
ICAM3
Inhibitory
PDCD1
LAG3
TIGIT
CTLA4-TM
CTLA4_all
BTLA
Th1 profile
CCR5
TBX21
IFNG
CXCR3
IL18RAP
IL18R1
IL12RB1
IFNAR2
CD46
STAT4
Inflammasome and IL18 signaling
PYCARD
GBP5
IL18RAP
IL18R1
CASP1
MYD88
IRAK1
IRAK4
Metabolism
G6PD
GAPDH
GPI
Cytotoxic molecules
GZMA
PRF1
GNLY
GZMK
CTSC
Exhaustion
PDCD1
KLRG1
LAG3
BATF
TIGIT
SH2D1A
CTLA4_all
BTLA
PRDM1
MX1
IRF4
Proapoptotic
PYCARD
BCL2L11
CASP3
TP53
CASP1
CRADD
CASP2
PML
CASP8
BAX
TGFbeta
TGFBR1
SMAD3
TGFB1
Log2 Fold Change (R vs D)

Within the $CD8^+$ T cell population (**Figure 40**) we also observed upregulation of genes associated to T cell activation and its regulation (*ZAP70, LCK, FYN, LCP2, MAPKs, JAK-STATs, HLA-DRA, G6PD, GAPDH, PTPN*s), effector functions (*GZMA, GZMB, PRF1, TNFSF10, CTSC*), adhesion (*CX3CR1, ITGAX, SELPLG, ITGAM, ITGB1, ITGAL, ITGB2, ITGA4, ITGA5, ICAM3*) and chemotaxis (*CX3CR1, CCR5, CXCR3, CCL5, CCL4, IL16*). We also noted an enrichment of inhibitory receptors (*HAVCR2, CD160, PDCD1, CTLA4, LAG3, KLRD1, CD244, KLRG1, SLAMF7*) and genes associated with exhausted cells (*HAVCR2, BATF, CD160, PDCD1, CTLA4, EOMES, TBX21, LAG3, CASP3, CD244, KLRG1, SH2D1A*) (Crawford et al., 2014; Man et al., 2017; Thorp et al., 2015; Wherry et al., 2007). Compared to the changes within the $CD4^+$ T cell subset, in $CD8^+$ T cells we observed an enrichment of genes linked to NOTCH (*NOTCH1, NOTCH2, RUNX1, IKZF1, TGFB1, CD46*) and NF-κB (*RELA, IKBKAP, TBK1, IKBKB, IKBKG, IKBKE, CHUK, MALT1*) signaling pathways. Interestingly, NOTCH1 and NOTCH2 have been reported to be expressed by activated $CD8^+$ T cells and the NOTCH signaling pathway seems to affect the transcription of key molecules controlling effector differentiation (T-bet and Eomes) and function (cytokines and cytolytic molecules) (Cho et al., 2009; Duval et al., 2015; Maekawa et al., 2008).

Among the genes downregulated in the recipients, we noted naïve-associated genes (*IL7R, LEF1, TCF7, CCR7* in both cohorts; *CXCR4, CD28, IL6ST* in cohort 1; *PTK2* in cohort 2) (Griffith et al., 2014; Holmes et al., 2005; Willinger et al., 2005, 2006) and genes involved in the WNT signaling pathway (*TCF7, LEF1, NT5E*). TCF7 and LEF1 are highly expressed in naïve $CD8^+$ T cells and their expression is downregulated following TCR or IL15R engagement *in vitro* and antigen encounter *in vivo* (Willinger et al., 2006). In line with this observation, downregulation of naïve-associated genes and enrichment of genes associated with memory cells (*CD45R0, CX3CR1, CCR5, EOMES, CD160, TBX21, KLRG1*) (Weng et al., 2012; Willinger et al., 2005) after HSCT could indicate the acquisition of an effector memory phenotype in response to host antigens and/or IL15 signaling, and a decreased abundance of naïve T cells.

Of note, one of the genes displaying the highest fold change in gene expression in both $CD4^+$ and $CD8^+$ T cells from recipients compared to their donors encodes the fractalkine receptor CX3CR1. Increases in $CX3CR1^+$ $CD4^+$ T cells have been reported in pathological conditions such as rheumatoid arthritis and inflammatory bowel disease (Kobayashi et al., 2007; Nanki et al., 2002). Moreover, CX3CR1 expression on T cells has been correlated with increased expression of

type 1 cytokines and cytotoxic molecules (Nanki et al., 2002). Within the $CD8^+$ compartment CX3CR1 identifies three distinct effector and memory T cell subsets. CX3CR1 expression was shown to correlate with the degree of effector differentiation, being highly expressed on effector memory cells (Gerlach et al., 2016). Increased *CX3CR1* expression in T cells after transplantation could therefore indicate changes in T cell polarization, migratory properties and a shift towards a memory/activated phenotype due to the lymphopenic and inflammatory environment present in HSCT recipients.

Figure 40 HSCT is associated with major transcriptomic changes in CD8$^+$ T cells
(A) Heatmap showing the gene expression profile of CD8$^+$ T cells in donors and recipients at day 90 post-HSCT in cohort 2. In the heatmap columns represent samples and are ordered by hierarchical clustering, while rows represent genes and are ranked by fold change. Yellow indicates high levels of expression and blue indicates low levels of expression. Paired t-test (donors *versus* recipients) with false discovery rate correction Q=1%. 221 genes are differentially expressed between donors and recipients (18 donor-recipient pairs). Comparable results are observed in cohort 1 (heatmap not shown). (B) Histograms representing selected genes upregulated in the recipients compared to the donors in cohort 1 (blue bars) and in cohort 2 (red bars). The fold change between recipients and donors is shown for each gene in the two cohorts. The presented genes were grouped according to their presumed function based on information available in public databases or in the literature.

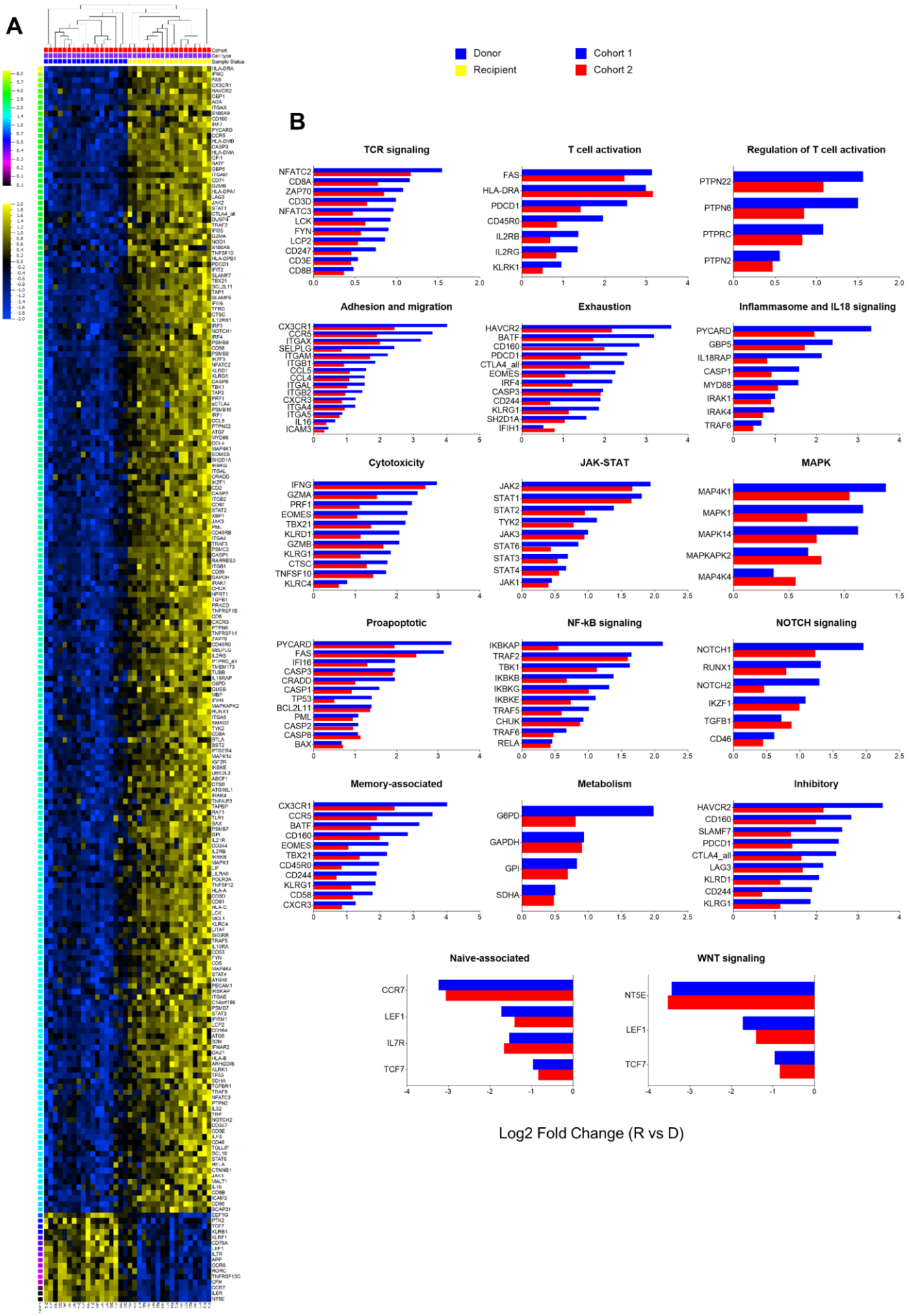
A
Cohort
Cell type
Sample Status
B
Donor
Recipient
Cohort 1
Cohort 2
TCR signaling
NFATC2
CD8A
ZAP70
CD3D
NFATC3
LCK
FYN
LCP2
CD247
CD3E
CD8B
T cell activation
FAS
HLA-DRA
PDCD1
CD45R0
IL2RB
IL2RG
KLRK1
Regulation of T cell activation
PTPN22
PTPN6
PTPRC
PTPN2
Adhesion and migration
CX3CR1
CCR5
ITGAX
SELPLG
ITGAM
ITGB1
CCL5
CCL4
ITGAL
ITGB2
CXCR3
ITGA4
ITGA5
IL16
ICAM3
Exhaustion
HAVCR2
BATF
CD160
PDCD1
CTLA4_all
EOMES
IRF4
CASP3
CD244
KLRG1
SH2D1A
IFIH1
Inflammasome and IL18 signaling
PYCARD
GBP5
IL18RAP
CASP1
MYD88
IRAK1
IRAK4
TRAF6
Cytotoxicity
IFNG
GZMA
PRF1
EOMES
TBX21
KLRD1
GZMB
KLRG1
CTSC
TNFSF10
KLRC4
JAK-STAT
JAK2
STAT1
STAT2
TYK2
JAK3
STAT6
STAT3
STAT4
JAK1
MAPK
MAP4K1
MAPK1
MAPK14
MAPKAPK2
MAP4K4
Proapoptotic
PYCARD
FAS
IFI16
CASP3
CRADD
CASP1
TP53
BCL2L11
PML
CASP2
CASP8
BAX
NF-kB signaling
IKBKAP
TRAF2
TBK1
IKBKB
IKBKG
IKBKE
TRAF5
CHUK
TRAF6
RELA
NOTCH signaling
NOTCH1
RUNX1
NOTCH2
IKZF1
TGFB1
CD46
Memory-associated
CX3CR1
CCR5
BATF
CD160
EOMES
TBX21
CD45R0
CD244
KLRG1
CD58
CXCR3
Metabolism
G6PD
GAPDH
GPI
SDHA
Inhibitory
HAVCR2
CD160
SLAMF7
PDCD1
CTLA4_all
LAG3
KLRD1
CD244
KLRG1
Naive-associated
CCR7
LEF1
IL7R
TCF7
WNT signaling
NT5E
LEF1
TCF7
Log2 Fold Change (R vs D)

5.2 Transcriptomic profile of CD4$^+$ and CD8$^+$ T cells in donors and in recipients early after HSCT

To investigate T cell transcriptomic changes associated with immune reconstitution at an early time point after HSCT, we analysed the gene expression profiles of CD4$^+$ and CD8$^+$ T cells from recipients at day 30 posttransplant compared to their donors (cohort 3). Already at day 30 after transplantation, the gene expression profile of T cells in the recipients is profoundly different compared to the one of the donors, with the majority of the genes analysed being upregulated after transplantation. In particular, in CD4$^+$ T cells we identified 175 genes differentially expressed between donors and recipients (Q=5%). Of these, 170 are upregulated and only 5 are downregulated in the recipients after transplantation. Similarly, in CD8$^+$ T cells we found 134 genes differentially expressed (Q=5%), of which only 3 are downregulated in the recipients after transplantation (**Figure 42**). Comparative analysis of the differentially expressed transcripts between donors and recipients at day 90 (cohorts 1 and 2) as compared to day 30 (cohort 3) following HSCT revealed a great overlap of the differentially expressed genes in both CD4$^+$ and CD8$^+$ T cells (**Figure 41**). This suggests that the changes in the T cell transcriptome observed three months after transplantation are in great part already detectable one month posttransplant.

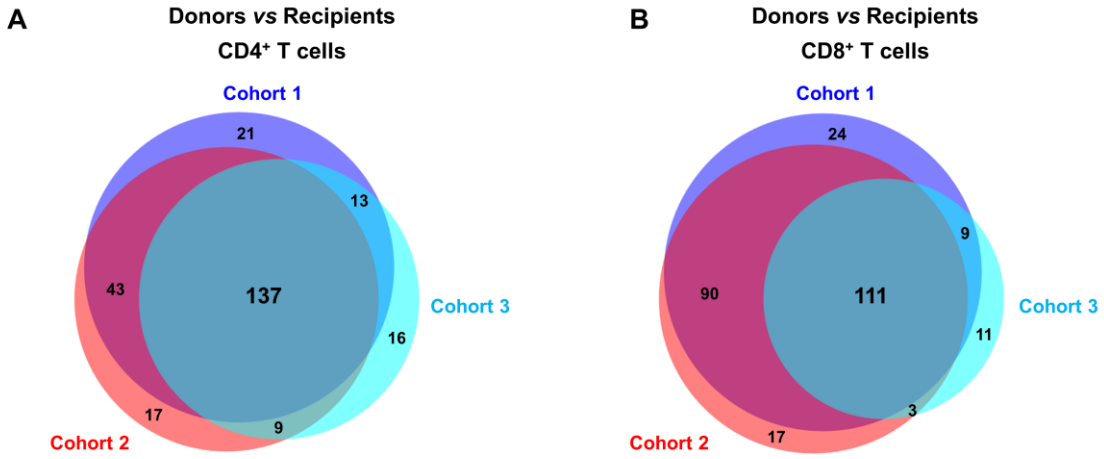

Figure 41 The majority of the T cell transcriptomic changes observed at day 90 post-HSCT are already detectable in the recipients one month after transplantation
Weighted Venn diagrams showing the number of transcripts differentially expressed that are shared in the three cohorts when comparing donors and recipients (paired t-test with FDR correction at Q=1% for cohorts 1 and 2 and Q=5% for cohort 3). Cohort 1 includes 18 donor-recipients couples for both cell populations. Cohort 2 includes 18 couples for CD4$^+$ T cells and 17 couples for CD8$^+$ T cells. Cohort 3 includes 10 couples for CD4$^+$ T cells and 8 couples for CD8$^+$ T cells.

In particular, gene associated with T cell activation (*ZAP70, FYN, LCP2, NFATC, NFATC3, GAPDH, G6PD, FAS*), effector functions (*IFNG, GZMA, GZMB, PRF1, FAS*), adhesion and migration (*CX3CR1,* Integrins, *CXCR3, CXCR6, CCR5, CCL5*), and co-inhibitory receptors (*LAG3, PDCD1, HAVCR2, TIGIT, CTLA4*) are upregulated in the recipients at day 30 post-HSCT compared to the donors. Moreover, as observed three months after transplant, already at day 30 posttransplant we noted the upregulation of some genes related to IL18 signaling and inflammasome biology (*IL18R1, IL18RAP, MYD88, IRAK1, IRAK4, PYCARD, GBP5*) and some proapoptotic genes (*BAX, CASP1, CASP2, CASP3, CASP8*). Only 5 and 3 genes were downregulated in $CD4^+$ and $CD8^+$ T cells respectively. Of these, *CCR7* and *PTK2* have been reported to be highly expressed in naïve T cells (**Figure 42**) (Griffith et al., 2014; Holmes et al., 2005).

Figure 42 Major transcriptomic changes are already detectable in T cells 30 days after HSCT
Heatmaps showing the gene expression profiles of $CD4^+$ (A) and $CD8^+$ (B) T cells in donors and recipients at day 30 post-HSCT in cohort 3. In the heatmap columns represent samples and are ordered by hierarchical clustering, while rows represent genes and are ranked by fold change. Yellow indicates high levels of expression and blue indicates low levels of expression. Paired t-test (donors *versus* recipients) with false discovery rate correction Q=5%. 175 genes are differentially expressed between donors and recipients in $CD4^+$ T cells (10 donor-recipient pairs) and 134 genes are differentially expressed in $CD8^+$ T cells (8 donor-recipient pairs).

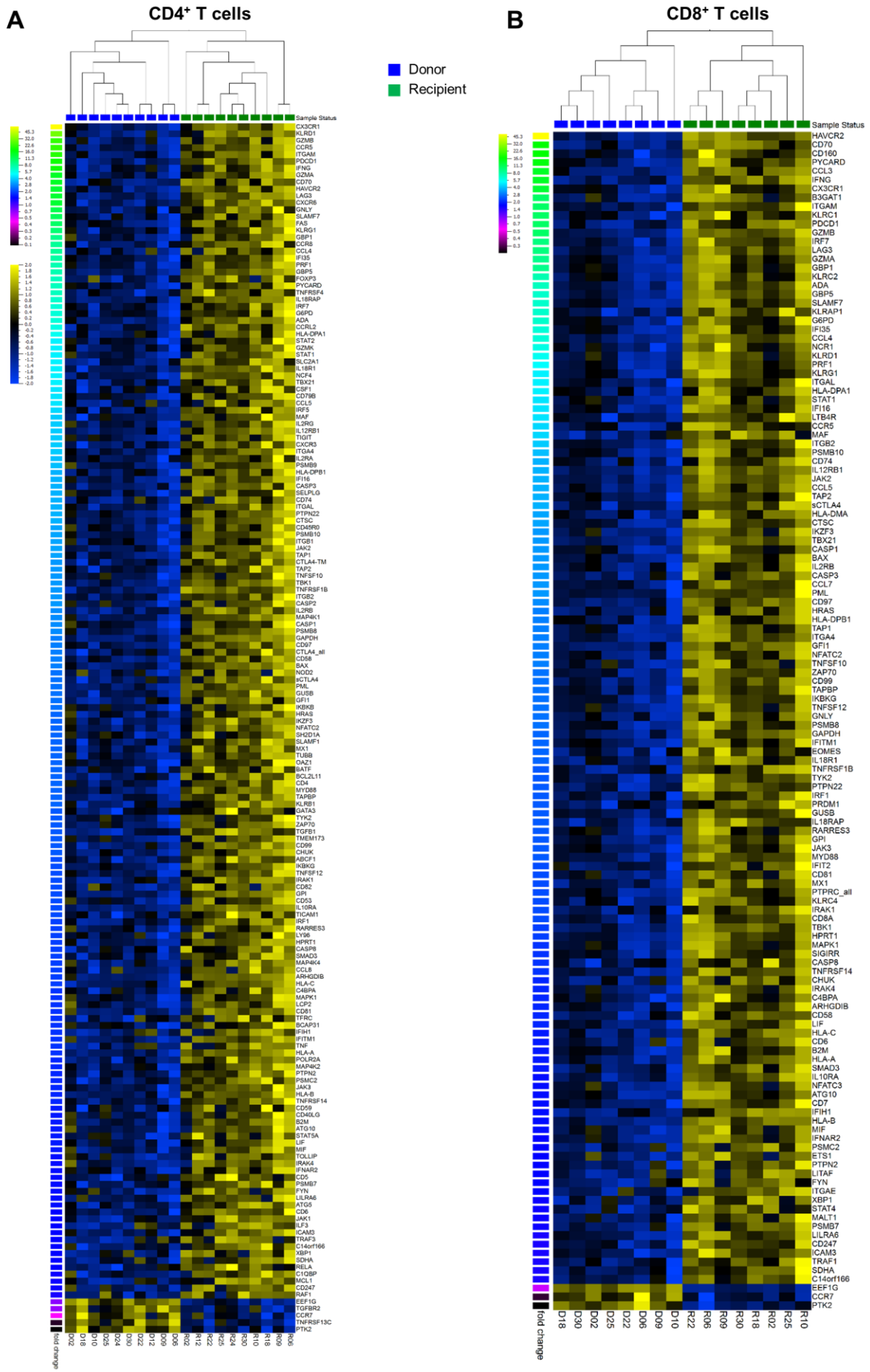
A
CD4+ T cells
Donor
Recipient
Sample Status
fold change
B
CD8+ T cells
Sample Status
fold change

5.2.1 Pathway enrichment in recipients 30 days after HSCT compared to their donors

To functionally interpret the differentially expressed genes in $CD4^+$ and $CD8^+$ T cells from recipients at day 30 post-HSCT compared to their donors, we applied the QuSAGE algorithm using 53 of the gene modules we designed. QuSAGE analysis on the T cell transcriptome at this early time point revealed a statistically significant enrichment of 40 and 32 gene modules in $CD4^+$ and $CD8^+$ T cells, respectively (**Figure 43**). All enriched modules had an increased pathway activity in the recipients compared to the donors. Among the gene sets displaying the strongest increase in pathway activity with the lowest FDR in $CD4^+$ T cells we observed *IL2 signaling*, coinhibitory receptors (*Coinhibitory*), *CTL-Cytotoxicity*, *Th1 profile* and *Memory* modules, followed by *T cell activation* and *NLR-inflammasome*, confirming the pattern observed at day 90 post-transplant.

Similarly, in $CD8^+$ T cells, gene modules enrichment ranking in the recipients confirmed what observed three months after transplantation, with *Coinhibitory*, *CTL-Cytotoxicity*, *Exhaustion-up* and *IFN-induced* being the modules displaying the highest increase in pathway activity.

PBMCs isolated from recipients and donors of cohorts 1 and 2 had been cryopreserved, while blood samples from subjects of this third cohort were processed immediately after collection. For technical reasons, samples had to be processed and analysed using slightly different protocols: (i) due to the limited number of cells available from the biobank and cell loss caused by the freezing and thawing procedures, we obtained lower RNA yields for the two cryopreserved cohorts compared to the freshly collected samples. Gene expression analysis was thus performed starting with a lower RNA input leading to loss of lowly expressed genes that fell under the background level; (ii) due to a lower number of donor-recipient couples available in this cohort, the two-group comparison has been performed with a less stringent FDR correction (Q=5%). However, despite these technical differences, we could reproduce the T cell gene expression signature associated with HSCT in the recipients in these three independent cohorts.

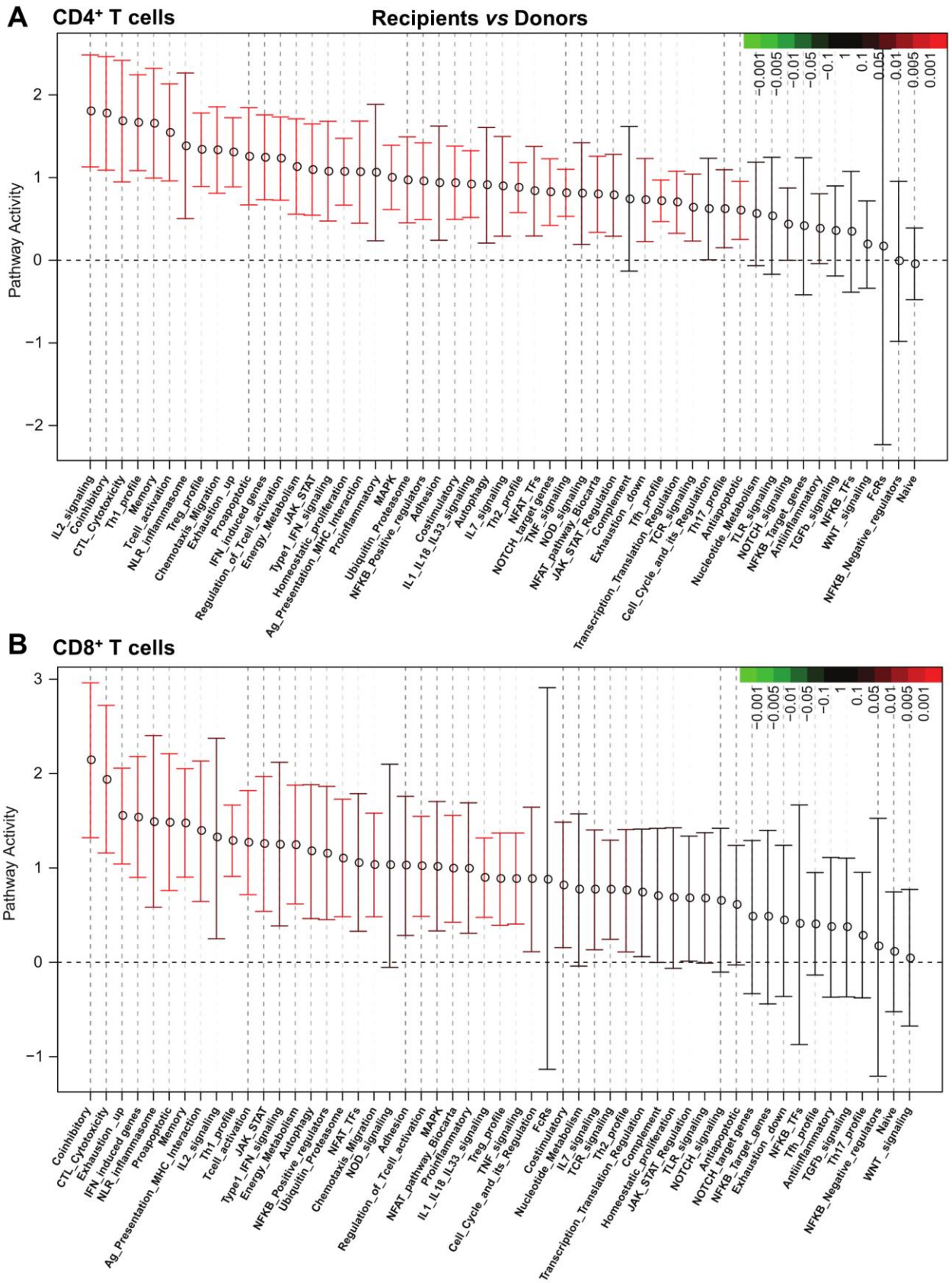

Figure 43 Enriched pathways in recipients at day 30 after HSCT

QuSAGE analysis on CD4+ (A) and CD8+ (B) T cell transcriptome in recipients at day 30 post-HSCT compared to their respective donors before transplant in cohort 3. For each pathway, the mean fold change and the 95% confidence interval are plotted and colour-coded according to their False Discovery Rate (FDR)-corrected P-values when compared to zero. Red and green bars indicate a statistically significant increased or decreased pathway activity respectively, in the recipients compared to the donors.

In summary, these data suggest that allogeneic HSCT is associated with major transcriptomic changes in $CD4^+$ and $CD8^+$ T cells. These changes are already detectable in the recipients at early time points (day 30) posttransplant and they persist over time (until three months post-HSCT). In the "empty" environment of the host, donor T cells acquire an activated phenotype with upregulation of genes associated to T cell activation, adhesion, migration and effector functions. The presence of a proinflammatory environment resulting from the release of danger signals and inflammatory mediators following the conditioning regimen induces the polarization of T helper (Th) 1 and Th17 (for $CD4^+$ T cells) and T cytotoxic (Tc1) and Tc17 cells (for $CD8^+$ T cells) (Ramadan and Paczesny, 2015). Our data suggest that after HSCT $CD4^+$ T cells acquire a Th1-like profile with upregulation of *TBX21* (encoding the transcription factor T-bet) and other genes typically associated with Th1 cells such as *IFNG*, *CXCR3*, *IL12RB1* and *CD46*. Of note, CD46 co-stimulation has been implicated in both the initiation and resolution of the Th1 response. Intracellularly activated complement components and the NLRP3 inflammasome seem to be fundamental for human Th1 induction and regulation (Arbore et al., 2016; Hess and Kemper, 2016). Interestingly, some genes involved in complement activation and regulation such as *ITGB2, ITGAM* and *CD59* are also upregulated in the recipients after HSCT. In addition to the aforementioned genes involved in complement regulation, in cohort 3 we noted the upregulation of *C1QBP* and *C4BPA* and of *SLC2A1* (encoding the glucose transporter GLUT1) in $CD4^+$ T cells from transplant recipients, supporting the hypothesis that the complement pathway might be involved in immune changes associated with allogeneic HSCT. It has been recently highlighted that complement pathways play a role in regulating T cell biology through the regulation of cell metabolism, cell differentiation to Th1 profile or response to inflammasome (Arbore and Kemper, 2016; Hess and Kemper, 2016). During the Th1 induction phase cells display high levels of glycolysis and oxidative phosphorylation (OXPHOS) required for IFNγ secretion (West et al., 2018). In line with this concept, $CD4^+$ T cells after HSCT showed upregulation of many genes encoding enzymes involved in glucose metabolism and OXPHOS such as glucose-6-phosphate dehydrogenase (*G6PD*), glyceraldehyde-3-phosphate dehydrogenase (*GAPDH*), glucose-6-phosphate isomerase (*GPI*) and succinate dehydrogenase complex flavoprotein subunit A (*SDHA*).

Compared to $CD4^+$ T cells, $CD8^+$ T cells have been reported to be more responsive to IL15 signaling and to undergo peripheral expansion more rapidly in lymphopenic conditions, with

acquisition of a memory phenotype (Lauvau and Goriely, 2016; Sprent and Surh, 2011). The transcriptional networks involved in this unconventional differentiation process are not completely understood, yet Eomesodermin (Eomes), an important T cell T-box transcription factor, seems to play a central role in driving these cells to acquire a memory phenotype and it controls the expression of IL2Rβ, the transducing IL15 receptor beta chain (Gordon et al., 2011; Lauvau and Goriely, 2016). Interestingly, after transplantation we noticed in $CD8^+$ T cells an increased expression of both *EOMES* and *IL2RB*, as well as many genes associated with memory cells. Moreover, *GZMB* and other cytotoxic molecules (*PRF1*, *GZMA*) reported to be induced in response to IL15 in the absence of antigen or TCR stimulation (Dulphy et al., 2008; Liu et al., 2002; Tamang et al., 2006), are upregulated in $CD8^+$T cells following transplantation. On the contrary, *TCF7* and *LEF1*, belonging to the WNT signaling pathway, are downregulated, consistent with the acquisition of an effector memory phenotype in response to alloantigens or IL15 stimulation (Willinger et al., 2006).

Furthermore, the combination of antigen-driven and homeostatic T cell expansion in lymphopenic recipients has been suggested to be a potent driver of T cell exhaustion, similarly to what has been described in the context of chronic viral infections (Kahan et al., 2015; Valujskikh and Li, 2012; Wherry and Kurachi, 2015). Chronic stimulation by host antigens might therefore lead to the upregulation of genes associated with cell exhaustion. It should be noted, however, that beyond being associated with an "exhausted" phenotype, the expression profile of several inhibitory receptors changes depending on the differentiation and activation status of the cell. Legat and colleagues reported that the inhibitory receptors PD1, CD244, KLRG1, CD160 and to a lesser extent Tim-3 are particularly upregulated with differentiation. Moreover, the authors showed that multiple inhibitory receptors are positively correlated to T cell activation (Legat et al., 2013), suggesting that the upregulation of genes encoding inhibitory receptors might reflect the activation and differentiation of the cells rather than an exhausted state.

Finally, the overrepresentation of genes associated with memory cells and the downregulation of naïve-associated genes is consistent with the depletion of the naïve T cell pool and the enrichment of memory cells observed at the cellular level. Since we sorted and analysed $CD4^+$ and $CD8^+$ T cells in bulk and not at the single-cell level, this observation might reflect the difference in abundance of naïve and memory subsets in the recipients compared to the donors.

Taken together these data indicate that donor T cells undergo major transcriptomic changes in the "environment" of the recipient after HSCT. In particular, T cells seem to acquire an activated phenotype with features of effector memory cells in both $CD4^+$ and $CD8^+$ compartments, while markers of naïve cells are underrepresented. $CD4^+$ T cells display a pattern of gene expression resembling a Th1 profile, while $CD8^+$ T cells are characterized by an upregulation of genes related to cytotoxic functions and of many of co-inhibitory receptors. In both compartments we noted an upregulation of genes associated with T cell exhaustion. This could be linked to chronic stimulation by host persistent antigens. These changes were detectable in the T cell transcriptome already at day 30 post-transplant and persisted until the later time point analysed, three months after transplantation, indicating that the effects of the transplantation procedure on the reconstituting immune system last several months.

5.3 Reconstitution and transcriptomic profile of $CD14^+$ monocytes in recipients after HSCT

Following HSCT, monocytes are the first cells to engraft, rapidly followed by granulocytes, platelets, and NK cells (Storek et al., 2008). Human monocytes represent an heterogenous populations with distinct phenotypic and functional characteristics. They can be classified in at least three subsets based on the expression of the LPS co-receptor CD14 and the receptor for the Fc portion of immunoglobulin G (FcγRIII) CD16. The major population, termed classical monocytes, accounts for about 90% of all monocytes and is characterized by high CD14 but no CD16 expression ($CD14^{++}$ $CD16^-$). $CD16^+$ cells account for about 10% of human monocytes and are further subdivided into the intermediate subset, with high CD14 and low CD16 ($CD14^{++}CD16^+$), and the non-classical subset with high CD16 but with relatively lower CD14 expression ($CD14^+CD16^{++}$). A developmental relationship from classical by intermediate to non-classical has been proposed, with the intermediate subset representing a transitional population bridging between the classical and the non-classical monocyte subsets (Ziegler-Heitbrock et al., 2010). Classical monocytes are thought to be a highly versatile subset, capable of responding to a variety of stimuli and mediate tissue repair or immune functions (Wong et al., 2011). The intermediate subset is likely to be predisposed to exert important functions in transplantation due to its ability to present antigens and to induce T cell proliferation, as these cells express higher levels of genes encoding MHC II molecules and genes involved in antigen processing and protein turnover (Wong et al., 2011; Zawada et al., 2011). Intermediate monocytes are considered to have proinflammatory functions, as they were shown to expand in inflammatory conditions (Wong et al., 2011; Ziegler-Heitbrock et al., 2010) and to produce high levels of inflammatory cytokines such as TNFα, IL12 and IFNγ upon challenge (Frankenberger et al., 1996; Zawada et al., 2011; Ziegler-Heitbrock and Hofer, 2013). It is unclear, however, whether shifts in CD16-positive monocytes reported in many inflammatory diseases were caused by an increase of CD16-positive cells or rather selective increases of intermediate or non-classical monocyte subsets (Zawada et al., 2011). Non-classical monocytes were shown to have patrolling function and to produce low levels of proinflammatory cytokines in response to bacteria-derived stimuli, but high levels of anti-inflammatory and wound healing factors (Cros et al., 2010; Thomas et al., 2015) Transcriptomic analyses demonstrated specific gene expression signatures that distinguish the three monocyte subsets (Ingersoll et al., 2010; Wong et al., 2011; Zawada et al., 2011). The dynamics of

reconstitution of the three different monocyte subsets and their role in the context of acute GVHD are unclear.

5.3.1 Expansion of CD16-expressing monocytes in recipients after transplantation

To investigate whether immune reconstitution after HSCT is associated with imbalances in monocyte subset distribution compared to the donors before transplant, we quantified classical, intermediate and non-classical monocyte subsets in 10 donor-recipient couples (in the absence of GVHD) from cohort 2 by flow cytometry. As shown in **Figure 44**, we assessed the frequency of the three monocyte subsets within the $CD14^+$ population based on CD14 and CD16 expression. To identify transcriptomic changes associated with HSCT, we also sorted total $CD14^+$ monocytes and performed gene expression profiling.

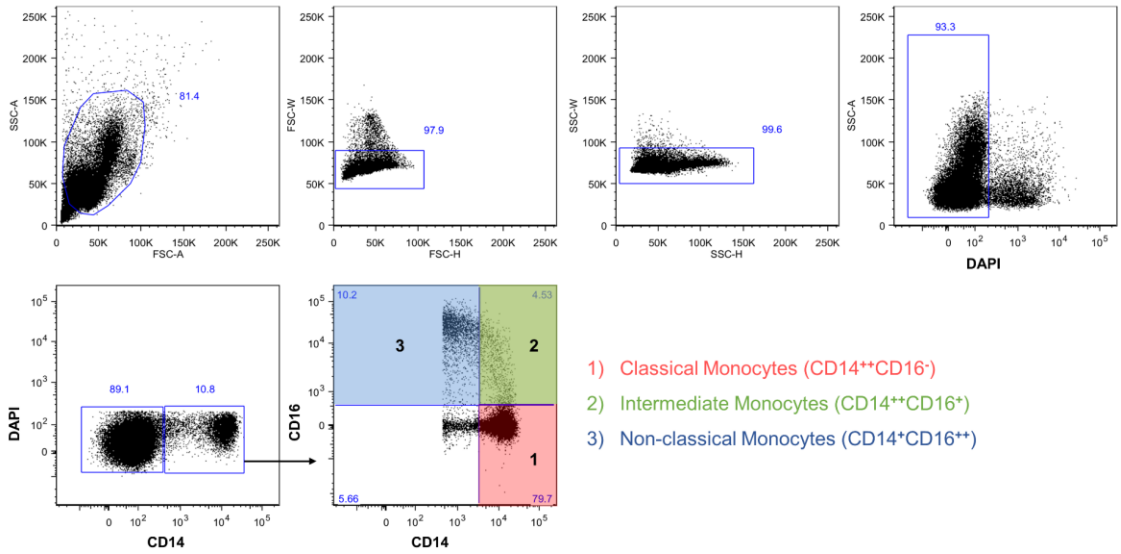

Figure 44 Identification of monocyte subsets in donors and recipients after HSCT
Gating strategy used to define classical ($CD14^{++}CD16^-$), intermediate ($CD14^{++}CD16^+$) and non-classical ($CD14^+CD16^{++}$) monocytes subsets in 10 donors and their recipients 90 days after HSCT. Representative staining on a donor's sample.

Three months after transplantation, we observed in the recipients an increased frequency of total $CD14^+$ monocytes compared to the donors, consistent with a rapid recovery of this cell population following HSCT. Within the total $CD14^+$ population, we noted an expansion of CD16-expressing cells, with increased percentages of both the intermediate and the non-classical subsets, paralleled by a decrease of classical monocytes, as shown in **Figure 45**. After HSCT, classical monocytes have been shown to be the first to recover, followed by the intermediate and non-classical subsets (Rogacev et al., 2015). In line with reports describing an expansion of CD16-

expressing monocytes in various inflammatory diseases (Ziegler-Heitbrock, 2015), the increased frequencies of the intermediate and non-classical subsets we observed in the recipients compared to the donors could be linked to the establishment of a proinflammatory milieu in the post-HSCT period.

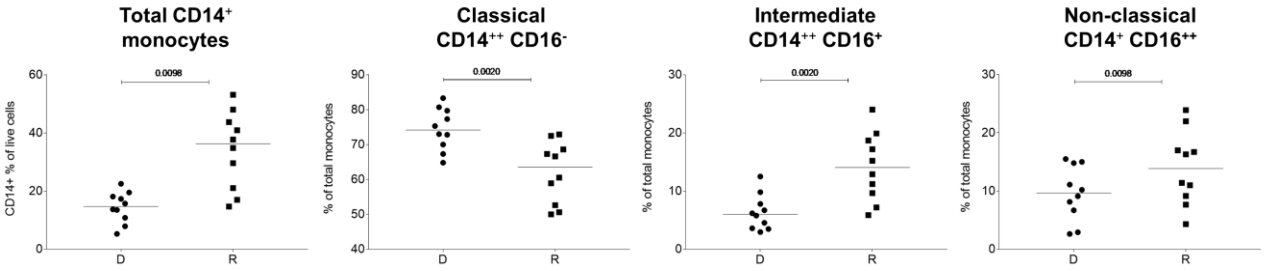

Figure 45 Expansion of CD16-expressing monocyte subsets in recipients after HSCT
Frequency of total $CD14^+$ monocytes, calculated as percentage of live DAPI-negative cells, and frequencies of classical ($CD14^{++}CD16^-$), intermediate ($CD14^{++}CD16^+$) and non-classical ($CD14^+CD16^{++}$) monocytes within the $CD14^+$ population in 10 recipients (R) at day 90 post-HSCT compared to their respective sibling donors (D) in cohort 2. Horizontal bars indicate the median. P-values were calculated using a Wilcoxon matched-pairs t test (donor *versus* respective recipient) and are indicated above the graph. Differences are considered significant for P-values < 0.05.

5.3.2 Monocyte transcriptomic profile in donors and recipients after HSCT

To characterize the impact of HSCT on the transcriptomic profile of monocytes, we measured gene expression of sorted unstimulated monocytes from 10 donors and from the corresponding recipients 90 days after HSCT. Molecular profiling was performed with the nCounter technology using the NanoString Human PanCancer Immune profile codeset. Major changes in gene expression were detected in monocytes from recipients after transplantation compared to their donors. We identified 172 genes differentially expressed between donors and recipients (FDR correction Q=10%). Of these, 164 were upregulated and only 8 were downregulated in the recipients after transplantation, as shown in the heatmap in **Figure 46A**. Consistent with the expansion of the intermediate and non-classical subsets detected at the cellular level, molecular profiling showed that monocytes from HSCT recipients displayed a gene expression profile reminiscent of CD16-expressing cells with upregulation of many genes that have been reported to be expressed in intermediate and non-classical monocytes. In line with an intermediate phenotype, we observed the upregulation of many genes involved in antigen processing and presentation (*TAP1, TAP2, TAPBP, CTSL, CTSS, HLA-A, -B, -C, -DRA, DMA, -DMB, -DPA1, -DPB1*), the

costimulatory molecule *CD40*, and the receptors *MARCO, CMKLR1, FCGR3A* (encoding CD16) and *CCR2* (Martinez, 2009; Wacleche et al., 2018; Wong et al., 2011). We also noticed an enrichment of several complement components and genes involved in complement regulation and activation (*C1QA, C1QB, C2, C3AR1, CD46, CFD, CR1, ITGAX, ITGB2, SERPING1*). As reported by Wong and colleagues these genes are most highly expressed by $CD16^+$ cells, in particular by non-classical monocytes (Wong et al., 2011). In addition, other genes typically associated with non-classical monocytes, such as *CD79B, CX3CR1, FCGR3A* and *ICAM2* (Wong et al., 2011) are enriched in the recipients. Amongst the upregulated transcripts we also noticed many interferon-induced genes (*BST2, CXCL10, IFI16, IFI27, IFI35, IFIH1, IFIT1, IFIT2, IFITM1, IFITM2, IRFs, ISG15, ISG20, MX1*). Upregulation of these genes could be linked to the presence of danger signals, including DAMPs and PAMPs, released post-conditioning and/or following GVHD prophylaxis therapy (including MTX), resulting in the activation of TLR signaling. In addition, the cytokine milieu of the posttransplant period could also lead to the induction of IFN-inducible programs (Ramadan and Paczesny, 2015). Interestingly, we noted the upregulation of the proinflammatory mediators *IL15* and *IL15RA* (encoding the subunit IL-15Rα), whose expression has also been reported to be IFN-induced (Hakim et al., 2016), *IL27* and *CXCL10* (**Figure 46B**). The levels of IL15 have been reported to be increased in recipients after transplantation (Dulphy et al., 2008; Matsuoka et al., 2010; Thiant et al., 2016) and to play an important role in the expansion and survival of T cell (in particular memory $CD8^+$ T cells) and NK cell subsets (Carson et al., 1997). IL15 signals through a heterotrimeric receptor that involves the common γ chain (CD132 or IL2Rγ), the IL2/IL15 receptor β (CD122 or IL2Rβ) and a third unique receptor subunit IL15Rα. IL15Rα on the cell surface presents IL15 *in trans* to neighbouring cells that express IL2Rβ and IL2Rγ (Waldmann, 2013). Upregulation of the genes encoding both IL15 and its receptor subunit IL15Rα in monocytes after HSCT could play a role in the expansion of memory T cells as well as of the $CD56^{bright}$ subset of NK cells that is observed in the recipients after transplantation (Dulphy et al., 2008). Changes in the frequency of the different NK cell subsets and the transcriptomic profile of NK cells in recipients after HSCT will be discussed in the next section. IL27, a member of the IL6/IL12 family, plays a role in both innate and adaptive responses. In adaptive immunity, it has been shown to cooperate with IL12 in promoting IFNγ production by $CD4^+$ and $CD8^+$ T cells and in inducing Th1 differentiation. Overexpression of *IL27* in monocytes after HSCT could be linked to the shift towards a Th1 profile observed at the gene

expression level in $CD4^+$ T cells from recipients following transplantation. Moreover, the overexpression of *CXCL10* could be involved in a cross-talk between monocytes and cells expressing the CXCL10 receptor CXCR3 and influence $CXCR3^+$ lymphocyte trafficking.

Monocytes are relatively undifferentiated and plastic cells and they have been shown to rapidly acquire discrete gene expression profiles in response to different cytokines such as IFN, IL4/IL13 or TGFβ (Martinez et al., 2006). In the context of HSCT, their transcriptome could thus provide a snapshot of the cytokine milieu they are exposed to and how these cells respond.

Figure 46 Transcriptomic profile of CD14$^+$ monocytes after HSCT
(A) Heatmap showing the gene expression profile of CD14$^+$ monocytes in 10 donors and their corresponding recipients at day 90 post-HSCT in cohort 2. In the heatmap columns represent samples and are ordered by hierarchical clustering, while rows represent genes and are ranked by fold change. Yellow indicates high levels of expression and blue indicates low levels of expression. Paired t-test (donors *versus* recipients) with false discovery rate correction Q=10%. 172 genes are differentially expressed between donors and recipients. (B) Histograms representing selected genes upregulated in 10 recipients compared to the donors in cohort 2. The fold change between recipients and donors is shown for each gene. The presented genes were grouped according to their presumed function based on information available in public databases or in the literature.

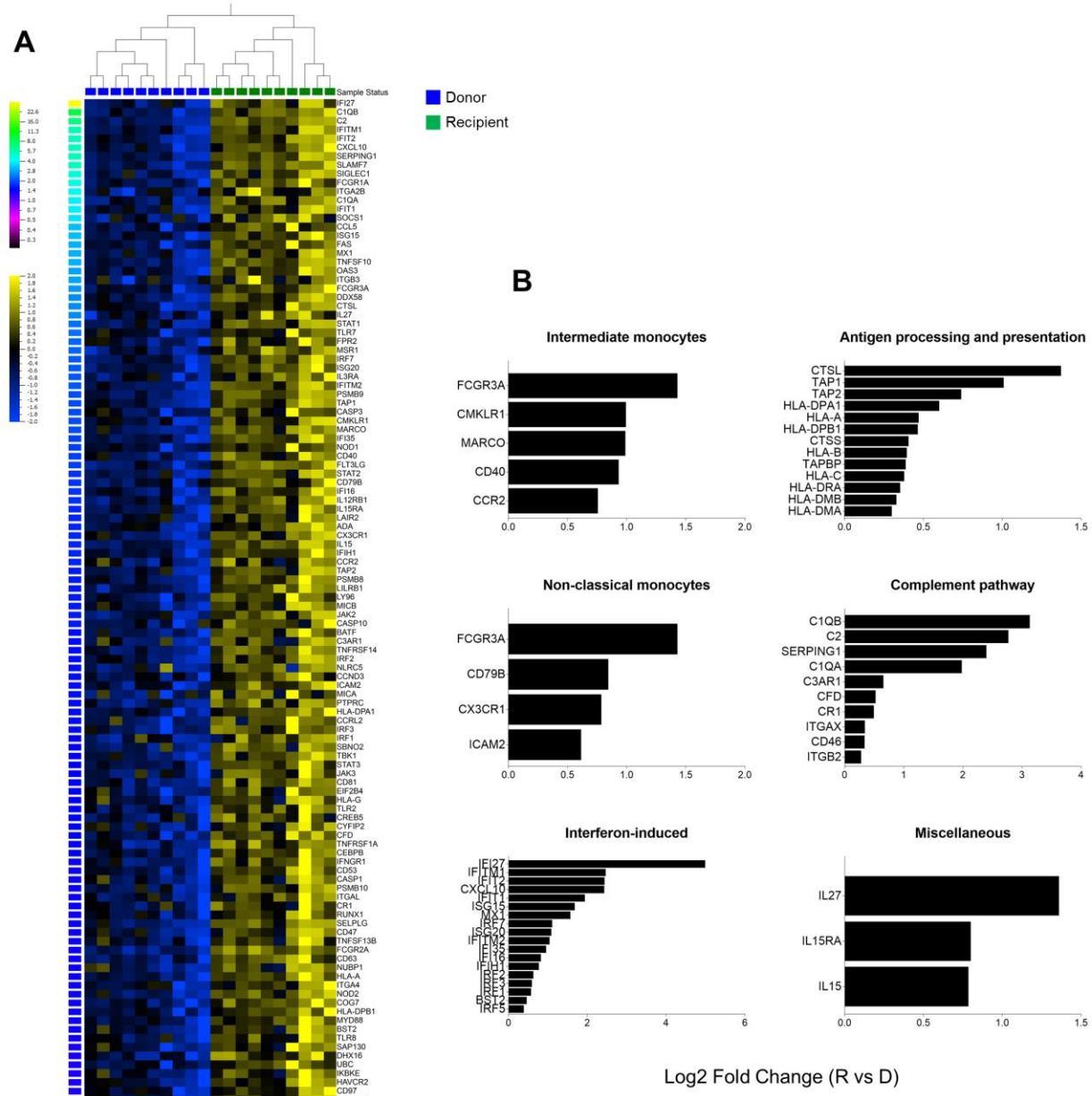
A
Sample Status
Donor
Recipient
B
Intermediate monocytes
FCGR3A
CMKLR1
MARCO
CD40
CCR2
Antigen processing and presentation
CTSL
TAP1
TAP2
HLA-DPA1
HLA-A
HLA-DPB1
CTSS
HLA-B
TAPBP
HLA-C
HLA-DRA
HLA-DMB
HLA-DMA
Non-classical monocytes
FCGR3A
CD79B
CX3CR1
ICAM2
Complement pathway
C1QB
C2
SERPING1
C1QA
C3AR1
CFD
CR1
ITGAX
CD46
ITGB2
Interferon-induced
IFI27
IFITM1
IFIT2
CXCL10
IFIT1
ISG15
MX1
IRF7
ISG20
IFITM2
IFI35
IFI16
IFIH1
IRF2
IRF3
BST2
IRF5
Miscellaneous
IL27
IL15RA
IL15
Log2 Fold Change (R vs D)

Next, we applied QuSAGE analysis with 46 gene modules we designed for this cell population. The complete list of the gene modules constructed and used for this analysis is described in **Annex Table 7**. As shown in **Figure 47**, of the 46 gene sets tested, 27 displayed a statistically significant increased pathway activity in the recipients. Consistent with the results described above, IFN-induced genes (*IFN-induced*), *Non-classical monocytes* and the complement pathway (*Complement*) were the modules with the highest increase in pathway activity followed by *Cytotoxicity*, *M1-like monocytes*, *JAK-STAT*, *Ubiquitin-proteasome* and *Intermediate monocytes*.

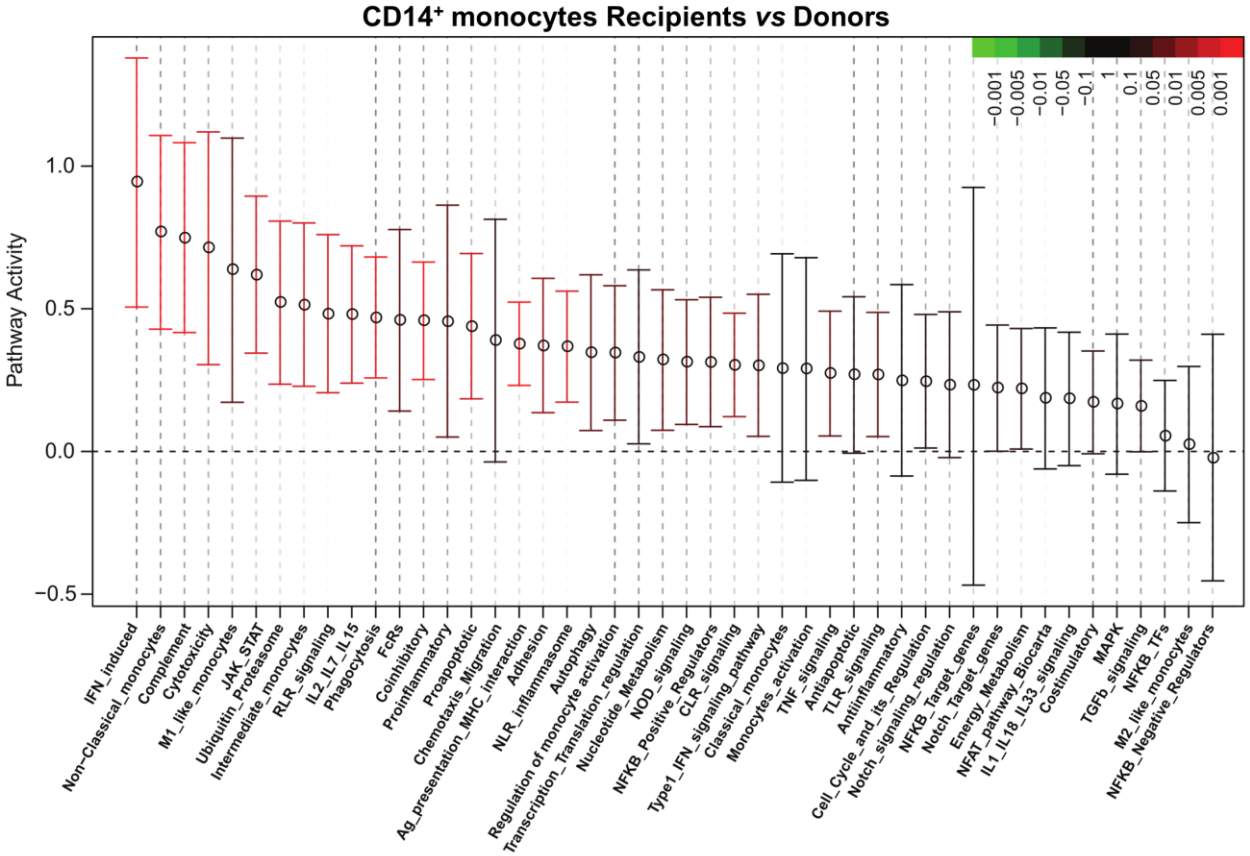

Figure 47 Enriched pathways in monocytes from recipients at day 90 after HSCT
QuSAGE analysis on CD14⁺ monocyte transcriptome in 10 recipients at day 90 post-HSCT compared to their respective donors before transplant in cohort 2. For each pathway, the mean fold change and the 95% confidence interval are plotted and colour-coded according to their False Discovery Rate (FDR)-corrected P-values when compared to zero. Red and green bars indicate a statistically significant increased or decreased pathway activity respectively, in the recipients compared to the donors.

Taken together, these data indicate that blood monocytes undergo major changes both in their subset distribution and in their gene expression profile following HSCT. In particular, the reconstituting monocyte population is characterized by an expansion of CD16-expressing cells while the classical monocyte subset displayed a decreased frequency. The gene expression profiling mirrored this increased abundance of intermediate and non-classical monocytes in the recipients, with overrepresentation of many genes that have been reported to be expressed in these cell subsets. The presence of an inflammatory environment, might drive the expansion of these $CD16^+$ subsets. In turn these cells contribute producing inflammatory mediators (e.g. IL15, IL27 and CXCL10) that can influence other cell populations such as T and NK cells. Stimulation of innate cells via TLRs results in upregulation of MHC expression as well as that of costimulatory molecules (e.g. CD40) and production of proinflammatory cytokines. This affects T cell activation and proliferation, and the inflammatory environment generated by TLR responses polarizes T helper cells towards a Th1 profile (Ramadan and Paczesny, 2015).

5.4 Reconstitution and transcriptomic profile of CD56^{+} NK cells in recipients after HSCT

Following HSCT, NK cells are the first donor-derived lymphocyte subset to recover, and may therefore play an important role in the protection against infections and tumours before T cell immunity is restored (Storek et al., 2008). NK cells, originally defined by their natural cytotoxicity against tumour cells, are now recognized as a separate lymphocyte lineage with both cytotoxicity and cytokine production effector functions (Vivier et al., 2008). In human, NK cells are defined phenotypically by their expression of CD56 (Neural Cell Adhesion Molecule, NCAM) and by the lack of the T cell co-receptor CD3. However, a subset of CD56-negative cells has also been identified. These CD56^{-} cells are rare in healthy individuals, but have been reported to increase in chronic viral infections (Björkström et al., 2010). Based on the surface density of CD56, NK cells can be divided into CD56^{dim} and CD56^{bright} subsets. The majority (around 90%) of human peripheral blood NK cells are CD56^{dim} and express high levels of the receptor for the Fc portion of immunoglobulin G (FcγRIII) CD16, whereas around 10% are CD56^{bright}CD16^{dim} or CD56^{bright}CD16^{-}. Unique phenotypic, functional and homing properties have been described for the CD56^{bright} and CD56^{dim} subsets (Cooper et al., 2001a). CD56^{bright} NK cells are believed to be poorly cytotoxic, while they are the primary source of immunoregulatory cytokines. Constitutive expression of the high-affinity heterotrimeric IL2R (IL2Rαβγ) as well as the c-kit receptor confers to this subset high proliferative response to IL2. On the contrary, CD56^{dim} NK cells are highly cytotoxic and contain much more perforin, granzymes and cytolytic granules compared to the CD56^{bright} subset. Differential expression of chemokine receptors and adhesion molecules results in divergent migratory properties, with CD56^{bright} NK cells preferentially migrating to secondary lymphoid organs and CD56^{dim} cells migrating to acute inflammatory sites (Poli et al., 2009). The developmental relationship between the CD56^{bright} and CD56^{dim} subsets has been debated for a long time and is still an unresolved issue (Michel et al., 2016). Collective evidence seems to support the hypothesis that CD56^{bright} cells represent immature precursors of the more differentiated CD56^{dim} subset. In this view, CD56^{bright} CD16^{dim} cells would be an intermediate stage between the most immature (CD56^{bright} CD16^{-}) and the most mature (CD56^{dim} CD16^{+}) cell types (Chan et al., 2007; Poli et al., 2009). However, it has been reported that activated CD56^{dim}CD16^{bright} cells can upregulate CD56 and lose CD16, so that at least a fraction of them might represent activated NK cells and not precursors (Michel et al., 2016).

5.4.1 CD56^{bright} NK cell expansion in recipients following HSCT

To investigate the dynamics of NK cell reconstitution after HSCT, we next analysed by flow cytometry the frequency of different NK cell subsets in 10 recipients (without GVHD) at day 90 following transplantation compared to their sibling donors. As shown in **Figure 48**, we defined total NK cells as CD14^{-}Lin^{-}CD56$^{+/-}$CD16$^{+/-}$. Within this population we identified five different subsets based on the relative expression of CD56 and CD16: 1) CD56^{bright} CD16^{-}; 2) CD56^{bright}CD16^{+}; 3) CD56^{dim}CD16^{-}; 4) CD56^{dim}CD16^{+} and 5) CD56^{-}CD16^{+}. In healthy individuals populations 3 and 5 are rare (Poli et al., 2009). To identify transcriptomic changes associated with HSCT, we also sorted total CD56^{+} NK cells and performed gene expression profiling.

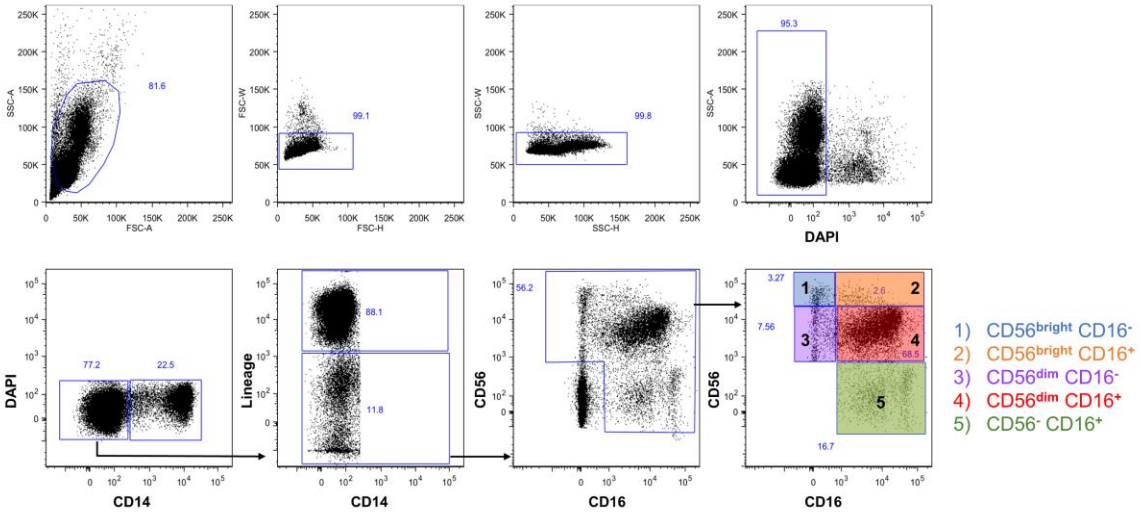

Figure 48 Identification of NK cell subsets in donors and recipients after HSCT
Gating strategy used to define different NK cell subsets based on CD56 and CD16 expression, in 10 donors and their recipients 90 days after HSCT. Total NK cells are defined as CD14^{-}Lin^{-}CD56$^{+/-}$CD16$^{+/-}$. Within this population we identified five different subsets: 1) CD56^{bright} CD16^{-}; 2) CD56^{bright}CD16^{+}; 3) CD56^{dim}CD16^{-}; 4) CD56^{dim}CD16^{+} and 5) CD56^{-}CD16^{+}. Lineage channel includes the markers CD3, CD19, TCRαβ, TCRγδ. Representative staining on a donor's sample.

Recipients after transplantation displayed an increased frequency of total NK cells (**Figure 49**), in keeping with these cells being among the first lymphocytes to repopulate the peripheral blood after allogeneic or autologous transplantation (Storek et al., 2008).

Moreover, within the NK cell population, we noted altered frequencies of the different subsets in the recipients compared to their donors. In particular, we observed a significant enrichment of the $CD56^{bright}CD16^{-}$ and $CD56^{bright}CD16^{+}$ subsets, while the $CD56^{dim}CD16^{+}$ cells are decreased. On the contrary, no significant differences were observed for the $CD56^{dim}CD16^{-}$ and $CD56^{-}CD16^{+}$ subsets.

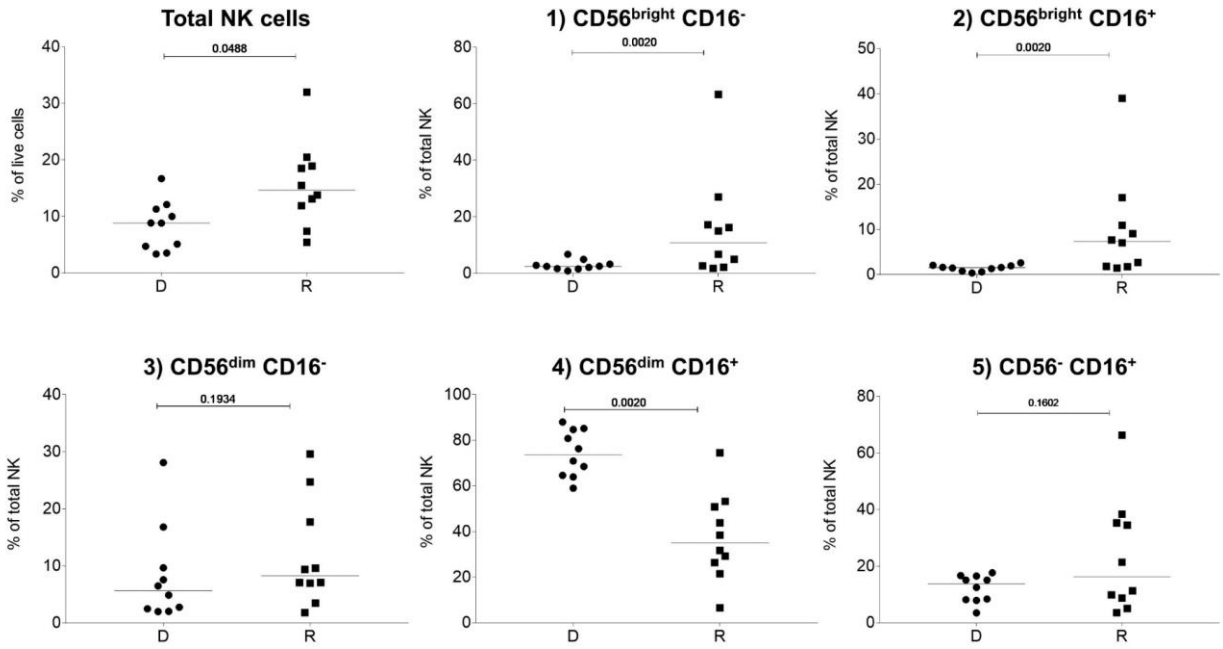

Figure 49 Reconstituting NK cells display a $CD56^{bright}$ phenotype
The frequency of total NK cells, defined as shown in Figure 48, was calculated as percentage of live DAPI-negative cells. Within total NK cells we quantified the percentages of 1) $CD56^{bright}$ $CD16^{-}$; 2) $CD56^{bright}CD16^{+}$; 3) $CD56^{dim}CD16^{-}$; 4) $CD56^{dim}CD16^{+}$ and 5) $CD56^{-}CD16^{+}$ in 10 recipients (R) at day 90 post-HSCT compared to their respective sibling donors (D) in cohort 2. Horizontal bars indicate the median. P-values were calculated using a Wilcoxon matched-pairs t test (donor *versus* respective recipient) and are indicated above the graph. Differences are considered significant for P-values < 0.05.

This increased percentage of $CD56^{bright}$ cells is consistent with data in the literature describing an expansion of the $CD56^{bright}$ NK subset after HSCT (Dulphy et al., 2008; Jacobs et al., 1992). The equilibrium between the two $CD56^{dim}$ and $CD56^{bright}$ subsets has been reported to be altered for at least one year after transplantation (Dulphy et al., 2008). NK cells constitutively express several cytokine receptors including IL1R, IL12R, IL15R and IL18R, and their phenotype changes rapidly when cells are stimulated with cytokines such as IL2, IL15 and IL18 (Cooper et al., 2001a; Storek et al., 2008). The presence of an IL15-rich environment following HSCT (Matsuoka et al.,

2010), as well as the presence of other inflammatory cytokines, might therefore influence the dynamics of NK cells reconstitution.

5.4.2 Transcriptomic profile of NK cells following HSCT

To investigate the changes in gene expression associated with HSCT and immune reconstitution within the NK cell population, we sorted $CD56^{+}$ NK cells from 10 donors before transplant and from the corresponding recipients 90 days after HSCT and we performed molecular profiling using the NanoString Human PanCancer Immune profile codeset. For two donors we could not obtain enough RNA to assess gene expression due to low cell numbers, therefore final transcriptomic analysis included a total of 8 donor-recipient pairs. As shown in the heatmap in **Figure 50A**, we identified 87 genes differentially expressed between donors and recipients (FDR correction Q=10%). Of these, 67 are upregulated and 20 are downregulated in the recipients after transplantation. Transcriptomic profile revealed that NK cells from the recipients display an enrichment of many transcripts associated with $CD56^{bright}$ cells such as *NCAM1, KIT, IL2RA, IL7R, KLRC1* and *2, CXCR3, SELL, IL18R1* and *ITGAX* (Hanna et al., 2004; Poli et al., 2009; Wendt et al., 2006). On the contrary, genes typically expressed by $CD56^{dim}$ NK cells (*CD247, CD244, GZMM, CD160, IGF1R, CD6*) are downregulated in the recipients compared to the donors. Downregulated genes also included some genes related to cell activation and cytotoxicity (*FYN, LCK, GZMM, CTSH, CD40, LY9*). Amongst the upregulated genes in NK cells from the recipients, we also observed genes associated with cell activation (*DPPA, CD9, IL2RA, HAVCR2, AGK, IL18R1, FCER1G, JAK-STATs*) and genes involved in adhesion and migration (*CCR1, CCR2, CCR5, CXCR3, CXCR6, FUT7* and *LGALS3*). Interestingly, some of these genes (*CCR1, CCR5, IL12RB2, IL18R1, AGK, HAVCR2*) have been reported to be specifically upregulated in NK cells stimulated with cytokines (IL12 and IL18) compared to other stimulation methods such as direct cell recognition or stimuli mimicking antibody-dependent cell-mediated cytotoxicity (ADCC) (Costanzo et al., 2018). We also noted an upregulation of many interferon-induced genes (*OAS3; MX1, IRF7, IRF1, IFI35, ISG20, BST2, IFITM1, IFITM2*). In addition, *IL1RL1* (encoding the IL33 receptor, ST2) showed the highest fold change in the recipients compared to the donors before transplant. IL33 is constitutively expressed by epithelial cells and is released upon tissue damage or necrosis functioning as an "alarmin". During irradiation and/or chemotherapy, tissue damage in the host leads to the release of various DAMPs, PAMPs and cytokines, including IL33 (Griesenauer and Paczesny, 2017). It was shown that IL33 cooperates with IL12 to directly induce

IFNγ production from NK cells. IL33 was found to be at least as potent as IL18 in promoting Th1-oriented effector responses (Smithgall et al., 2008).

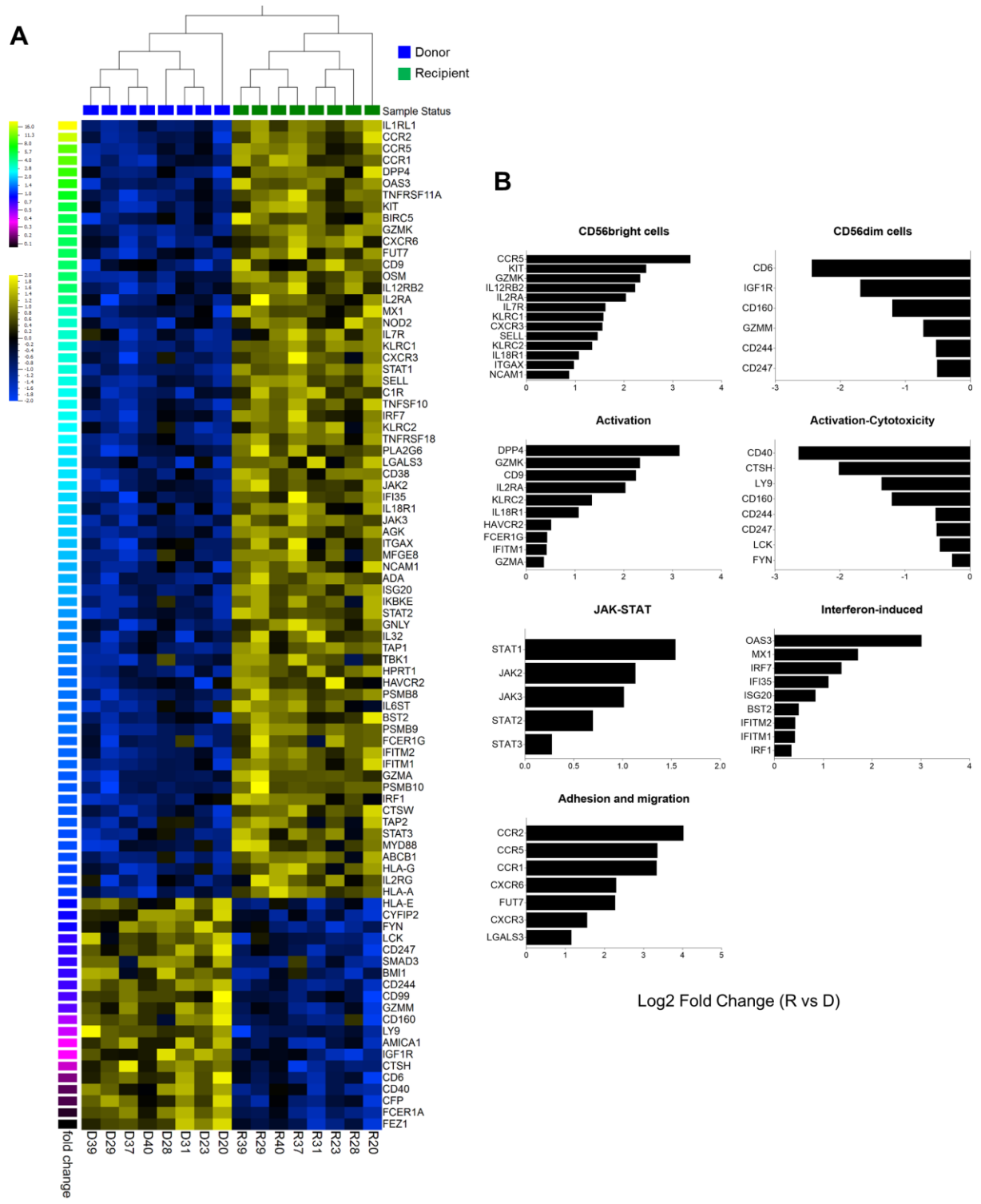

Figure 50 Transcriptomic profile of CD56^{+} NK cells after HSCT

(A) Heatmap showing the gene expression profile of CD56^{+} NK cells in 8 donors and their corresponding recipients at day 90 post-HSCT in cohort 2. In the heatmap columns represent samples and are ordered by hierarchical clustering, while rows represent genes and are ranked by fold change. Yellow indicates high levels of expression and blue indicates low levels of expression. Paired t-test (donors *versus* recipients) with false discovery rate correction Q=10%. 87 genes are differentially expressed between donors and recipients. (B) Histograms representing selected genes upregulated in recipients compared to the donors in cohort 2. The log2 of the fold change between recipients and donors is shown for each gene. The presented genes were grouped according to their presumed function based on information available in public databases or in the literature.

Next, we applied QuSAGE analysis with 49 gene modules we designed for this cell population. The complete list of the gene modules constructed and used for this analysis is described in **Annex Table 8**. Of the 49 gene sets tested, 6 displayed a statistically significant increased pathway activity in the recipients, while 1 was decreased (**Figure 51**). Consistent with the results described above, the module *NK CD56^{bright}* showed the highest increase in pathway activity, while the module including genes associated with CD56^{dim} cells (*NK CD56^{dim}*) was decreased, even though it did not reach statistical significance. Enriched modules with the lowest FDR included IFN-induced genes (*IFN-induced*), *Ubiquitin-Proteasome*, *JAK-STAT*, followed by *IL2-IL7-IL15 signaling* and *Proinflammatory molecules*. On the contrary the module *FcRs*, including genes encoding Fc receptors, displayed a significant decrease in pathway activity in the recipients.

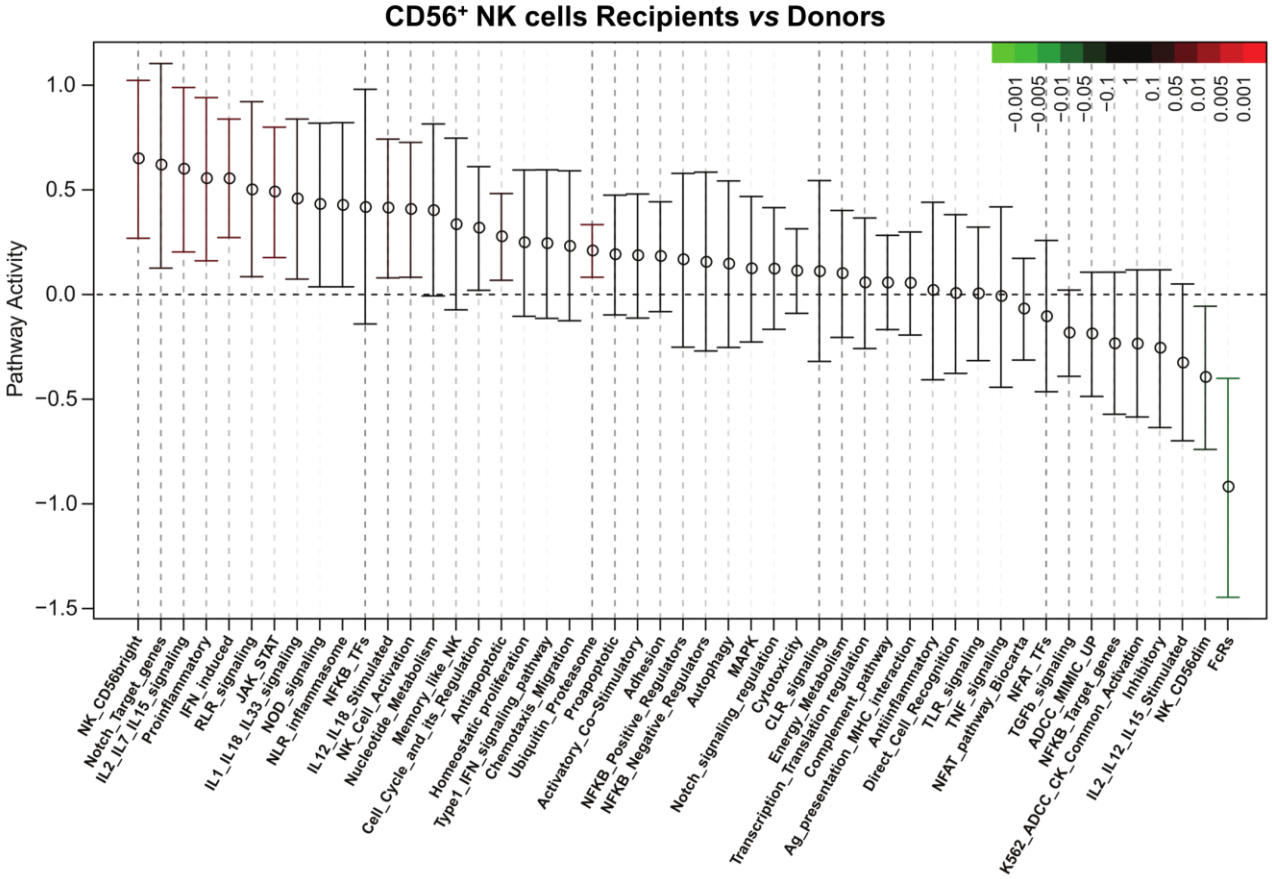

Figure 51 Enriched pathways in NK cells from recipients at day 90 after HSCT
QuSAGE analysis on CD56^{+} NK cell transcriptome in 8 recipients at day 90 post-HSCT compared to their respective donors before transplant in cohort 2. For each pathway, the mean fold change and the 95% confidence interval are plotted and colour-coded according to their False Discovery Rate (FDR)-corrected P-values when compared to zero. Red and green bars indicate a statistically significant increased or decreased pathway activity respectively, in the recipients compared to the donors.

Taken together the results described in this section show that following HSCT, the reconstitution of the NK cell population is characterized by an expansion of the $CD56^{bright}$ subsets with a parallel decrease of $CD56^{dim}$ $CD16^{+}$ cells. As reported by Dulphy and colleagues, we also found that three months after transplantation the percentage of $CD56^{bright}$ $CD16^{dim}$ cells is increased (Dulphy et al., 2008). These cells have been proposed to represent an intermediate population between the more immature $CD56^{bright}$ $CD16^{-}$ subset and the terminally differentiated $CD56^{dim}CD16^{+}$ NK cells (Chan et al., 2007; Dulphy et al., 2008; Poli et al., 2009). Consistent with the increased abundance of $CD56^{bright}$ cells, transcriptomic profiling of NK cells from recipients at day 90 post-transplant revealed a gene expression signature typical of the $CD56^{bright}CD16^{-}$ subset, while genes associated with $CD56^{dim}$ cells and cytotoxicity are underrepresented. The $CD56^{bright}$ NK cell subset is believed to have immunomodulatory properties and shape innate and adaptive immune responses through cytokine production (Michel et al., 2016). Monocyte-derived cytokines (monokines) present in the microenvironment influence NK cell activation and function, and different combinations of these soluble factors have been shown to induce a distinct cytokine repertoire by NK cells (Cooper et al., 2001b). Cytokines present in the host environment posttransplant might therefore drive the reconstitution dynamics and the functional properties of NK cells after HSCT, with IL15 inducing strong proliferation of the $CD56^{bright}$ subset and other inflammatory monokines such as IL12 and IL18 shaping NK cell responses. In line with a regulatory role of the $CD56^{bright}$ NK cell subset, these cells have been shown to produce the anti-inflammatory purine nucleoside adenosine through a CD38-mediated pathway and to inhibit $CD4^{+}$ T cell proliferation (Morandi et al., 2015). Interestingly, *CD38* was found to be upregulated in the recipients compared to their donors, suggesting an immunoregulatory role of these cells following HSCT.

In summary, molecular profiling of $CD4^{+}$, $CD8^{+}$ T cells, NK cells and monocytes after transplantation revealed major transcriptomic changes in all four cell populations compared to the donors before transplant. Collectively the results seem to suggest that the danger signals released as a consequence of the conditioning regimen and GVHD prophylaxis (MTX) and the cytokine-rich environment present in the recipients after transplantation play an important role in driving the dynamics of immune reconstitution and in shaping both innate and adaptive immune responses in the HSCT recipients.

5.5 Gene expression signature of GVHD onset

The success of allogeneic HSCT is limited by graft-versus-host disease that remains one of the major complications following HSCT accompanied by significant morbidity and mortality. Despite pharmacological prophylaxis, about 25-40% of patients undergoing HSCT develop acute GVHD after transplantations using HLA-identical sibling donors (Jagasia et al., 2012; Kanda et al., 2016). The underlying mechanisms responsible for this immune escape and alloreactivity that occur despite ongoing immunosuppression leading to GVHD development in humans are still unclear. To investigate the molecular mechanisms at the T cell level associated with human aGVHD, we sorted $CD4^+$ and $CD8^+$ T cells from recipients without GVHD and at acute GVHD onset, before the start of the steroid therapy, and performed gene expression profiling using nCounter technology.

5.5.1 T cell transcriptomic signature at GVHD onset in cohorts 1 and 2

We first assessed the gene expression profile of sorted $CD4^+$ and $CD8^+$ T cells from recipients with and without GVHD in cohorts 1 and 2. For these two cohorts, blood was collected either at GVHD onset or at day 90 after HSCT for the recipients that did not develop acute GVHD. To increase the power of our analysis, we combined the samples from the two cohorts. Since the two cohorts differ in the proportions of type of conditioning (reduced intensity or myeloablative), we included in the analysis only the patients receiving a reduced intensity conditioning (RIC) to reduce the heterogeneity of the pooled dataset. We could not perform the same analysis including the patients receiving a myeloablative conditioning due to insufficient number of samples. Moreover, to better identify transcriptomic changes associated with GVHD, we excluded the recipients that developed mild aGVHD (grade 1) and thus focused our analysis on patients that experienced a more severe disease (grade 2-4). Based on these criteria, the final analysis included 20 recipients at GVHD onset and 19 No GVHD recipients for $CD4^+$ T cells, while for $CD8^+$ T cells we could include 20 GVHD and 20 No GVHD recipients. Differences in the numbers of samples included are due to the RNA yields that could be obtained according to the number of cells available.

Transcriptomic profile of CD4$^+$ T cells showed differential expression of 48 genes in patients with GVHD compared to No GVHD recipients (FDR<10%). Of these, 5 were upregulated and 43 were downregulated at GVHD onset (**Figure 52**).

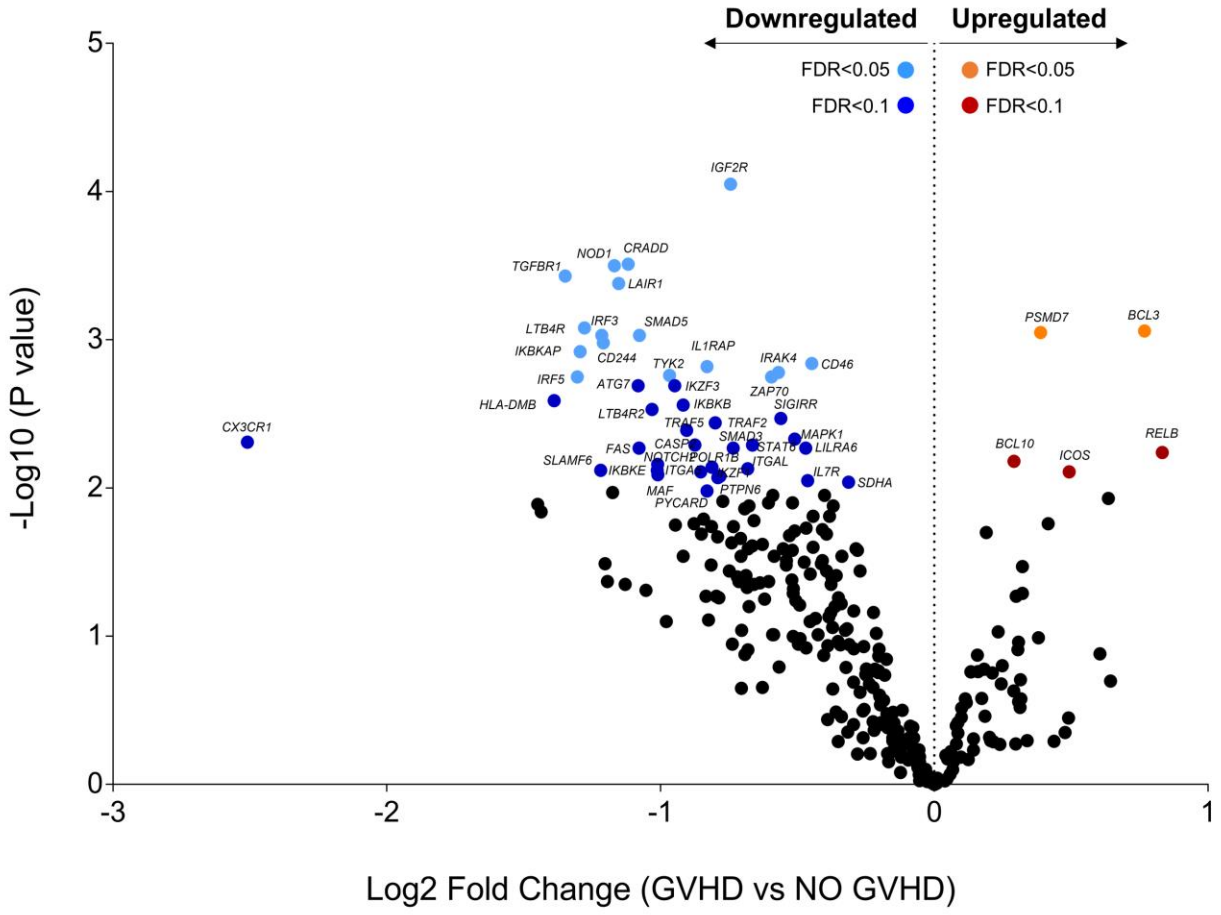

Figure 52 Gene expression profile of CD4$^+$ T cells at GVHD onset
Transcriptomic profile of CD4$^+$ T cells from 20 patients at GVHD onset compared to 19 patients without GVHD in cohorts 1 and 2. In the volcano plot, the x-axis specifies the log2 of the fold change and the y-axis the negative logarithm to the base 10 of the t-test P-values. Red and blue dots represent transcripts significantly up- or downregulated in recipients at GVHD onset compared to No GVHD recipients, respectively, with FDR<10%. Orange and light blue dots represent transcripts significantly up- or downregulated in recipients at GVHD onset compared to No GVHD recipients respectively, with FDR<5%. P-values were calculated using an unpaired t test. Adjusted P-values (FDR) were calculated using the method of Benjamini-Hochberg to correct for multiple comparisons.

QuSAGE analysis revealed 6 modules with a significant decrease in pathway activity at GVHD onset. Interestingly, the module most significantly downregulated is *TGFβ signaling* (**Figure 53A**). Closer inspection of the differentially expressed genes within this module showed that $CD4^+$ T cells from recipients at GVHD onset had significantly lower expression levels of genes encoding TGFBR1, SMAD3 and IGF2R compared to the No GVHD group (**Figure 53B**).

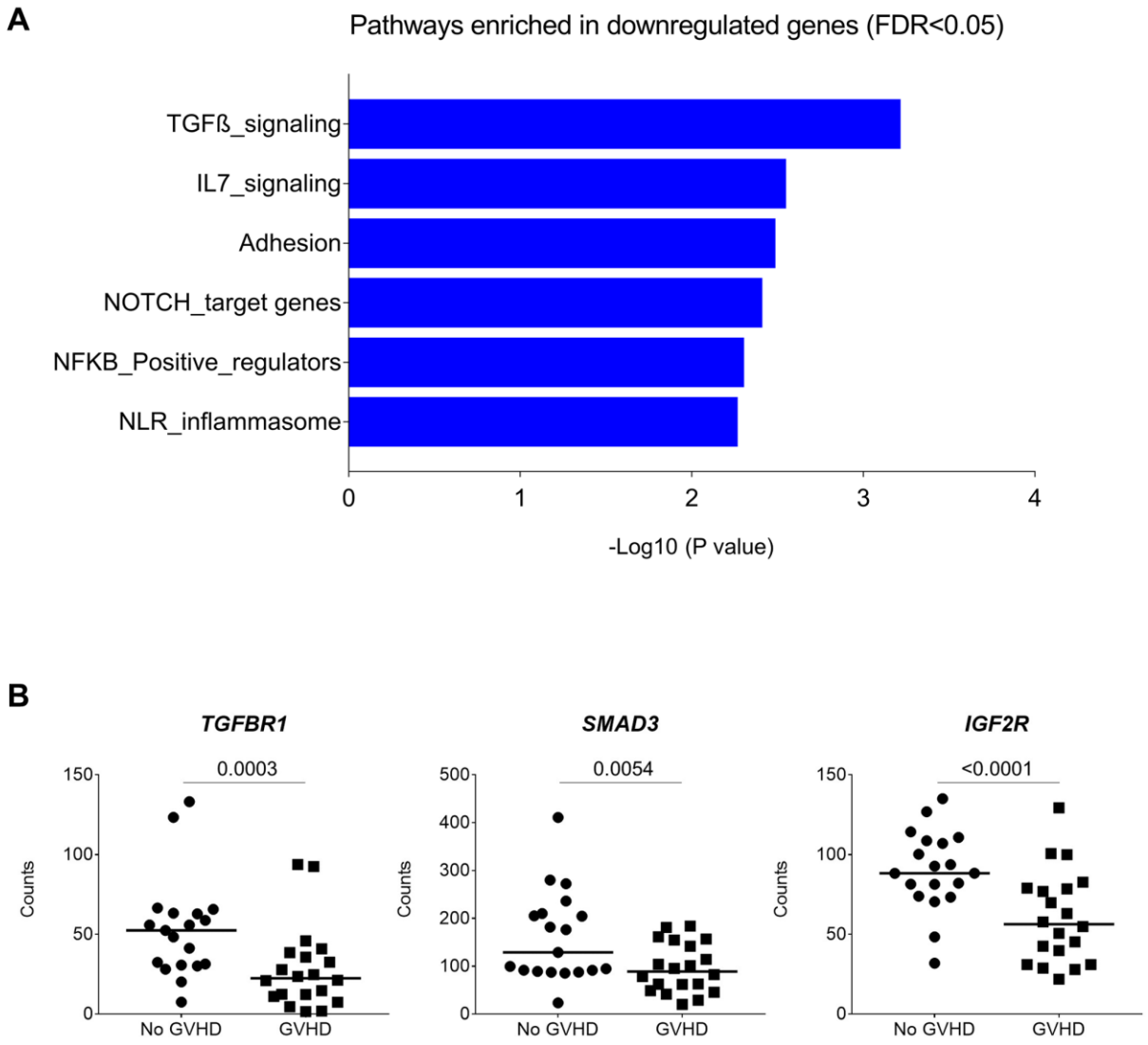

Figure 53 Genes involved in the TGFβ signaling pathway are downregulated at GVHD onset
(A) Results of the QuSAGE analysis conducted on the $CD4^+$ T cell transcriptome from GVHD and No GVHD recipients. Plotted is the negative logarithm to the base 10 of the P-values for the 6 modules with significantly different pathway activity (FDR<5%) at GVHD onset compared to No GVHD recipients. (B) Transcript levels of *TGFBR1*, *SMAD3* and *IGF2R* in $CD4^+$ T cells from recipients without GVHD (No GVHD) and at GVHD onset (GVHD). These genes showed decreased expression at GVHD onset compared to recipients without GVHD ($P < 0.05$, FDR < 10%). P-values were calculated using an unpaired t test. Adjusted P-values (FDR) were calculated using the method of Benjamini-Hochberg to correct for multiple comparisons.

TGFβ is a pleiotropic cytokine involved in a wide range of physiological processes. The TGFβ receptor complex is composed of TGFβRI and TGFβRII. Upon ligand binding TGFβ signaling is primarily mediated through the Smad family of transcription factors. However, non-canonical Smad-independent pathways are also present (Oh and Li, 2013). The role of TGFβ in both self and transplantation tolerance is well established (Regateiro et al., 2011) and it has been proposed as an important modulator of the alloresponse leading to aGVHD (Carli et al., 2012). SMAD3 is a key component of TGFβ signaling and the lack of SMAD3 was shown to dramatically increase the frequency and severity of GVHD after allogeneic hematopoietic cell transplantation in a SMAD3 knock-out mouse model (Giroux et al., 2011). *IGF2R*, encoding insulin-like growth factor 2 (IGF2) and mannose 6-phospate receptor, has been reported to be expressed at higher levels in $CD4^+CD25^+Foxp3^+$ Treg cells compared to T effectors and to enhance TGFβ release (Yang et al., 2014). Moreover, Furlan and colleagues identified IGF2R as a key proapoptotic gene underrepresented in T cells in breakthrough acute GVHD compared to healthy controls in a NHP model of GVHD (Furlan et al., 2016).

In recipients at GVHD onset, we noticed the upregulation of genes involved in the NF-κB signaling pathway such as *RELB*, *BCL10*, and *BCL3* (**Figure 54**). We also observed the upregulation of *PSMD7*, coding for a component of the 26S proteasome (26S proteasome non-ATPase regulatory subunit 7). The ubiquitin-proteasome system (UPS) is involved in the regulation of inflammatory responses and it plays an important role in the activation of NF-κB (Chen, 2005). $CD4^+$ T cells at GVHD onset also showed upregulation of *ICOS*, a member of the CD28 superfamily, induced on $CD4^+$ and $CD8^+$ T cells during T cell activation (Hutloff et al., 1999) (**Figure 54**). Using a model of xeno-GVHD in NOD-scid gamma (NSG) mice, Burlion and colleagues showed that blocking human ICOS alleviated GVHD without impairing GVL, suggesting that ICOS could be a promising target in GVHD prevention while preserving the beneficial GVL effect (Burlion et al., 2017).

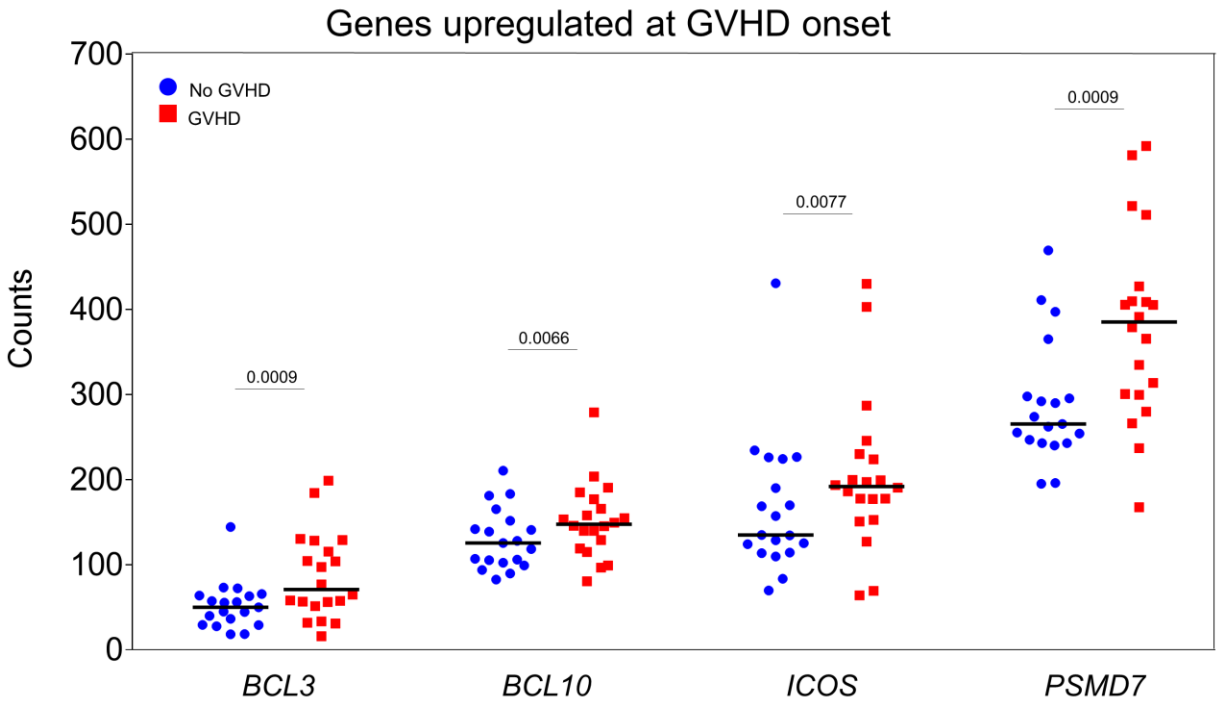

Figure 54 Genes upregulated in CD4⁺ T cells at GVHD onset
Transcript levels of *BCL3, BCL10, ICOS,* and *PSMD7* in CD4⁺ T cells from recipients without GVHD (blue dots) and at GVHD onset (red squares). These genes showed increased expression at GVHD onset compared to recipients without GVHD ($P < 0.05$, FDR < 10%). P-values were calculated using an unpaired t test. Adjusted P-values (FDR) were calculated using the method of Benjamini-Hochberg to correct for multiple comparisons.

CD8$^+$ T cells from recipients at GVHD onset showed differential expression of 134 genes compared to recipients without GVHD (FDR<5%). In particular, we observed the upregulation of 23 genes, while 111 transcripts were downregulated at GVHD onset (**Figure 55**).

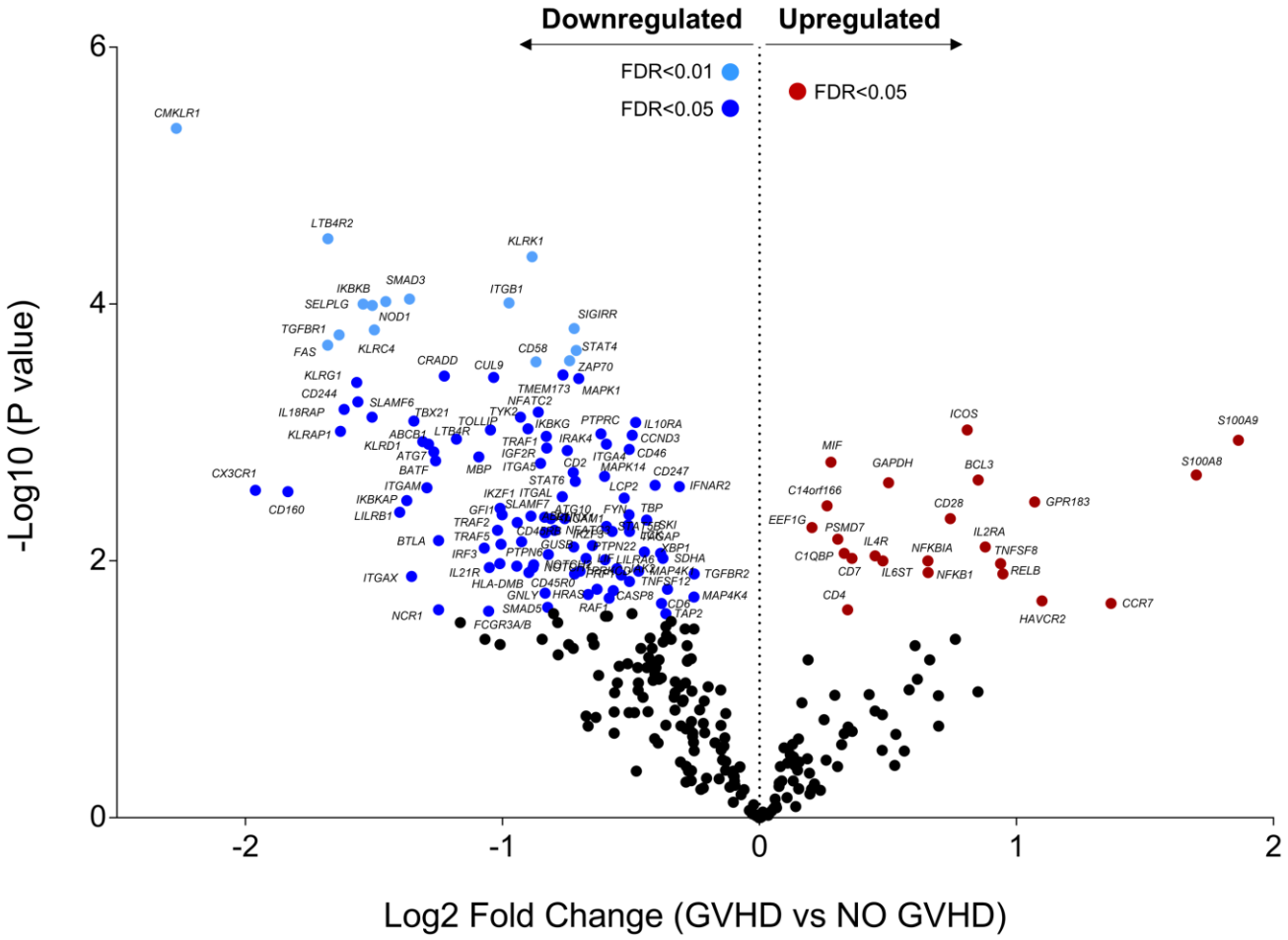

Figure 55 Gene expression profile of CD8$^+$ T cells at GVHD onset
Transcriptomic profile of CD8$^+$ T cells from 20 patients at GVHD onset compared to 20 patients without GVHD in cohorts 1 and 2. In the volcano plot, the x-axis specifies the log2 of the fold change and the y-axis the negative logarithm to the base 10 of the t-test P-values. Red and blue dots represent transcripts significantly up- or downregulated in recipients at GVHD onset compared to No GVHD recipients, respectively, with FDR<5%. Light blue dots represent transcripts significantly downregulated in recipients at GVHD onset compared to No GVHD recipients with FDR<1%. P-values were calculated using an unpaired t test. Adjusted P-values (FDR) were calculated using the method of Benjamini-Hochberg to correct for multiple comparisons.

Among the transcripts upregulated in patients with GVHD we observed genes involved in NF-κB signaling such as *NFKB1*, *RELB*, *BCL3* and the negative regulator *NFKBIA* (**Figure 56**). Similarly to what was observed in $CD4^+$ T cells, also in $CD8^+$ T cells we noticed the upregulation of the gene encoding the proteasome subunit PSMD7 as well as the costimulatory molecule ICOS. In addition, $CD8^+$ T cells displayed increased expression of the costimulatory molecule *CD28*, the inflammatory mediator *MIF* (macrophage migratory inhibitory factor) and the glycolytic enzyme *GAPDH*. The switch from oxidative phosphorylation to aerobic glycolysis is the hallmark of T cell activation and Chang and colleagues showed that aerobic glycolysis facilitates full effector status and IFNγ production in T cells (Chang et al., 2013). Moreover, among the transcripts upregulated at GVHD onset we noted genes encoding proteins that have been proposed as biomarkers for GVHD such as IL2Rα (Paczesny et al., 2009), Tim-3 (encoded by HAVCR2) (McDonald et al., 2015) and the "calprotectin" genes *S100A8* (calgranulin A) and *S100A9* (calgranulin B) (Paczesny et al., 2013; Reinhardt et al., 2014). Of note, consistent with data in the literature reporting a preferential expression of S100A8 and S100A9 in innate cells, especially phagocytes (Wong et al., 2011; Xia et al., 2018), the observed expression levels of these two genes in $CD8^+$ T cells are low. Interestingly, upregulation of *IL2RA*, *HAVCR2*, *S100A8* and *S100A9* has been described in $CD3^+$ T cells during GVHD in a NHP model (Furlan et al., 2015), suggesting a potential pathogenic role in human acute GVHD.

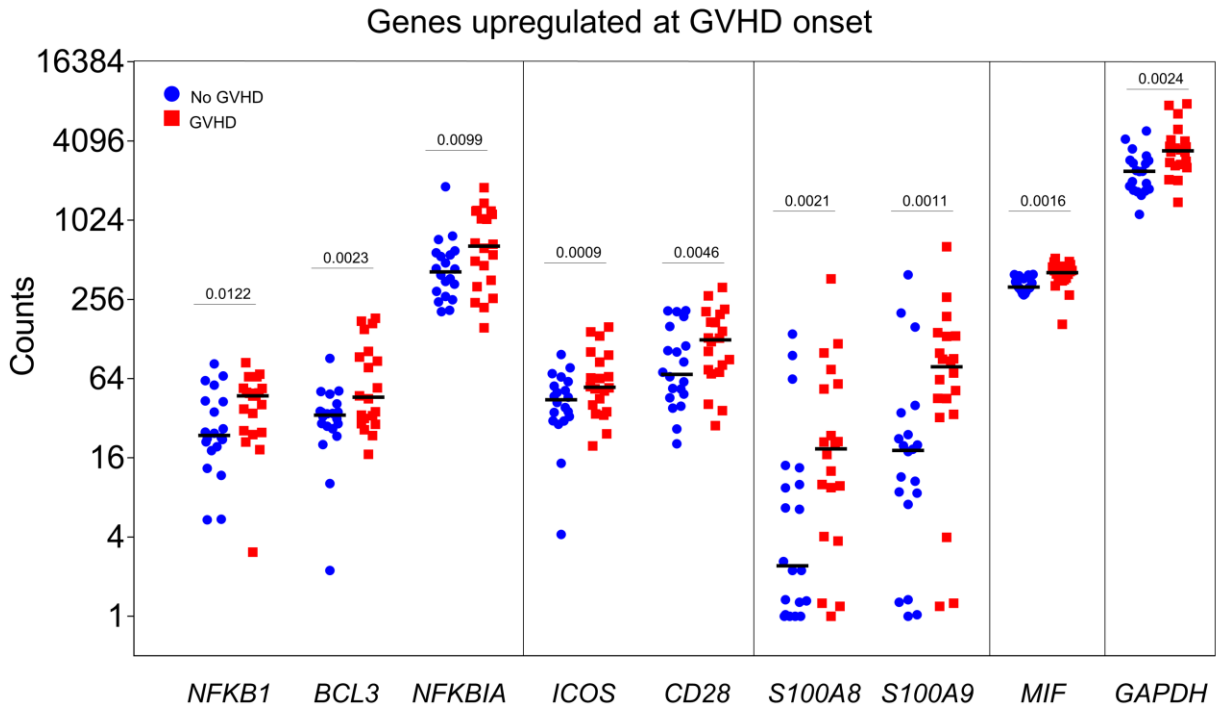

Figure 56 Genes upregulated in CD8$^+$ T cells at GVHD onset
Transcript levels of *NFKB1*, *BCL3*, *NFKBIA*, *ICOS*, *CD28*, *S100A8*, *S100A9*, *MIF* and *GAPDH* in CD8$^+$ T cells from recipients without GVHD (blue dots) and at GVHD onset (red squares). These genes showed increased expression at GVHD onset compared to recipients without GVHD ($P < 0.05$, FDR < 5%). P-values were calculated using an unpaired t test. Adjusted P-values (FDR) were calculated using the method of Benjamini-Hochberg to correct for multiple comparisons.

QuSAGE analysis on the transcriptomic profile of CD8$^+$ T cells showed 24 genes modules significantly different between recipients at GVHD onset and patients without GVHD. Of these, 23 had a significant decrease in pathway activity and only one module was significantly upregulated at GVHD onset. As shown in **Figure 57**, the module displaying increased pathway activity at GVHD onset was the *NF-κB-TFs* module, including the NF-κB transcription factors *NFKB1*, *NFKB2*, *RELA* and *RELB*. A wide set of stimuli such as bacterial components (e.g. LPS), proinflammatory cytokines, viruses, DNA damaging agents, T- and B- cell mitogens and antigens binding to the TCR can initiate the activation of the NF-κB pathway (Karin and Ben-Neriah, 2000; Vallabhapurapu and Karin, 2009). This suggests an important role of the NF-κB signaling pathway in alloreactive T cells mediating GVHD in humans.

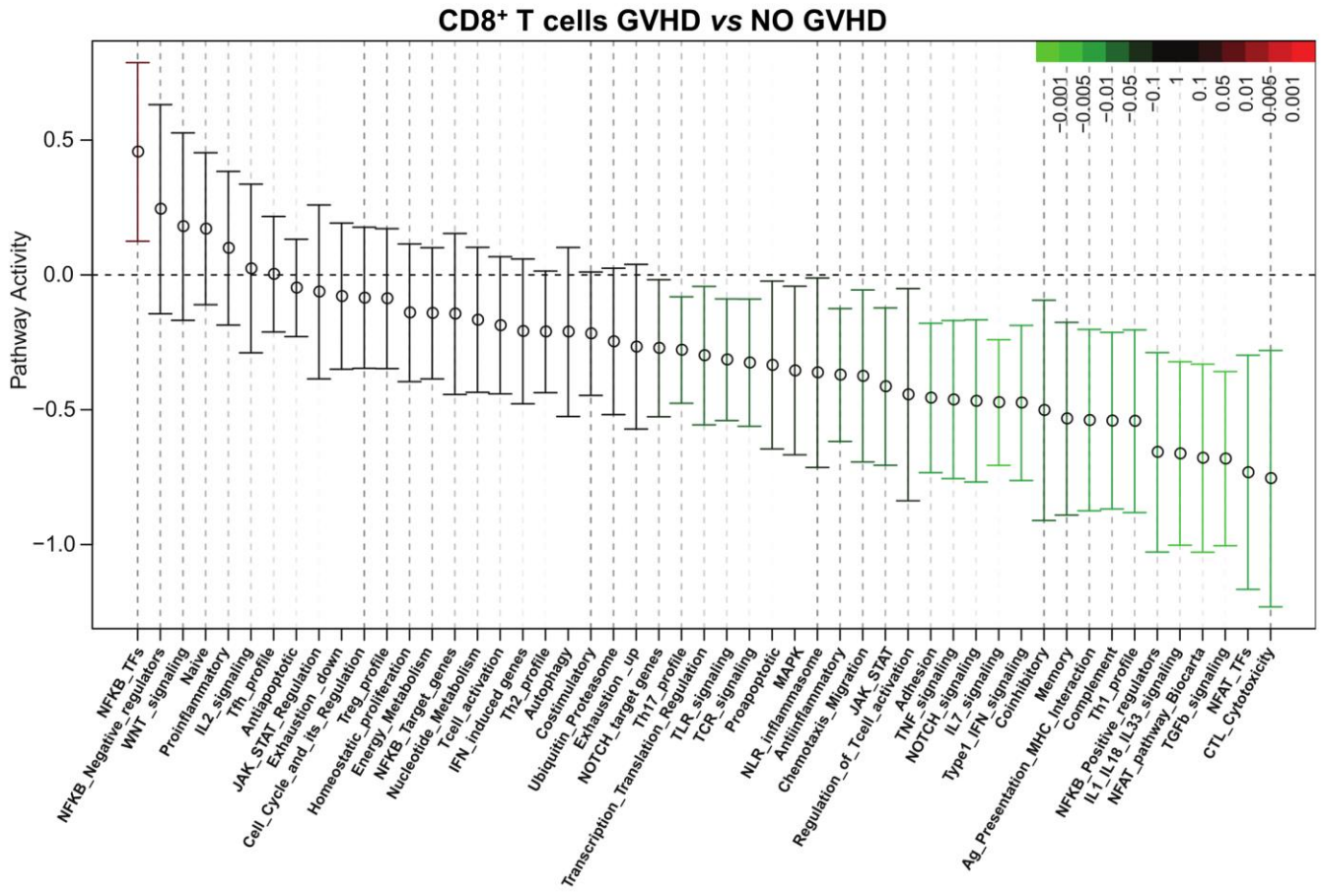

Figure 57 Enriched pathways in CD8⁺ T cells at GVHD onset

QuSAGE analysis on the CD8⁺ T cell transcriptome in 20 recipients at GVHD onset compared to 20 recipients without GVHD from cohorts 1 and 2. For each pathway, the mean fold change and the 95% confidence interval are plotted and colour-coded according to their False Discovery Rate (FDR)-corrected P-values when compared to zero. Red and green bars indicate a statistically significant increased or decreased pathway activity respectively, in recipients at GVHD onset compared to recipients without GVHD.

Similar to CD4$^+$ T cells, the module most significantly downregulated in CD8$^+$ T cells at GVHD onset was the *TGFβ signaling* module (P=0.00005, FDR=0.002). Within the modules with significantly decreased pathway activity we also observed the *Coinhibitory* and the *Anti-inflammatory* modules. Transcript levels of representative genes belonging to these modules are shown in **Figure 58.** CD8$^+$ T cells from recipients at GVHD onset displayed downregulation of genes involved in TGFβ signaling (*TGFBR1, TGFBR2, SMAD3, IGF2R)* as well as genes encoding inhibitory receptors (*LAIR1, LILRB1, BTLA, KLRG1*) (Chen and Flies, 2013; Kang et al., 2016; Murphy et al., 2006; Odorizzi and Wherry, 2012) and molecules mediating immunosuppressive signals (e.g. *IL10RA*) (Saraiva and O'Garra, 2010), suggesting that a decreased expression of genes involved in the regulation and dampening of the immune response might be implicated in GVHD development.

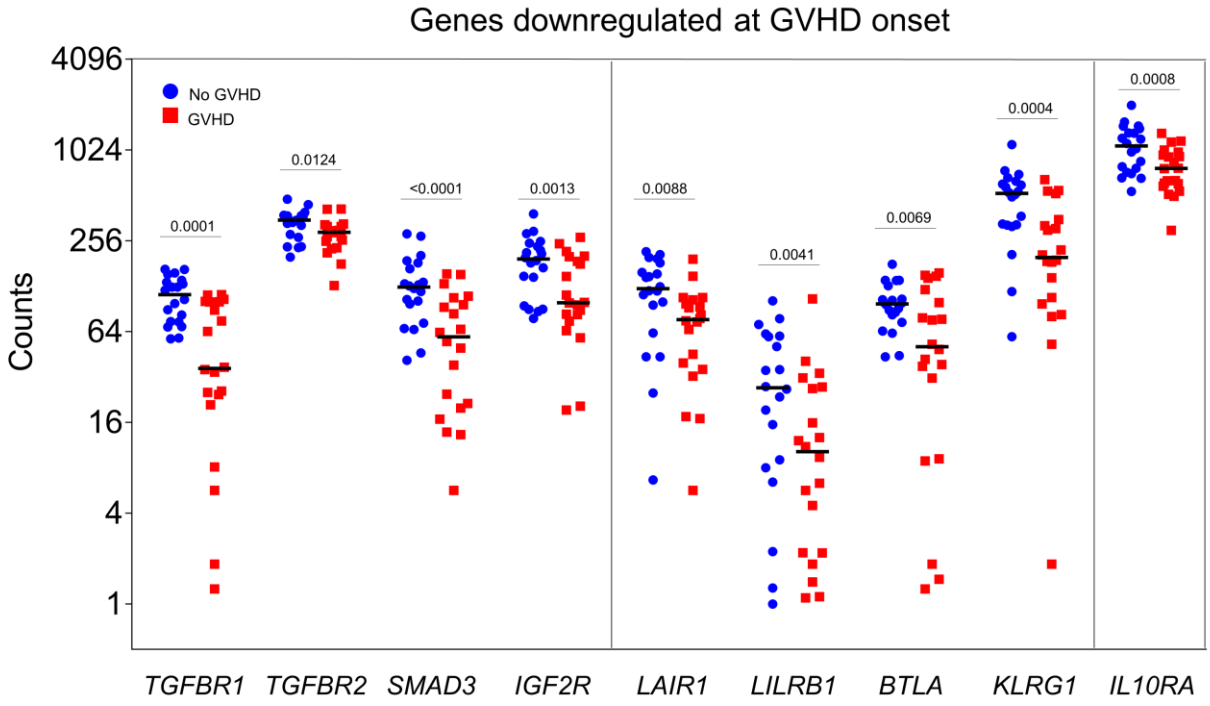

Figure 58 Genes downregulated in CD8$^+$ T cells at GVHD onset
Transcript levels of *TGFBR1, TGFBR2, SMAD3, IGFR2, LAIR1, LILRB1, BTLA, KLRG1,* and *IL10RA* in CD8$^+$ T cells from recipients without GVHD (blue dots) and at GVHD onset (red squares). These genes showed decreased expression at GVHD onset compared to recipients without GVHD (P < 0.05, FDR < 5%). P-values were calculated using an unpaired t test. Adjusted P-values (FDR) were calculated using the method of Benjamini-Hochberg to correct for multiple comparisons.

However, we also noted that other modules including genes involved in T cell activation and effector functions such as the modules *CTL-Cytotoxicity*, *NFAT signaling* and NFAT transcription factors (*NFAT-TFs*), *NF-κB positive regulators*, *Th1 profile* and *JAK-STAT* displayed a decrease in pathway activity. Given the importance of $CD8^+$ T cells in mediating aGVHD (Ferrara et al., 2009), more work is necessary to define the role of these signaling pathways in aGVHD development.

A key element in the pathogenesis of both acute and chronic GVHD is the migration of activated T cells to target organs. This process is mediated by adhesion molecules, such as integrins and selectins, as well as chemokine-chemokine receptor interactions (Castor et al., 2012). For example, CXCL10-CXCR3 interactions have been associated with the recruitment of T cells in cutaneous acute GVHD (Piper et al., 2007). Chemokine-mediated recruitment of effector cells into target organs might be associated with a depletion of these cells in the blood. In line with this hypothesis, Hakim and colleagues reported a significantly reduced frequency of circulating $CD4^+$ and $CD8^+$ $CXCR3^+$ T cells in patients with extensive skin chronic GVHD, as compared with those with less skin involvement or healthy controls (Hakim et al., 2016). We could thus speculate that at GVHD onset a proportion of alloreactive T cells might have migrated to the target tissues and therefore be depleted in peripheral blood. This could explain the gene expression signature characterized by an underrepresentation of many genes associated with T cell activation and effector functions observed in recipients at GVHD onset.

However, we cannot exclude that the difference in the time of sampling between the GVHD and the No GVHD groups, may affect the level of immune reconstitution and therefore the gene expression profile.

5.5.2 Gene expression profile of T cells at GVHD onset in cohort 3

To address this question, we next analysed the transcriptomic changes associated with GVHD onset in recipients from cohort 3, for which blood samples were collected either at day 30 post-HSCT, for recipients without GVHD, or at GVHD onset, and processed the same day of the blood sampling. Because the median delay of GVHD onset is day 39 posttransplant in this cohort, the timepoint at which the blood was collected in the GVHD and No GVHD groups is more similar compared to cohorts 1 and 2 in which No GVHD recipients were sampled at day 90 post-HSCT. Given the limited number of recipients available in this cohort (10 GVHD *vs* 10 No GVHD recipients), statistical analysis was performed with a less stringent FDR threshold.

Transcriptomic analysis of $CD4^+$ T cells from recipients at GVHD onset compared to recipients in the absence of GVHD revealed a gene expression signature involving the upregulation of 10 genes (*S1PR1, CRADD, IL21R, IL32, IL1R2, SIGIRR, GPR183, JAK3, TLR1* and *MIF* (approaching significance)), while 2 genes were downregulated (*IFIH1* and *NCR1*) (P-value < 0.05, FDR <27%) (**Figure 59**). Among the transcripts upregulated in the recipients at GVHD onset we noted genes encoding the proinflammatory mediators IL32 and MIF. IL32 is a proinflammatory cytokine originally identified in IL2-activated T and NK cells (Dahl et al., 1992). IL32 expression is increased after T cell activation and its proinflammatory activity seems to involve the degradation of the NF-κB inhibitor IκB, leading to the activation of NF-κB, as well as phosphorylation of mitogen-activated protein p38 (Kim et al., 2005). IL32 expression has been shown to be induced by TNFα (Stirewalt et al., 2008), which is upregulated in transplant recipients together with other inflammatory mediators such as IL1 and IL6, resulting in the "cytokine storm" important for the initiation of the graft-versus-host reaction (Antin and Ferrara, 1992; Henden and Hill, 2015). On the other hand, IL32 has been reported to induce TNFα (Kim et al., 2005), suggesting a possible amplification loop between these two cytokines. In line with our observation, Marcondes and colleagues reported increased *IL32* mRNA levels in blood leukocytes from patients with GVHD compared to patients without GVHD as well as upregulation of both IL32 mRNA and protein levels in cells exposed to allogeneic stimulator cells in comparison to autologous controls in a mixed lymphocytes culture system (Marcondes et al., 2011).

Similarly to what was described for IL32, also MIF has been reported to be involved in a proinflammatory loop in which MIF and TNFα induce each other's production (Calandra et al., 1994). Moreover, it was shown that T cell activation elicits MIF release and that anti-MIF antibodies inhibited T cell proliferation and IL2 production *in vitro* and suppressed antigen-driven T cell activation *in vivo,* suggesting an important regulatory role of this factor in T cell activation (Bacher et al., 1996). Interestingly, a role for MIF in alloreactivity has been reported, with studies describing an upregulation of MIF during alloimmune responses after kidney and bone marrow transplantation (Lan et al., 1998; Lo et al., 2002; Toubai et al., 2009). Of note, MIF serum levels were found to be increased at GVHD onset and both MIF mRNA and protein were upregulated in skin and gut biopsies from patients with GVHD. This increase in local MIF expression in aGVHD was associated with infiltration of activated T cells and macrophages in allogeneic HSCT recipients (Lo et al., 2002; Toubai et al., 2009).

Within the other genes found to be upregulated in $CD4^+$ T cells at GVHD onset, we noted the presence of genes whose products have been investigated as pharmacological targets for GVHD prevention or therapy in preclinical studies, such as sphingosine-1-phosphate receptor 1 (S1PR1) and Janus kinase 3 (JAK3). S1PR1 is a G-protein-coupled receptor for the bioactive lipid sphingosine-1-phosphate (S1P) involved in various cellular processes including lymphocyte trafficking and inflammatory responses. S1P-S1PR1-mediated T cell migration is important for T cell egress from the thymus into the circulation and for lymphocyte retention in inflamed tissues (Aoki et al., 2016; Chi, 2011). Additionally, S1PR1 signaling has been implicated in T cell differentiation, driving the generation of Th1 cells while inhibiting Treg development (Chi, 2011; Liu et al., 2010). To date, a number of functional antagonists of S1P receptors have been developed such as the immunosuppressant FTY720 (Fingolimod, Gilenya, Novartis), that binds to all S1P receptors except S1PR2 (Brinkmann et al., 2010), and the S1PR1-selective agonist CYM-5442 (CYM) (Gonzalez-Cabrera et al., 2008). S1P antagonism has been shown to reduce acute GVHD (Smith et al., 2017; Zeiser and Blazar, 2017). In particular, it was reported that CYM treatment in a mouse model of GVHD was associated with a decreased percentage of activated $CD69^+$ T cells as well as decreased Th1 response (Cheng et al., 2015).

Janus kinases (JAKs) are important mediators in GVHD pathogenesis, transducing inflammatory signals downstream cytokine receptors (Yamaoka et al., 2004). Consistent with a role of JAK3 in GVHD, it was reported that mice receiving JAK3-deficient T cells developed a milder disease as compared to the ones receiving wild type T cells (Hechinger et al., 2015). Moreover, the JAK3 inhibitor tofacitinib was shown to reduce the expansion and activation of $CD8^+$ T cells in a murine model of GVHD (Okiyama et al., 2014). Interestingly, at GVHD onset we also noticed the upregulation of the gene encoding the IL21 receptor (*IL21R*), which signals using the shared subunit common γ chain and through JAK3 recruitment (Yamaoka et al., 2004). IL21 has been implicated in GVHD pathophysiology and IL21 blockade has been shown to ameliorate GVHD in murine models (Hippen et al., 2012; Oh et al., 2010).

No statistically significant differences were observed in $CD8^+$ T cells in recipients at GVHD onset compared to No GVHD recipients in this cohort.

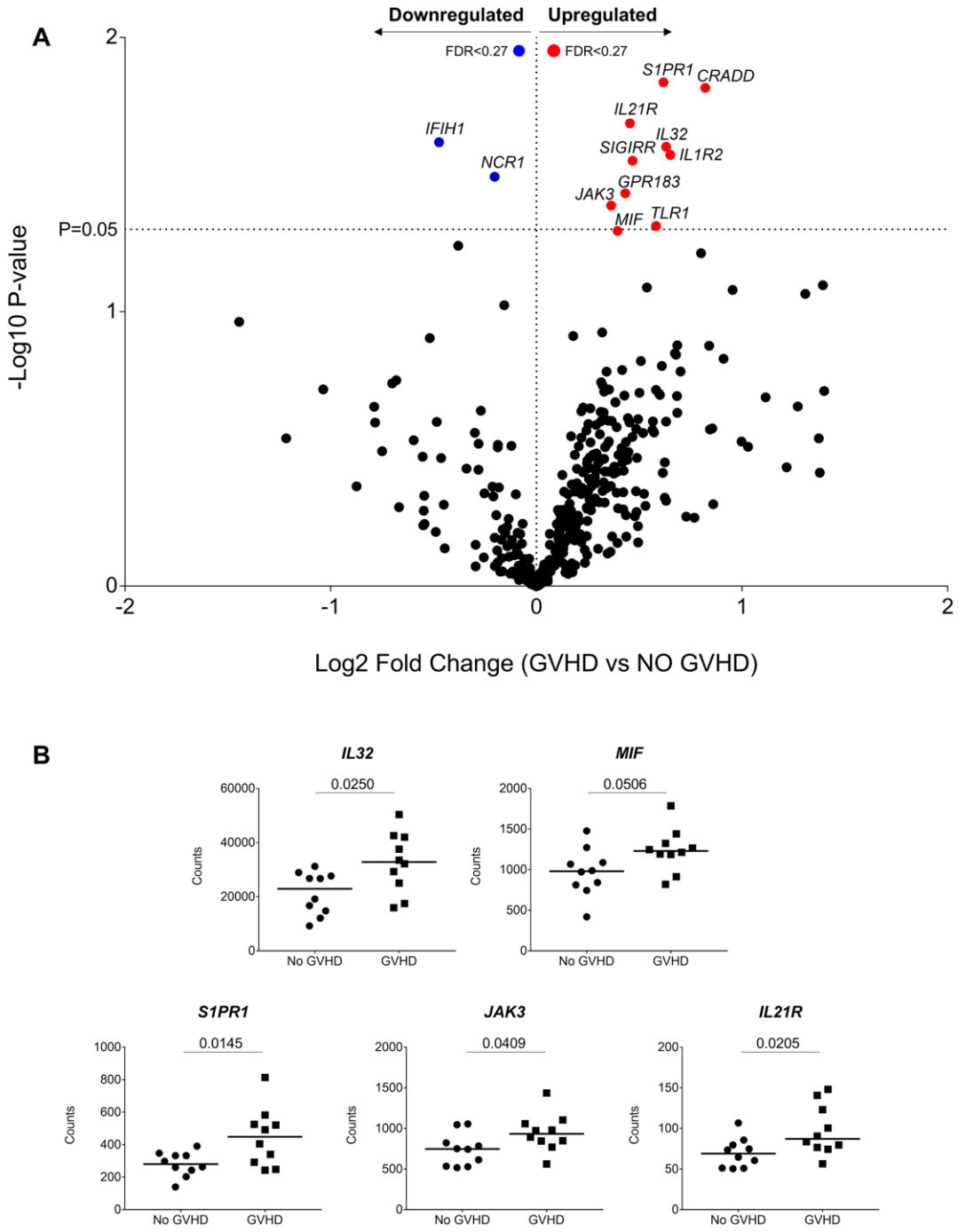

Figure 59 Gene expression profile of CD4⁺ T cells at GVHD onset

(A) Transcriptomic changes of CD4⁺ T cells from 10 patients at GVHD onset compared to 10 patients without GVHD in cohort 3. In the volcano plot the x-axis specifies the log2 of the fold change and the y-axis the negative logarithm to the base 10 of the t-test P-values. Red and blue dots represent transcripts significantly up- or downregulated in recipients at GVHD onset compared to No GVHD recipients, respectively. P-values were calculated using an unpaired t test. Adjusted P-values (FDR) were calculated using the method of Benjamini-Hochberg to correct for multiple comparisons. (B) Transcript levels of *IL32*, *MIF*, *S1PR1*, *JAK3* and *IL21R* in CD4⁺ T cells from recipients without GVHD (No GVHD) and at GVHD onset (GVHD).

In summary, T cell transcriptome analysis in patients at GVHD onset compared to recipients without GVHD revealed upregulation of genes involved in NF-κB signaling (*NFKB1*, *RELB* and *BCL3*) as well as costimulatory molecules (*ICOS, CD28*) and proinflammatory mediators (*MIF*, *S100A8*, *S100A9*). On the contrary, genes involved in TGFβ signaling (*TGFBR1, TGFBR2, SMAD3*) and encoding receptors mediating immunoregulatory and immunosuppressive signals, such as inhibitory receptors (*LAIR1, LILRB1, BTLA*, KLRG1) and IL10Rα were downregulated, suggesting that a decreased expression of regulatory and inhibitory molecules might be involved in GVHD development.

Moreover, in cohort 3 we observed upregulation of inflammatory mediators such as *IL32* and *MIF*, as well as molecules involved in cytokine signal transduction (*IL21R* and *JAK3*) and cell migration and trafficking (*S1PR1*).

Of note, in this third cohort the downregulation of genes associated with T cell activation and effector functions observed in cohorts 1 and 2 was not found, supporting the importance of matching the time of sampling between the GVHD and No GVHD groups to avoid confounding effects.

Among the genes upregulated in T cells at GVHD onset, many could represent potential therapeutic targets to prevent or treat GVHD. However, confirmation in a bigger cohort of patients is needed. Ideally the groups of recipients with and without GVHD should be time-matched to avoid biases due to different timing in immune reconstitution.

Discussion

Allogeneic hematopoietic stem cell transplantation is a unique and highly specialized medical procedure that provides a form of "immune rescue" for patients with defects in their hematopoietic system. The transplant enables the regeneration of a competent donor-derived immune system, following a conditioning regimen that ablate the existing abnormal lymphohematopoietic system. Over the past decades, HSCT has become an essential component of the treatment of a variety of malignant and non-malignant hematologic disorders that were before considered untreatable. Since 1957, when the first HSCT was performed by E.D. Thomas and colleagues, outstanding advances in the field have led to remarkable improvements in clinical results. However, the success of allogeneic HSCT is still heavily influenced by the occurrence of graft-versus-host disease that remains the main factor contributing to non-relapse mortality and morbidity, limiting the broader applicability of this procedure.

The early period after HSCT, before and during the engraftment phase, is characterized by the activation and the maturation of APCs, and the rapid amplification of donor T cells that ultimately leads to the development of GVHD or paves the way to immune tolerance. The cellular and molecular mechanisms underlying immune reconstitution and acute GVHD development in humans are still incompletely understood, and much of our knowledge of the biology of acute GVHD derives from preclinical studies. However, differences between humans and animal models hamper the direct translation of the findings from preclinical studies to the clinical setting (Socie and Blazar, 2009). Thus, it is essential to improve our understanding of the disease processes in humans, to make progress in the diagnosis, prognosis, prophylaxis and treatment of GVHD. Of note, compared to the controlled and standardized settings in preclinical models, studies in human patients are complicated by the limited sample availability and by many clinical and biological confounding factors that can make the interpretation of the results particularly challenging.

To address these issues, we have investigated the phenotypic and molecular characteristics of immune cells in patients after HSCT and in their HLA-identical sibling donors, with the goal of defining immune parameters associated with the recovery of donor-derived immunity and with the development of acute GVHD. In particular, in our study we addressed three main questions: (i) What are the cellular and molecular mechanisms at play in the reconstitution of a functional immune system after HSCT in the absence of acute GVHD? (ii) Can we identify cellular and/or molecular correlates associated with acute GVHD onset in recipients after HSCT? and (iii) Can

we identify signatures of “dangerous donors”, stronger alloresponders that are more likely to elicit acute GVHD in their recipients?

To answer these questions, we have analysed three independent cohorts of HLA-identical donor-recipient pairs undergoing HSCT, in which we profiled the distribution of different T cell subsets and their proliferative status using spectral flow cytometry; and we assessed the gene expression signatures of sorted immune cell populations in the donors before transplant and in their recipients, either at aGVHD onset or at day 30 or 90 for the recipients that did not develop aGVHD.

1 How does the donor immune system react to the environment of the host after HSCT?

After transplantation, the reconstitution of a functional, donor-derived immune system in the recipient is an essential component for successful outcome, important for the long-term recovery and survival of patients undergoing HSCT (Van Den Brink et al., 2013, 2015). Reconstitution is a highly dynamic and complex process, with the different immune cell subsets recovering at different rates. Innate immunity recovers within the first weeks and months after HSCT, followed by reconstitution of the adaptive immune system that occurs over a longer period, and can take months and even years to regenerate a functional immunity (Chaudhry et al., 2017; Storek et al., 2008).

The dynamics of reconstitution of different immune subsets after transplantation have been extensively investigated (de Koning et al., 2016; Ogonek et al., 2016; Pankratova and Chukhlovin, 2016; Park et al., 2015; Storek et al., 2008; Xhaard et al., 2014). However, a comprehensive analysis of the frequencies of different T cell subsets and their proliferative status, together with gene expression profile of immune cell populations in recipients after HSCT and in their respective sibling donors has never been performed.

1.1 Dynamics of T cell immune reconstitution after HSCT

To investigate the dynamics of reconstitution of the different T cell subsets after HSCT, we designed two flow cytometry panels that enable the detection of all major T cell subsets and their proliferative status. We first assessed the recovery of the different T cell subpopulations at day 90 posttransplant, in recipients that did not develop acute GVHD, compared to their respective sibling donors, in two independent cohorts of donor-recipient couples (cohorts 1 and 2).

Three months after HSCT, we observed in the recipients an incomplete reconstitution of the T cell compartment. In particular, $CD4^+$ T cells recover more slowly than $CD8^+$ T cells, leading to an inversion of the CD4/CD8 ratio. This observation is in line with data in the literature describing an inverted CD4/CD8 ratio in recipients after HSCT compared to healthy donors (Lum, 1987; Seggewiss and Einsele, 2010). The inversion of the CD4/CD8 ratio posttransplant, due to an inefficient recovery of $CD4^+$ T cells relative to $CD8^+$ T cells, has been attributed to a greater reliance of $CD4^+$ T cells for regeneration *via* the thymic-dependent pathway (Mackall et al.,

1997b), while $CD8^+$ T cells undergo lymphopenia-dependent expansion more efficiently than $CD4^+$ T cells. Studies in mice showed that $CD8^+$ T cells survive better and engage faster in homeostatic proliferation than $CD4^+$ T cells. Moreover, the homeostatic expansion of $CD8^+$ T cells is not limited to lymphoid organs as for $CD4^+$ T cells, leading to a faster recovery of $CD8^+$ T cells (Bender et al., 1999; Dai and Lakkis, 2001; Ernst et al., 1999; Ferreira et al., 2000).

To investigate the T cell migratory properties and the distribution of T helper subsets following HSCT, we analysed the expression of the chemokine receptors CXCR3, CCR6, CRTH2 and CXCR5 in donors and recipients. While many studies investigated the migratory properties of T cells during GVHD (Jaksch et al., 2005; Palmer et al., 2010; Wysocki et al., 2005), changes in the expression of chemokine receptors as a consequence of the transplantation procedure, in the absence of GVHD, have not been characterized. Our results indicate that after HSCT, in the absence of aGVHD, the expression pattern of chemokine receptors is altered in both $CD4^+$ and $CD8^+$ T cells compared to the donors before transplant. In particular, within $CD4^+$ T lymphocytes, we observed an increase of cells able to migrate to mucosal sites ($CCR6^+$) (Lee et al., 2013a), whereas the proportions of cells with a Th1-like ($CXCR3^+$) (Groom and Luster, 2011) and Tfh-like ($CXCR5^+$) (Crotty, 2011) profile were decreased. The decrease of $CXCR3^+$ cells was also observed in the $CD8^+$ T cell population. On the other hand, within the $CD8^+$ compartment the percentage of $CXCR5^+$ cells was increased in the recipients, contrarily to what was observed within $CD4^+$ T cells. Early after HSCT, tissue damage caused by the conditioning regimen and release of proinflammatory cytokines result in the establishment of an inflammatory environment in the recipients (Min et al., 2001; Welniak et al., 2007). Inflammatory stimuli can lead to the upregulation of chemokines and their receptors (Mackay, 2001; Rossi and Zlotnik, 2000), thus the changes in chemokine receptor expression that we observed in HSCT recipients could be driven by the cytokine milieu present in the host microenvironment after transplantation. For example, CCL20, the ligand for CCR6, has been reported to be upregulated in response to various inflammatory cytokines (such as TNFα, IL1, IFNγ) and CCR6 itself is upregulated in T cells by inflammatory stimuli (Lee et al., 2013a). On the other hand, differential expression of chemokine receptors could also reflect altered frequencies of naïve and effector/memory subsets, as these proteins are up- or downregulated according to the activation and differentiation status of the cell (Rossi and Zlotnik, 2000; Sallusto and Lanzavecchia, 2009). CXCR5, the hallmark of Tfh cells, is also expressed on subsets of circulating $CD4^+$ and $CD8^+$ memory cells (Quigley et al., 2007;

Schaerli et al., 2000). CXCR3 is highly expressed on memory and effector cells, especially with a Th1/Tc1 profile, while it is absent on naïve cells (Groom and Luster, 2011). However, given the observed increase in memory cells after HSCT, the decrease of circulating CXCR3-expressing cells in both $CD4^+$ and $CD8^+$ compartments could indicate a depletion due to recruitment of these cells into peripheral sites, as CXCR3 enables cells to access sites that are otherwise restricted (Groom and Luster, 2011).

Analysis of the distribution of different naïve and memory subsets in recipients revealed a depletion of the naïve T cell pool paralleled by an increase of cells with an effector memory phenotype in both $CD4^+$ and $CD8^+$ compartments. This observation is consistent with data in the literature showing that following T cell replete HSCT, initial recovery of the T cell compartment relies mainly on the peripheral expansion of memory T cells present in the graft, driven by cytokines (IL7, IL15 and IL2), as well as the lymphopenia and allogeneicity that characterize the host environment posttransplant (Chaudhry et al., 2017; Fry and Mackall, 2005; Toubert et al., 2012). It is only at later time points that *de novo* generation of naïve T cells in the thymus occurs and replenishes the naïve T cell pool (Krenger et al., 2011; Mackall et al., 2009; Seggewiss and Einsele, 2010). Moreover, in lymphopenic conditions naive cells are more likely to respond to weak or low-affinity antigens (Goldrath and Bevan, 1999b). In these conditions, homeostatic proliferation of naïve T cells is associated with the acquisition of a memory-like phenotype (Tchao and Turka, 2012), potentially explaining the skewing of the T cell compartment toward a memory phenotype after transplantation. Interestingly, assessment of Ki-67 expression showed an increased proliferation of all $CD4^+$ and $CD8^+$ T naïve and memory subsets analysed in the recipients compared to the donors, despite post-HSCT pharmacologic immunosuppression. Our observation is consistent with the study of Alho et al. describing increased proliferation of $CD4^+$ and $CD8^+$ naïve, central memory and effector memory T cell subsets in recipients. The increased proliferation compared to healthy donors was observed at different time points, from one to 24 months after HSCT. In particular, in this study the authors report a peak of proliferation within the T_{CM} and T_{EM} subsets in both $CD4^+$ and $CD8^+$ compartments at six months post-HSCT (Alho et al., 2016). However, differently from our study, this work included patients receiving grafts from both matched related, matched unrelated and mismatched unrelated donors, resulting in a more heterogenous study population compared to our setting, in which only HLA-identical siblings were included. In addition, comparison between donors and recipients involved a group of unrelated

healthy donors and not the corresponding donors from which the recipients received the graft, while in our study cells from the same donor were analysed before HSCT and in the "environment" of the recipient posttransplant. Matsuoka et al. also reported a higher proliferation rate of T cells in a cohort of patients after allogeneic hematopoietic stem cell transplantation compared to healthy donors, and these cells had predominantly a memory phenotype ($CD45RA^-$).

In the same study the authors observed a more pronounced proliferation in the Treg population than in conventional T cells (Matsuoka et al., 2010). Our analysis of the reconstitution of the Treg population three months after HSCT, revealed an increased percentage of $CD4^+$ $Foxp3^+$ Treg cells in the recipients compared to the donors and, consistent with the study from Matsuoka and colleagues, Treg cells in the recipients displayed increased proliferation compared to the donors. In addition, in the recipients Tregs displayed increased proliferation compared to conventional $CD4^+$ T cells. These data indicate that in the lymphopenic environment of the host after HSCT, both conventional T cells and regulatory T cells undergo strong proliferation, and that cell proliferation is more evident for regulatory T cells. Increased T cell proliferation in recipients after HSCT could be driven by cytokine-mediated signals, given the fact that many studies reported increased availability of the homeostatic cytokines IL7 and IL15 after transplantation (De Bock et al., 2013; Dulphy et al., 2008; Matsuoka et al., 2010), as well as stimulation by host alloantigens. However, Tregs seem to respond differently than conventional T cells to homeostatic signals in the host and their proliferation appears to be mainly driven by $CD4^+$ T cell lymphopenia (Matsuoka et al., 2010). Moreover, within the reconstituting Treg subset in the recipients, we observed increased frequencies of cells expressing the functional markers CTLA4, PD1 and ICOS, suggesting a potential mechanism aimed at counterbalancing the proinflammatory environment of the host.

In a recent study conducted by Lakshmikanth and colleagues, mass cytometry and proximity extension assay (PEA) were used to profile different immune cell populations present in blood and serum proteins, respectively, in 26 patients after HSCT. Analysis of the most abundant proteins revealed four principal patterns, of which one was represented by a "3 month burst" that included proteins whose concentration increased around 3 months after HSCT. Three months after HSCT is the same time point at which blood samples from recipients that did not develop aGVHD were collected in our cohorts (1 and 2). Interestingly, the "3 months burst" displayed an enrichment of proteins involved in "cell proliferation" and "IL2 signaling upregulated", suggesting that during

this phase of immune reconstitution these processes are particularly active (Lakshmikanth et al., 2017). These observations are interesting, as some of our findings at a similar time point, such as increased proliferation of T cell subsets and increased frequency of Tregs in recipients after HSCT could be related with the serum protein profile patterns described by Lakshmikanth et al. In particular, we could speculate that the "IL2 signaling upregulated" profile could explain the increased Treg frequency in the HSCT recipients. It has to be noted that while we included in our analysis only patients without aGVHD, in the aforementioned study both patients with and without aGVHD were included.

To also investigate the dynamics of T cell reconstitution at an earlier time point after transplantation, we analysed a third cohort of donor-recipient couples for which recipients' blood samples were collected at day 30 (instead of day 90) post-HSCT. One month after transplantation, we observed in the recipients a decrease of the absolute counts of all major lymphocyte populations (total lymphocytes, $CD4^+$ T cells, $CD8^+$ T cell, B cells) compared to the donors, while NK cell numbers remained stable, consistent with a rapid recovery of this cell subset after HSCT (Storek et al., 2008). The inversion of the CD4/CD8 ratio observed at day 90 posttransplant was already detectable at this early time point. While the decrease of naïve T cells was already detectable at day 30 post-HSCT, the increase of cells with an effector/memory phenotype was not observed at this early time point, indicating that the skewing of the T cell compartment toward a memory phenotype as a result of homeostatic peripheral expansion of mature donor T cells might take some months to become evident after HSCT.

1.2 T cell gene expression profile during immune reconstitution following HSCT

To investigate the molecular mechanisms underlying T cell immune reconstitution and expansion after HSCT, we profiled the transcriptome of sorted $CD4^+$ and $CD8^+$ T cells from donors before transplant and from patients without aGVHD on day 90 post-HSCT. Our gene expression analysis revealed that HSCT is associated with major transcriptomic changes in both $CD4^+$ and $CD8^+$ T cells in recipients compared to their donors. In particular, we observed that the majority of the genes analysed were upregulated and only few genes were downregulated in the recipients in both cell populations. Importantly, we found a great degree of overlap of the differentially expressed genes between the two cohorts, and changes in gene expression occurred in the same direction in the two independent cohorts.

Using Quantitative Set Analysis for Gene Expression (QuSAGE) and identification of differentially expressed gene signatures, we found that donor T cells react to environment of the host by acquiring an activated phenotype with upregulation of genes associated with T cell activation and its regulation, adhesion and migration, and effector functions, especially linked to a Th1-profile and cytotoxicity. QuSAGE analysis showed that the pathways and biological processes most affected in the recipients after transplantation included the *NLR-inflammasome* module, the *Memory* module, the *Th1 profile* and *CTL-Cytotoxicity* modules; followed by gene sets related to T cell activation, interferon-induced genes, proapoptotic genes and genes associated with exhausted cells and inhibitory receptors, all displaying an increased pathway activity after HSCT. Upregulation of genes associated with exhaustion and inhibitory receptor was more evident within the $CD8^+$ T cell population. Interestingly, modules with a significant reduction in pathway activity in the recipients included *WNT signaling* and the *Naïve* gene modules in both cohorts. Consistent with our flow cytometry data, which demonstrated in the recipients a depletion of the naïve T cell pool and an increase of cells with an effector memory phenotype, similar findings could be observed also at the transcriptomic level, with an enrichment of many genes reported to be expressed in memory T cells and an underrepresentation of naïve T cell-associated genes. On the contrary, while cellular profiling in the recipients posttransplant showed a decrease of cells with a Th1-like phenotype ($CXCR3^+$), at the gene expression level our data suggest that after HSCT $CD4^+$ T cells acquire a Th1-like profile with upregulation of *TBX21* (encoding the transcription factor T-bet) and other genes typically associated with Th1 cells such as *IFNG*, *CXCR3* and *IL12RB1*. Given the complex nature of the cellular environment in transplant recipients, transcriptomic analyses on individual cell populations or at the single-cell level will help unravel the heterogeneity and complexity of the reconstituting immune system following HSCT.

Of note, in the two cohorts the ranking of the enriched modules based on the pathway activity in the QuSAGE analysis was almost overlapping, further indicating the reproducibility of our observations in these two independent cohorts. Moreover, the changes in gene expression observed in cohorts 1 and 2 at day 90 post-transplant, were in great part reproduced and already detectable in the T cell transcriptome at day 30 posttransplant (cohort 3), indicating that the effects of the transplantation procedure on the reconstituting immune system can be detected early after HSCT during the engraftment phase and persist over time.

Several factors, such as the type of conditioning regimen, the source of stem cells, the GVHD prophylaxis administered as well as infections (such as CMV replication) can influence the immune reconstitution after HSCT (Itzykson et al., 2015; Lakshmikanth et al., 2017; Toubert, 2008). Changes in the host environment related to the conditioning regimen, especially the establishment of a proinflammatory milieu, and the increased availability of homeostatic cytokines such as IL7 and IL15 in the recipients, can influence and shape the immune reconstitution after HSCT. In particular, the T cell transcriptome in the recipients after HSCT could reflect alterations due to the presence of inflammatory cytokines that affect T cell polarization and migratory properties and a shift towards a memory/activated phenotype in HSCT recipients.

Immunophenotyping revealed increased T cell proliferation in HSCT recipients, and transcriptomic analysis showed the upregulation of the gene encoding IFNγ despite administration of CSA that strongly inhibits TCR-mediated signaling (Matsuda and Koyasu, 2000). In general, IFNγ production by T cells depends on TCR-mediated T cell activation (referred as "acquired" T cell activation pathway). However, a combination of IL12 and IL18 has been reported to synergistically induce IFNγ production by T cells in a TCR-independent manner (named "innate" T cell activation pathway) (Nakanishi et al., 2001; Yang et al., 1999). In particular, Yang et al. showed that the TCR-dependent and TCR-independent IFNγ induction pathways are pharmacologically distinct, with TCR-induced IFNγ production being CSA sensitive, while the IL12/IL18-induced pathway being completely CSA resistant (Yang et al., 1999). Translated to our study, this observation argues in favour of an effect of proinflammatory cytokines (IL12 and IL18) in the host in shaping T cell responses and reconstitution after HSCT in the presence of pharmacological immunosuppression. Moreover, genes involved in IL18 signaling were observed to be upregulated in the recipients after HSCT, further corroborating this hypothesis.

Even though the release of danger signals and inflammatory mediators as a consequence of the conditioning regimen is believed to last only a few weeks after HSCT, our data suggest that three months after HSCT a "signature" indicative of T cell activation and stimulation by inflammatory mediators is still present. Whether and to which extent the sequelae of the conditioning regimen can influence gene expression at the time points analysed in our study, and the potential impact of other factors (such as age, gender, CMV serostatus/reactivation, GVHD prophylaxis) remains to be further investigated. Multivariate analysis methods to identify the impact of pre and post-transplant variables on the gene expression profile after HSCT could be performed and will help

elucidate the mechanisms underlying reconstitution of a donor-derived immune system in transplant recipients. However, large cohorts of patients are needed for this kind of approaches to reach the required statistical power (Green, 1991; Wilson Van Voorhis and Morgan, 2007).

1.3 HSCT is associated with changes in NK cell and monocyte subset distribution and gene expression profile in recipients compared to their donors

In a subgroup of patients and donors of cohort 2, we additionally assessed the cellular subset distribution and the gene expression profile of NK cells and monocytes.

1.3.1 Expansion of CD56^{bright} NK cells after HSCT

NK cells reappear rapidly after allogeneic HSCT (Chan et al., 2018; Chklovskaia et al., 2004) and are the predominant circulating lymphoid cell subset in the host during the first few months (Benjamin et al., 2010). To investigate the dynamics of NK cell reconstitution after transplantation we analysed the frequency of different NK cell subsets in 10 recipients without GVHD at day 90 posttransplant, and compared it to their sibling donors. Our analysis showed that, three months after transplantation, recipients had a significantly increased frequency of total NK cells compared to the donors. This observation is consistent with studies in the literature describing high frequencies of NK cells in HSCT recipients compared to healthy subjects (Dulphy et al., 2008; Pical-Izard et al., 2015), and is in keeping with a rapid recovery of this cell subset compared to T and B lymphocytes (Storek et al., 2008).

In healthy individuals, peripheral blood CD56^{+}CD3^{-} NK cells are mainly represented by the CD56^{dim} subset, while CD56^{bright} cells are less abundant and account for about only 10% of circulating NK cells (Cooper et al., 2001a). Our data indicate that NK cell reconstitution after HSCT is associated with an altered subset distribution compared to healthy donors. We observed a significant expansion of the CD56^{bright} subset in the recipients, while the frequency of CD56^{dim}CD16^{+} cells was decreased. This finding is in agreement with other studies reporting that after HSCT NK cells are predominantly CD56^{bright} (Chklovskaia et al., 2004; Dulphy et al., 2008; Jacobs et al., 1992; Pical-Izard et al., 2015; Vukicevic et al., 2010). This preferential expansion of the CD56^{bright} NK subset is likely due to the high cytokine levels in patients after HSCT, and it has been related to the increased levels of the cytokine IL15 observed post-HSCT (Dulphy et al., 2008). It has also been shown that, when stimulated by IL2 or IL15, CD56^{bright} NK cells proliferate much more vigorously than CD56^{dim} NK cells (Carson et al., 1994; Cooper et al., 2001a). Moreover, CD56^{bright} CD16^{-} NK cells express IL7Rα (CD127), whereas the CD56^{dim} population is CD127^{-} (Vosshenrich et al., 2006), suggesting that IL7 levels posttransplant might modulate the proliferation and function of these cells. The enrichment of the CD56^{bright} subset in the recipients

has been reported to persist for several months (at least 6 months) after HSCT (Dulphy et al., 2008; Pical-Izard et al., 2015) and could also be linked to the GVHD prophylaxis with CSA, which was shown to reduce the proliferation of $CD56^{dim}$ NK cells to a greater extent compared to the $CD56^{bright}$ subset (Wang et al., 2007).

Gene expression analysis of total $CD56^{+}$ NK cells from recipients three months after HSCT showed a significant enrichment of transcripts characteristic of $CD56^{bright}$ cells while genes typically expressed by $CD56^{dim}$ NK cells were underrepresented compared to the donors. Interestingly, some of the genes enriched in NK cells in recipients after HSCT (*CCR1, CCR5, IL12RB2, IL18R1, AGK, HAVCR2*) have been reported to be specifically upregulated in NK cells stimulated with cytokines (IL12 and IL18) compared to other stimulation methods (Costanzo et al., 2018), suggesting that cytokines in the host environment influence the gene expression signature as well as the subset distribution of this cell population after transplantation. Although it was not assessed in our study, NK cell functional properties have been reported to be altered after transplantation (Ullah et al., 2016). In particular, Pical-Izard and colleagues showed that while the degranulation capacity and the chemokine production was similar to healthy controls, target cell-induced TNFα and IFNγ production was severely impaired in reconstituting NK cells, and remained low until 6 months posttransplant (Pical-Izard et al., 2015). On the contrary, Dulphy et al. reported increased IFNγ production by recipient $CD56^{bright}$ NK cells upon IL12/IL18 stimulations as compared with donors. The authors propose that after HSCT, $CD56^{bright}$ NK cells might get activated by IL15, probably through trans-presentation by dendritic cells and/or monocytes (Dulphy et al., 2008).

1.3.2 Expansion of $CD16^{+}$ monocytes after HSCT

Following HSCT, monocytes are the first cells to engraft (Storek et al., 2008). However, the dynamics of reconstitution of the different monocyte subsets and the role played by monocytes in the defence against infections after HSCT are poorly understood. Three months after transplantation, we observed in recipients without GVHD an increased frequency of total monocytes compared to the donors, consistent with a rapid recovery of this cell population. Increased proportions of total monocytes after HSCT compared to healthy controls were reported by Hainz et al. (Hainz et al., 2005). Within the $CD14^{+}$ monocyte population we observed an enrichment of $CD16^{+}$ cells, with increased percentages of both the intermediate ($CD14^{++}CD16^{+}$) and the non-classical ($CD14^{+}CD16^{++}$) subsets, paralleled by a decrease of classical monocytes

($CD14^{++}CD16^{-}$). After transplantation, classical monocytes have been previously shown to be the first to recover, followed by the intermediate and non-classical subsets. In this study monocyte subpopulation frequencies plateaued early after HSCT, at day 8-10 posttransplant for classical monocytes, at day 10-12 for the intermediate subsets and at day 14-16 for non-classical monocytes (Rogacev et al., 2015). Beyond the field of transplantation, CD16-expressing monocyte subsets have been reported to be expanded in various inflammatory conditions (Ziegler-Heitbrock, 2015). This suggests that classical monocytes recover first and that the host inflammatory environment post-HSCT might drive the expansion of the $CD16^{+}$ subsets. A developmental relationship from classical by intermediate to non-classical has been proposed (Ziegler-Heitbrock et al., 2010). Maturation of the classical monocytes into intermediate and non-classical monocytes in response to the host environment might explain the decreased frequency of the classical subset and the increase of $CD16^{+}$ cells observed in the recipients three months after HSCT. Immunosuppressive agents such as CSA, tacrolimus, MMF and MTX, do not seem to alter monocyte subset distribution (Rogacev et al., 2015). In line with our observation of altered monocyte subset distribution in recipients after transplantation, Döring et al. reported a significant decrease of classical ($CD14^{++}CD16^{-}$) monocytes and an increase of the intermediate ($CD14^{++}CD16^{+}$) monocyte subset on day 60 posttransplant compared to healthy controls (Döring et al., 2015).

Gene expression profiling of total $CD14^{+}$ monocytes also reflected the increased abundance of intermediate and non-classical monocytes found at the cellular level. In fact, in the recipients, we observed an enrichment of many genes that have been reported to be highly expressed in intermediate and non-classical monocyte subsets. Genes typically expressed by intermediate monocytes that were upregulated in the recipients included transcripts encoding proteins involved in antigen processing and presentation, the costimulatory molecule *CD40* and the receptors *MARCO, CMKLR1, FCGR3A* (encoding for CD16) and *CCR2* (Martinez, 2009; Wacleche et al., 2018; Wong et al., 2011). We also observed an upregulation of several complement components and genes involved in complement regulation and activation, which are highly expressed by non-classical monocytes (Wong et al., 2011). In addition, other genes typically associated with non-classical monocytes, such as *CD79B, CX3CR1, FCGR3A* and *ICAM2* (Wong et al., 2011) were enriched in the recipients. Interestingly, the transcriptomic profile of monocytes from HSCT recipients displayed an upregulation of many interferon-induced genes. Many factors, such as the presence of danger signals (e.g. DAMPs and PAMPs) that trigger pattern recognition receptor

(PRRs) signaling, cytokines present in the host environment, or reactivation of viruses (such as CMV) in the absence of optimal T cell functions, could explain this IFN-induced gene signature.

Chan et al. assessed the gene expression profile of monocytes following CMV infection *in vitro* and described a unique M1/M2 polarization signature skewed toward the M1 activation phenotype (Chan et al., 2008). In our QuSAGE analysis, we observed an enrichment of the M1-like signature in monocytes from HSCT recipients compared to the donors. Although all recipients included in this analysis received a graft from a CMV^+ donor, and were either CMV^+ or CMV^- (5 couples D^+/R^+, 4 couples D^+/R^-, one couple with unknown status), hierarchical clustering of the monocyte transcriptomic profile in recipients and donors, did not indicate a segregation according to the CMV serostatus mismatch (D^+/R^+ or D^+/R^-). We did not correlate the monocyte gene expression profile with clinical parameters such as CMV reactivation after HSCT, because the low patient number. Other factors that could determine a M1-like signature are microorganism-related molecules such as LPS, or inflammatory cytokines such as TNFα or IFNγ (Italiani and Boraschi, 2014) present in the host environment. To which extent the observed gene expression signature could be explained by viral infection, cytokine stimulation or other factors in the post-HSCT period remains to be assessed.

In a recent study investigating the role of monocytes in chronic GVHD, Hakim and colleagues found that multiple IFN-inducible genes were upregulated in monocytes from cGVHD patients compared to healthy donors and patients without cGVHD (Hakim et al., 2016). Although we did not observe any significant difference in the monocyte transcriptomic profile between recipients with and without aGVHD (data not shown), it would be interesting to assess whether upregulation of such IFN-induced signature early after transplantation could be correlated with the future occurrence of cGVHD at later time points.

Moreover, it would be interesting to correlate the observed cellular and/or gene expression signatures with clinical data, to investigate whether specific clinical parameters are associated with changes in cell distribution and/or transcriptomic profiles after HSCT.

2 Can we identify cellular and/or gene expression signatures associated with GVHD onset?

Validated diagnostic, prognostic and predictive tests for acute GVHD occurrence and responsiveness to therapy are not yet available in routine clinical care (Paczesny, 2018). Future progress in the field of GVHD for the diagnosis, prognosis, prophylaxis and treatment requires a better understanding of disease processes in humans. Much of our understanding of the biology of GVHD derives from studies in animal models (Socie and Blazar, 2009). The complex and multifactorial nature of GVHD pathophysiology, together with limited access to biological specimens, especially from GVHD target organs, make the study of the mechanisms involved in the development of this disease in humans particularly challenging. Although donor T cells have been shown to be critical to the pathophysiology of acute and chronic GVHD (Choi et al., 2010; Socie and Blazar, 2009), the precise mechanisms underlying their functions remain unclear.

The goal of this part of the project was to assess whether acute GVHD onset is associated with imbalances in specific immune cell populations, to identify potential "pathogenic" cell subsets, and to analyse the transcriptomic profile of immune cell populations involved in GVHD pathogenesis, to identify gene expression signatures associated with GVHD onset that could provide insight into the molecular mechanisms underlying GVHD development in humans.

2.1 Cellular correlates of acute GVHD onset

To investigate potential alterations in the T cell subset distribution associated with aGVHD development, we first compared the frequency of $CD3^+$, $CD4^+$ and $CD8^+$ T cells in recipients at aGVHD onset, before administration of the steroid therapy, and in recipients without aGVHD in cohorts 1 and 2. We reasoned that identification of specific cell subsets altered in GVHD patients would suggest that these cells play a role in GVHD development. Our analysis showed that in recipients at aGVHD onset the $CD3^+$ T cell compartment was characterized by an increased frequency of $CD4^+$ T cells and a decrease of $CD8^+$ T cells. Recipients at GVHD onset are thus characterized by a CD4/CD8 ratio that is generally, but not in all patients, greater than one, indicating an enrichment of $CD4^+$ T cells and suggesting an important role of these cells in GVHD development. In most murine models, $CD4^+$ T cells have been shown to play an important role in GVHD induction through different mechanisms: either stimulating $CD8^+$ T cell proliferation *via*

IL2 production, or by the generation of effector proteins such as TNF and IFNγ, or *via* cytolytic activity mediated by Fas/FasL (Coghill et al., 2011). We did not detect any significant difference in T helper subset distribution based on chemokine receptor expression between GVHD and No GVHD recipients.

Within the $CD8^+$ T cell compartment we observed in patients at GVHD onset an increase of $CXCR3^+CCR6^+$ and a trend toward an increase of $CXCR3^+$ cells, compared to patients without GVHD. This finding suggests a differential regulation of $CD4^+$ and $CD8^+$ T cell migratory properties during aGVHD. In particular, we observed a significant increase of the small fraction of $CD8^+$ T cells expressing both chemokine receptors CXCR3 and CCR6, which are important for access into inflamed and mucosal tissues (Groom and Luster, 2011; Lee et al., 2013a), indicating that these cells might be more prone to leave the periphery to migrate to GVHD target organs. In our experimental setting, we cannot determine whether the increased CD4/CD8 ratio observed at aGVHD onset is due to an expansion of the $CD4^+$ T cell subset or to a depletion of $CD8^+$ T cells in the periphery following their recruitment in GVHD target organs. However, in the latter case we would expect homing of activated T cells to target tissues to be associated with a decrease of these cells in peripheral blood. For example, a decrease of circulating $CD161^+$ $CCR6^+$ T cells has been reported in patients with aGVHD, and has been related to their recruitment toward $CCL20^+$ target tissues (Van Der Waart et al., 2012). While we observed an increase of $CXCR3^+CCR6^+$ $CD8^+$ T cells, no significant differences were found at GVHD onset in the frequency of circulating single $CXCR3^+$ $CD8^+$ and $CCR6^+$ $CD8^+$ T cells. Our data seem therefore to indicate that the increased CD4/CD8 ratio corresponds to an expansion of the $CD4^+$ T cell subset, rather than to increased homing of $CD8^+$ T cells.

Analysis of the different naïve and memory T cell subsets in recipients with and without aGVHD revealed that recipients at GVHD onset had a significant increase of cells with a $T_{SCM\text{-}like}$ phenotype compared to recipients without GVHD in both $CD4^+$ and $CD8^+$ compartments. Consistent with the notion that memory cells do not seem to trigger GVHD (Huang and Chao, 2017), our data indicate that at GVHD onset there is an increased frequency of cells belonging to less differentiated subsets, in particular $T_{SCM\text{-}like}$, while cells with an effector memory phenotype showed a trend towards a decrease, especially in the $CD8^+$ compartment. The increase of $T_{SCM\text{-}like}$ cells at GVHD onset is intriguing. T_{SCM} have been initially identified in a mouse model of human GVHD against minor histocompatibility antigens, in which they were shown to sustain alloreactive

T cells mediating GVHD upon serial transplantation into allogeneic hosts (Zhang et al., 2005). Subsequently, Gattinoni and colleagues reported the identification of T_{SCM} in humans (Gattinoni et al., 2011), but an association between this cell subset and human aGVHD has not been described. The property of T_{SCM} to sustain the generation of all memory and effector T cell subsets while maintaining their own pool through self-renewal (Gattinoni et al., 2011; Zhang et al., 2005) has implications for GVHD pathophysiology. T_{SCM} cells could represent a cellular reservoir for alloreactive T cells in recipients developing GVHD, sustaining the production of alloreactive donor T cells in the presence of host persistent antigens. Further investigation including additional markers for a more detailed phenotypic characterization together with functional studies should be performed to elucidate the role of this cell subset in human aGVHD. However, their low frequency in peripheral blood makes this kind of analyses particularly challenging.

Despite the increased frequency of $CD4^+$ and $CD8^+$ $T_{SCM\text{-}like}$ and T_{CM} cells observed at GVHD onset, we did not detect any clear difference in the proliferative status of the different cell subsets between recipients with and without GVHD. Interestingly, in a NHP model of acute GVHD, Furlan and colleagues reported a T cell signature characterized by antiapoptotic skewing and proposed that, in the setting of clinical GVHD that occurs in the presence of ongoing immunosuppression, T cell persistence rather than strong proliferation might be involved in GVHD pathogenesis (Furlan et al., 2016).

We next analysed the cellular profile associated with aGVHD in cohort 3, for which samples were collected either at aGVHD onset or at day 30 post-HSCT for the recipients that did not develop GVHD. Absolute counts at GVHD onset showed a significant increase of $CD3^+$ and $CD4^+$ T cell numbers compared to patients in the absence of GVHD, while a trend toward an increase was present for $CD8^+$ T cells. Consistent with the increased counts of $CD3^+$ T cells at GVHD onset, we also observed an increased percentage of $CD3^+$ T cells within the lymphocyte population in recipients developing GVHD compared to No GVHD patients. These findings are in line with the report from Podgorny et al. describing that high counts of both $CD4^+$ and $CD8^+$ T cells at day 28 precede aGVHD onset, suggesting involvement of both cell types in GVHD induction (Podgorny et al., 2014). In this cohort, we did not find the increased CD4/CD8 ratio at GVHD onset observed in cohorts 1 and 2. Since in cohort 3 samples from the GVHD and No GVHD groups have been collected at a more similar time point compared to cohorts 1 and 2, we cannot

exclude the possibility that an imbalance in immune reconstitution might be present, as in cohorts 1 and 2 non-GVHD patients were sampled at a later time during the reconstitution process, compared to patients with GVHD. However, given the slower reconstitution of $CD4^+$ compared to $CD8^+$ T cells (Seggewiss and Einsele, 2010), we would expect at day 30 post-HSCT (median delay of GVHD onset is around day 30) a lower frequency of $CD4^+$ T cells compared to day 90 posttransplant (time of sampling of the No GVHD group), suggesting that the increased CD4/CD8 ratio observed at GVHD onset in cohorts 1 and 2 might be linked to GVHD development rather than being solely an effect of the time of observation. Confirmation of these findings in a cohort of patients with time-matched samples between the GVHD and No GVHD groups is necessary to avoid possible confounding effects due to the time of observation.

2.2 T cell gene expression signature at acute GVHD onset

To investigate genes and pathways involved in GVHD pathogenesis, we performed gene expression profiling of sorted $CD4^+$ and $CD8^+$ T cells from recipients without GVHD and at GVHD onset, before the start of the steroid therapy.

While major changes in gene expression were detected in $CD4^+$ and $CD8^+$ T cells from recipients compared to their donors, indicating a strong effect of the transplantation procedure on the transcriptomic profile, identification of a gene expression signature associated with aGVHD onset has proven to be more challenging. We reasoned that, while the HSCT procedure strongly affects the engrafted immune cells, differences within the recipient group might be harder to capture, and possibly more influenced by confounding factors, resulting in a weaker signature.

To increase the power of our analysis, we combined the samples from cohorts 1 and 2, and to reduce the heterogeneity of the pooled dataset we included only patients receiving a reduced intensity conditioning (RIC). Moreover, to better identify transcriptomic changes associated with GVHD, we focused our analysis on the patients that experienced a more severe disease (grade 2-4) and excluded the patients with grade 1 aGVHD.

Transcriptomic profile of $CD4^+$ T cells revealed differential expression of 48 genes in patients with GVHD compared to No GVHD recipients (FDR<10%), of which 5 were upregulated and 43 were downregulated at GVHD onset. QuSAGE analysis showed that the gene module most significantly downregulated in GVHD recipients was *TGFβ signaling*. In particular, we observed lower expression levels of genes encoding TGFBR1, SMAD3 and IGF2R at GVHD onset

compared to the No GVHD group. On the contrary, transcripts that displayed an upregulation in recipients at GVHD onset included genes involved in the NF-κB signaling pathway (*RELB, BCL10, BCL3*), the proteasome subunit *PSMD7* and the costimulatory molecule *ICOS.*

In $CD8^+$ T cells we observed more marked changes between the two recipient groups compared to $CD4^+$ T cells, with differential expression of 134 genes (FDR<5%), of which 23 genes were upregulated and 111 were downregulated at GVHD onset. As for $CD4^+$ T cells we observed upregulation of genes involved in NF-κB signaling (*NFKB1*, *RELB*, *BCL3* and *NFKBIA*), the proteasome subunit *PSMD7*, as well as the costimulatory molecule *ICOS.* In addition, within the $CD8^+$ T cell subset we found an increased expression of the costimulatory molecule *CD28*, the inflammatory mediator *MIF* and the glycolytic enzyme *GAPDH.* QuSAGE analysis showed increased pathway activity of the gene module including NF-κB transcription factors, suggesting that in both $CD4^+$ and $CD8^+$ compartments the NF-κB signaling pathway plays an important role in alloreactive T cells mediating GVHD. This finding is consistent with the central role of this pathway in mediating TCR signaling and T cell activation and differentiation (Oh and Ghosh, 2013), supporting a key role of NF-κB signaling in GVHD pathogenesis. Consistently, inhibition of NF-κB was shown to protect mice from lethal GVHD (Vodanovic-Jankovic et al., 2006).

Similar to $CD4^+$ T cells, we observed in $CD8^+$ T cells downregulation of genes involved in TGFβ signaling (*TGFBR1, TGFBR2, SMAD3, IGF2R*) at GVHD onset. In addition, genes encoding inhibitory receptors (*LAIR1, LILRB1, BTLA, KLRG1*) (Chen and Flies, 2013; Kang et al., 2016; Murphy et al., 2006; Odorizzi and Wherry, 2012) and molecules mediating immunosuppressive signals (e.g. *IL10RA*) (Saraiva and O'Garra, 2010) were also downregulated in GVHD recipients, suggesting that a deficient expression of genes involved in the regulation and dampening of the immune response might be implicated in GVHD development. However, we also noted the downregulation of genes involved in T cell activation and effector functions. This is somewhat counterintuitive and further investigation is necessary to elucidate the role of these signaling pathways in GVHD development.

Given the difference in the time point of sampling between the GVHD and No GVHD groups, we cannot exclude that this might affect the level of immune reconstitution and therefore the gene expression profile. To address this issue, we analysed the T cell transcriptome in recipients of the third cohort, for which the time points of sampling for the GVHD and No GVHD groups are more similar. Transcriptomic analysis of $CD4^+$ T cells in this cohort revealed upregulation of genes

encoding the proinflammatory mediators IL32 and MIF, molecules involved in cytokine signal transduction, such as *IL21R* and *JAK3*, and genes involved in cell migration and trafficking such as *S1PR1*. Our finding of increased expression of *IL32* and *MIF* in T cells at GVHD onset is in agreement with other studies in the literature reporting increased MIF serum levels (Lo et al., 2002; Toubai et al., 2009) as well as increased MIF mRNA and protein expression in skin and colonic biopsies (Lo et al., 2002) and increased IL32 mRNA expression in blood leukocytes (Marcondes et al., 2011) in GVHD recipients compared to patients without GVHD, and might indicate a pathogenic role of these cytokines in the T cell alloimmune response mediating acute GVHD in humans. In particular, these cytokines have been shown to induce other inflammatory mediators (e.g. TNFα and IFNγ), suggesting that they could be involved in a self-amplifying proinflammatory loop (Calandra et al., 1994; Kim et al., 2005; Stirewalt et al., 2008). Of note, given its induced expression in response to glucocorticoids and its ability to counter-regulate the immunosuppressive action of glucocorticoids (Calandra et al., 1995; Leng et al., 2009), MIF has been proposed as a potential factor that could be involved in steroid resistance in glucocorticoid-refractory acute GVHD. (Pidala and Anasetti, 2010).

To date, only a few studies in small cohorts analysed the gene expression profile associated with acute GVHD in humans (Buzzeo et al., 2008; Takahashi et al., 2008; Verner et al., 2012). These studies used microarray analysis on either bulk PBMCs (Buzzeo et al., 2008; Verner et al., 2012) or microbead-enriched immune cell subpopulations ($CD4^+$ T cells, $CD8^+$ T cells, $CD56^+$ NK cells, $CD14^+$ monocytes) (Takahashi et al., 2008) and identified non-overlapping sets of genes up- or downregulated before or at GVHD onset. The small patient numbers analysed, as well as differences in the experimental and clinical setting among these studies and as compared to our analysis make it difficult to compare the results and identify shared gene expression signatures that could shed light on the mechanisms involved in GVHD development in humans.

3 Can we identify “dangerous donors”?

Progress in HLA typing techniques has greatly improved donor selection for allogeneic HSCT based on histocompatibility (Petersdorf, 2008). However, evidence from animal and human studies indicates that histoincompatibility is necessary, but not sufficient, to induce fatal GVHD (Fontaine et al., 1991; Gleichmann et al., 1984; Martin, 1991; Via and Shearer, 1988). Beyond mismatches at MHC loci, factors such as alloantigens tissue distribution and non-HLA gene polymorphisms (e.g. at genes encoding cytokines) influence the risk of developing GVHD and disease severity (Dickinson and Charron, 2005; Gam et al., 2017; Spierings, 2014).

It has also been proposed that quantitative or qualitative differences in donor immune responses could define “dangerous donors”, stronger alloresponders that are more likely to induce GVHD in their recipients. The identification of these characteristics would allow a better donor selection minimizing the risk of GVHD (Baron et al., 2007). To this end, Baron et al. measured the transcriptomic profiles of $CD4^+$ and $CD8^+$ T cells from allogeneic donors and suggested a dominant impact of the donor gene expression profile on the occurrence of chronic GVHD in the recipients. The authors reported that the risk of cGVHD was influenced by the activity of genes that regulate diverse cellular functions in donor T cells, including TGFβ signaling and cell proliferation (Baron et al., 2007). However, donor gene expression signatures associated with acute GVHD development in the recipients have not been identified.

To address this question, the third goal of our study was to try to define cellular and/or molecular parameters in the donors that could indicate an increased risk of developing aGVHD for the recipients. We thus stratified the donors according to the aGVHD status of the corresponding recipients and compared the frequencies and numbers of the different immune cell populations as well as the gene expression profiles in donors whose recipients developed aGVHD and donors whose recipients did not. In our cohorts and with our experimental settings, we could not detect any significant differences in immune cell composition or gene expression signatures in the peripheral blood of the donors before transplant that could indicate a higher risk for the recipients to develop aGVHD.

Further investigation including for example genome-wide gene expression profiling or analysis of stimulated cells may help identify signatures of “dangerous donors” that can improve the process of donor selection.

We are currently extending our immunophenotype analysis with unsupervised approaches. In particular, we are applying two different algorithms for unsupervised analysis, FlowSOM (Van Gassen et al., 2015) and CITRUS (Bruggner et al., 2014), to integrate the traditional analysis done with manual gating, that relies on defined cell populations, and gain insight into cell subpopulations that might have been missed in the original manual gating and that could better discriminate donors and recipients, recipients with and without aGVHD or donors whose recipients developed or not aGVHD.

Conclusions and Perspectives

In conclusion, our study provides insights into the cellular and molecular mechanisms involved in the reconstitution of a donor-derived immune system after HSCT, and in the development of acute GVHD in humans. Immunophenotyping revealed that immune reconstitution in recipients after transplantation is associated with several homeostatic imbalances compared to the donor's immune system before transplant. Gene expression profiling of different immune cell subsets showed major transcriptomic changes in recipients following HSCT compared to their sibling donors. In particular, signals present in the environment of the host following the transplantation procedure, such as proinflammatory mediators and cytokines, seems to be the main drivers in determining and shaping the process of immune reconstitution. Comparison of recipients without GVHD and at GVHD onset allowed the identification of cellular and molecular correlates associated with the development of aGVHD. Our data demonstrate that comprehensive analysis of the distribution of different immune cell subsets with flow cytometry together with gene expression profiling can contribute to elucidate the processes involved in immune reconstitution and GVHD development in humans.

Immune cell subsets such as $CD4^+$ T cells, $CD8^+$ T cells, NK cells and monocytes are not homogeneous populations, thus it would be interesting to extend our investigation using other methodologies that enable genome-wide analysis on low-frequency cells, such as single-cell RNA-sequencing. Such approach would allow to better understand the role of more specific cell subpopulations in immune reconstitution after HSCT and in aGVHD development. In addition, the analysis of immune cell populations in peripheral blood does not always mirror the situation in tissues, but the availability of biopsies from GVHD target organs is limited and makes the study of the mechanisms underlying this disease in humans particularly challenging. Longitudinal analyses of large cohorts of transplant patients including both peripheral blood and target organ specimens would be of particular importance for future investigations in order to elucidate disease processes in humans and guide novel strategies for GVHD prevention and treatment.

In our analysis, for cohorts 1 and 2, the time point of sampling between the GVHD and No GVHD recipient groups was not perfectly matched. The degree to which this difference affects the cellular and molecular profiling is not clear and, ideally, it would be beneficial to confirm our findings in a more time-matched setting.

Studies with larger patient cohorts including comprehensive assessment of frequencies and numbers of different immune cell populations as well as their functional properties are needed to draw conclusions regarding the impact of specific cell subsets on clinical outcome and GVHD development after HSCT. New techniques such as single-cell RNA sequencing and mass cytometry, can help unravel the heterogeneity and complexity of the reconstituting immune system following HSCT. In addition, profiling of cytokines and chemokines in the serum at different time points, and correlation of these secretome data with cellular and molecular signatures could help elucidate the mechanisms underlying immune reconstitution and provide biomarkers for HSCT outcome and occurrence of complications, such as GVHD or viral reactivation. Standardization of both clinical (e.g. therapeutic regimens and criteria for GVHD diagnosis) and experimental procedures (e.g. flow cytometric identification of different cell subsets or time points evaluated after HSCT) between centres is pivotal to enable data comparison between studies and facilitate multicentre studies. The rapid advances in the technologies available, together with national and international initiatives, such as CRYOSTEM biobank, that provide invaluable samples for clinical and translational research, will hopefully bring in the near future insights into the mechanisms underlying GVHD development that will help design new preventive and therapeutic strategies to be applied in the clinics.

Annex

Fluorochrome	Version 1 [a]	Version 2 [a]	Version 3 [a]	Version 4 [a,b]	Version 5 [a,c]
BV421	CD95	CD95	CD95	CD95	CD95
V450	CD3	CD3	CD3	CD3	CD3
VioGreen					CD45R0
V500	CD4	CD4	CD4	CD4	
BV570	CD8	CD8	CD8	CD8	CD8
BV605	CD62L	CD62L			PD1
BV650	CD117	CD27	CD27	CD27	CD27
BV711	CCR6	CCR6	CCR6	CCR6	CCR6
BV750					CD4
BV786	CD45RA	CD45R0	CD45RA	CD45RA	CD45RA
FITC	eF520	eF520	eF520	eF520	eF520
FITC	CD34	CD34	CD34	CD34	CD34
FITC	CD11c	CD11c	CD11c	CD11c	CD11c
FITC	CD14	CD14	CD14	CD14	CD14
FITC	CD19	CD19	CD19	CD19	CD19
BB515		CD122	CD45R0	CD45R0	
PerCP-Cy5.5	CD161	CCR7	CXCR5	CXCR5	CXCR5
PE	TCRgδ	TCRgδ	TCRgδ	TCRgδ	CD122
PE	TCRvδ2	TCRvδ2	TCRvδ2	TCRvδ2	
PE-CF594	CRTH2	CRTH2	CRTH2	CRTH2	CRTH2
PE-Cy7	CXCR3	CXCR3	CXCR3	CXCR3	CXCR3

a Cohort 3
b Cohort 1
c Cohort 2

Table 4 Panel 1, markers used for surface staining

Fluorochrome	Version 1 [a]	Version 2 [a]	Version 3 [a,b]	Version 4 [a,c]
BV421	KI67	CD95	CD95	CD25
V450	CD3	CD3	CD3	CD3
V500	CD4	CD4	CD4	CD4
BV570	CD8	CD8	CD8	CD8
BV605	CD62L	Ki67	Ki67	Ki67
BV650		CD27	CD27	CD27
BV711	PD1	PD1	PD1	PD1
BV786	CD45RA	CD45RA	CD45RA	CD45RA
FITC	eF520	eF520	eF520	eF520
PerCP-Cy5.5	ICOS	ICOS	ICOS	ICOS
PE	FoxP3	FoxP3	FoxP3	FoxP3
PE-CF594	CTLA4	CTLA4	CTLA4	CTLA4
PE-Cy7	HLADR	HLADR	HLADR	CD127

a Cohort 3

b Cohort 1

c Cohort 2

Table 5 Panel 2, markers used for intracellular staining

Module	Genes
Adhesion	*CD2, CD58, CD99, CEACAM1, ICAM1, ICAM2, ICAM3, ITGA4, ITGA5, ITGA6, ITGAE, ITGAL, ITGAM, ITGAX, ITGB1, ITGB2, PECAM1, SELL, CD164, CD6, CD9, CD97, CX3CR1, DPP4, LGALS3, PLAUR, PTK2, SELPLG, SRC, TGFBI, CD53, APP, CTNNB1, CEACAM6, CEACAM8, ITGA2B*
Antigen Presentation and MHC Interaction	*HLA-A, HLA-B, HLA-C, B2M, TAP1, TAP2, TAPBP, CD74, HLA-DMA, HLA-DMB, HLA-DOB, HLA-DPA1, HLA-DPB1, HLA-DRA, CTSS, KLRC1, KLRC2, KLRC3, KLRC4, KLRD1, KLRF1, KLRK1, LILRA1, LILRA3, LILRA6, LILRB1, LILRB2, LILRB4, CD4, CD8A, CD8B, MR1, XBP1, LILRA2, CD1D*
Antiapoptotic	*MCL1, TRAF4, MIF, TRAF1, NFKB1, CDKN1A, MALT1, RELA, TNFAIP3, BCL2, TNFRSF1B, LGALS3, PTK2, RAF1, IKZF3, TNFRSF10C, IL2RA, IL2RB, IL2RG*
Anti-inflammatory	*IL10, IL10RA, TGFB1, TGFBR1, TGFBR2, IL4R, IL11RA, CD83*
Autophagy	*ATG10, ATG12, ATG5, ATG7, ATG16L1, TOLLIP, TNFAIP3, IL2RG, IFI16, ABL1, PTPN22, S100A8, S100A9, XBP1, FKBP5*
Cell cycle and its Regulation	*CCND3, CDKN1A, TP53, ABL1, ATM, AHR, BAX, BCL2, IKZF1, MAPK1, PML, RARRES3, PRKCD, PTK2, SRC, S100A8, S100A9, CEBPB, ILF3, NFATC2*
Chemotaxis and Migration	*CCL3, CCL4, CCL5, CCL7, CCL8, CCR1, CCR2, CCR5, CCR6, CCR7, CCR8, CCRL2, CMKLR1, CX3CR1, CXCR1, CXCR2, CXCR3, CXCR4, CXCR6, IL16, S1PR1, GPR183, LTB4R, LTB4R2, PPBP, MUC1, CXCL1*
Coinhibitory	*BTLA, CD160, CD22, CD244, CD5, CD96, CTLA4_all, HAVCR2, KIR3DL2, KLRG1, LAG3, LAIR1, PDCD1, PECAM1, TIGIT, TNFRSF14, CTLA4-TM, sCTLA4, KLRD1, CEACAM1, LILRB1, LILRB4, SLAMF7, KIR3DL1*
Complement	*C1QBP, C1R, C2, C4BPA, C6, CD46, CD55, CD59, CFD, CFH, CFP, CR1, CR2, ITGAM, ITGAX, ITGB2, SERPING1*
Costimulatory	*ADA, CD2, CD24, CD27, CD28, CD40, CD40LG, CD6, CD81, CD82, CD53, DPP4, ICOS, TNFRSF13C, TNFRSF14, TNFRSF4, TNFRSF8, TNFRSF9, TNFSF4, TNFSF8, TRAF1, LTBR, SLAMF1, TRAF2, TRAF3, TRAF5, TNFRSF1B, CD99, CD86, CD80, SLAMF6, FCGR3A/B, ICOSLG*
CTL-Cytotoxicity	*CD160, EOMES, PRDM1, GNLY, GZMA, GZMB, GZMK, IFNAR1, IFNAR2, IFNG, IL12RB1, IL21R, KLRC1, KLRD1, KLRF1, KLRG1, PRF1, TBX21, TNF, TNFSF10, XCL1, B3GAT1, CXCR3, CTSC, FCGR3A/B, KLRC2, KLRC3, KLRC4, NCAM1, NCR1*
Energy and Metabolism	*ALAS1, CD36, CD74, G6PD, GAPDH, GPI, MAPK14, MIF, SDHA, SLC2A1, XBP1, CEACAM1, PTGS2*
Exhaustion-down	*CD28, ETS1, ICAM2, IFNAR1, IL2RB, IL7R, LEF1, MAP4K4, TCF7, IL18R1*
Exhaustion-up	*BATF, BTLA, CASP3, CCL3, CCL4, CCRL2, CD160, CD244, CD27, CD7, CD80, CD9, CTLA4_all, CXCL10, ENTPD1, EOMES, HAVCR2, ICOS, IFIH1, IKZF2, IL10, IL21, IRF4, JAK3, KLRG1, LAG3, LILRB4, MX1, NFATC1, NFIL3, NFKBIA, NFKBIZ, PDCD1, PRDM1, PTGER4, SH2D1A, TBX21, TNFRSF4, TNFRSF9, TIGIT, MAF*
FcRs	*FCER1A, FCER1G, FCGR2A, FCGR2A/C, FCGR2B, FCGR3A/B, FCGRT*
Homeostatic proliferation	*CD24, CD5, IL21R, IL2RA, IL2RB, IL2RG, IL7R*
IFN-induced genes	*BST2, CD74, GBP1, HLA-A, HLA-B, HLA-C, IFI16, IFIH1, IFIT2, IFITM1, IRF1, IRF3, IRF4, IRF5, IRF7, IRF8, JAK1, MX1, PML, SOCS1, SOCS3, STAT1, STAT2, TNFSF10, IFNGR1, CXCL10, IFI35, PSMB8*
IL1-IL18-IL33_signaling	*EGR1, IL18R1, IL18RAP, IL1R2, IL1RAP, IL1RL1, IRAK1, IRAK2, IRAK3, IRAK4, MYD88, SIGIRR, TOLLIP, TRAF6*
IL2 signaling	*IL2RA, IL2RB, IL2RG*
IL6 signaling	*IL6R, IL6ST*
IL7 signaling	*IL7R, IL2RG, CD46, GFI1*

JAK-STAT	*JAK1, JAK2, JAK3, TYK2, STAT1, STAT2, STAT3, STAT4, STAT5A, STAT5B, STAT6*
JAK-STAT Regulation	*CISH, PTPN2, PTPN6, PTPRC_all, SOCS1, SOCS3*
MAPK	*DUSP4, HRAS, MAP4K1, MAP4K2, MAP4K4, MAPK1, MAPK14, MAPKAPK2, RAF1*
Memory	*BATF, BCL6, CASP1, CCL5, CCR2, CCR5, CCR6, CD160, CD2, CD244, CD45R0, CD58, CD7, CD74, CDKN1A, CFH, CX3CR1, CXCR3, DUSP4, EOMES, FAS, GZMA, GZMB, GZMK, HLA-DPA1, HLA-DPB1, HLA-DRA, ICAM1, IFNG, IFNGR1, IL10RA, IL12RB1, IL18R1, IL18RAP, IL2RB, IL2RG, IL7R, ITGA4, ITGA5, ITGAL, ITGAM, ITGB1, ITGB2, KIR3DL2, KLRC1, KLRF1, KLRG1, LGALS3, LY96, MAF, NCF4, NFATC2, NFATC3, NOD2, PRDM1, PRF1, PTPN22, S100A9, SLAMF1, SMAD3, TBX21, TNF, TNFRSF1B, TNFSF10*
Naïve	*CCR7, CD27, CD28, CD45RA, CD45RB, CD7, CTSC, CXCR4, FKBP5, IL6ST, IL7R, LEF1, PECAM1, POU2F2, PTK2, S1PR1, SELL, SOCS3, TCF7*
NFAT pathway Biocarta	*HRAS, LIF, MAPK1, MAPK14, NFATC1, NFATC2, NFATC3, RAF1*
NFAT TFs	*NFATC1, NFATC2, NFATC3*
NFKB Negative regulators	*NFKBIA, TNFAIP3, NFKBIZ, TRAF3*
NFKB Positive regulators	*BCL10, BTK, CHUK, IKBKAP, IKBKB, IKBKE, IKBKG, MALT1, MAP4K4, TBK1, TRAF4, TRAF2, TRAF5, TRAF6*
NFKB target genes	*BCL2, BCL3, CCL4, CXCL2, CYBB, ICAM1, IL8, NFKBIA, PTGS2, TNF, TNFAIP3, TNFSF13B, TRAF1, TRAF2, VCAM1*
NFKB TFs	*NFKB1, NFKB2, RELA, RELB*
NLR-inflammasome	*BCL2, CASP1, GBP5, NLRP3, PYCARD*
NOD signaling	*TRAF6, TRAF4, NOD1, NOD2*
NOTCH signaling	*APP, CD46, ETS1, IKZF1, NOTCH1, NOTCH2, RUNX1, TGFB1, TGFBR2*
NOTCH target genes	*BATF, BCL2, CDKN1A, GATA3, IL2RA, IL7R, NFKB2, NOTCH1, TBX21, TCF7, CR2*
Nucleotide Metabolism	*HPRT1, NT5E, ENTPD1, ADA, POLR1B, POLR2A, BST1*
Proapoptotic	*BAX, BCL10, BCL2L11, CASP1, CASP2, CASP3, CASP8, CRADD, CTSC, CTSS, FADD, FAS, IFI16, LTBR, MX1, PYCARD, CTSG, TNFRSF1B, TNFRSF8, TNFRSF9, TNFSF12, TP53, TRAF3, BCAP31, CD2, CD27, PDCD2, PML, OAZ1, ARHGDIB*
Proinflammatory	*CCL20, CCL3, CCL4, CCL5, CCR1, CCR2, CCR5, CSF1, CXCR2, IFNG, IL12A, IL32, IL6R, IL6ST, IL8, MIF, PTAFR, PTGER4, PTGS2, S100A8, S100A9, TNF, CXCL10, LITAF, IL23A*
Regulation of T cell activation	*DUSP4, PTPN2, PTPN22, PTPN6, PTPRC_all, GBP1, CR1, EGR2, MBP*
T cell activation	*CCR5, CD2, CD27, CD28, CD40LG, CD45R0, CD58, CD70, CD82, CD83, CD86, CD97, CEACAM1, CTLA4_all, CXCR3, DPP4, FAS, G6PD, GAPDH, HLA-DPA1, HLA-DPB1, HLA-DRA, ICAM1, ICOS, IL2RA, IL2RB, IL2RG, ITGAL, KLRK1, LGALS3, PDCD1, PLAUR, TAGAP, TFRC, TNFRSF4, TNFRSF8, TNFRSF9, TNFSF8, CD6, EGR1, FCGR3A/B*
TCR signaling	*BCL10, CD247, CD3D, CD3E, CD4, CD8A, CD8B, FYN, HRAS, LCK, LCP2, MALT1, MAPK1, NFATC1, NFATC2, NFATC3, NFKB1, RAF1, RELA, ZAP70, TRAF6, SYK*
Tfh profile	*CXCL13, IL21, PDCD1, ICOS, BCL6, CD40LG, IL21R, IL6R, IL6ST, SH2D1A, CXCR4, STAT1, STAT3*
TGFβ signaling	*TGFB1, TGFBR1, TGFBR2, SMAD3, SMAD5, TGFBI, SKI, IGF2R, ZEB1, MAPK1*
Th1 profile	*TBX21, CCR5, CXCR3, IFNG, TNF, LTA, STAT1, STAT4, IL12RB1, IFNAR1, IFNAR2, IFNGR1, CD46, IL18R1, IL18RAP, IL12A*

Th17 profile	*IL21, TGFBR1, TGFBR2, IL6R, IL6ST, IL1RAP, IL23R, IL12RB1, RORC, STAT3, CCR6, KLRB1, IL21R, AHR, BATF, IRF4, MAF, ZBTB16*
Th2 profile	*IL4R, GATA3, STAT6, CCR8, CXCR4, GFI1, IL11RA, IL1RL1*
TLR signaling	*TLR1, TLR2, TLR3, TLR4, TLR5, TLR8, CD36, MYD88, TOLLIP, IRAK1, IRAK2, IRAK4, TOLLIP, TICAM1, TBK1, BCL10, MALT1, TRAF6, CD14, LY96*
TNF signaling	*TNF, LTA, TNFRSF1B, FADD, TRAF1, TRAF2, TRAF3, TRAF5, LTBR, TNFSF12, TNFRSF14*
Transcription and Translation Regulation	*AIRE, APP, C14orf166, CTNNB1, EGR2, EOMES, IKBKAP, ILF3, ABCF1, EEF1G, POLR1B, POLR2A, TBP, PML, BATF3*
Treg profile	*FOXP3, IL10, TGFB1, TGFBR1, TGFBR2, LIF, LGALS3, RUNX1, STAT5A, STAT5B, CCR5, CCR6, CCR8, IL2RA, CTLA4-TM, CTLA4_all, sCTLA4, ENTPD1, LAG3, NT5E, IL2RB, IL2RG*
Type1 IFN signaling	*IFNAR1, IFNAR2, JAK1, TYK2, STAT1, STAT2, STAT3, STAT4, TMEM173*
Ubiquitin-Proteasome	*PSMB10, PSMB5, PSMB7, PSMB8, PSMB9, PSMC2, PSMD7, CUL9, UBE2L3*
WNT signaling	*CTNNB1, TCF4, TCF7, LEF1*

Table 6 Gene modules designed for T cells and used in QuSAGE analysis

Module	Genes
Adhesion	*JAM3, ALCAM, CD58, CX3CR1, ITGA2B, ITGAE, ITGB3, ITGA5, ITGAX, ITGAM, ICAM1, ICAM2, ICAM3, ICAM4, ITGA4, ITGAL, ITGB1, ITGB2, ITGA1, CD164, CD9, CD99, PLAUR, SELPLG, CD97, SIGLEC1, PECAM1, PVR, SELL, THBS1, APP, LGALS3, PLAU, TNFRSF12A, AMICA1, CD33, CD53, CD63*
Ag Presentation and MHC interaction	*HLA-DMB, HLA-DPA1, HLA-DPB1, HLA-DRA, HLA-DRB4, MR1, PSMB7, PSMB9, TAP1, TAP2, TAPBP, HLA-DOB, HLA-A, HLA-B, HLA-C, HLA-DMA, KLRF1, KLRK1, HLA-E, HLA-G, LILRA1, LILRB2, LILRB3, LILRB1, CD74, CTSL, CTSS, LILRA5, CD1A, CD1C, CD37, CD1D*
Antiapoptotic	*BCL2, CDKN1A, AKT3, IL3RA, CSF2RB, TNFRSF1B, TNF, HRAS, TNFAIP3, BCL2L1, CHUK, IKBKB, IKBKG, LGALS3, MIF, NFKB1, RELA, TRAF2, CX3CR1, CD40, FYN, CSF1R, PDGFC, ANP32B, TNFRSF10C*
Anti-inflammatory	*ADORA2A, ANXA1, FPR2, IDO1, IL10, IL10RA, IL13RA1, IL1R2, IL1RN, IL27, IL4R, MAF, TGFB1, SBNO2*
Autophagy	*ABL1, ATG10, ATG12, ATG16L1, ATG5, ATG7, IFI16, S100A8, TOLLIP, TFEB, LAMP1, LAMP2, MEFV*
Cell cycle and its regulation	*ABL1, BAX, BCL2, BID, CCND3, CDKN1A, CEBPB, CSF1R, CSF2RB, EP300, ETS1, HRAS, ILF3, IRF2, MAF, MAPK1, NUP107, PRKCD, S100A8, THBS1, TNFSF10, TP53, INPP5D, S100A12, NFATC2, PIN1, TFRC, TLK2, ANP32B, CYLD, FLT3, IGF1R*
Chemotaxis and Migration	*CCL2, CCL20, CCL3, CCL3L1, CCL4, CCL5, CCL8, CCR1, CCR2, CCR5, CCRL2, CD99, CKLF, CMKLR1, CX3CR1, CXCL10, CXCL11, CXCL16, CXCL2, CXCL5, IL8, CXCL9, CXCR2, CXCR4, HCK, IL16, LGALS3, PPBP, THBD, VEGFA, FPR2, LYN, ANXA1, FYN, CD47, CD81, LRP1, FUT7*
Classical monocytes	*BATF, BST1, CCL3L1, CCR1, CCR2, CD14, CD163, CD1D, CD36, CD9, CD99, CLEC5A, CREB5, IL8, CXCR2, EGR1, F13A1, F2RL1, FCGR1A, FUT7, IL10, IL13RA1, IL1B, ITGA5, ITGAM, LYN, OSM, PLAUR, PTGS2, S100A12, S100A8, SELL, SERPINB2, THBS1, TLR4, TNFSF12, TREM1*
CLR signaling	*BCL10, CARD9, CD63, CLEC4A, CLEC4C, CLEC5A, CLEC6A, CLEC7A, FCER1G, IRF5, MRC1, PRKCD, PYCARD, SYK*
Coinhibitory	*CD86, IDO1, LILRB2, LILRB3, LILRB1, TNFRSF14, PDCD1LG2, HAVCR2*
Complement	*ITGAX, ITGB2, ITGAM, C1QA, C1QB, C2, C5, THBD, C3, C3AR1, CD46, CD55, CD59, CFD, CR1, CREB5, SERPING1, C1QBP, CFP*
Costimulatory	*CD86, TNFSF14, CD40, PVR, TNFRSF14, CD48, CD58, LILRA5, ICOSLG, TNFSF8, TNFSF15, CD244, CD84, TNFSF4, CD4, CD8A*
Cytotoxicity	*CTSH, CYBB, FCGR1A, FCGR2A, FCGR3A, GNLY, GZMA, GZMB, GZMK, IFNAR1, IFNAR2, IFNGR1, IL1B, MICA, MICB, NCF4, PRF1, SLAMF7, TNF, TNFSF10, TNFSF12, TREM1, TUBB, GZMH*
Energy and Metabolism	*AGK, ALAS1, CD36, CD74, G6PD, GPI, MAPK14, MIF, MTMR14, PIK3CD, PIK3CG, PLA2G6, PTGS2, SDHA*
FcRs	*FCER1A, FCER1G, FCER2, FCGR1A, FCGR2A, FCGR2B, FCGR3A*
IFN induced	*BST2, CD74, CXCL10, CXCL9, EGR1, HLA-A, HLA-B, HLA-C, HLA-E, HLA-G, IFI16, IFI27, IFI35, IFIH1, IFIT1, IFIT2, IFITM1, IFITM2, IFNA17, IFNAR1, IFNAR2, IFNGR1, IKBKE, IRF1, IRF2, IRF3, IRF4, IRF5, IRF7, IRF8, ISG15, ISG20, JAK1, MX1, OAS3, PSMB8, SOCS1, STAT1, STAT2, TNFSF10, TYK2*
IL1-IL18-IL33-signaling	*EGR1, IL18, IL1B, IL1R2, IL1RAP, IL1RN, IRAK1, IRAK2, IRAK4, MAP3K7, MYD88, SIGIRR, TAB1, TOLLIP, TRAF6, ECSIT*
IL2-IL7-IL15	*IL15RA, IL2RG, STAT3, STAT5B, JAK1, JAK3, IL15*
Intermediate monocytes	*CCR2, CCR5, CD14, CD163, CD1D, CD38, CD40, CD74, CD86, CMKLR1, CSF1R, CX3CR1, CXCR4, FCGR3A, GPI, HLA-A, HLA-B, HLA-C, HLA-DOB, HLA-DPA1, HLA-DPB1, HLA-DRA, ICAM1, IFNAR2, IL10, IL12RB1, IRF1, ISG20, ITGAM, MARCO, MERTK, TLR2, TLR4, TLR5, TNF, TNFSF10*
JAK-STAT	*STAT1, STAT2, STAT3, STAT5B, STAT6, JAK1, JAK2, JAK3, TYK2, PTPRC, SOCS1*

M1-like monocytes	*CCL2, CCL20, CCL3, CCL4, CCL5, CCL8, CD68, CD86, CXCL10, CXCL11, CXCL9, FAS, IDO1, IFNGR1, IL15, IL15RA, IL1B, IRF1, IRF7, MARCO, PSMB9, PTGS2, TLR2, TLR4, TNF, TNFSF10*
M2-like monocytes	*CCL2, CD163, CD36, CLEC7A, CXCR4, EGR2, FCER1A, IL10, IL13RA1, IL1R2, IL1RAP, IL1RN, IL21R, IL4R, IRF4, MAF, MRC1, MSR1, SOCS1, TLR5, NRP1, IGF1R*
MAPK	*HRAS, DUSP6, MAP2K1, MAP2K2, MAP2K4, MAP3K1, MAP3K5, MAP3K7, MAP4K2, MAPK1, MAPK14, MAPK3, MAPK8, MAPKAPK2*
Monocytes activation	*ADORA2A, CCL2, CCL3, CCL4, CCL5, CD74, CD83, CSF1, CSF1R, CXCL2, IL8, EGR1, FCER2, FCGR1A, FPR2, HLA-DRA, IFNGR1, IL1B, IL2RG, IRF1, LYN, NFKB1, NFKBIA, PTGS2, REL, SERPINB2, TNF, CD4, TNFSF13, SLC11A1*
NFAT pathway Biocarta	*HRAS, MAP2K1, MAPK1, MAPK14, MAPK3, MAPK8, MEF2C, NFATC1, NFATC2, NFATC3, PIK3CG*
NFKB Negative Regulators	*TNFAIP3, NFKBIA, TRAF3*
NFKB Positive Regulators	*BCL10, BTK, CHUK, IKBKB, IKBKE, IKBKG, TBK1, TRAF2, TRAF6*
NFKB Target genes	*BCL2, CCL4, CXCL2, CYBB, ICAM1, IL1B, IL8, NFKBIA, PLAU, PTGS2, TNF, TNFAIP3, TNFSF13B, TRAF2*
NFKB TFs	*NFKB1, NFKB2, RELA, RELB, REL*
NLR-inflammasome	*BCL2, BCL2L1, CASP1, CASP8, FADD, IFI16, MEFV, NLRC5, NLRP3, NOD2, PRKCD, PYCARD, TXNIP*
NOD signaling	*CARD9, CHUK, IKBKB, IKBKE, IKBKG, IRF3, IRF7, MAP3K7, MAVS, NOD1, NOD2, RIPK2, TAB1, TANK, TBK1, TNFAIP3, TRAF2, TRAF3, TRAF6*
Non-Classical monocytes	*ADA, C1QA, C1QB, C2, C3, CD79B, CD97, CSF1R, CTSL, CX3CR1, CXCR4, CYFIP2, FCGR3A, HCK, ICAM2, IFITM1, IFITM2, IL12RB1, IL1B, IL3RA, ITGAL, ITGAX, ITGB2, LILRB1, LILRB2, LTB, LYN, MAF, PIK3CG, PTGDR2, PTPRC, RUNX3, SH2D1B, SLAMF7, SPN, TNF, TNFRSF8*
Notch signaling regulation	*TGFB1, NOTCH1, RUNX1, ETS1, PSEN1, APP, CD46, ITCH, PSEN2*
Notch Target genes	*BCL2, CDKN1A, BATF, NOTCH1, NFKB2*
Nucleotide Metabolism	*ADA, ENTPD1, HPRT1, NT5E, POLR2A*
Phagocytosis	*PIK3CD, PIK3CG, ITGB3, ITGAX, ITGAM, ITGAL, ITGB1, ITGB2, PTPRC, PLA2G6, FCGR1A, CD163, NT5E, SIGLEC1, CD47, CD36, FCGR2A, PECAM1, FCGR2B, FCGR3A, MARCO, CYBB, MAP2K1, MAPK1, MAPK3, HCK, SYK, LYN, ANXA1, FYN, MERTK, FCER1G, PRKCD, SLC11A1, LRP1, AXL*
Proapoptotic	*BAX, BCL10, BID, CASP1, CASP10, CASP3, CASP8, CTSS, FADD, FAS, IFI16, LTBR, MX1, PYCARD, TNFRSF10B, TNFRSF1A, TNFRSF1B, TNFRSF8, TNFSF12, TNFSF15, TP53, TRAF3, ETS1, CD47, MAP3K5, CYLD, CTSH, CTSL*
Proinflammatory	*CCL2, CCL20, CCL3, CCL4, CCL5, CCL8, CCR1, CCR2, CCR5, CD163, CSF1, CSF1R, CSF2RB, CXCL10, CXCL2, IL8, CXCR2, IL15, IL15RA, IL17RA, IL18, IL1B, IL27, IL2RG, IL32, IL3RA, IL6R, IL6ST, LILRA5, MIF, OSM, PTGS2, S100A12, S100A8, TNF, TNFRSF1A, TNFSF4, CXCL9*
Regulation of monocyte activation	*BTK, FYN, IFNGR1, IL4R, LYN, PIK3CD, PIK3CG, SOCS1, TGFB1, TNFAIP3, TOLLIP, IL10RA, SH2B2, AXL, LCN2*
RLR signaling	*DDX58, FADD, IFIH1, IKBKE, IRF3, IRF7, MAVS, TANK, TBK1, TRAF2, TRAF3, TRAF6*
TGFβ signaling	*IGF2R, MAPK1, SMAD2, SMAD3, TFE3, TGFB1, MAP3K7*
TLR signaling	*AKT3, BCL10, CASP8, CD14, CD36, FADD, IKBKE, IRAK1, IRAK2, IRAK4, LY96, MAP3K7, MYD88, PIK3CD, TAB1, TBK1, TICAM1, TICAM2, TIRAP, TLR1, TLR2, TLR4, TLR5, TLR6, TLR7, TLR8, TOLLIP, TRAF3, TRAF6, CD180, LY86, ECSIT*
TNF signaling	*FADD, LTBR, MAP3K5, MAP3K7, PIK3CD, TAB1, TNF, TNFRSF14, TNFRSF1A, TNFRSF1B, TNFSF12, TRAF2, TRAF3*

Transcription and Translation regulation	*ABCF1, APP, ATF2, CNOT10, CNOT4, CREB1, EGR2, EIF2B4, EP300, ERCC3, GTF3C1, IFI27, ILF3, MAPK3, MEF2C, MRPS5, POLR2A, RPS6, YTHDF2, ZNF143, SBNO2, ATF1, BCL6, BMI1, CD3EAP, ELK1, EWSR1, FOS, POU2F2, GPATCH3, HDAC3, SAP130, ZC3H14, DDX50, DHX16, EDC3, FCF1, SF3A3, USP39*
Type1 IFN signaling pathway	*AKT3, IFNAR2, STAT1, STAT2, STAT3, STAT5B, STAT6, JAK1, TYK2, IFNA17, IFNAR1, NFKB1*
Ubiquitin-Proteasome	*PSMB7, PSMB9, PSMB8, PSMB10, PSMD7, UBC, TRIM39*

Table 7 Gene modules designed for monocytes and used in QuSAGE analysis

Module	Genes
Activatory and Co-Stimulatory	*CD160, CD2, CD244, CD247, CD27, CD38, CD44, CD59, CD7, FCER1G, FCGR3A, FYN, IFNAR1, IFNAR2, IL12RB1, IL15RA, IL18R1, IL21R, IL2RA, ITGA4, ITGA5, ITGAL, ITGAM, ITGAX, ITGB1, ITGB2, KLRC2, KLRD1, KLRF1, KLRK1, NCR1, SH2D1A, SLAMF6, SLAMF7, SYK, ZAP70, FCGR2A, LILRA5, CD84, TNFRSF4, LCK, PTPRC, LYN, TNFRSF9, TNFRSF18, TNFRSF14, CD48, ITK, LCP1, LY9, TXK, CD40*
ADCC mimic_up	*BCL2, GPI, IGF2R, CCL3, CCL3L1, CCR7, CD83, CSF2, HLA-DRA, IL21R, IL2RA, IRF4, TNF, TNFRSF9, XCL2*
Adhesion	*ALCAM, CD2, CD53, CD58, CD44, CD9, CX3CR1, ICAM1, ICAM2, ICAM3, ITGA1, ITGA4, ITGA5, ITGA6, ITGAE, ITGAL, ITGAM, ITGAX, ITGB1, ITGB2, SELL, NCAM1, CD63, PVR, CD96, AMICA1, APP, CD6, CD97, CD99, DPP4, LGALS3, PECAM1, SELPLG, THBS1, PLAUR*
Ag presentation and MHC interaction	*HLA-DMB, HLA-DPA1, HLA-DPB1, HLA-DRA, HLA-DRB4, MR1, PSMB7, PSMB9, TAP1, TAP2, TAPBP, HLA-DOB, HLA-A, HLA-B, HLA-C, HLA-DMA, KLRF1, KLRC2, KLRC1, KLRD1, KLRK1, HLA-E, HLA-G, LILRA1, LILRB2, LILRB1, CD74, CTSS, LILRA4, LILRA5, CD1C, CD37, CD1D, MICB, MICA*
Antiapoptotic	*BCL2, BIRC5, CDKN1A, AKT3, TNFRSF1B, HMGB1, HRAS, TNFAIP3, BCL2L1, CHUK, IKBKB, IKBKG, NFKB1, RELA, TRAF2, LGALS3, MIF, FYN, TNFSF11, S100B, ANP32B, IL18R1, IL2RA, IL2RB, IL2RG, IL15RA, CD160*
Anti-inflammatory	*ADORA2A, ANXA1, IDO1, IL10RA, IL11RA, IL13RA1, IL4R, MAF, TGFB1, SBNO2*
Autophagy	*ABL1, ATG10, ATG16L1, ATG5, ATG7, IFI16, S100A8, TOLLIP, TFEB, LAMP1, HMGB1*
Cell cycle and its regulation	*ABL1, BAX, BCL2, BIRC5, CCND3, CDK1, CDKN1A, HRAS, TP53, CEBPB, CREBBP, EP300, ETS1, ILF3, IRF2, MAF, MAPK1, NUP107, PRKCD, S100A8, THBS1, TNFSF10, TTK, INPP5D, S100A12, S100B, NFATC2, PIN1, TFRC, TLK2, ANP32B, CYLD, IGF1R, IL2RA, IL2RB, IL2RG, IL15RA, CD81, IL21R, IL12RB1, IL12RB2, IL18R1, IFNAR1*
Chemotaxis and Migration	*CCR1, CCR2, CCR5, CCR7, CCRL2, CCL3, CCL3L1, CCL4, CCL5, CMKLR1, CX3CR1, IL8, CXCL16, CXCR1, CXCR2, CXCR3, CXCR4, CXCR6, CD81, CD47, CD99, CKLF, FUT7, FYN, PIK3CG, LCK, IL16, LGALS3, PPBP, XCL2IL2RB, IL2RG, IL15RA, CD4, HCK*
CLR signaling	*BCL10, CARD9, CD63, CLEC4A, CLEC4C, FCER1G, IRF5, MRC1, PRKCD, PYCARD, SYK*
Complement	*ITGAX, ITGB2, ITGAM, C1R, THBD, C3AR1, CD46, CD59, C1QBP, CFP*
Cytotoxicity	*CD244, CD84, CTSH, CTSS, CTSW, FCGR3A, GNLY, GZMA, GZMB, GZMH, GZMK, GZMM, IFNAR1, IFNAR2, IFNGR1, KLRC2, KLRK1, LAMP1, LTA, LTB, NCR1, PRF1, SH2D1A, SH2D1B, TNF, TNFSF10, KLRD1, HMGB1, CD8A*
Energy and Metabolism	*AGK, ALAS1, CD36, CD74, G6PD, GPI, MAPK14, MIF, MTMR14, PIK3CD, PIK3CG, PLA2G6, RORA, SDHA*
FcRs	*FCER1A, FCER1G, FCGR2A, FCGR2B, FCGR3A*
Homeostatic proliferation	*IL15RA, IL2RB, IL2RG, CD44, IFNG, ITGAL*
IFN-induced	*BST2, CD74, HLA-A, HLA-B, HLA-C, HLA-E, HLA-G, IFI16, IFI27, IFI35, IFIH1, IFIT1, IFIT2, IFITM1, IFITM2, IFNAR1, IFNAR2, IFNGR1, IKBKE, IRF1, IRF2, IRF3, IRF4, IRF5, IRF7, IRF8, ISG15, ISG20, JAK1, MX1, OAS3, PSMB8, SOCS1, STAT1, STAT2, TNFSF10, TYK2*
IL1-IL18-IL33 signaling	*IL18, IL18R1, IL18RAP, IL1RAP, IL1RL1, IRAK1, IRAK2, IRAK4, MAP3K7, MYD88, SIGIRR, TAB1, TOLLIP, TRAF6, ECSIT*
IL12-IL18 stimulated_up	*AGK, BATF, CCR1, CCR5, CD44, CD97, GZMB, HAVCR2, ICAM1, IFNG, IL12RB2, IL18R1, IL4R, IRF8, ITGA1, NFKB1, NFKBIA, SLAMF7, CCL3,*

	CCL3L1, CCR7, CD83, CSF2, HLA-DRA, IL21R, IL2RA, IRF4, TNF, TNFRSF9, XCL2
IL2-IL7-IL15 signaling	*IL15RA, IL2RG, STAT3, STAT5B, IL2RB, IL7R, JAK1, JAK3, IL15, IL2RA*
Inhibitory	*BTLA, CD244, CD33, CD96, FCGR2B, KIR3DL1, KIR3DL2, KLRB1, KLRC1, KLRD1, KLRG1, LILRB1, LILRB2, TIGIT, CD81, HAVCR2, LAG3, PDGFRB, ITK*
JAK-STAT	*STAT1, STAT2, STAT3, STAT5B, STAT4, STAT6, JAK1, JAK2, JAK3, TYK2, PTPRC, SOCS1*
K562-ADCC-CK common activation_up	*CCL3, CCL3L1, CCR7, CD83, CSF2, HLA-DRA, IL21R, IL2RA, IRF4, TNF, TNFRSF9, XCL2*
K562 direct recognition_up	*CD86, CDK1, FOS, GAGE1, TNFRSF9, TNFSF14, CCL3, CCL3L1, CCR7, CD83, CSF2, HLA-DRA, IL21R, IL2RA, IRF4, TNF, XCL2*
MAPK	*HRAS, DUSP4, DUSP6, MAP2K1, MAP2K2, MAP2K4, MAP3K1, MAP3K5, MAP3K7, MAP4K2, MAPK1, MAPK14, MAPK3, MAPK8, MAPKAPK2*
Memory-like NK	*CD2, FCGR3A, IFNG, IL2RA, KLRC1, KLRC2, KLRD1, KLRG1, LILRB1, NCR1, SPN*
NFAT pathway Biocarta	*CREBBP, HRAS, MAP2K1, MAPK1, MAPK14, MAPK3, MAPK8, MEF2C, NFATC1, NFATC2, NFATC3, PIK3CG*
NFAT TFs	*NFATC1, NFATC2, NFATC3*
NFKB Negative Regulators	*TNFAIP3, NFKBIA, TRAF3*
NFKB Positive Regulators	*BCL10, BTK, CHUK, IKBKB, IKBKE, IKBKG, TBK1, TRAF2, TRAF6, CARD11*
NFKB Target genes	*BCL2, CCL4, CYBB, ICAM1, IL8, NFKBIA, TNF, TNFAIP3, TNFSF13B, TRAF2*
NFKB TFs	*NFKB1, NFKB2, RELA, RELB, REL*
NK CD56bright	*CCR5, CCR7, CD2, CD44, CD59, CD74, CXCR3, CXCR4, GNLY, GZMK, HLA-DMA, HLA-DMB, HLA-DPA1, HLA-DRA, ICAM1, ICAM3, IFNG, IL18, IL18R1, IL2RA, IL2RB, IL2RG, IL7R, IRF4, ITGA5, ITGAM, ITGAX, KIT, KLRB1, KLRC1, KLRC2, KLRD1, LTB, NCR1, NOTCH1, SELL, TCF7, TGFB1, TNF, TNFSF10, NCAM1, IL12RB1, IL12RB2, FLT3LG, PLA2G6*
NK CD56dim	*BATF, CCL3, CCL4, CCL5, CD160, CD244, CD247, CD53, CD58, CD6, CMKLR1, CX3CR1, CXCR1, CXCR2, FCGR3A, GTF3C1, GZMA, GZMB, GZMM, ICAM2, IFI16, IGF1R, IGF2R, IL21R, ITGAE, ITGAL, KIR3DL1, KIR3DL2, KLRC2, KLRD1, KLRG1, LAIR2, LILRB1, MAF, MAP3K7, MEF2C, PRF1, SELPLG, TNFRSF1B, IL8, PECAM1*
NK cell activation	*CASP8, CD2, CD244, CD44, CD53, CD59, CD63, CD70, CD81, CD86, CD9, DPP4, FCER1G, GZMA, GZMB, GZMK, HAVCR2, HLA-DRA, IFITM1, IFNG, IL15, IL18, IL18R1, IL21R, IL2RA, IL2RB, ITGB2, KLRC2, KLRG1, KLRK1, LAMP1, NCR1, PIK3CD, SELL, SLAMF6, SLAMF7, STAT5B, TNF, TNFSF14, TNFSF4, SPN, TNFSF4, RUNX3*
NLR-inflammasome	*BCL2, BCL2L1, CASP1, CASP8, IFI16, NLRC5, NLRP3, NOD2, PRKCD, PYCARD*
NOD signaling	*CARD9, CHUK, IKBKB, IKBKE, IKBKG, IRF3, IRF7, MAP3K7, MAVS, NOD1, NOD2, RIPK2, TAB1, TANK, TBK1, TNFAIP3, TRAF2, TRAF3, TRAF6*
Notch signaling and regulation	*TGFB1, NOTCH1, RUNX1, ETS1, PSEN1, APP, CD46, ITCH, PSEN2*
Notch Target genes	*BCL2, CDKN1A, BATF, IL7R, IL2RA, NOTCH1, TCF7, TBX21, NFKB2*
Nucleotide Metabolism	*ADA, ENTPD1, HPRT1, NT5E, POLR2A, BST1, CD38*
Proapoptotic	*BAX, BCL10, CASP1, CASP3, CASP8, FAS, TNFRSF1A, TNFRSF1B, TP53, CD2, CD27, CTSH, CTSW, CTSS, IFI16, MX1, PYCARD, TNFRSF9, TNFSF12, TRAF3, ETS1, MAP3K5, CYLD, CYFIP2*
Proinflammatory	*CCL3, CCL4, CCL5, CCR1, CCR2, CCR5, CSF2, IL8, CXCR2, HMGB1, IFNG, IL15, IL15RA, IL17RA, IL18, IL2RA, IL2RB, IL2RG, IL32, IL3RA,*

	IL6R, IL6ST, LILRA5, LTA, MIF, OSM, S100A12, S100A8, TNF, TNFRSF11A, TNFRSF1A, TNFSF4, TNFSF8
Resting vs IL2-IL12-IL15-stim NK cell_up	*CCL4, NFATC1, PIN1*
RLR signaling	*DDX58, IFIH1, IKBKE, IRF3, IRF7, MAVS, TANK, TBK1, TRAF2, TRAF3, TRAF6*
TGFβ signaling	*IGF2R, MAPK1, SMAD2, SMAD3, TGFB1, MAP3K7*
TLR signaling	*AKT3, BCL10, CASP8, CD14, CD36, IKBKE, IRAK1, IRAK2, IRAK4, MAP3K7, MYD88, PIK3CD, TAB1, TBK1, TICAM1, TIRAP, TLR1, TLR10, TLR3, TLR6, TOLLIP, TRAF3, TRAF6, CD180, LY86, ECSIT*
TNF signaling	*LTA, MAP3K5, MAP3K7, PIK3CD, TAB1, TNF, TNFRSF14, TNFRSF1A, TNFRSF1B, TNFSF12, TRAF2, TRAF3*
Transcription and Translation regulation	*ABCF1, APP, ATF2, CNOT10, CNOT4, CREB1, CREBBP, EIF2B4, EOMES, EP300, ERCC3, GTF3C1, IFI27, ILF3, MAPK3, MEF2C, MRPS5, POLR2A, RPS6, TBP, YTHDF2, ZNF143, SBNO2, ATF1, BCL6, BMI1, CD3EAP, ELK1, EWSR1, FOS, POU2F2, GPATCH3, HDAC3, SAP130, ZC3H14, DDX50, DHX16, EDC3, FCF1, SF3A3, USP39*
Type1 IFN signaling pathway	*AKT3, IFNAR2, STAT1, STAT2, STAT3, STAT5B, STAT4, STAT6, JAK1, TYK2, IFNAR1, NFKB1*
Ubiquitin-Proteasome	*PSMB7, PSMB9, PSMB8, PSMB10, PSMD7, UBC, TRIM39*

Table 8 Gene modules designed for NK cells and used in QuSAGE analysis

List of Abbreviations

ADCC	antibody-dependent cell-mediated cytotoxicity
ALL	acute lymphoblastic leukemia
AML	acute myeloid leukemia
APC	antigen presenting cell
ATG	anti-thymocyte globulin
BM	bone marrow
BMT	bone marrow transplantation
CB	cord blood
CCL	C-C motif ligand
CCR7	C-C chemokine receptor type 7
CD	cluster of differentiation
CML	chronic myeloid leukemia
CMV	cytomegalovirus
CSA	cyclosporine A
CTL	cytotoxic T lymphocyte
CTLA4	anti-cytotoxic T-lymphocyte-associated antigen 4
CXCL	CXC ligand
CXCR4	CX chemokine receptor 4
Cy	cyclophosphamide
DAMP	damage-associated molecular pattern
DAPI	4′,6-diamidino-2-phenylindole
DC	dendritic cell
DLA	dog leukocyte antigen
DLI	donor lymphocyte infusion
DMSO	dimethyl sulfoxide
DNA	Deoxyribonucleic acid
EBMT	European Bone Marrow Transplant
FACS	fluorescence-activated cell sorting
FasL	Fas ligand
FCS	fetal calf serum
FDR	false discovery fate
FMO	fluorescence minus one
FOV	fields of view
Foxp3	Forkhead box P3
G6PD	glucose-6-phosphate dehydrogenase
GAPDH	glyceraldehyde 3-phosphate dehydrogenase
G-CSF	granulocyte colony-stimulating factor
GH	growth hormone

GI	gastrointestinal
GO	Gene Ontology
GPI	glucose-6-phosphate isomerase
GSEA	Gene Set Enrichment Analysis
GVHD	graft-versus-host disease
GVL	graft-versus-leukemia
GVT	graft-versus-tumour
HGF	hepatocyte growth factor
HLA	human leukocyte antigen
HPE	homeostatic peripheral expansion
HSC	hematopoietic stem cell
HSCT	hematopoietic stem cell transplantation
ICOS	Inducible-Costimulator
IFN	interferon
Ig	immunoglobulin
IGF2	insulin-like growth factor 2
IL	interleukin
IL2Rα	IL2 receptor alpha chain
IL2Rβ	IL2 receptor beta chain
IL2Rγ	IL2 receptor common γ chain
JAK	Janus kinase
KEGG	Kyoto Encyclopedia of Genes and Genomes
KGF	keratinocyte growth factor
KIR	killer-cell immunoglobulin-like receptor
LPS	lipopolysaccharide
MAC	myeloablative conditioning
Mb	megabases
mDC	myeloid dendritic cell
mHA	minor histocompatibility antigen
MHC	major histocompatibility complex
MIF	macrophage migratory inhibitory factor
miR	micro RNA
MMF	mycophenolate mofetil
mRNA	messenger ribonucleic acids
mSigDB	molecular Signatures Database
MTX	methotrexate
NCAM	Neural Cell adhesion Molecule
NF-κB	nuclear factor kappa-light-chain-enhancer of activated B cells
NHP	non-human primate
NK	natural killer
NMA	non-myeloablative

NO	nitride oxide
NOD2	nucleotide-binding oligomerization domain-containing 2
NSG	NOD-scid gamma
OXPHOS	oxidative phosphorylation
PAMP	pathogen-associated molecular pattern
PBMC	peripheral blood mononuclear cell
PBS	Phosphate Buffer Saline
PBSC	peripheral blood mobilized stem cell
PCA	Principal Component Analysis
PCR	polymerase chain reaction
PD1	programmed cell death 1
pDC	plasmocytoid dendritic cell
PDL1	programmed cell death ligand 1
PFA	paraformaldehyde
PSGL1	P-selectin ligand 1
QuSAGE	Quantitative Set Analysis of Gene expression
REGα	regeneration islet-derived 3α
RIC	reduced intensity conditioning
RIN	RNA integrity number
rpm	revolutions per minute
RPMI	Roswell Park Memorial Institute
S1P	sphingosine-1-phosphate
S1PR1	sphingosine-1-phosphate receptor 1
SCFA	short chain fatty acid
SCID	severe combined immunodeficiency
SD	standard deviation
SDF-1	stromal derived factor-1
SDHA	succinate dehydrogenase complex flavoprotein subunit A
SELL	L-selectin
SNP	single nucleotide polymorphism
SR	steroid-refractory
TBI	total body irradiation
T_{CM}	central memory T cell
TCR	T cell receptor
T_{EFF}	effector T cell
T_{EM}	effector memory T cell
TGFβ	transforming growth factor β
Tim-3	T cell immunoglobulin mucin 3
TLR	Toll-like receptor
T_N	naive T cell

TNF	tumour necrosis factor
TNFR1	tumour necrosis factor receptor 1
TNFα	tumour necrosis factor-alpha
TRAIL	TNF-related apoptosis-inducing ligand
TREC	T cell receptor rearrangement excision DNA circles
Treg	regulatory T cell
TRM	transplant-related mortality
T_{SCM}	T stem cell memory
TWEAK	TNF-like weak inducer of apoptosis
UPS	ubiquitin-proteasome system

List of figures

List of tables

References

Afzali, B., Lombardi, G., and Lechler, R.I. (2008). Pathways of major histocompatibility complex allorecognition. Curr. Opin. Organ Transplant. *13*, 438–444.

Alho, A.C., Kim, H.T., Chammas, M.J., Reynolds, C.G., Matos, T.R., Forcade, E., Whangbo, J., Nikiforow, S., Cutler, C.S., Koreth, J., et al. (2016). Unbalanced recovery of regulatory and effector T cells after allogeneic stem cell transplantation contributes to chronic GVHD. Blood *127*, 646–657.

Anasetti, C. (2008). What are the most important donor and recipient factors affecting the outcome of related and unrelated allogeneic transplantation? Best Pract. Res. Clin. Haematol. *21*, 691–697.

Antin, J.H., and Ferrara, J.L. (1992). Cytokine dysregulation and acute graft-versus-host disease. Blood *80*, 2964–2968.

Aoki, M., Aoki, H., Ramanathan, R., Hait, N.C., and Takabe, K. (2016). Sphingosine-1-Phosphate Signaling in Immune Cells and Inflammation: Roles and Therapeutic Potential. Mediators Inflamm. *2016*.

Appelbaum, F.R. (2003). The Current Status of Hematopoietic Cell Transplantation. Annu. Rev. Med. *54*, 491–512.

Appelbaum, F.R. (2007). Hematopoietic-Cell Transplantation at 50. N. Engl. J. Med. *375*, 1472–1475.

Arai, S., Arora, M., Wang, T., Spellman, S.R., He, W., Couriel, D.R., Urbano-Ispizua, A., Cutler, C.S., Bacigalupo, A.A., Battiwalla, M., et al. (2015). Increasing Incidence of Chronic Graft-versus-Host Disease in Allogeneic Transplantation: A Report from the Center for International Blood and Marrow Transplant Research. Biol. Blood Marrow Transplant. *21*, 266–274.

Arbore, G., and Kemper, C. (2016). A novel "complement–metabolism–inflammasome axis" as a key regulator of immune cell effector function. Eur. J. Immunol. *46*, 1563–1573.

Arbore, G., West, E.E., Spolski, R., Robertson, A.A.B., Klos, A., Rheinheimer, C., Dutow, P., Woodruff, T.M., Yu, Z.X., O'Neill, L.A., et al. (2016). T helper 1 immunity requires complement-driven NLRP3 inflammasome activity in CD4+ T cells. Science (80-.). *352*.

Asano, T., Meguri, Y., Yoshioka, T., Kishi, Y., Iwamoto, M., Nakamura, M., Sando, Y., Yagita, H., Koreth, J., Kim, H.T., et al. (2017). PD-1 modulates regulatory T cell homeostasis during low-dose IL-2 therapy. Blood *129*, 2186–2197.

Bacher, M., Metz, C.N., Calandra, T., Mayer, K., Chesney, J., Lohoff, M., Gemsa, D., Donnelly, T., and Bucala, R. (1996). An essential regulatory role for macrophage migration inhibitory factor in T-cell activation. Proc. Natl. Acad. Sci. U. S. A. *93*, 7849–7854.

Bacigalupo, A., Ballen, K., Rizzo, D., Giralt, S., Lazarus, H., Ho, V., Apperley, J., Slavin, S., Pasquini, M., Sandmaier, B.M., et al. (2009). Defining the Intensity of Conditioning Regimens: Working Definitions. Biol. Blood Marrow Transplant. *15*, 1628–1633.

Ballen, K.K., Gluckman, E., and Broxmeyer, H.E. (2013). Umbilical cord blood transplantation : the first

25 years and beyond. Blood *122*, 491–498.

Banchereau, R., Hong, S., Cantarel, B., Baldwin, N., Baisch, J., Edens, M., Cepika, A.M., Acs, P., Turner, J., Anguiano, E., et al. (2016). Personalized Immunomonitoring Uncovers Molecular Networks that Stratify Lupus Patients. Cell *165*, 551–565.

Barnes, D.W., and Loutit, J.F. (1954). What is the recovery factor in spleen? Nucleonics *12*, 68–71.

Barnes, D.W., and Loutit, J.F. (1957). Treatment of murine leukaemia with x-rays and homologous bone marrow: II. Br. J. Haematol. *3*, 241–252.

Barnes, D.W., Corp, M.J., Loutit, J.F., and Neal, F.E. (1956). Treatment of Murine Leukaemia With X Rays and Homologous bone marrow. Preliminary communication. Br. Med. J. *2*, 626–627.

Baron, C., Somogyi, R., Greller, L.D., Rineau, V., Wilkinson, P., Cho, C.R., Cameron, M.J., Kelvin, D.J., Chagnon, P., Roy, D.C., et al. (2007). Prediction of Graft-versus-host disease in humans by donor gene-expression profiling. PLoS Med. *4*, 0069–0083.

Baron, F., Storer, B., Maris, M.B., Storek, J., Piette, F., Metcalf, M., White, K., Sandmaier, B.M., Maloney, D.G., Storb, R., et al. (2006). Unrelated Donor Status and High Donor Age Independently Affect Immunologic Recovery after Nonmyeloablative Conditioning. Biol. Blood Marrow Transplant. *12*, 1176–1187.

Van Bekkum, D.W., Vos, O., and Weyzen, W.W. (1959). The pathogenesis of the secondary disease following foreign bone marrow transplantation in irradiated mice. Bull. Soc. Int. Chir. *18*, 302–314.

Van Bekkum, D.W., Roodenburg, J., Heidt, P.J., and van der Waaij, D. (1974). Mitigation of secondary disease of allogeneic mouse radiation chimeras by modification of the intestinal microflora. J. Natl. Cancer Inst. *52*, 401–404.

Bender, J., Mitchell, T., Kappler, J., and Marrack, P. (1999). CD4+ T cell division in irradiated mice requires peptides distinct from those responsible for thymic selection. J. Exp. Med. *190*, 367–374.

Benjamin, J.E., Gill, S., and Negrin, R.S. (2010). Biology and clinical effects of natural killer cells in allogeneic transplantation. Curr. Opin. Oncol. *22*, 130–137.

Benjamini, Y., and Hochberg, Y. (1995). Controlling the False Discovery Rate: A Practical and Powerful Approach to Multiple Testing. J. R. Stat. Soc. Ser. B *57*, 289–300.

Beres, A.J., and Drobyski, W.R. (2013). The role of regulatory T cells in the biology of graft versus host disease. Front. Immunol. *4*, 1–9.

Berhanu, D., Mortari, F., De Rosa, S.C., and Roederer, M. (2003). Optimized lymphocyte isolation methods for analysis of chemokine receptor expression. J. Immunol. Methods *279*, 199–207.

Bethge, W.A., Hegenbart, U., Stuart, M.J., Storer, B.E., Maris, M.B., Flowers, M.E.D., Maloney, D.G., Chauncey, T., Bruno, B., Agura, E., et al. (2004). Adoptive immunotherapy with donor lymphocyte infusions after allogeneic hematopoietic cell transplantation following nonmyeloablative conditioning.

103, 790–795.

Billingham, R.E. (1966). The biology of graft-versus-host reactions. Harvey Lect. *62*, 21–78.

Billingham, R.E., and Brent, L. (1959). Quantitative studies on tissue transplantation immunity. IV. Induction of tolerance in newborn mice and studies on the phenomenon of runt disese. Philos. Trans. R. Soc. B Biol. Sci. *242*, 439–477.

Björkström, N.K., Ljunggren, H.-G., and Sandberg, J.K. (2010). CD56 negative NK cells: origin, function, and role in chronic viral disease. Trends Immunol. *31*, 401–406.

Blazar, B.R., Murphy, W.J., and Abedi, M. (2012). Advances in graft-versus-host disease biology and therapy. Nat. Rev. Immunol. *12*, 443–458.

Bleakley, M., and Riddell, S.R. (2004). Molecules and mechanisms of the graft-versus-leukaemia effect. Nat. Rev. Cancer *4*, 371–380.

Bleakley, M., Heimfeld, S., Loeb, K.R., Jones, L. a, Chaney, C., Seropian, S., Gooley, T. a, Sommermeyer, F., Riddell, S.R., and Shlomchik, W.D. (2015). Outcomes of acute leukemia patients transplanted with naive T cell – depleted stem cell grafts. J. Clin. Invest. *125*, 1–13.

De Bock, M., Fillet, M., Hannon, M., Seidel, L., Merville, M.P., Gothot, A., Beguin, Y., and Baron, F. (2013). Kinetics of IL-7 and IL-15 Levels after Allogeneic Peripheral Blood Stem Cell Transplantation following Nonmyeloablative Conditioning. PLoS One *8*, 1–9.

Bonneville, M., O'Brien, R.L., and Born, W.K. (2010). γδ T cell effector functions: A blend of innate programming and acquired plasticity. Nat. Rev. Immunol. *10*, 467–478.

Bortin, M.M. (1970). A compendium of reported human bone marrow transplants. Transplantation *9*, 571–587.

Boyman, O., Létourneau, S., Krieg, C., and Sprent, J. (2009). Homeostatic proliferation and survival of naïve and memory T cells. Eur. J. Immunol. *39*, 2088–2094.

Van Den Brink, M.R.M., and Burakoff, S.J. (2002). Cytolytic pathways in haematopoietic stem-cell transplantation. Nat. Rev. Immunol. *2*, 273–281.

Van Den Brink, M.R., Leen, A.M., Baird, K., Merchant, M., Mackall, C., and Bollard, C.M. (2013). Enhancing Immune Reconstitution: From Bench to Bedside. Biol. Blood Marrow Transplant. *19*, S79–S83.

Van Den Brink, M.R.M., Alpdogan, Ö., and Boyd, R.L. (2004). Strategies to enhance T-cell reconstitution in immunocompromised patients. Nat. Rev. Immunol. *4*, 856–867.

Van Den Brink, M.R.M., Velardi, E., and Perales, M.-A. (2015). Immune reconstitution following stem cell transplantation. Hematol. Am Soc Hematol Educ Program. 215–219.

Brinkmann, V., Billich, A., Baumruker, T., Heining, P., Schmouder, R., Francis, G., Aradhye, S., and Burtin, P. (2010). Fingolimod (FTY720): Discovery and development of an oral drug to treat multiple

sclerosis. Nat. Rev. Drug Discov. *9*, 883–897.

Bruggner, R. V, Bodenmiller, B., Dill, D.L., Tibshirani, R.J., and Nolan, G.P. (2014). Automated identification of stratifying signatures in cellular subpopulations. Proc. Natl. Acad. Sci. U. S. A. *111*, E2770-7.

Burlion, A., Brunel, S., Petit, N.Y., Olive, D., and Marodon, G. (2017). Targeting the human T-Cell Inducible COStimulator molecule with a monoclonal antibody prevents graft-vs-host disease and preserves graft vs leukemia in a xenograft murine model. Front. Immunol. *8*.

Buzzeo, M.P., Yang, J., Casella, G., and Reddy, V. (2008). A preliminary gene expression profile of acute graft-versus-host disease. Cell Transpl. *17*, 489–494.

Calandra, T., Bernhagen, J., Mitchell, R.A., and Bucala, R. (1994). The Macrophage Is an Important and Previously Unrecognized Source of Macrophage Migration Inhibitory Factor. J. Exp. Med. *179*, 1895–1902.

Calandra, T., Bernhagen, J., Metz, C.N., Spiegel, L.A., Bacher, M., Donnelly, T., Cerami, A., and Bucala, R. (1995). MIF as a glucocorticoid-induced modulator of cytokine production. Nature *377*, 68–71.

Carli, C., Giroux, M., and Delisle, J.S. (2012). Roles of Transforming Growth Factor-β in Graft-versus-Host and Graft-versus-Tumor Effects. Biol. Blood Marrow Transplant. *18*, 1329–1340.

Carson, W.E., Giri, J.G., Lindemann, M.J., Linett, M.L., Ahdieh, M., Paxton, R., Anderson, D., Eisenmann, J., Grabstein, K., and Caligiuri, M. a (1994). Interleukln (IL) 15 Is a Novel Cytoklne That Activates Human Natural Killer Cells via Components of the IL-2 Receptor. J. Exp. Med. *180*.

Carson, W.E., Fehniger, T.A., Haldar, S., Eckhert, K., Lindemann, M.J., Lai, C.F., Croce, C.M., Baumann, H., and Caligiuri, M.A. (1997). A potential role for interleukin-15 in the regulation of human natural killer cell survival. J. Clin. Invest. *99*, 937–943.

Castor, M.G.M., Pinho, V., and Teixeira, M.M. (2012). The role of chemokines in mediating graft versus host disease: Opportunities for novel therapeutics. Front. Pharmacol. *3*.

Champlin, R. (2003). Selection of Autologous or Allogeneic Transplantation. In Holland-Frei Cancer Medicine. 6th Edition., B. Decker, ed. p.

Chan, A., Hong, D.-L., Atzberger, A., Kollnberger, S., Filer, A.D., Buckley, C.D., McMichael, A., Enver, T., and Bowness, P. (2007). CD56bright Human NK Cells Differentiate into CD56dim Cells: Role of Contact with Peripheral Fibroblasts. J. Immunol. *179*, 89–94.

Chan, G., Bivins-Smith, E.R., Smith, M.S., Smith, P.M., and Yurochko, A.D. (2008). Transcriptome Analysis Reveals Human Cytomegalovirus Reprograms Monocyte Differentiation toward an M1 Macrophage. J. Immunol. *181*, 698–711.

Chan, Y.L.T., Zuo, J., Inman, C., Croft, W., Begum, J., Croudace, J., Kinsella, F., Maggs, L., Nagra, S., Nunnick, J., et al. (2018). NK cells produce high levels of IL-10 early after allogeneic stem cell

transplantation and suppress development of acute GVHD. Eur. J. Immunol. *48*, 316–329.

Chang, C., Curtis, J.D., Maggi, L.B., Faubert, B., Villarino, A. V, Sullivan, D.O., Huang, S.C., Windt, G.J.W. Van Der, Blagih, J., Qiu, J., et al. (2013). Posttranscriptional Control of T Cell Effector Function by Aerobic Glycolysis. Cell *153*, 1239–1251.

Chang, Y.J., Zhao, X.Y., Huo, M.R., and Huang, X.J. (2009). Expression of CD62L on donor CD4+ T cells in allografts: Correlation with graft-versus-host disease after unmanipulated allogeneic blood and marrow transplantation. J. Clin. Immunol. *29*, 696–704.

Chaudhry, M.S., Velardi, E., Malard, F., and van den Brink, M.R.M. (2017). Immune Reconstitution after Allogeneic Hematopoietic Stem Cell Transplantation: Time To T Up the Thymus. J. Immunol. *198*, 40–46.

Chen, Z.J. (2005). Ubiquitin signalling in the NF-kB pathway. Nat. Cell Biol. *7*, 758–765.

Chen, L., and Flies, D.B. (2013). Molecular mechanisms of T cell co-stimulation and co-inhibition. Nat. Rev. Immunol. *13*, 227–242.

Chen, B.J., Deoliveira, D., Cui, X., Le, N.T., Son, J., Whitesides, J.F., Chao, N.J., and Dc, W. (2007). Inability of memory T cells to induce graft-versus-host disease is a result of an abortive alloresponse. Blood *109*, 3115–3123.

Cheng, Q., Ma, S., Lin, D., Mei, Y., Gong, H., Lei, L., Chen, Y., Zhao, Y., Hu, B., Wu, Y., et al. (2015). The S1P 1 receptor-selective agonist CYM-5442 reduces the severity of acute GVHD by inhibiting macrophage recruitment. Cell. Mol. Immunol. *12*, 681–691.

Chérel, M., Choufi, B., Trauet, J., Cracco, P., Dessaint, J.P., Yakoub-Agha, I., and Labalette, M. (2014). Naive subset develops the most important alloreactive response among human CD4+ T lymphocytes in Human Leukocyte Antigen-identical related setting. Eur. J. Haematol. *92*, 491–496.

Chi, H. (2011). Sphingosine-1-phosphate and immune regulation: Trafficking and beyond. Trends Pharmacol. Sci. *32*, 16–24.

Chiesa, M. Della, Falco, M., Podesta, M., Locatelli, F., Moretta, L., Frassoni, F., and Moretta, A. (2012). Phenotypic and functional heterogeneity of human NK cells developing after umbilical cord blood transplantation : a role for human cytomegalovirus ? Blood *119*, 399–410.

Chklovskaia, E., Nowbakht, P., Nissen, C., Gratwohl, A., Bargetzi, M., and Wodnar-filipowicz, A. (2004). Reconstitution of dendritic and natural killer – cell subsets after allogeneic stem cell transplantation : effects of endogenous flt3 ligand. *103*, 3860–3868.

Cho, O.H., Shin, H.M., Miele, L., Golde, T.E., Fauq, A., Minter, L.M., and Osborne, B.A. (2009). Notch Regulates Cytolytic Effector Function in CD8+ T Cells. J. Immunol. *182*, 3380–3389.

Choi, S.W., Levine, J.E., and Ferrara, J.L.M. (2010). Pathogenesis and Management of Graft versus Host Disease. Immunolo Allergy Clin North Am *30*, 75–101.

Coghill, J.M., Sarantopoulos, S., Moran, T.P., Murphy, W.J., Blazar, B.R., and Serody, J.S. (2011). Effector CD4+ T cells, the cytokines they generate, and graft-versus-host disease: something old and something new. Blood *117*, 3268–3276.

Colonna, M., Trinchieri, G., and Liu, Y.J. (2004). Plasmacytoid dendritic cells in immunity. Nat. Immunol. *5*, 1219–1226.

Cooper, M.A., Fehniger, T.A., and Caligiuri, M.A. (2001a). The biology of human natural killer-cell subsets. Trends Immunol. *22*, 633–640.

Cooper, M.A., Fehniger, T.A., Turner, S.C., Chen, K.S., Ghaheri, B.A., Ghayur, T., Carson, W.E., and Caligiuri, M.A. (2001b). Human natural killer cells : a unique innate immunoregulatory role for the CD56 bright subset. Blood *97*, 3146–3151.

Copelan, E.A. (2006). Hematopoietic Stem-Cell Transplantation. N. Engl. J. Med. *354*, 1813–1826.

Cosmi, L., Annunziato, F., Iwasaki, M., Galli, G., Manetti, R., Maggi, E., Nagata, K., and Romagnani, S. (2000). CRTH2 is the most reliable marker for the detection of circulating human type 2 Th and type 2 T cytotoxic cells in health and disease. Eur. J. Immunol. *30*, 2972–2979.

Costanzo, M.C., Kim, D., Creegan, M., Lal, K.G., Ake, J.A., Currier, J.R., Streeck, H., Robb, M.L., Michael, N.L., Bolton, D.L., et al. (2018). Transcriptomic signatures of NK cells suggest impaired responsiveness in HIV-1 infection and increased activity post-vaccination. Nat. Commun. *9*, 1–16.

Craig, F.E., and Foon, K.A. (2008). Flow cytometric immunophenotyping for hematologic neoplasms. Blood *111*, 3941–3967.

Crawford, A., Angelosanto, J.M., Kao, C., Doering, T.A., Odorizzi, P.M., Barnett, B.E., and Wherry, E.J. (2014). Molecular and Transcriptional Basis of CD4+ T Cell Dysfunction during Chronic Infection. Immunity *40*, 289–302.

Cros, J., Cagnard, N., Woollard, K., Patey, N., Zhang, S.Y., Senechal, B., Puel, A., Biswas, S.K., Moshous, D., Picard, C., et al. (2010). Human CD14dim Monocytes Patrol and Sense Nucleic Acids and Viruses via TLR7 and TLR8 Receptors. Immunity *33*, 375–386.

Crotty, S. (2011). Follicular Helper CD4 T Cells (TFH). Annu. Rev. Immunol. *29*, 621–663.

D'Souza, A., and Fretham, C. (2017). Current Uses and Outcomes of Hematopoietic Cell Transplantation (HCT): CIBMTR Summary Slides.

Dahl, C.A., Schall, R.P., He, H.L., and Cairns, J.S. (1992). Identification of a novel gene expressed in activated natural killer cells and T cells. J. Immunol. *148*, 597–603.

Dai, Z., and Lakkis, F.G. (2001). Cutting Edge: Secondary Lymphoid Organs Are Essential for Maintaining the CD4, But Not CD8, Naive T Cell Pool. J. Immunol. *167*, 6711–6715.

Dickinson, A.M., and Charron, D. (2005). Non-HLA immunogenetics in hematopoietic stem cell transplantation. Curr. Opin. Immunol. *17*, 517–525.

Dickinson, A.M., Norden, J., Li, S., Hromadnikova, I., Schmid, C., and Dickinson, A.M. (2017). Graft-versus-Leukemia effect Following Hematopoietic Stem Cell Transplantation for Leukemia. Front. Immunol. *8*.

Distler, E., Bloetz, A., Albrecht, J., Asdufan, S., Hohberger, A., Frey, M., Schnürer, E., Thomas, S., Theobald, M., Hartwig, U.F., et al. (2011). Alloreactive and leukemia-reactive T cells are preferentially derived from naïve precursors in healthy donors: Implications for immunotherapy with memory T cells. Haematologica *96*, 1024–1032.

Dolstra, H., Fredrix, H., Van Der Meer, A., De Witte, T., Figdor, C., and Van De Wiel-Van Kemenade, E. (2001). TCR γδ cytotoxic T lymphocytes expressing the killer cell-inhibitory receptor p58.2 (CD158b) selectively lyse acute myeloid leukemia cells. Bone Marrow Transplant. *27*, 1087–1093.

Dong, S., Maiella, S., Xhaard, A., Pang, Y., Wenandy, L., Larghero, J., Becavin, C., Benecke, A., Bianchi, E., Socié, G., et al. (2013). Multiparameter single-cell profiling of human CD4+FOXP3+ regulatory T-cell populations in homeostatic conditions and during graft-versus-host disease. Blood *122*, 1802–1812.

Döring, M., Cabanillas Stanchi, K.M., Haufe, S., Erbacher, A., Bader, P., Handgretinger, R., Hofbeck, M., and Kerst, G. (2015). Patterns of monocyte subpopulations and their surface expression of HLA-DR during adverse events after hematopoietic stem cell transplantation. Ann. Hematol. *94*, 825–836.

Doulatov, S., Notta, F., Laurenti, E., and Dick, J.E. (2012). Hematopoiesis: A human perspective. Cell Stem Cell *10*, 120–136.

Dulphy, N., Haas, P., Busson, M., Belhadj, S., Peffault de Latour, R., Robin, M., Carmagnat, M., Loiseau, P., Tamouza, R., Scieux, C., et al. (2008). An Unusual CD56bright CD16low NK Cell Subset Dominates the Early Posttransplant Period following HLA-Matched Hematopoietic Stem Cell Transplantation. J. Immunol. *181*, 2227–2237.

Dutt, S., Tseng, D., Ermann, J., George, T.I., Liu, Y.P., Davis, C.R., Fathman, C.G., and Strober, S. (2007). Naive and Memory T Cells Induce Different Types of Graft-versus-Host Disease. J. Immunol. *179*, 6547–6554.

Dutta, B., Wallqvist, A., and Reifman, J. (2012). PathNet: A tool for pathway analysis using topological information. Source Code Biol. Med. *7*, 1–12.

Duval, F., Mathieu, M., and Labrecque, N. (2015). Notch controls effector CD8+ T cell differentiation. Oncotarget *6*, 21787–21788.

Edinger, M., Hoffmann, P., Ermann, J., Drago, K., Garrison Fathman, C., Strober, S., and Negrin, R.S. (2003). CD4+CD25+ regulatory T cells preserve graft-versus-tumor activity while inhibiting graft-versus-host disease after bone marrow transplantation. Nat. Med. *9*, 1144–1150.

Erlich, H.A., Opelz, G., and Hansen, J. (2001). HLA DNA typing and transplantation. Immunity *14*, 347–356.

Ernst, B., Lee, D.S., Chang, J.M., Sprent, J., and Surh, C.D. (1999). The peptide ligands mediating positive selection in the thymus control T cell survival and homeostatic proliferation in the periphery. Immunity *11*, 173–181.

Falkenburg, J.H.F., and Warren, E.H. (2011). Graft versus Leukemia Reactivity after Allogeneic Stem Cell Transplantation. Biol. Blood Marrow Transplant. *17*, S33–S38.

Ferrara, J.L., and Reddy, P. (2006). Pathophysiology of graft-versus-host disease. Semin. Hematol. *43*, 3–10.

Ferrara, J.L., Levine, J.E., Reddy, P., and Holler, E. (2009). Graft-versus-host disease. Lancet *373*, 1550–1561.

Ferreira, C., Barthlott, T., Garcia, S., Zamoyska, R., and Stockinger, B. (2000). Differential Survival of Naive CD4 and CD8 T Cells. J. Immunol. *165*, 3689–3694.

Foley, B., Cooley, S., Verneris, M.R., Pitt, M., Curtsinger, J., Luo, X., Lanier, L.L., Weisdorf, D., Miller, J.S., Dc, W., et al. (2012). Cytomegalovirus reactivation after allogeneic transplantation promotes a lasting increase in educated NKG2C+ natural killer cells with potent function. Blood *119*, 2665–2674.

Fontaine, P., Langlais, J., and Perreault, C. (1991). Evaluation of in vitro cytotoxic T lymphocyte assays as a predictive test for the occurrence of graft vs host disease. Immunogenetics *34*, 222–226.

Fontenot, J.D., Gavin, M.A., and Alexander, R.Y. (2003). Foxp3 Programs the Development and Function of CD4+ CD25+ Regulatory T cells. Nat. Immunol. *4*, 330–336.

Ford, C.E., Hamerton, J.L., Barnes, D.W., and Loutit, J.F. (1956). Cytological identification of radiation-chimaeras. Nature *177*, 452–454.

Fowler, D.H., and Gress, R.E. (2000). Th2 and Tc2 Cells in the Regulation of GVHD, GVL, and Graft Rejection: Considerations for the Allogeneic Transplantation Therapy of Leukemia and Lymphoma. Leuk. Lymphoma *38*, 221–234.

Fowler, D.H., Breglio, J., Nagel, G., Eckhaus, M.A., and Gress, R.E. (1996). Allospecific CD8+ Tc1 and Tc2 populations in graft-versus-leukemia effect and graft-versus-host disease. J. Immunol. *157*, 4811–4821.

Frankenberger, M., Sternsdorf, T., Pechumer, H., and Ziegler-Heitbrock, H.W.L. (1996). Differential Cytokine Expression in Human Blood Monocyte Subpopulations: A Polymerase Chain Reaction Analysis. Blood *87*, 373–377.

Freitas, A.A., and Rocha, B. (2000). Population Biology of Lymphocytes: The flight for survival. Annu. Rev. Immunol. *6*, 83–111.

Fry, T.J., and Mackall, C.L. (2005). Immune reconstitution following hematopoietic progenitor cell transplantation: challenges for the future. Bone Marrow Transplant. *35*, S53–S57.

Fujimaki, K., Maruta, A., Yoshida, M., Kodama, F., Matsuzaki, M., Fujisawa, S., Kanamori, H., and

Ishigatsubo, Y. (2001). Immune reconstitution assessed during five years after allogeneic bone marrow transplantation. Bone Marrow Transplant. *27*, 1275–1281.

Furlan, S.N., Watkins, B., Tkachev, V., Flynn, R., Cooley, S., Ramakrishnan, S., Singh, K., Giver, C., Hamby, K., Stempora, L., et al. (2015). Transcriptome analysis of GVHD reveals aurora kinase a as a targetable pathway for disease prevention. Sci. Transl. Med. *7*.

Furlan, S.N., Watkins, B., Tkachev, V., Cooley, S., Panoskaltsis-mortari, A., Betz, K., Brown, M., Hunt, D.J., Schell, J.B., Zeleski, K., et al. (2016). Systems analysis uncovers inflammatory Th/Tc17-driven modules during acute GVHD in monkey and human T cells. Blood *128*, 2568–2580.

Gam, R., Shah, P., Crossland, R.E., Norden, J., Dickinson, A.M., and Dressel, R. (2017). Genetic association of hematopoietic stem cell transplantation outcome beyond histocompatibility genes. Front. Immunol. *8*.

Van Gassen, S., Callebaut, B., Van Helden, M.J., Lambrecht, B.N., Demeester, P., Dhaene, T., and Saeys, Y. (2015). FlowSOM: Using self-organizing maps for visualization and interpretation of cytometry data. Cytometry *87*, 636–645.

Gattinoni, L., Lugli, E., Ji, Y., Pos, Z., Paulos, C.M., Quigley, M.F., Almeida, J.R., Gostick, E., Yu, Z., Carpenito, C., et al. (2011). A human memory T cell subset with stem cell-like properties. Nat. Med. *17*, 1290–1297.

Gattinoni, L., Speiser, D.E., Lichterfeld, M., and Bonini, C. (2017). T memory stem cells in health and disease. Nat. Med. *23*, 18–27.

Geiss, G.K., Bumgarner, R.E., Birditt, B., Dahl, T., Dowidar, N., Dunaway, D.L., Fell, H.P., Ferree, S., George, R.D., Grogan, T., et al. (2008). Direct multiplexed measurement of gene expression with color-coded probe pairs. Nat. Biotechnol. *26*, 317–325.

Geneugelijk, K., Thus, K.A., and Spierings, E. (2014). Predicting alloreactivity in transplantation. J. Immunol. Res. *2014*.

Gerlach, C., Moseman, E.A., Loughhead, S.M., Alvarez, D., Zwijnenburg, A.J., Waanders, L., Garg, R., de la Torre, J.C., and von Andrian, U.H. (2016). The Chemokine Receptor CX3CR1 Defines Three Antigen-Experienced CD8 T Cell Subsets with Distinct Roles in Immune Surveillance and Homeostasis. Immunity *45*, 1270–1284.

Gill, S., and Porter, D.L. (2013). Reduced-intensity hematopoietic stem cell transplants for malignancies: harnessing the graft-versus-tumor effect. Annu. Rev. Med. *64*, 101–117.

Gill, S., Olson, J.A., and Negrin, R.S. (2009). Natural Killer Cells in Allogeneic Transplantation: Effect on Engraftment, Graft- versus-Tumor, and Graft-versus-Host Responses. Biol. Blood Marrow Transplant. *15*, 765–776.

Giroux, M., Delisle, J.S., Gauthier, S.D., Heinonen, K.M., Hinsinger, J., Houde, B., Gaboury, L., Brochu,

S., Wu, J., Hébert, M.J., et al. (2011). SMAD3 prevents graft-versus-host disease by restraining Th1 differentiation and granulocyte-mediated tissue damage. Blood *117*, 1734–1744.

Gleichmann, E., Pals, S., Rolink, A., and Radaszkiewicz, T Gleichmann, H. (1984). Graft-versus-host reactions: Clues to the etiopathology of a spectrum of immunological diseases. Immunol. Today *5*, 324–332.

Glucksberg, H., Storb, R., Fefer, A., Buckner, C.D., Neiman, P.E., Clift, R.A., Lerner, K.G., and Thomas, E.D. (1974). Clinical manifestations of graft-versus-host disease in human recipients of marrow from HL-A-matched sibling donors. Transplantation *18*, 295–304.

Goldrath, A.W., and Bevan, M.J. (1999a). Selecting and maintaining a diverse T-cell repertoire. Nature *402*, 255–262.

Goldrath, A.W., and Bevan, M.J. (1999b). Low-affinity ligands for the TCR drive proliferation of mature CD8+T cells in lymphopenic hosts. Immunity *11*, 183–190.

Gonzalez-Cabrera, P.J., Jo, E., Sanna, M.G., Brown, S., Leaf, N., Marsolais, D., Schaeffer, M.-T., Chapman, J., Cameron, M., Guerrero, M., et al. (2008). Full Pharmacological Efficacy of a Novel S1P1 Agonist That Does Not Require S1P-Like Headgroup Interactions. Mol. Pharmacol. *74*, 1308–1318.

Gordon, S.M., Carty, S.A., Kim, J.S., Zou, T., Smith-Garvin, J., Alonzo, E.S., Haimm, E., Sant'Angelo, D.B., Koretzky, G.A., Reiner, S.L., et al. (2011). Requirements for Eomesodermin and PLZF in the development of innate-like CD8+T cells. J. Immunol. *186*, 4573–4578.

Goulmy, E. (1996). Human minor histocompatibility antigens. Curr. Opin. Immunol. *8*, 75–81.

Gratwohl, A. (2008). Chapter 6. Principles of conditioning. EBMT-ESH Handb. 128–146.

Gratwohl, A., Hermans, J., Goldman, J.M., Arcese, W., Carreras, E., Devergie, A., Frassoni, F., Gahrton, G., Kolb, H.J., Niederwieser, D., et al. (1998). Risk assessment for patients with chronic myeloid leukaemia before allogeneic blood or marrow transplantation. Chronic Leukemia Working Party of the European Group for Blood and Marrow Transplantation. Lancet *352*, 1087–1092.

Green, S.B. (1991). How Many Subjects Does It Take To Do A Regression Analysis? Multivariate Behav. Res. *26*, 499–510.

Grégori, G., Rajwa, B., Patsekin, V., Jones, J., Furuki, M., Yamamoto, M., and Paul Robinson, J. (2014). Hyperspectral Cytometry. In High-Dimensional Single Cell Analysis: Mass Cytometry, Multi-Parametric Flow Cytometry and Bioinformatic Techniques, H.G. Fienberg, and G.P. Nolan, eds. (Berlin, Heidelberg: Springer Berlin Heidelberg), pp. 191–210.

Griesenauer, B., and Paczesny, S. (2017). The ST2/IL-33 axis in immune cells during inflammatory diseases. Front. Immunol. *8*.

Griffith, J.W., Sokol, C.L., and Luster, A.D. (2014). Chemokines and Chemokine Receptors: Positioning Cells for Host Defense and Immunity. Annu. Rev. Immunol. *32*, 659–702.

Groom, J.R., and Luster, A.D. (2011). CXCR3 in T cell function. Exp. Cell Res. *317*, 620–631.

Gyurkocza, B., and Sandmaier, B.M. (2014). Conditioning regimens for hematopoietic cell transplantation : one size does not fi t all. Blood *124*, 344–353.

Hainz, U., Obexer, P., Winkler, C., Sedlmayr, P., Takikawa, O., Greinix, H., Lawitschka, A., Pötschger, U., Fuchs, D., Ladisch, S., et al. (2005). Monocyte-mediated T-cell suppression and augmented monocyte tryptophan catabolism after human hematopoietic stem-cell transplantation. Blood *105*, 4127–4134.

Hakim, F.T., Cepeda, R., Kaimei, S., Mackall, C.L., McAtee, N., Zujewski, J., Cowan, K., and Gress, R.E. (1997). Constraints on CD4 recovery postchemotherapy in adults: thymic insufficiency and apoptotic decline of expanded peripheral CD4 cells. Blood *90*, 3789–3798.

Hakim, F.T., Memon, S., Jin, P., Matin, M., Wang, H., Rehman, N., Yan, X., Rose, J., Mays, J.W., Dhamala, S., et al. (2016). Upregulation of IFN-Inducible and Damage-Response Pathways in Chronic Graft-versus-Host Disease. J. Immunol. *197*, 3490–3503.

Hamann, D., Baars, P.A., Rep, M.H.G., Hooibrink, B., Kerkhof-Garde, S.R., Klein, M.R., and Lier, R.A.W. v. (1997). Phenotypic and Functional Separation of Memory and Effector Human CD8+ T Cells. J. Exp. Med. *186*, 1407–1418.

Handgretinger, R., and Schilbach, K. (2018). The potential role of γδ T cells after allogeneic HCT for leukemia. Blood *131*, 1063–1072.

Hanna, J., Bechtel, P., Zhai, Y., Youssef, F., McLachlan, K., and Mandelboim, O. (2004). Novel Insights on Human NK Cells' Immunological Modalities Revealed by Gene Expression Profiling. J. Immunol. *173*, 6547–6563.

Hatzimichael, E., and Tuthill, M. (2010). Hematopoietic stem cell transplantation. Stem Cells Cloning *3*, 105–117.

Hechinger, A., Smith, B.A.H., Flynn, R., Hanke, K., Mcdonald-hyman, C., Taylor, P.A., Pfeifer, D., Leonhardt, F., Prinz, G., Dierbach, H., et al. (2015). Therapeutic activity of multiple common γ-chain cytokine inhibition in acute and chronic GVHD. Blood *125*, 570–581.

Henden, A.S., and Hill, G.R. (2015). Cytokines in Graft-versus-Host Disease. J. Immunol. *194*, 4604–4612.

Henel, G., and Schmitz, J. (2007). Basic Theory and Clinical Applications of Flow Cytometry. Lab. Med. *38*, 428–436.

Henig, I., and Zuckerman, T. (2014). Hematopoietic Stem Cell Transplantation—50 Years of Evolution and Future Perspectives. Rambam Maimonides Med. J. *5*, 1–15.

Hess, C., and Kemper, C. (2016). Complement-Mediated Regulation of Metabolism and Basic Cellular Processes. Immunity *45*, 240–254.

Hill, G.R., and Ferrara, J.L. (2000). The primacy of the gastrointestinal tract as a target organ of acute graft-

versus-host disease: rationale for the use of cytokine shields in allogeneic bone marrow transplantation. Blood *95*, 2754–2759.

Hill, L., Alousi, A., Kebriaei, P., Mehta, R., Rezvani, K., and Shpall, E. (2018). New and emerging therapies for acute and chronic graft versus host disease. Ther. Adv. Hematol. *9*, 21–46.

Hippen, K.L., Bucher, C., Schirm, D.K., Bearl, A.M., Brender, T., Mink, K.A., Waggie, K.S., De Latour, R.P., Janin, A., Curtsinger, J.M., et al. (2012). Blocking IL-21 signaling ameliorates xenogeneic GVHD induced by human lymphocytes. Blood *119*, 619–628.

Holler, E., Rogler, G., Brenmoehl, J., Hahn, J., Herfarth, H., Greinix, H., Dickinson, A.M., Socié, G., Wolff, D., Fischer, G., et al. (2006). Prognostic significance of NOD2/CARD15 variants in HLA-identical sibling hematopoietic stem cell transplantation: effect on long-term outcome is confirmed in 2 independent cohorts and may be modulated by the type of gastrointestinal decontamination. Blood *107*, 4189–4193.

Holmes, S., He, M., Xu, T., and Lee, P.P. (2005). Memory T cells have gene expression patterns intermediate between naive and effector. Proc. Natl. Acad. Sci. U. S. A. *102*, 5519–5523.

Holtan, S.G., Marcelo, P., and Weisdorf, D.J. (2014). Acute graft-versus-host disease: A bench-to-bedside update. Blood *124*, 363–373.

Horowitz, M.M., Gale, R.P., Sondel, P.M., Goldman, J.M., Kersey, J., Kolb, H.J., Rimm, A.A., Ringdén, O., Rozman, C., and Speck, B. (1990). Graft-versus-leukemia reactions after bone marrow transplantation. Blood *75*, 555–562.

Huang, W., and Chao, N.J. (2017). Memory T cells: A helpful guard for allogeneic hematopoietic stem cell transplantation without causing graft-versus-host disease. Hematol. Oncol. Stem Cell Ther. *10*, 211–219.

Huang, D.W., Sherman, B.T., and Lempicki, R.A. (2009). Bioinformatics enrichment tools: Paths toward the comprehensive functional analysis of large gene lists. Nucleic Acids Res. *37*, 1–13.

Hülsdünker, J., and Zeiser, R. (2015). Insights into the pathogenesis of GvHD: What mice can teach us about man. Tissue Antigens *85*, 2–9.

Hutloff, A., Dittrich, A.M., Beier, K.C., Eljaschewitsch, B., Kraft, R., Anagnostopoulos, I., and Kroczek, R.A. (1999). ICOS is an inducible T-cell co-stimulator structurally and functionally related to CD28. Nature *397*, 263–266.

Di Ianni, M., Falzetti, F., Carotti, A., Terenzi, A., Castellino, F., Bonifacio, E., Del Papa, B., Zei, T., Iacucci Ostini, R., Cecchini, D., et al. (2011). Tregs prevent GVHD and promote immune reconstitution in HLA-haploidentical transplantation. Blood *117*, 3921–3928.

Ichiba, T., Teshima, T., Kuick, R., Misek, D.E., Liu, C., Takada, Y., Maeda, Y., Reddy, P., Williams, D.L., Hanash, S.M., et al. (2003). Early changes in gene expression profiles of hepatic GVHD uncovered by

oligonucleotide microarrays. Blood *102*, 763–771.

Ingersoll, M., Spanbroek, R., Lottaz, C., Gautier, E., Frankenberger, M., Hoffmann, R., Lang, R., Haniffa, M., Collin, M., Tacke, F., et al. (2010). Comparison of gene expression profiles between human and mouse monocyte subsets. Blood *115*, 10–20.

Italiani, P., and Boraschi, D. (2014). From monocytes to M1/M2 macrophages: Phenotypical vs. functional differentiation. Front. Immunol. *5*.

Ito, T., Hanabuchi, S., Wang, Y.H., Park, W.R., Arima, K., Bover, L., Qin, F.X.F., Gilliet, M., and Liu, Y.J. (2008). Two Functional Subsets of FOXP3+Regulatory T Cells in Human Thymus and Periphery. Immunity *28*, 870–880.

Itzykson, R., Robin, M., Moins-Teisserenc, H., Delord, M., Busson, M., Xhaard, A., Sicre De Fontebrune, F., Peffault De Latour, R., Toubert, A., and Socie, G. (2015). Cytomegalovirus shapes long-term immune reconstitution after Allogeneic stem cell transplantation. Haematologica *100*, 114–123.

Jacobs, R., Stoll, M., Stratmann, G., Leo, R., Link, H., and Schmidt, R.E. (1992). CD16- CD56+ natural killer cells after bone marrow transplantation. Blood *79*, 3239–3244.

Jacobson, L.O., Marks, E.K., Robson, M.J., Gaston, E.O., and Zirkle, R.E. (1949). The effect of spleen protection on mortality following x-irradiation. J. Lab. Clin. Med. *34*, 1538–1543.

Jagasia, M., Arora, M., Flowers, M.E.D., Chao, N.J., Mccarthy, P.L., Cutler, C.S., Urbano-ispizua, A., Pavletic, S.Z., Haagenson, M.D., Zhang, M., et al. (2012). Risk factors for acute GVHD and survival after hematopoietic cell transplantation. Blood *119*, 296–307.

Jaksch, M., Remberger, M., and Mattsson, J. (2005). Increased gene expression of chemokine receptors is correlated with acute graft-versus-host disease after allogeneic stem cell transplantation. Biol. Blood Marrow Transplant. *11*, 280–287.

Janeway CA, J., Travers, P., and Walport, M. (2001). The major histocompatibility complex and its functions. In Immunobiology: The Immune System in Health and Disease., p.

Jenq, R.R., and van den Brink, M.R.M. (2010). Allogeneic haematopoietic stem cell transplantation: individualized stem cell and immune therapy of cancer. Nat. Rev. Cancer *10*, 213–221.

Jones, J.M., Wilson, R., and Bealmear, P.M. (1971). Mortality and gross pathology of secondary disease in germfree mouse radiation chimeras. Radiat. Res. *45*, 577–588.

Josefowicz, S.Z., Lu, L.-F., and Rudensky, A.Y. (2012). Regulatory T Cells: Mechanisms of Differentiation and Function. Annu. Rev. Immunol. *30*, 531–564.

Juric, M.K., Ghimire, S., Ogonek, J., Weissinger, E.M., Holler, E., van Rood, J.J., Oudshoorn, M., Dickinson, A., and Greinix, H.T. (2016). Milestones of hematopoietic stem cell transplantation - From first human studies to current developments. Front. Immunol. *7*.

Juvet, S.C., Whatcott, A.G., Bushell, A.R., and Wood, K.J. (2014). Harnessing Regulatory T cells for

clinical use in transplantation: The end of the beginning. Am. J. Transplant. *14*, 750–763.

Kahan, S.M., Wherry, E.J., and Zajac, A.J. (2015). T cell exhaustion during persistent viral infections. Virology *479–480*, 180–193.

Kanda, J., Brazauskas, R., Hu, Z.H., Kuwatsuka, Y., Nagafuji, K., Kanamori, H., Kanda, Y., Miyamura, K., Murata, M., Fukuda, T., et al. (2016). Graft-versus-Host Disease after HLA-Matched Sibling Bone Marrow or Peripheral Blood Stem Cell Transplantation: Comparison of North American Caucasian and Japanese Populations. Biol. Blood Marrow Transplant. *22*, 744–751.

Kang, X., Kim, J., Deng, M., John, S., Chen, H., Wu, G., Phan, H., and Zhang, C.C. (2016). Inhibitory leukocyte immunoglobulin-like receptors: Immune checkpoint proteins and tumor sustaining factors. Cell Cycle *15*, 25–40.

Kappel, L.W., Goldberg, G.L., King, C.G., Suh, D.Y., Smith, O.M., Ligh, C., Holland, A.M., Grubin, J., Mark, N.M., Liu, C., et al. (2009). IL-17 contributes to CD4-mediated graft-versus-host disease. Blood *113*, 945–952.

Karin, M., and Ben-Neriah, Y. (2000). Phosphorilation Meets Ubiquitination: The Control of NF-KB Activity. Annu. Rev. Immunol. *18*, 621–663.

Kedia, S., Acharya, P.S., Mohammad, F., Nguyen, H., Asti, D., Mehta, S., Pant, M., and Mobarakai, N. (2013). Infectious Complications of Hematopoietic Stem Cell Transplantation. J. Stem Cell Res. Ther. *s3*, 1–8.

Khatri, P., Sirota, M., and Butte, A.J. (2012). Ten years of pathway analysis: Current approaches and outstanding challenges. PLoS Comput. Biol. *8*.

Khwaja, A., Bjorkholm, M., Gale, R.E., Levine, R.L., Jordan, C.T., Ehninger, G., Bloomfield, C.D., Estey, E., Burnett, A., Cornelissen, J.J., et al. (2016). Acute myeloid leukaemia. Nat. Rev. Dis. Prim. *2*.

Kim, S.H., Han, S.Y., Azam, T., Yoon, D.Y., and Dinarello, C.A. (2005). Interleukin-32: A cytokine and inducer of TNFα. Immunity *22*, 131–142.

Klein, J., and Sato, A. (2000). The HLA system - First of Two Parts. N. Engl. J. Med. *343*, 702–709.

Kobayashi, T., Okamoto, S., Iwakami, Y., Nakazawa, A., Hisamatsu, T., Chinen, H., Kamada, N., Imai, T., Goto, H., and Hibi, T. (2007). Exclusive increase of CX3CR1+CD28−CD4+ T cells in inflammatory bowel disease and their recruitment as intraepithelial lymphocytes. Inflamm. Bowel Dis. *13*, 837–846.

Kolb, H.J., Schattenberg, a, Goldman, J.M., Hertenstein, B., Jacobsen, N., Arcese, W., Ljungman, P., Ferrant, a, Verdonck, L., Niederwieser, D., et al. (1995). Graft-versus-leukemia effect of donor lymphocyte transfusions in marrow grafted patients. Blood *86*, 2041–2050.

Kondo, T., Takata, H., and Takiguchi, M. (2007). Functional expression of chemokine receptor CCR6 on human effector memory CD8+ T cells. Eur. J. Immunol. *37*, 54–65.

de Koning, C., Plantinga, M., Besseling, P., Boelens, J.J., and Nierkens, S. (2016). Immune Reconstitution

after Allogeneic Hematopoietic Cell Transplantation in Children. Biol. Blood Marrow Transplant. *22*, 195–206.

Korngold, R., and Sprent, J. (1978). Lethal graft-versus-host disease after bone marrow transplantation across minor histocompatibility barriers in mice. Prevention by removing mature T cells from marrow. J. Exp. Med. *148*, 1687–1698.

Koyama, M., and Hill, G.R. (2016). Alloantigen presentation and graft-versus-host disease: fuel for the fire. Blood *127*, 2963–2970.

Koyama, M., Kuns, R.D., Olver, S.D., Raffelt, N.C., Wilson, Y.A., Don, A.L.J., Lineburg, K.E., Cheong, M., Robb, R.J., Markey, K.A., et al. (2012). Recipient nonhematopoietic antigen-presenting cells are sufficient to induce lethal acute graft-versus-host disease. Nat. Med. *18*, 135–142.

Krenger, W., Blazar, B.R., and Holla, G.A. (2011). Thymic T-cell development in allogeneic stem cell transplantation. Blood *117*, 6768–6776.

Lafarge, X. (2017). What compatibility in 2017 for the haematopoietic stem cell transplantation? Transfus. Clin. Biol. *24*, 124–130.

Lakshmikanth, T., Olin, A., Chen, Y., Mikes, J., Fredlund, E., Remberger, M., Omazic, B., and Brodin, P. (2017). Mass Cytometry and Topological Data Analysis Reveal Immune Parameters Associated with Complications after Allogeneic Stem Cell Transplantation. Cell Rep. *20*, 2238–2250.

Lan, H.Y., Yang, N., Brown, F.G., Isbel, N.M., Nikolic-Paterson, D.J., Mu, W., Metz, C.N., Bacher, M., Atkins, R.C., and Bucala, R. (1998). Macrophage migration inhibitory factor expression in human renal allograft rejection. Transplantation *66*, 1465–1471.

Lauvau, G., and Goriely, S. (2016). Memory CD8+ T Cells: Orchestrators and Key Players of Innate Immunity? PLOS Pathog. *12*.

Lee, A.Y.S., Eri, R., Lyons, A.B., Grimm, M.C., and Korner, H. (2013a). CC chemokine ligand 20 and its cognate receptor CCR6 in mucosal T cell immunology and inflammatory bowel disease: Odd couple or axis of evil? Front. Immunol. *4*.

Lee, S.E., Cho, B.S., Kim, J.H., Yoon, J.H., Shin, S.H., Yahng, S.A., Eom, K.S., Kim, Y.J., Kim, H.J., Lee, S., et al. (2013b). Risk and prognostic factors for acute GVHD based on NIH consensus criteria. Bone Marrow Transplant. *48*, 587–592.

Legat, A., Speiser, D.E., Pircher, H., Zehn, D., and Fuertes Marraco, S.A. (2013). Inhibitory receptor expression depends more dominantly on differentiation and activation than “exhaustion” of human CD8 T cells. Front. Immunol. *4*.

Leng, L., Wang, W., Roger, T., Merk, M., Wuttke, M., Calandra, T., and Bucala, R. (2009). Glucocorticoid-induced MIF expression by human CEM T cells. Cytokine *48*, 177–185.

Li, H.W., and Sykes, M. (2012). Emerging concepts in haematopoietic cell transplantation. Nat. Rev.

Immunol. *12*, 403–416.

Li, W., Liu, L., Gomez, A., Zhang, J., Ramadan, A., Zhang, Q., Choi, S.W., Zhang, P., Greenson, J.K., Liu, C., et al. (2016). Proteomics analysis reveals a Th17-prone cell population in presymptomatic graft-versus-host disease. JCI Insight *1*.

Liberzon, A., Subramanian, A., Pinchback, R., Thorvaldsdóttir, H., Tamayo, P., and Mesirov, J.P. (2011). Molecular signatures database (MSigDB) 3.0. Bioinformatics *27*, 1739–1740.

Little, M., and Storb, R. (2002). History of haematopoietic stem-cell transplantation. Nat. Rev. Cancer *2*, 231–238.

Liu, G., Yang, K., Burns, S., Shrestha, S., and Chi, H. (2010). The S1P1-mTOR axis directs the reciprocal differentiation of Th1 and Treg cells. Nat. Immunol. *11*, 1047–1056.

Liu, K., Catalfamo, M., Li, Y., Henkart, P. a, and Weng, N. (2002). IL-15 mimics T cell receptor crosslinking in the induction of cellular proliferation, gene expression, and cytotoxicity in CD8+ memory T cells. Proc. Natl. Acad. Sci. U. S. A. *99*, 6192–6197.

Ljungman, P., Bregni, M., Brune, M., Cornelissen, J., De Witte, T., Dini, G., Einsele, H., Gaspar, H.B., Gratwohl, A., Passweg, J., et al. (2010). Allogeneic and autologous transplantation for haematological diseases, solid tumours and immune disorders: current practice in Europe 2009. Bone Marrow Transplant. *45*, 219–234.

Ljungman, P., Hakki, M., and Boeckh, M. (2011). Cytomegalovirus in hematopoietic stem cell transplant recipients. Hematol. Oncol. Clin. North Am. *25*, 151–169.

Lo, J.W.S., Leung, A.Y.H., Huang, X.R., Lie, A.K.W., Metz, C., Bucala, R., Liang, R., and Lan, H.Y. (2002). Macrophage migratory inhibitory factor (MIF) expression in acute graft-versus-host disease (GVHD) in allogeneic hemopoietic stem cell transplant recipients. Bone Marrow Transplant. *30*, 375–380.

Locatelli, F., Pende, D., Falco, M., Della Chiesa, M., Moretta, A., and Moretta, L. (2018). NK Cells Mediate a Crucial Graft-versus-Leukemia Effect in Haploidentical-HSCT to Cure High-Risk Acute Leukemia. Trends Immunol. *39*, 577–590.

Lorenz, E., Uphoff, D., Reid, T.R., and Shelton, E. (1951). Modification of Irradiation Injury in Mice and Guinea Pigs by Bone Marrow Injections. J. Natl. Cancer Inst. *12*, 197–201.

Lorenz, E., Schwartz, D.A., Martin, P.J., Gooley, T., Lin, M.T., Chien, J.W., Hansen, J.A., and Clark, J.G. (2001). Association of TLR4 mutations and the risk for acute GVHD after HLA-matched-sibling hematopoietic stem cell transplantation. Biol. Blood Marrow Transplant. *7*, 384–387.

Loschi, M., Porcher, R., Peffault de Latour, R., Vanneaux, V., Robin, M., Xhaard, A., Sicre de Fontebrune, F., Larghero, J., and Socie, G. (2015). High Number of Memory T Cells Is Associated with Higher Risk of Acute Graft-versus-Host Disease after Allogeneic Stem Cell Transplantation. Biol. Blood Marrow

Transplant. *21*, 569–574.

Lugli, E., Dominguez, M.H., Gattinoni, L., Chattopadhyay, P.K., Bolton, D.L., Song, K., Klatt, N.R., Brenchley, J.M., Vaccari, M., Gostick, E., et al. (2013). Superior T memory stem cell persistence supports long-lived T cell memory. J. Clin. Invest. *123*, 594–599.

Vander Lugt, M.T., Braun, T.M., Hanash, S., Ritz, J., Ho, V.T., Antin, J.H., Zhang, Q., Wong, C.-H., Wang, H., Chin, A., et al. (2013). ST2 as a marker for risk of therapy-resistant graft-versus-host disease and death. N. Engl. J. Med. *369*, 529–539.

Lum, L.G. (1987). The kinetics of immune reconstitution after human marrow transplantation. Blood *69*, 369–380.

Lupu, M., and Storb, R. (2007). Five decades of progress in haematopoietic cell transplantation based on the preclinical canine model. Vet. Comp. Oncol. *5*, 14–30.

Mackall, C.L., Hakim, F.T., and Gress, R.E. (1997a). T-cell regeneration: All repertoires are not created equal. Immunol. Today *18*, 245–251.

Mackall, C.L., Fleisher, T.A., Brown, M.R., Andrich, M.P., Chen, C.C., Feuerstein, I.M., Magrath, I.T., Wexler, L.H., Dimitrov, D.S., and Gress, R.E. (1997b). Distinctions between CD8+ and CD4+ T-cell regenerative pathways result in prolonged T-cell subset imbalance after intensive chemotherapy. Blood *89*, 3700–3707.

Mackall, C.L., Fry, T., Gress, R., Peggs, K., Storek, J., and Toubert, A. (2009). Background to hematopoietic cell transplantation, including post transplant immune recovery. Bone Marrow Transplant. *44*, 457–462.

Mackay, C.R. (2001). Chemokines: Immunology's high impact factors. Nat. Immunol. *2*, 95–101.

Maekawa, Y., Minato, Y., Ishifune, C., Kurihara, T., Kitamura, A., Kojima, H., Yagita, H., Sakata-Yanagimoto, M., Saito, T., Taniuchi, I., et al. (2008). Notch2 integrates signaling by the transcription factors RBP-J and CREB1 to promote T cell cytotoxicity. Nat. Immunol. *9*, 1140–1147.

Magenau, J., Runaas, L., and Reddy, P. (2016). Advances in understanding the pathogenesis of graft-versus-host disease. Br. J. Haematol. *173*, 190–205.

Mahnke, Y.D., Brodie, T.M., Sallusto, F., Roederer, M., and Lugli, E. (2013). The who's who of T-cell differentiation: Human memory T-cell subsets. Eur. J. Immunol. *43*, 2797–2809.

Main, J.M., and Prehn, R.T. (1955). Successful skin homografts after the administration of high dosage X radiation and homologous bone marrow. J. Natl. Cancer Inst. *15*, 1023–1029.

Majhail, N.S. (2017). Long-term complications after hematopoietic cell transplantation. Hematol. Oncol. Stem Cell Ther.

Man, K., Gabriel, S.S., Liao, Y., Gloury, R., Preston, S., Henstridge, D.C., Pellegrini, M., Zehn, D., Berberich-Siebelt, F., Febbraio, M.A., et al. (2017). Transcription Factor IRF4 Promotes CD8+T Cell

Exhaustion and Limits the Development of Memory-like T Cells during Chronic Infection. Immunity *47*, 1129–1141.e5.

Marcondes, A.M., Li, X., Tabellini, L., Bartenstein, M., Kabacka, J., Sale, G.E., Hansen, J.A., Dinarello, C.A., and Deeg, H.J. (2011). Inhibition of IL-32 activation by alfa-1 antitrypsin suppresses alloreactivity and increases survival in an allogeneic murine marrow transplantation model. Blood *118*, 5031–5039.

Markey, K. a., Macdonald, K.P. a, and Hill, G.R. (2014). The biology of graft-versus-host disease : experimental systems instructing clinical practice. Blood *124*, 354–363.

Markiewicz, M., Sobczyk-Kruszelnicka, M., Dzierzak Mietla, M., Koclega, A., Zielinska, P., and Kyrcz-Krzemien, S. (2013). Progress in Hematopoietic Stem Cell Transplantation. Innov. Stem Cell Transplant.

Martin, P. (1991). Increased disparity for minor histocompatibility antigens as a potential cause of increased GVHD risk in marrow transplantation from unrelated donors compared with related donors. Bone Marrow Transpl. *8*, 217–223.

Martin, P.J., Levine, D.M., Storer, B.E., Warren, E.H., Zheng, X., Nelson, S.C., Smith, A.G., MortensenJ, B.K., and Hansen, J.A. (2017). Genome-wide minor histocompatibility matching as related to the risk of graft-versus-host disease. Blood *129*, 791–798.

Martinez, F.O. (2009). The transcriptome of human monocyte subsets begins to emerge. J. Biol. *8*.

Martinez, F.O., Gordon, S., Locati, M., and Mantovani, A. (2006). Transcriptional Profiling of the Human Monocyte-to-Macrophage Differentiation and Polarization: New Molecules and Patterns of Gene Expression. J. Immunol. *177*, 7303–7311.

Martinon, F., Gaide, O., Pétrilli, V., Mayor, A., and Tschopp, J. (2007). NALP Inflammasomes: A central role in innate immunity. Semin. Immunopathol. *29*, 213–229.

Mathé, G., Amiel, J.L., Schwarzenberg, L., Cattan, A., and Schneider, M. (1965). Adoptive Immunotherapy of Acute Leukemia : Experimental and Clinical Results. Cancer Res. *25*, 1525–1531.

Mathewson, N.D., Jenq, R., Mathew, A. V, Koenigsknecht, M., Hanash, A., Toubai, T., Oravecz-Wilson, K., Wu, S.-R., Sun, Y., Rossi, C., et al. (2016). Gut microbiome–derived metabolites modulate intestinal epithelial cell damage and mitigate graft-versus-host disease. Nat. Immunol. *17*, 505–513.

Matsuda, S., and Koyasu, S. (2000). Mechanisms of action of cyclosporine. Immunopharmacology *47*, 119–125.

Matsuoka, K. (2018). Low-dose interleukin-2 as a modulator of Treg homeostasis after HSCT: current understanding and future perspectives. Int. J. Hematol. *107*, 130–137.

Matsuoka, K., Kim, H.T., Mcdonough, S., Bascug, G., Warshauer, B., Koreth, J., Cutler, C., Ho, V.T., Alyea, E.P., Antin, J.H., et al. (2010). Altered regulatory T cell homeostasis in patients with CD4+ lymphopenia following allogeneic hematopoietic stem cell transplantation. J. Clin. Invest. *120*, 1479–

1493.

McDonald-Hyman, C., Turka, L.A., and Blazar, B.R. (2015). Advances and challenges in immunotherapy for solid organ and hematopoietic stem cell transplantation. Sci. Transl. Med. *7*.

McDonald, G.B., Tabellini, L., Storer, B.E., Lawler, R.L., Martin, P.J., and Hansen, J.A. (2015). Plasma biomarkers of acute GVHD and nonrelapse mortality: Predictive value of measurements before GVHD onset and treatment. Blood *126*, 113–120.

McLornan, D.P. (2013). Principles of haematopoietic stem cell transplantation. Medicine (Baltimore). *41*, 302–305.

Mehta, R.S., and Rezvani, K. (2016). Immune reconstitution post allogeneic transplant and the impact of immune recovery on the risk of infection. Virulence *7*, 901–916.

Menegatti, S., Rouilly, V., Latis, E., Yahia, H., Mascia, E., Leloup, C., Duffy, D., Urrutia, A., Achouri, E., Quintana-Murci, L., et al. Immune response profiling reveals signaling networks mediating TNF-blocker function and correlates of therapeutic responses in spondyloarthritis. Submitted.

Michel, T., Poli, A., Cuapio, A., Briquemont, B., Iserentant, G., Ollert, M., and Zimmer, J. (2016). Human CD56 ^{bright} NK Cells: An Update. J. Immunol. *196*, 2923–2931.

Michonneau, D., Sagoo, P., Breart, B., Garcia, Z., Celli, S., and Bousso, P. (2016). The PD-1 Axis Enforces an Anatomical Segregation of CTL Activity that Creates Tumor Niches after Allogeneic Hematopoietic Stem Cell Transplantation. Immunity *44*, 143–154.

Min, C.K., Lee, W.Y., Min, D.J., Lee, D.G., Kim, Y.J., Park, Y.H., Kim, H.J., Lee, S., Kim, D.W., Lee, J.W., et al. (2001). The kinetics of circulating cytokines including IL-6, TNF-α, IL-8 and IL-10 following allogeneic hematopoietic stem cell transplantation. Bone Marrow Transplant. *28*, 935–940.

Miura, Y., Thoburn, C., Bright, E., Phelps, M., Shin, T., Matsui, E., Matsui, W., Arai, S., Fuchs, E., Vogelsang, G., et al. (2004). Association of Foxp3 regulatory gene expression with graft-versus-host disease. Blood *104*, 2187–2193.

Morandi, F., Horenstein, A.L., Chillemi, A., Quarona, V., Chiesa, S., Imperatori, A., Zanellato, S., Mortara, L., Gattorno, M., Pistoia, V., et al. (2015). CD56 bright CD16 − NK Cells Produce Adenosine through a CD38-Mediated Pathway and Act as Regulatory Cells Inhibiting Autologous CD4 + T Cell Proliferation. J. Immunol. *195*, 965–972.

Morris, E.S., and Hill, G.R. (2007). Advances in the understanding of acute graft-versus-host disease. Br. J. Haematol. *137*, 3–19.

Moser, B. (2015). CXCR5, the defining marker for follicular B helper T (TFH) cells. Front. Immunol. *6*.

Moy, R.H., Huffman, A.P., Richman, L.P., Crisalli, L., Wang, X.K., Hoxie, J.A., Mick, R., Emerson, S.G., Zhang, Y., Vonderheide, R.H., et al. (2017). Clinical and immunologic impact of CCR5 blockade in graft-versus-host disease prophylaxis. Blood *129*, 906–916.

Mullally, A., and Ritz, J. (2007). Beyond HLA : the significance of genomic variation for allogeneic hematopoietic stem cell transplantation. Blood *109*, 1355–1362.

Murphy, K.M., Nelson, C.A., and Šedý, J.R. (2006). Balancing co-stimulation and inhibition with BTLA and HVEM. Nat. Rev. Immunol. *6*, 671–681.

Murphy, W.J., Welniak, L.A., Taub, D.D., Wiltrout, R.H., Taylor, P.A., Vallera, D.A., Kopf, M., Young, H., Longo, D.L., and Blazar, R. (1998). Differential effects of the absence of interferon-gamma and IL-4 in acute graft-versus-host disease after allogeneic bone marrow transplantation in mice. J. Clin. Invest. *102*, 1742–1748.

Nakanishi, K., Yoshimoto, T., and Okamura, H. (2001). Interleukin-18 regulates both Th1 and Th2 responses. Annu. Rev. Immunol. *19*, 423–474.

Nanki, T., Imai, T., Nagasaka, K., Urasaki, Y., Nonomura, Y., Taniguchi, K., Hayashida, K., Hasegawa, J., Yoshie, O., and Miyasaka, N. (2002). Migration of CX3CR1-positive T cells producing type 1 cytokines and cytotoxic molecules into the synovium of patients with rheumatoid arthritis. Arthritis Rheum. *46*, 2878–2883.

Nassereddine, S., Rafei, H., Elbahesh, E., and Tabbara, I. (2017). Acute Graft Versus Host Disease: A Comprehensive Review. Anticancer Res. *37*, 1547–1555.

Nikolic, B., Lee, S., Bronson, R.T., Grusby, M.J., and Sykes, M. (2000). Th1 and Th2 mediate acute graft-versus-host disease , each with distinct end-organ targets. J. Clin. Invest. *105*, 1289–1298.

Norkin, M., and Wingard, J.R. (2017). Recent advances in hematopoietic stem cell transplantation. F1000 Res. *6*.

Nowak, J. (2008). Role of HLA in hematopoietic SCT. Bone Marrow Transpl. *42*, S71-76.

Nowell, P.C., Cole, L.J., Habermeyer, J.G., and John, G. (1956). Growth and Continued Function of Rat Marrow Cells in X-radiated Mice. Cancer Res. *16*, 258–261.

O'Shea, J.J., and Paul, W.E. (2010). Mechanisms Underlying Lineage Commitment and Plasticity of Helper CD4+ T Cells. Science (80-.). *327*, 1098–1102.

Odorizzi, P.M., and Wherry, E.J. (2012). Inhibitory Receptors on Lymphocytes: Insights from Infections. J. Immunol. *188*, 2957–2965.

Ogonek, J., Juric, M.K., Ghimire, S., Varanasi, P.R., Holler, E., Greinix, H., and Weissinger, E. (2016). Immune reconstitution after allogeneic hematopoietic stem cell transplantation. Front. Immunol. *7*.

Oh, H., and Ghosh, S. (2013). NF-κB: Roles and Regulation In Different CD4+ T cell subsets. Immunol. Rev. *252*, 41–51.

Oh, S.A., and Li, M.O. (2013). TGFb : Guardian of T Cell Function. J. Immunol. *191*, 3973–3979.

Oh, I., Ozaki, K., Meguro, A., Hatanaka, K., Kadowaki, M., Matsu, H., Tatara, R., Sato, K., Iwakura, Y., Nakae, S., et al. (2010). Altered Effector CD4+ T Cell Function in IL-21R-/- CD4+ T Cell-Mediated

Graft-Versus-Host Disease. J. Immunol. *185*, 1920–1926.

Okiyama, N., Furumoto, Y., Villarroel, V.A., Linton, J.T., Tsai, W.L., Gutermuth, J., Ghoreschi, K., Gadina, M., O'Shea, J.J., and Katz, S.I. (2014). Reversal of CD8 T-cell-mediated mucocutaneous graft-versus-host-like disease by the JAK inhibitor tofacitinib. J. Invest. Dermatol. *134*, 992–1000.

Paczesny, S. (2018). Biomarkers for post-transplantation outcomes. Blood *131*, 2193–2204.

Paczesny, S., Krijanovski, O.I., Braun, T.M., Choi, S.W., Clouthier, S.G., Kuick, R., Misek, D.E., Cooke, K.R., Kitko, C.L., Weyand, A., et al. (2009). A biomarker panel for acute graft-versus-host disease. Blood *113*, 273–278.

Paczesny, S., Raiker, N., Brooks, S., and Mumaw, C. (2013). Graft-versus-host disease biomarkers: Omics and personalized medicine. Int. J. Hematol. *98*, 275–292.

Palmer, L.A., Sale, G.E., Balogun, J.I., Li, D., Jones, D., Molldrem, J.J., Storb, R.F., and Ma, Q. (2010). Chemokine Receptor CCR5 Mediates AlloImmune Responses in Graft-versus-Host Disease. Biol. Blood Marrow Transplant. *16*, 311–319.

Pankratova, O.S., and Chukhlovin, A.B. (2016). Time course of immune recovery and viral reactivation following hematopoietic stem cell transplantation. Cell. Ther. Transplant. *55*, 1866–8836.

Park, B.G., Park, C.-J., Jang, S., Chi, H.-S., Kim, D.-Y., Lee, J.-H., Lee, J.-H., and Lee, K.-H. (2015). Reconstitution of lymphocyte subpopulations after hematopoietic stem cell transplantation: comparison of hematologic malignancies and donor types in event-free patients. Leuk. Res. *39*, 1334–1341.

Passweg, J.R., Halter, J., Bucher, C., Gerull, S., Heim, D., Rovó, A., Buser, A., Stern, M., and Tichelli, A. (2012). Hematopoietic stem cell transplantation: A review and recommendations for follow-up care for the general practitioner. Swiss Med. Wkly. *142*.

Pavletic, S.Z., and Fowler, D.H. (2012). GVHD - Are we making progress in GVHD prophylaxis and treatment? Hematol. Am. Soc. Hematol. Educ. Progr. *2012*, 251–264.

Perdomo-Celis, F., Taborda, N.A., and Rugeles, M.T. (2017). Follicular CD8+ T Cells: Origin, Function and Importance during HIV Infection. Front. Immunol. *8*.

Petersdorf, E.W. (2008). Optimal HLA matching in hematopoietic cell transplantation. Curr. Opin. Immunol. *20*, 588–593.

Petersdorf, E.W. (2013). Genetics of graft-versus-host disease: The major histocompatibility complex. Blood Rev. *27*, 1–12.

Petersdorf, E.W. (2017a). Which factors influence the development of GVHD in HLA-matched or mismatched transplants? Best Pract. Res. Clin. Haematol. *30*, 333–335.

Petersdorf, E.W. (2017b). Role of major histocompatibility complex variation in graft-versus-host disease after hematopoietic cell transplantation. F1000 Res. *6*.

Pical-Izard, C., Crocchiolo, R., Granjeaud, S., Kochbati, E., Just-Landi, S., Chabannon, C., Frassati, C.,

Picard, C., Blaise, D., Olive, D., et al. (2015). Reconstitution of Natural Killer Cells in HLA-Matched HSCT after Reduced-Intensity Conditioning: Impact on Clinical Outcome. Biol. Blood Marrow Transplant. *21*, 429–439.

Pidala, J., and Anasetti, C. (2010). Glucocorticoid-Refractory Acute Graft-versus-Host Disease. Biol. Blood Marrow Transplant. *16*, 1504–1518.

Pidala, J., Bloom, G.C., Eschrich, S., Sarwal, M., Enkemann, S., Betts, B.C., Beato, F., Yoder, S., and Anasetti, C. (2015). Tolerance associated gene expression following allogeneic hematopoietic cell transplantation. PLoS One *10*.

Piper, K.P., Horlock, C., Curnow, S.J., Arrazi, J., Nicholls, S., Mahendra, P., Craddock, C., and Moss, P.A. (2007). CXCL10-CXCR3 interactions play an important role in the pathogenesis of acute graft-versus-host disease in the skin following allogeneic stem-cell transplantation. Blood *110*, 3827–3832.

Podgorny, P.J., Liu, Y., Dharmani-Khan, P., Pratt, L.M., Jamani, K., Luider, J., Auer-Grzesiak, I., Mansoor, A., Williamson, T.S., Ugarte-Torres, A., et al. (2014). Immune cell subset counts associated with graft-versus-host disease. Biol. Blood Marrow Transplant. *20*, 450–462.

Poli, A., Michel, T., Thérésine, M., Andrès, E., Hentges, F., and Zimmer, J. (2009). CD56 bright natural killer (NK) cells: an important NK cell subset. Immunology *126*, 458–465.

Porter, D., Roth, M., McGarigle, C., Ferrara, J., and Antin, J. (1994). Induction of graft-versus-host disease as immunotherapy for relapsed chronic myeloid leukemia. N. Engl. J. Med. *330*, 100–106.

Przepiorka, D., Weisdorf, D., Martin, P., Klingemann, H.G., Beatty, P., Hows, J., and Thomas, E.D. (1995). 1994 Consensus Conference on Acute GVHD Grading. Bone Marrow Transplant. *15*, 825–828.

Quigley, M.F., Gonzalez, V.D., Granath, A., Andersson, J., and Sandberg, J.K. (2007). CXCR5+ CCR7- CD8 T cells are early effector memory cells that infiltrate tonsil B cell follicles. Eur. J. Immunol. *37*, 3352–3362.

Ramadan, A., and Paczesny, S. (2015). Various forms of tissue damage and danger signals following hematopoietic stem-cell transplantation. Front. Immunol. *6*.

Reddy, P., and Ferrara, J.L.M. (2003). Immunobiology of acute graft-versus-host disease. Blood Rev. *17*, 187–194.

Regateiro, F.S., Howie, D., Cobbold, S.P., and Waldmann, H. (2011). TGF-β in transplantation tolerance. Curr. Opin. Immunol. *23*, 660–669.

Reinhardt, K., Foell, D., Vogl, T., Mezger, M., Wittkowski, H., Fend, F., Federmann, B., Gille, C., Feuchtinger, T., Lang, P., et al. (2014). Monocyte-Induced Development of Th17 Cells and the Release of S100 Proteins Are Involved in the Pathogenesis of Graft-versus-Host Disease. J. Immunol. *193*, 3355–3365.

Reis, M., Ogonek, J., Qesari, M., Borges, N.M., Nicholson, L., Preußner, L., Dickinson, A.M., Wang, X.

nong, Weissinger, E.M., and Richter, A. (2016). Recent developments in cellular immunotherapy for HSCT-associated complications. Front. Immunol. *7*.

Ringnér, M. (2008). What is principal component analysis? Nat. Biotechnol. *26*, 303–304.

Rock, K.L., Reits, E., and Neefjes, J. (2016). Present Yourself! By MHC Class I and MHC Class II Molecules. Trends Immunol. *37*, 724–737.

Rogacev, K.S., Zawada, A.M., Hundsdorfer, J., Achenbach, M., Held, G., Fliser, D., and Heine, G.H. (2015). Immunosuppression and monocyte subsets. Nephrol. Dial. Transplant. *30*, 143–153.

Romano, M., Tung, S.L., Smyth, L.A., and Lombardi, G. (2017). Treg therapy in transplantation: a general overview. Transpl. Int. *30*, 745–753.

Roncarolo, M.G., and Battaglia, M. (2007). Regulatory T-cell immunotherapy for tolerance to self antigens and alloantigens in humans. Nat. Rev. Immunol. *7*, 585–598.

Van Rood, J.J., and Van Leeuwen, A. (1963). Leukocyte Grouping. A Method and Its Application. J. Clin. Invest. *42*, 1382–1390.

Van Rood, J.J., Eernisse, J., and Van Leeuwen, A. (1958). Leucocyte antibodies in sera from pregnant women. Nature *181:*, 1735–6.

Roopenian, D., Choi, E.Y., and Brown, A. (2002). The immunogenomics of minor histocompatibility antigens. Immunol. Rev. *190*, 86–94.

Rossi, D., and Zlotnik, A. (2000). The Biology of Chemokines and Their Receptor. Annu. Rev. Immunol. *18*, 217–242.

Roy, D.C., and Perreault, C. (2017). Major vs minor histocompatibility antigens. Blood *129*, 664–666.

Ruggeri, L., Capanni, M., Urbani, E., Perruccio, K., Shlomchik, W.D., Tosti, A., Posati, S., Rogaia, D., Frassoni, F., Aversa, F., et al. (2002). Effectiveness of donor natural killer cell alloreactivity in mismatched hematopoietic transplants. Science (80-.). *295*, 2097–2100.

Ruggeri, L., Mancusi, A., Capanni, M., Urbani, E., Carotti, A., Stern, M., Pende, D., Perruccio, K., Burchielli, E., Topini, F., et al. (2007). Donor natural killer cell allorecognition of missing self in haploidentical hematopoietic transplantation for acute myeloid leukemia : challenging its predictive value. Blood *110*, 433–440.

Ruutu, T., Gratwohl, A., De Witte, T., Afanasyev, B., Apperley, J., Bacigalupo, A., Dazzi, F., Dreger, P., Duarte, R., Finke, J., et al. (2014). Prophylaxis and treatment of GVHD: EBMT-ELN working group recommendations for a standardized practice. Bone Marrow Transplant. *49*, 168–173.

Sadeghi, B., Al-Chaqmaqchi, H., Al-Hashmi, S., Brodin, D., Hassan, Z., Abedi-Valugerdi, M., Moshfegh, A., and Hassan, M. (2013). Early-phase GVHD gene expression profile in target versus non-target tissues: kidney, a possible target? Bone Marrow Transplant. *48*, 284–293.

Sakaguchi, S., Sakaguchi, N., Asano, M., Itoh, M., and Toda, M. (1995). Immunologic self-tolerance

maintained by activated T cells expressing IL-2 receptor alpha-chains (CD25). Breakdown of a single mechanism of self-tolerance causes various autoimmune diseases. J. Immunol. *155*, 1151–1164.

Sallusto, F., and Lanzavecchia, A. (2009). Heterogeneity of CD4+ memory T cells: Functional modules for tailored immunity. Eur. J. Immunol. *39*, 2076–2082.

Sallusto, F., Lenig, D., Mackay, C.R., and Lanzavecchia, A. (1998). Flexible Programs of Chemokine Receptor Expression on Human Polarized T Helper 1 and 2 Lymphocytes. J. Exp. Med. *187*, 875–883.

Sallusto, F., Lenig, D., Förster, R., Lipp, M., and Lanzavecchia, A. (1999). Two subsets of memory T lymphocytes with distinct homing potential and effector functions. Nature *401*, 708–712.

Santos, G.W. (1989). Busulfan (Bu) and cyclophosphamide (Cy) for marrow transplantation. Bone Marrow Transplant. *4*, 236–239.

Saraiva, M., and O'Garra, A. (2010). The regulation of IL-10 production by immune cells. Nat. Rev. Immunol. *10*, 170–181.

Schaerli, P., Willimann, K., Lang, A.B., Lipp, M., Loetscher, P., and Moser, B. (2000). CXC Chemokine Receptor 5 Expression Defines Follicular Homing T Cells with B Cell Helper Function. J. Exp. Med. *192*, 1553–1562.

Schmitt, N., Bentebibel, S.E., and Ueno, H. (2014). Phenotype and functions of memory Tfh cells in human blood. Trends Immunol. *35*, 436–442.

Scholzen, T., and Gerdes, J. (2000). The Ki-67 protein: from the known and the unknown. J. Cell. Physiol. *182*, 311–322.

Seggewiss, R., and Einsele, H. (2010). Immune reconstitution after allogeneic transplantation and expanding options for immunomodulation : an update. Blood *115*, 3861–3868.

Shallis, R.M., Terry, C.M., and Lim, S.H. (2017). Changes in intestinal microbiota and their effects on allogeneic stem cell transplantation. Am. J. Hematol. 1–7.

Shlomchik, D.S. (2007). Graft-versus-host disease. Nat. Rev. Immunol. *7*, 340–352.

Shono, Y., and Van Den Brink, M.R.M. (2018). Gut microbiota injury in allogeneic haematopoietic stem cell transplantation. Nat. Rev. Cancer *18*, 283–295.

Shono, Y., Docampo, M.D., Peled, J.U., Perobelli, S.M., Velardi, E., Tsai, J.J., Slingerland, A.E., Smith, O.M., Young, L.F., Gupta, J., et al. (2016). Increased GVHD-related mortality with broad-spectrum antibiotic use after allogeneic hematopoietic stem cell transplantation in human patients and mice. Sci. Transl. Med. *8*.

Simonetta, F., Alvarez, M., and Negrin, R.S. (2017). Natural Killer Cells in Graft-versus-Host-Disease after Allogeneic Hematopoietic Cell Transplantation. Front. Immunol. *8*.

Singh, A.K., and McGuirk, J.P. (2016). Allogeneic stem cell transplantation: A historical and scientific overview. Cancer Res. *76*, 6445–6451.

Singh, S.P., Zhang, H.H., Foley, J.F., Hedrick, M.N., and Farber, J.M. (2008). Human T Cells That Are Able to Produce IL-17 Express the Chemokine Receptor CCR6. J. Immunol. *180*, 214–221.

Slavin, S., Naparstek, E., Nagler, A., Ackerstein, A., Kapelushnik, J., and Or, R. (1995). Allogeneic cell therapy for relapsed leukemia after bone marrow transplantation with donor peripheral blood lymphocytes. Exp. Hematol. *23*, 1553–1562.

Smith, P., O'Sullivan, C., and Gergely, P. (2017). Sphingosine 1-Phosphate Signaling and Its Pharmacological Modulation in Allogeneic Hematopoietic Stem Cell Transplantation. Int. J. Mol. Sci. *18*, 2027.

Smithgall, M.D., Comeau, M.R., Park Yoon, B.R., Kaufman, D., Armitage, R., and Smith, D.E. (2008). IL-33 amplifies both Th1- and Th2-type responses through its activity on human basophils, allergen-reactive Th2 cells, iNKT and NK Cells. Int. Immunol. *20*, 1019–1030.

Socie, G., and Blazar, B.R. (2009). Acute graft-versus-host disease : from the bench to the bedside. Blood *114*, 4327–4336.

Spierings, E. (2014). Minor histocompatibility antigens: Past, present, and future. Tissue Antigens *84*, 374–360.

Sprent, J., and Surh, C.D. (2011). Normal T cell homeostasis: The conversion of naive cells into memory-phenotype cells. Nat. Immunol. *12*, 478–484.

Staffas, A., Burgos, M., and Van Den Brink, M.R.M. (2017). The intestinal microbiota in allogeneic hematopoietic cell transplant and graft-versus-host disease. Blood *129*, 927–934.

Stern, L., McGuire, H., Avdic, S., Rizzetto, S., Fazekas de St Groth, B., Luciani, F., Slobedman, B., and Blyth, E. (2018). Mass Cytometry for the assessment of immune reconstitution after hematopoietic stem cell transplantation. Front. Immunol. *9*.

Stikvoort, A., Chen, Y., Rådestad, E., Törlén, J., Lakshmikanth, T., Björklund, A., Mikes, J., Achour, A., Gertow, J., Sundberg, B., et al. (2017). Combining flow and mass cytometry in the search for biomarkers in chronic graft-versus-host disease. Front. Immunol. *8*.

Stirewalt, D.L., Mhyre, A.J., Marcondes, M., Pogosova-Agadjanyan, E., Abbasi, N., Radich, J.P., and Deeg, H.J. (2008). Tumour necrosis factor-induced gene expression in human marrow stroma: Clues to the pathophysiology of MDS? Br. J. Haematol. *140*, 444–453.

Storb, R., Prentice, R.L., Buckner, C.D., Clift, R.A., Appelbaum, F., Deeg, J., Doney, K., Hansen, J.A., Mason, M., Sanders, J.E., et al. (1983). Graft-versus-host disease and survival in patients with aplastic anemia treated by marrow grafts from HLA-identical siblings. Beneficial effect of a protective environment. N. Engl. J. Med. *308*, 302–307.

Storek, J., Geddes, M., Khan, F., Huard, B., Helg, C., Chalandon, Y., Passweg, J., and Roosnek, E. (2008). Reconstitution of the immune system after hematopoietic stem cell transplantation in humans. Semin.

Immunopathol. *30*, 425–437.

Subramanian, A., Tamayo, P., Mootha, V.K., Mukherjee, S., Ebert, B.L., Gillette, M.A., Paulovich, A., Pomeroy, S.L., Golub, T.R., Lander, E.S., et al. (2005). Gene set enrichment analysis: A knowledge-based approach for interpreting genome-wide expression profiles. Proc. Natl. Acad. Sci. U. S. A. *102*, 15545–15550.

Sugerman, P.B., Faber, S.B., Willis, L.M., Petrovic, A., Murphy, G.F., Pappo, J., Silberstein, D., and Van Den Brink, M.R.M. (2004). Kinetics of gene expression in murine cutaneous graft-versus-host disease. Am. J. Pathol. *164*, 2189–2202.

Sullivan, K.M., Weiden, P.L., Storb, R., Witherspoon, R.P., Fefer, A., Fisher, L., Buckner, C.D., Anasetti, C., Appelbaum, F.R., and Badger, C. (1989). Influence of acute and chronic graft-versus-host disease on relapse and survival after bone marrow transplantation from HLA-identical siblings as treatment of acute and chronic leukemia. Blood *73*, 1720–1728.

Sung, A.D., and Chao, N.J. (2013). Concise Review: Acute Graft-Versus-Host Disease: Immunobiology, Prevention, and Treatment. Stem Cell Transl. Med. *2*, 25–32.

Sureda, A., Bader, P., Cesaro, S., Dreger, P., Duarte, R.F., Dufour, C., Falkenburg, J.H.F., Farge-Bancel, D., Gennery, A., Kröger, N., et al. (2015). Indications for allo- and auto-SCT for haematological diseases, solid tumours and immune disorders: current practice in Europe, 2015. Bone Marrow Transplant. *50*, 1037–1056.

Szyska, M., and Na, I.-K. (2016). Bone Marrow GvHD after Allogeneic Hematopoietic Stem Cell Transplantation. Front. Immunol. *7*.

Takahashi, N., Sato, N., Takahashi, S., and Tojo, A. (2008). Gene-expression profiles of peripheral blood mononuclear cell subpopulations in acute graft-vs-host disease following cord blood transplantation. Exp. Hematol. *36*, 1760–1774.

Tamang, D.L., Redelman, D., Alves, B.N., Vollger, L., Bethley, C., and Hudig, D. (2006). Induction of granzyme B and T cell cytotoxic capacity by IL-2 or IL-15 without antigens: Multiclonal responses that are extremely lytic if triggered and short-lived after cytokine withdrawal. Cytokine *36*, 148–159.

Tchao, N.K., and Turka, L.A. (2012). Lymphodepletion and homeostatic proliferation: Implications for transplantation. Am. J. Transplant. *12*, 1079–1090.

Thiant, S., Moutuou, M.M., Leboeuf, D., and Guimond, M. (2016). Homeostatic cytokines in immune reconstitution and graft-versus-host disease. Cytokine *82*, 24–32.

Thomas, E.D. (1999). A history of haemopoietic cell transplantation. Br. J. Haematol. *105*, 330–339.

Thomas, E.D., and Blume, K.G. (1999). Historical markers in the development of allogeneic hematopoietic cell transplantation. Biol. Blood Marrow Transplant. *5*, 341–346.

Thomas, E.D., Lochte, H.L., Lu, W.C., and Ferrebee, J.W. (1957). Intravenous Infusion of Bone Marrow

in Patients Receiving Radiation and Chemotherapy. N. Engl. J. Med. *257*, 491–496.

Thomas, E.D., Storb, R., Clift, R.A., Fefer, A., Johnson, F.L., Neiman, P.E., Lerner, K.G., Glucksberg, H., and Buckner, C.D. (1975). Bone-marrow transplantation. N. Engl. J. Med. *292*, 832–843, 895–902.

Thomas, E.D., Buckner, C.D., Banali, M., Cliff, R.A., Fefer, A., Flournoy, N., Goodell, B.W., Hickman, R.O., Lerner, K.G., Neiman, P.E., et al. (1977). One hundred patients with acute leukemia treated with chemotherapy, total body irradiation, and allogeneic marrow transplantation. Blood *49*, 511–533.

Thomas, G., Tacke, R., Hedrick, C.C., and Hanna, R.N. (2015). Nonclassical Patrolling Monocyte Function in the Vasculature. Arterioscler. Thromb. Vasc. Biol. *35*, 1306–1316.

Thorp, E.B., Stehlik, C., and Ansari, M.J. (2015). T-cell exhaustion in allograft rejection and tolerance. Curr. Opin. Organ Transplant. *20*, 37–42.

Tilly, G., Doan-Ngoc, T.M., Yap, M., Caristan, A., Jacquemont, L., Danger, R., Cadoux, M., Bruneau, S., Giral, M., Guerif, P., et al. (2017). IL-15 harnesses pro-inflammatory function of TEMRA CD8 in kidney-transplant recipients. Front. Immunol. *8*.

Toubai, T., Shono, Y., Nishihira, J., Ibata, M., Suigita, J., Kato, N., Ohkawara, T., Tone, S., Lowler, K.P., Ota, S., et al. (2009). Serum macrophage migration inhibitory factor (MIF) levels after allogeneic hematopoietic stem cell transplantation. Int. J. Lab. Hematol. *31*, 161–168.

Toubert, A. (2008). Chapter 15: Immune reconstitution after allogeneic HSCT. In EMBT Handbook, pp. 6–11.

Toubert, A., Glauzy, S., Douay, C., and Clave, E. (2012). Thymus and immune reconstitution after allogeneic hematopoietic stem cell transplantation in humans: Never say never again. Tissue Antigens *79*, 83–89.

Trop-Steinberg, S., Azar, Y., Bringer, R., and Or, R. (2015). Myc and AP-1 expression in T cells and T-cell activation in patients after hematopoietic stem cell transplantation. Clin Exp Med *15*, 189–203.

Truitt, R.L., and Atasoylu, A.A. (1991). Contribution of CD4+ and CD8+ T cells to graft-versus-host disease and graft-versus-leukemia reactivity after transplantation of MHC-compatible bone marrow. Bone Marrow Transplant. *8*, 51–58.

Ullah, M.A., Hill, G.R., and Tey, S.-K. (2016). Functional Reconstitution of Natural Killer Cells in Allogeneic Hematopoietic Stem Cell Transplantation. Front. Immunol. *7*.

Urrutia, A., Duffy, D., Rouilly, V., Posseme, C., Djebali, R., Illanes, G., Libri, V., Albaud, B., Gentien, D., Piasecka, B., et al. (2016). Standardized Whole-Blood Transcriptional Profiling Enables the Deconvolution of Complex Induced Immune Responses. Cell Rep. *16*, 2777–2791.

Vallabhapurapu, S., and Karin, M. (2009). Regulation and Function of NF-κB Transcription Factors in the Immune System. Annu. Rev. Immunol. *27*, 693–733.

Valujskikh, A., and Li, X.C. (2012). Memory T Cells and Their Exhaustive Differentiation. Curr. Opin.

Organ Transplant. *17*, 15–19.

Vandesompele, J., De Preter, K., Pattyn, F., Poppe, B., Van Roy, N., De Paepe, A., and Speleman, R. (2002). Accurate normalization of real-time quantitative RT-PCR data by geometric averaging of multiple internal control genes. Genome Biol. *3*, 1–11.

Verma, K., Ogonek, J., Varanasi, P.R., Luther, S., Bünting, I., Thomay, K., Behrens, Y.L., Mischak-Weissinger, E., and Hambach, L. (2017). Human CD8+ CD57- TEMRA cells: Too young to be called "old." PLoS One *12*.

Verner, J., Kabathova, J., Tomancova, A., Pavlova, S., Tichy, B., Mraz, M., Brychtova, Y., Krejci, M., Zdrahal, Z., Trbusek, M., et al. (2012). Gene expression profiling of acute graft-vs-host disease after hematopoietic stem cell transplantation. Exp. Hematol. *40*, 899–905.

Via, C.S., and Shearer, G.M. (1988). T-cell interactions in autoimmunity: Insights from a murine model of graft-versus-host disease. Immunol. Today *9*, 207–213.

Vincent, K., Roy, D.C., and Perreault, C. (2011). Next-generation leukemia immunotherapy. Blood *118*, 2951–2959.

Vivier, E., Tomasello, E., Baratin, M., Walzer, T., and Ugolini, S. (2008). Functions of natural killer cells. Nat. Immunol. *9*, 503–510.

Vodanovic-Jankovic, S., Hari, P., Jacobs, P., Komorowski, R., and Drobyski, W.R. (2006). NF-kB as a target for the prevention of graft-versus-host disease: Comparative efficacy of bortezomib and PS-1145. Blood *107*, 827–834.

Vosshenrich, C.A.J., García-Ojeda, M.E., Samson-Villéger, S.I., Pasqualetto, V., Enault, L., Goff, O.R. Le, Corcuff, E., Guy-Grand, D., Rocha, B., Cumano, A., et al. (2006). A thymic pathway of mouse natural killer cell development characterized by expression of GATA-3 and CD127. Nat. Immunol. *7*, 1217–1224.

Vriesendorp, H.M. (2003). Aims of conditioning. Exp. Hematol. *31*, 844–854.

Vukicevic, M., Chalandon, Y., Helg, C., Matthes, T., Dantin, C., Huard, B., Chizzolini, C., Passweg, J., and Roosnek, E. (2010). CD56 bright NK cells after hematopoietic stem cell transplantation are activated mature NK cells that expand in patients with low numbers of T cells. Eur. J. Immunol. *40*, 3246–3254.

Van Der Waart, A.B., Van Der Velden, W.J.F.M., Van Halteren, A.G.S., Leenders, M.J.L.G., Feuth, T., Blijlevens, N.M.A., van der Voort, R., and Dolstra, H. (2012). Decreased Levels of Circulating IL17-Producing CD161+CCR6+ T Cells Are Associated with Graft-versus-Host Disease after Allogeneic Stem Cell Transplantation. PLoS One *7*.

Wacleche, V.S., Tremblay, C.L., Routy, J.P., and Ancuta, P. (2018). The biology of monocytes and dendritic cells: Contribution to HIV pathogenesis. Viruses *10*, 1–31.

Waldmann, T.A. (2013). The Biology of IL-15: Implications for Cancer Therapy and the Treatment of Autoimmune Disorders. J. Investig. Dermatology Symp. Proc. *16*, S28–S30.

Wang, H., Grzywacz, B., Sukovich, D., Mccullar, V., Cao, Q., Lee, A.B., Blazar, R., Cornfield, D.N., Miller, J.S., and Verneris, M.R. (2007). The unexpected effect of cyclosporin A on CD56+CD16- and CD56+CD16+ natural killer cell subpopulations. Blood *110*, 1530–1539.

Wang, Y., Zhao, X., Ye, X., Luo, H., Zhao, T., Diao, Y., Zhang, H., Lv, M., Zhang, W., Huang, X., et al. (2015). Plasma microRNA-586 is a new biomarker for acute graft-versus-host disease. Ann. Hematol. *94*, 1505–1514.

Warren, E.H., and Deeg, H.J. (2013). Dissecting graft-versus-leukemia from graft-versus-host-disease using novel strategies. Tissue Antigens *81*, 183–193.

Warren, E.H., Greenberg, P.D., and Riddell, S.R. (1998). Cytotoxic T-lymphocyte-defined human minor histocompatibility antigens with a restricted tissue distribution. Blood *91*, 2197–2207.

Warren, E.H., Zhang, X.C., Li, S., Fan, W., Storer, B.E., Chien, J.W., Boeckh, M.J., Zhao, L.P., Martin, P.J., and Hansen, J.A. (2012). Effect of MHC and non-MHC donor / recipient genetic disparity on the outcome of allogeneic HCT. Blood *120*, 2796–2806.

Weiden, P.L., Flournoy, N., Thomas, E.D., Prentice, R., Fefer, A., Buckner, C.D., and Storb, R. (1979). Antileukemic effect of graft-versus-host disease in human recipients of allogeneic-marrow grafts. N. Engl. J. Med. *300*, 1068–1073.

Weiden, P.L., Sullivan, K.M., Flournoy, N., Storb, R., and Thomas, E.D. (1981). Antileukemic Effect of Chronic Graft-versus-Host Disease. N. Engl. J. Med. *304*, 1529–1533.

Welniak, L.A., Blazar, B.R., and Murphy, W.J. (2007). Immunobiology of Allogeneic Hematopoietic Stem Cell Transplantation. Annu. Rev. Immunol. *25*, 139–170.

Wendt, K., Wilk, E., Buyny, S., Buer, J., Schmidt, R.E., and Jacobs, R. (2006). Gene and protein characteristics reflect functional diversity of CD56dim and CD56bright NK cells. J. Leukoc. Biol. *80*, 1529–1541.

Weng, N., Araki, Y., and Subedi, K. (2012). The molecular basis of the memory T cell response: differential gene expression and its epigenetic regulation. Nat. Rev. Immunol. *12*, 306–315.

West, E.E., Kolev, M., and Kemper, C. (2018). Complement and the Regulation of T Cell Responses. Annu. Rev. Immunol. *36*, 309–338.

Wherry, E.J. (2011). T cell exhaustion. Nat. Immunol. *12*, 492–499.

Wherry, E.J., and Kurachi, M. (2015). Molecular and cellular insights into T cell exhaustion. Nat. Rev. Immunol. *15*, 486–499.

Wherry, E.J., Ha, S.J., Kaech, S.M., Haining, W.N., Sarkar, S., Kalia, V., Subramaniam, S., Blattman, J.N., Barber, D.L., and Ahmed, R. (2007). Molecular Signature of CD8+ T Cell Exhaustion during Chronic

Viral Infection. Immunity *27*, 670–684.

Williams, K.M., and Gress, R.E. (2008). Immune reconstitution and implications for immunotherapy following haematopoietic stem cell transplantation. Best Pract. Res. Clin. Haematol. *21*, 579–596.

Willinger, T., Freeman, T., Hasegawa, H., McMichael, A.J., and Callan, M.F.C. (2005). Molecular Signatures Distinguish Human Central Memory from Effector Memory CD8 T Cell Subsets. J. Immunol. *175*, 5895–5903.

Willinger, T., Freeman, T., Herbert, M., Hasegawa, H., McMichael, A.J., and Callan, M.F.C. (2006). Human Naive CD8 T Cells Down-Regulate Expression of the WNT Pathway Transcription Factors Lymphoid Enhancer Binding Factor 1 and Transcription Factor 7 (T Cell Factor-1) following Antigen Encounter In Vitro and In Vivo. J. Immunol. *176*, 1439–1446.

Wilson Van Voorhis, C.R., and Morgan, B.L. (2007). Understanding Power and Rules of Thumb for Determining Sample Sizes. Tutor. Quant. Methods Psychol. *3*, 43–50.

Wing, K., Onishi, Y., Prieto-Martin, P., Yamaguchi, T., Miyara, M., Fehervari, Z., Nomura, T., and Sakaguchi, S. (2008). CTLA-4 Control over Foxp3+ Regulatory T Cell Function. Science (80-.). *322*, 271–275.

Wong, K.L., Tai, J.J.-Y., Wong, W.-C., Han, H., Sem, X., Yeap, W.-H., Kourilsky, P., and Wong, S.-C. (2011). Gene expression profiling reveals the defining features of the classical, intermediate, and nonclassical human monocyte subsets. Blood *118*, e16–e31.

Wu, C.J., and Ritz, J. (2006). Induction of Tumor Immunity Following Allogeneic Stem Cell Transplantation. Adv. Immunol. *90*, 133–173.

Wysocki, C.A., Panoskaltsis-mortari, A., Blazar, B.R., and Serody, J.S. (2005). Leukocyte migration and graft-versus-host disease. Blood *105*, 4191–4199.

Xhaard, A., Moins-Teisserenc, H., Busson, M., Robin, M., Ribaud, P., Dhedin, N., Abbes, S., Carmagnat, M., Kheav, V.D., Maki, G., et al. (2014). Reconstitution of regulatory T-cell subsets after allogeneic hematopoietic SCT. Bone Marrow Transplant. *49*, 1089–1092.

Xia, C., Braunstein, Z., Toomey, A.C., Zhong, J., and Rao, X. (2018). S100 proteins as an important regulator of macrophage inflammation. Front. Immunol. *8*.

Xiao, B., Wang, Y., Li, W., Baker, M., Guo, J., Corbet, K., Tsalik, E.L., Li, Q., Palmer, S.M., Woods, C.W., et al. (2013). Plasma microRNA signature as a noninvasive biomarker for acute graft-versus-host disease. Blood *122*, 3365–3375.

Yaari, G., Bolen, C.R., Thakar, J., and Kleinstein, S.H. (2013). Quantitative set analysis for gene expression: A method to quantify gene set differential expression including gene-gene correlations. Nucleic Acids Res. *41*.

Yakoub-Agha, I., Saule, P., Depil, S., Micol, J.-B., Grutzmacher, C., Boulanger-Villard, F., Bauters, F.,

Jouet, J.-P., Dessaint, J.-P., and Labalette, M. (2006). A high proportion of donor CD4+ T cells expressing the lymph node-homing chemokine receptor CCR7 increases incidence and severity of acute graft-versus-host disease in patients undergoing allogeneic stem cell transplantation for hematological malignancy. Leukemia *20*, 1557–1565.

Yamaoka, K., Saharinen, P., Pesu, M., Holt, V.E.T., Silvennoinen, O., and O'Shea, J.J. (2004). The Janus kinases (Jaks). Genome Biol. *5*.

Yamazaki, T., Yang, X.O., Chung, Y., Fukunaga, A., Nurieva, R., Pappu, B., Martin-Orozco, N., Kang, H.S., Ma, L., Panopoulos, A.D., et al. (2008). CCR6 Regulates the Migration of Inflammatory and Regulatory T Cells. J. Immunol. *181*, 8391–8401.

Yang, G., Geng, X.R., Song, J.P., Wu, Y., Yan, H., Zhan, Z., Yang, L., He, W., Liu, Z.Q., Qiu, S., et al. (2014). Insulin-like growth factor 2 enhances regulatory T-cell functions and suppresses food allergy in an experimental model. J. Allergy Clin. Immunol. *133*, 1702–1708.e5.

Yang, J., Murphy, T.L., Ouyang, W., and Murphy, K.M. (1999). Induction of interferon-gamma production in Th1 CD4+ T cells: evidence for two distinct pathways for promoter activation. Eur. J. Immunol. *29*, 548–555.

Yap, M., Boeffard, F., Clave, E., Pallier, A., Danger, R., Giral, M., Dantal, J., Foucher, Y., Guillot-Gueguen, C., Toubert, A., et al. (2014). Expansion of Highly Differentiated Cytotoxic Terminally Differentiated Effector Memory CD8+ T Cells in a Subset of Clinically Stable Kidney Transplant Recipients: A Potential Marker for Late Graft Dysfunction. J. Am. Soc. Nephrol. *25*, 1856–1868.

Yi, T., Chen, Y., Wang, L., Du, G., Huang, D., Zhao, D., Johnston, H., Young, J., Todorov, I., Umetsu, D.T., et al. (2009). Reciprocal differentiation and tissue-specific pathogenesis of Th1, Th2, and Th17 cells in graft-versus-host disease. Blood *114*, 3101–3112.

Yuan, X., Cheng, G., and Malek, T.R. (2014). The importance of regulatory T-cell heterogeneity in maintaining self-tolerance. Immunol. Rev. *259*, 103–114.

Zakrzewski, J.L., Van Den Brink, M.R.M., and Hubbell, J.A. (2014). Overcoming immunological barriers in regenerative medicine. Nat. Biotechnol. *32*, 786–794.

Zawada, A.M., Rogacev, K.S., Rotter, B., Winter, P., Marell, R.R., Fliser, D., and Heine, G.H. (2011). SuperSAGE evidence for CD14 ++CD16 + monocytes as a third monocyte subset. Blood *118*, 50–62.

Zeiser, R., and Blazar, B.R. (2017). Acute Graft-versus-Host Disease — Biologic Process, Prevention, and Therapy. N. Engl. J. Med. *377*, 2167–2179.

Zeiser, R., Socié, G., and Blazar, B.R. (2016). Pathogenesis of acute graft-versus-host disease: from intestinal microbiota alterations to donor T cell activation. Br. J. Haematol. *175*, 191–207.

Zhang, L., Chu, J., Yu, J., and Wei, W. (2016). Cellular and molecular mechanisms in graft-versus-host disease. J. Leukoc. Biol. *99*, 279–287.

Zhang, P., Wu, J., Deoliveira, D., Chao, N.J., and Chen, B.J. (2012). Allospecific CD4+Effector Memory T Cells Do Not Induce Graft-versus-Host Disease in Mice. Biol. Blood Marrow Transplant. *18*, 1488–1499.

Zhang, Y., Joe, G., Hexner, E., Zhu, J., and Emerson, S.G. (2005). Host-reactive CD8+ memory stem cells in graft-versus-host disease. Nat. Med. *11*, 1299–1305.

Zhao, Y., Liu, Q., Yang, L., He, D., Wang, L., Tian, J., Li, Y., Zi, F., Bao, H., Yang, Y., et al. (2013). TLR4 inactivation protects from graft-versus-host disease after allogeneic hematopoietic stem cell transplantation. Cell. Mol. Immunol. *10*, 165–175.

Ziegler-Heitbrock, L. (2015). Blood monocytes and their subsets: Established features and open questions. Front. Immunol. *6*.

Ziegler-Heitbrock, L., and Hofer, T.P.J. (2013). Toward a refined definition of monocyte subsets. Front. Immunol. *4*.

Ziegler-Heitbrock, L., Ancuta, P., Crowe, S., Dalod, M., Grau, V., Hart, D.N., Leenen, P.J.M., Liu, Y., Macpherson, G., Randolph, G.J., et al. (2010). Nomenclature of monocytes and dendritic cells in blood. Blood *116*, e74–e80.